

INCREASING THE BIODEGRADATION RATE OF POLY(LACTIC ACID) IN
COMPOSTING CONDITIONS

By

Edgar Castro Aguirre

A DISSERTATION

Submitted to
Michigan State University
in partial fulfillment of the requirements
for the degree of

Packaging – Doctor of Philosophy

2018

ABSTRACT

INCREASING THE BIODEGRADATION RATE OF POLY(LACTIC ACID) IN COMPOSTING CONDITIONS

By

Edgar Castro Aguirre

Poly(lactic acid) (PLA), a well-known compostable and bio-based aliphatic polyester, has found applications in the medical, textile, plasticulture, and packaging industries. PLA has been blended with several polymers and compounded with different micro and nanoparticles to fulfill desirable properties and to extend its range of applications. The growing interest in PLA-based materials and other biodegradable polymers has required the development of methodologies to evaluate their biodegradability and understand the different factors affecting their biodegradation mechanisms and rate. One of the current limitations of biodegradable polymers, like PLA, is that they do not biodegrade as fast as other organic wastes during composting, affecting their general acceptance in industrial composting facilities. In this work, the results of two different approaches to accelerate the biodegradation rate of PLA are presented: 1) the addition of layered silicate nanoparticles to the PLA matrix, and 2) the addition of selective PLA-degrading microbial strains to the media, *i.e.*, bioaugmentation.

For structural changes, three different nanoclays were used as model systems due to their different surface characteristics but similar chemistry: organo-modified montmorillonite (OMMT), Halloysite nanotubes (HNT), and Laponite[®] RD (LRD). Additionally, the organo-modifier of OMMT (Cloisite[®] 30B), methyl, tallow, bis-2-hydroxyethyl, quaternary ammonium (QAC) was used to investigate its effects on the biodegradation of the polymer. PLA and PLA bio-nanocomposite films (BNCs) were

produced and fully characterized. Films were tested for biodegradation in simulated composting conditions by analysis of evolved CO₂ with an in-house built direct measurement respirometer. The molecular weight of the films was monitored during the biodegradation tests and correlated with the degradation kinetics. Additionally, a biofilm formation assay and scanning electron microscopy were used to evaluate microbial attachment on the surface of PLA and BNCs. The biodegradation test results showed a higher mineralization and microbial attachment of the films containing nanoclay in comparison to the pristine PLA. However, the effect of the nanoclays on the initial molecular weight and thickness played a crucial role in the evolution of CO₂.

For bioaugmentation, microorganisms present in the compost and capable of degrading PLA were isolated through an enrichment technique with PLA as the sole carbon source at 58°C. The isolates were identified as *Geobacillus* using 16S rRNA gene sequencing and further used to study the effect of bioaugmentation on the biodegradation rate of PLA and BNCs in solid environments. The results showed that bioaugmentation with *Geobacillus* increased the evolution of CO₂ and accelerated the biodegradation phase of PLA and BNCs when tested in compost and vermiculite inoculated with a compost-derived mixed culture.

This work provides the insights gained during the performance of different biodegradation tests and unique understanding about the biodegradation mechanism of PLA. Increasing the biodegradation rate of PLA-based materials will greatly benefit their general use and their acceptance in industrial composting facilities at their end of life.

Copyright by
EDGAR CASTRO AGUIRRE
2018

To my parents Roberto and Clementina,
brother and sister, Roberto Carlos and Denise

ACKNOWLEDGMENTS

I would like to acknowledge those who without their support, contribution, encouragement and inspiration this dissertation would not have been possible. I would like to express my deep gratitude to Dr. Rafael Auras, my research supervisor, for his patient guidance, enthusiastic encouragement and useful critiques during the planning and development of this work. Dr. Auras encouraged me to always give the best of me and taught me that every single problem has a simple solution if we try harder and think differently. I would like to express my very great appreciation to Dr. Susan Selke. Her comments and criticisms taught me about critical thinking and reasoning. I would also like to thank Dr. Maria Rubino for her valuable and constructive suggestions. I would like to offer my special thanks to Dr. Terence Marsh for his guidance in microbiology. His willingness to give his time so generously has been very much appreciated.

I wish to acknowledge the help provided by the members of Dr. Auras' research group (RAA group) who are not only partners but friends. Special thanks should be given to Fabiola Iniguez-Franco, Javiera Rubilar-Parra, Hayati Samsudin, Pooja Mayekar, Anibal Bher, Sadia Satti, and Wanwarang Limsukon. I would also like to extend my thanks to the undergraduate students: Connor Pettengill, Jason Shaffer, Julia Beaumier, Peter Kieffer, and Austin Barnaby for their invaluable help and time.

I am very thankful to my friends who became my Lansing family: Fabiola Iniguez-Franco, Javiera Rubilar-Parra, Hayati Samsudin, Pooja Mayekar, Jiyon Lee, Lisette Delgado-Aquije, Woranit Muangmala, Jin Zhang, Kikyung Kim, Trey Gase, Rijosh Cheruvathur, Anibal Bher, Ismael Povea-Garcerant, and Felipe Vogelsang for their support, encouragement and inspiration, and for making this journey better.

I would like to acknowledge the Mexican National Council for Science and Technology (CONACYT), and the Mexican Secretariat of Public Education (SEP) for providing a scholarship. I would like to extend my thanks to the School of Packaging (SoP), and the Center for Packaging Innovation and Sustainability (CPIS) for research funding support, to the Environmental Science and Policy Program (ESPP) for a summer research fellowship, and to the College of Agriculture and Natural Resources (CANR) for providing a dissertation completion fellowship. Without all this financial support my Ph. D. studies would not have been completed.

I would like to express my gratitude to the faculty from the School of Packaging, their teaching, guidance, and advices have not only helped me understand and improve my research, but also inspired me to continue working in the packaging field. I would also like to extend my gratitude to the staff from the School of Packaging for their support and constant willingness to help.

Finally, I wish to thank my family, especially my parents, Roberto Castro Diaz and Clementina Aguirre Jaimes, and siblings, Roberto Carlos and Denise Castro Aguirre, for their love and continuous support and encouragement, and for believing in me. I have no words to express my gratitude to them. I would also like to extend my gratitude to those who unintentionally I did not mention.

TABLE OF CONTENTS

LIST OF TABLES	xii
LIST OF FIGURES	xiv
KEY TO SYMBOLS AND ABBREVIATIONS	xxii
CHAPTER 1	
INTRODUCTION	1
1.0 Background and motivation	1
1.1 Overall goal and objectives	4
1.2 Dissertation overview	5
REFERENCES	7
CHAPTER 2	
POLY(LACTIC ACID) – MASS PRODUCTION, PROCESSING, INDUSTRIAL APPLICATIONS, AND END OF LIFE	13
2.0 Abstract	14
2.1 Introduction.....	14
2.2 PLA Resin Production	16
2.3 PLA Processing.....	25
2.3.1 Extrusion.....	26
2.3.2 Injection molding.....	30
2.3.3 Injection stretch blow molding.....	32
2.3.4 Cast film and sheet	33
2.3.5 Thermoforming	38
2.3.6 Other processes – Foaming and fibers.....	40
2.4 Tailoring PLA Properties.....	45
2.5 PLA Industrial Applications.....	50
2.5.1 Medical	51
2.5.2 Fibers and textiles.....	53
2.5.3 Packaging and serveware	56
2.5.4 Plasticsulture	63
2.5.5 Environmental remediation	66
2.5.6 Other applications.....	68
2.6 PLA Degradation	69
2.6.1 Hydrolysis	70
2.6.2 Thermal degradation.....	73
2.6.3 Photodegradation	77
2.7 End-of-life Scenarios for PLA	81
2.7.1 Source reduction (reuse)	83
2.7.2 Recycling	84
2.7.3 Composting.....	86
2.7.4 Incineration with energy recovery	91

2.7.5 Landfill	92
2.8 Environmental Footprint of PLA.....	93
2.9 Final Remarks	103
REFERENCES.....	107

CHAPTER 3

INSIGHTS ON THE AEROBIC BIODEGRADATION OF POLYMERS BY ANALYSIS OF EVOLVED CARBON DIOXIDE IN SIMULATED COMPOSTING CONDITION

3.0 Abstract	138
3.1 Introduction.....	139
3.2 Materials and Methods	151
3.2.1 Materials	151
3.2.1.1 Material processing and characterization	151
3.2.2 Biodegradation test.....	152
3.2.2.1 Compost source	153
3.2.2.2 Compost characterization	154
3.2.2.3 Preparation of inoculum solution	154
3.2.2.4 Biodegradation in compost.....	155
3.2.2.5 Biodegradation in vermiculite	155
3.3 Results and Discussion	156
3.3.1 Biodegradation: CO ₂ evolution and mineralization.....	156
3.3.1.1 Biodegradation in compost.....	157
3.3.1.2 Biodegradation in vermiculite	165
3.3.2 Environment-related factors affecting biodegradation.....	168
3.3.2.1 Microorganisms.....	168
3.3.2.2 Temperature	170
3.3.2.3 Oxygen availability	171
3.3.2.4 Water availability	172
3.3.3 Inoculum-related factors affecting biodegradation	175
3.3.3.1 Dry solids and volatile solids	176
3.3.3.2 pH	177
3.3.3.3 C/N.....	177
3.3.3.4 Compost activity	179
3.3.3.5 Other nutrients	181
3.3.3.6 Priming effect	183
3.3.4 Material-related factors affecting biodegradation	184
3.3.4.1 Chemical structure and properties	184
3.3.4.2 Concentration.....	188
3.3.4.3 Shape.....	189
3.3.4.4 Comparison among different biodegradation tests.....	190
3.3.5 Study Case: Biodegradation of Poly(lactic acid)	192
3.4 Final Remarks	197
APPENDICES	200
APPENDIX 3A: Material processing	201
APPENDIX 3B: Elemental analysis	202
APPENDIX 3C: Molecular weight determination	203
APPENDIX 3D: Compost source.....	204

APPENDIX 3E: Respirometric system.....	205
APPENDIX 3F: Calculation method.....	207
APPENDIX 3G: Determination of the calibration factor, optimal flow and cycle time	211
APPENDIX 3H: Compost physicochemical characteristics before and after the test	216
APPENDIX 3I: Compost nitrate and ammonium concentration	217
APPENDIX 3J: Summary of the results obtained from the eight different biodegradation tests	218
REFERENCES.....	220

CHAPTER 4

IMPACT OF NANOCCLAYS ON THE BIODEGRADATION OF POLY(LACTIC ACID) NANOCOMPOSITES

4.0 Abstract	232
4.1 Introduction.....	233
4.2 Materials and Methods	237
4.2.1 Materials	237
4.2.2 Processing of the PLA bio-nanocomposites	238
4.2.3 Characterization of the PLA bio-nanocomposites	238
4.2.4 Biodegradation evaluation	239
4.2.5 Size Exclusion Chromatography (SEC)	241
4.2.6 Microbial attachment.....	241
4.2.7 Statistical Analysis	243
4.3 Results and Discussion	243
4.3.1 Characterization of the PLA bio-nanocomposites	243
4.3.2 Biodegradation evaluation	246
4.3.3 Molecular Weight.....	257
4.3.4 Microbial attachment.....	262
4.4 Final Remarks	266
APPENDICES	268
APPENDIX 4A: Material processing	269
APPENDIX 4B: Material characterization	271
APPENDIX 4C: Physicochemical characteristics of the compost	276
APPENDIX 4D: Molecular weight determination	277
APPENDIX 4E: Biofilm formation	284
REFERENCES.....	287

CHAPTER 5

ENHANCING THE BIODEGRADATION RATE OF POLY(LACTIC ACID) FILMS AND PLA BIO-NANOCOMPOSITES IN SIMULATED COMPOSTING THROUGH BIOAUGMENTATION.....

5.0 Abstract	296
5.1 Introduction.....	297
5.2 Materials and Methods	299
5.2.1 Materials	299
5.2.1.1 Material processing and characterization.....	299

5.2.2	Isolation of PLA-degrading microbial strain.....	300
5.2.3	Identification of PLA-degrading microbial strain.....	301
5.2.4	Biodegradation evaluation	302
5.2.4.1	Preparation of the compost and vermiculite	302
5.2.4.2	Bioreactor setup	303
5.2.4.3	Bioaugmentation	304
5.2.5	Biofilm formation	304
5.2.6	Size Exclusion Chromatography (SEC).....	305
5.2.7	Statistical Analysis	305
5.3	Results and Discussion	305
5.3.1	Isolation and identification of PLA-degrading bacteria	305
5.3.2	Biodegradation Test.....	307
5.3.3	Molecular Weight.....	312
5.3.4	Biofilm test	315
5.4	Final Remarks	318
	APPENDICES	320
	APPENDIX 5A: Compost and vermiculite nutrient analysis	321
	APPENDIX 5B: Molecular weight	322
	APPENDIX 5C: Biofilm Test	324
	REFERENCES.....	325
CHAPTER 6		
CONCLUSIONS AND RECOMMENDATIONS.....		
6.0	Conclusions.....	331
6.1	Recommendations.....	334

LIST OF TABLES

Table 2.1 Properties and processing temperatures of selected commercially available Ingeo™ PLA resins	29
Table 2.2 Selected average optical, physical, mechanical, and barrier properties of PLA films reported from a number of studies using different grades of PLA, adapted and modified from Auras [49].	36
Table 2.3 Selected examples of packaging containers produced from PLA	60
Table 2.4 General requirements to test biodegradation under laboratory conditions and comparison between ASTM D5338 and ISO 14855 standards [334, 335], reproduced from Castro-Aguirre, E. [336].	89
Table 2.5 Environmental footprint of 1 kg of selected commercial polymer resins as available in Ecoinvent 3.2 and reported using Simapro 8.0.5 with ReCiPe (E) Midpoint Indicator considering the World as the geographical region.....	98
Table 3.1 Selected biodegradation tests in composting conditions reported in the literature and presented in reverse chronological order for 2015 through 1990, including information about the samples, compost and the main methods for assessing biodegradation.	142
Table 3.2 Initial M_n , M_w , and PI of the PLA samples	152
Table 3.3 Biodegradation test, materials, and media used for testing	153
Table 3.4 Detailed composition of 1 L of mineral solution.....	155
Table 3.5 Characteristics of the compost samples for each test and requirements according to ISO 14855 standard.....	176
Table 3.6 Physicochemical parameters and total nutrient analysis of different media used in the Nov15 test	183
Table 3A.1 Temperature profile and screw speed used for the production of the PLA films	201
Table 3B.1 Carbon, hydrogen, and nitrogen content of the tested materials	202
Table 3H.1 Physicochemical characteristics of the compost from the Feb13 and the Nov14 tests determined before and after the test	216
Table 3J.1 Summary of the results obtained from the eight different biodegradation tests	218

Table 4.1 Key for biodegradation test and labels of the samples.....	240
Table 4A.1 Processing conditions of the sample materials.....	270
Table 4B.1 Carbon, hydrogen, and nitrogen content of the tested materials	271
Table 4B.2 Thermal properties of the PLA and BNCs	273
Table 4B.3 Resistivity of the PLA and BNCs	274
Table 4B.4 Contact angle of the PLA and BNCs measured with water at room temperature.....	275
Table 4C.1 Physicochemical characteristics of the compost used in the different biodegradation tests	276
Table 4D.1 Initial M_n , M_w , and PDI of the PLA samples	278
Table 4D.2 Initial molecular weight and reduction rate of PLA and BNCs as estimated by the first order reaction of the form $M_n = M_{n0} \exp(-kt)$	283
Table 4E.1 Absorbance (600 nm) of a) PA at 23°C first iteration.....	285
Table 4E.2 Absorbance (600 nm) of a) CE at 58°C first iteration.....	286
Table 4E.3 Absorbance (600 nm) of PA at 23°C during the biofilm test	286
Table 4E.4 Absorbance (600 nm) of CE at 58°C during the biofilm test	286
Table 5.1 Carbon, hydrogen, and nitrogen content of the tested materials.....	300
Table 5.2 Initial physicochemical parameters of the compost and vermiculite used for biodegradation tests	303
Table 5.3 Identification of the microbial isolates using the MSU-RDP Sequence Match and the NCBI database.	307
Table 5.4 Absorbance (600 nm) of biofilm formation samples with <i>Pseudomonas aeruginosa</i> (PA) at 23°C	316
Table 5.5 Absorbance (600 nm) of biofilm formation samples with <i>Geobacillus</i> at 58°C	317
Table 5A.1 Physicochemical parameters and total nutrient analysis of different media used in the biodegradation test	321
Table 5B.1 Molecular weight reduction rate of PLA and PLA-OMMT5 in vermiculite with different levels of inoculation as estimated by the first order reaction of the form $M_n/M_{n0} = \exp(-kt)$	322

LIST OF FIGURES

Figure 2.1 Number of research reports published since 1990 based on the Web of Science search using keywords "PLA", "PLLA", "PDLA", "polylactic acid", "polylactide", and "poly(lactic acid)" [7].	15
Figure 2.2 Chemical structure of L(+) and D(-) lactic acid.	17
Figure 2.3 The manufacturing processes to produce high molecular weight PLA, adapted from Hartmann [17].	19
Figure 2.4 NatureWorks LLC commercial process for producing high molecular weight PLA, adapted from Auras <i>et al.</i> [2] and Vink <i>et al.</i> [5].	21
Figure 2.5 Diastereomeric structures of lactide (3,6-dimethyl-1,4-dioxane-2,5-dione). T_m of L-lactide, D-lactide, <i>meso</i> -lactide, and <i>rac</i> -lactide are 96, 96–97, 53, and 125°C, respectively, adapted from Vert <i>et al.</i> [18].	22
Figure 2.6 Major components of an injection molding machine showing the extruder (reciprocal screw) and clamp units. "Reprinted from Progress in Polymer Science, 33, Lim <i>et al.</i> , Processing technologies for poly (lactic acid), 820-852, Copyright (2008), with permission from Elsevier" [1].	31
Figure 2.7 Injection stretch blow molding (ISBM) of PLA bottle. "Reprinted from Progress in Polymer Science, 33, Lim <i>et al.</i> , Processing technologies for poly (lactic acid), 820-852, Copyright (2008), with permission from Elsevier" [1].	33
Figure 2.8 Biaxial oriented extrusion cast film machine, adapted from "Reprinted from Progress in Polymer Science, 33, Lim <i>et al.</i> , Processing technologies for poly (lactic acid), 820-852, Copyright (2008), with permission from Elsevier" [1].	35
Figure 2.9 Production of a thermoforming part, reproduced "Reprinted from Progress in Polymer Science, 33, Lim <i>et al.</i> , Processing technologies for poly (lactic acid), 820-852, Copyright (2008), with permission from Elsevier" [1].	39
Figure 2.10 Schematic of microcellular foaming process: a) batch process, b) continuous process; 1 to 6 are the main regions of the extruder; adapted from Matuana [64].	42
Figure 2.11 Schematic representation of melt spinning setup: (1) extruder drive, (2) single-extruder - 24 to 36:1 L/D ratio, (3) hopper, (4) screw, (5) manifold, (6) static mixer, (7) metering pump, (8) metering pump drive, (9) spin pack, (10) mesh filters, (11) distributor, (12) spinneret, (13) cross-flow quench chamber, (14) freshly spun yarn, (15) godet, (16) idler roller, (17) friction-driven winder, (18) yarn bobbin, adapted from Agrawal [67].	45

Figure 2.12 Selected biodegradable and non-biodegradable blends of PLA polymers: PLA-LDPE [89], PLA-LLDPE [90], PLLA-LLDPE [90-92], PLLA-HDPE [91], PLA-PS [93], PLLA-PEVA [94], PLLA-EVOH [95], PLA-TPO [96], PLLA-ABS [97], PLLA-PIP [98], PLA-PVOH [99], PLA-PHB [100] PLLA-PBS [101, 102], PLA-PBSA [103], PLA-PBAT [104, 105], PLLA-PTAT [106], PLA-PAE [107], PLA-PU [108], PLA-PEG [109], PLA-SPI [110], PLA-SPC [110], PLA-SF [111], PLA-TKGM [112], PLA-Chitosan [83, 113], PDLLA-Chitosan [114], PLLA-Chitosan [114], PLLA-PBSL [115], PLLA-PEO [116], PLLA-PCL [117-119], PDLLA-PCL [117], PLA-PCL [120], PLA-Starch [121-124], PLA-PHBHxx [125], PLA-PPC [126], PLA-PP [127], PLA-PC [128], PLA-PGS [129], PLA-PTT [130], and PLA-EGMA [131]..... 47

Figure 2.13 Average scale dimensions of selected fillers in PLA composites: MMT (montmorillonite) [168], CNT (carbon nanotube) [169], Ag [170], sisal [171], wood [168, 172, 173], MCC (microcrystalline cellulose) [174], sepiolite [168], cotton [175, 176], ramie [177, 178], MWCNT (multiwall carbon nanotube), graphene, algal [179, 180], tunicin [181], halloysite [148], talc3 [182], CaCO₃ [183], talc2 [182], CaSO₄ [184], talc1 [182], glass fiber [185, 186], abaca fiber [187], jute fiber [187], cotton fiber [187], hemp fiber [187], and flax fiber [186, 188]..... 50

Figure 2.14 (left) tomato plots covered with mulch films; (right) high tunnel or overwintering house. 65

Figure 2.15 Cradle to gate, grave, and cradle life cycle flowchart of plastic mulch films. After removal of conventional mulch films, they can be reused, recycled, incinerated, and/or landfilled. Biodegradable mulch provides the same end-of-life scenario routes and also can be composted. 66

Figure 2.16 Hydrolytic chain cleavage mechanisms of PLA in alkaline (a) and acidic (b) media. "Reprinted from Polymer, 42, Jong *et al.*, New insights into the hydrolytic degradation of poly(lactic acid): participation of the alcohol terminus, 2795-2802, Copyright (2001), with permission from Elsevier" [257]..... 72

Figure 2.17 Ln (M_n) as a function of time during hydrolysis of PLA films into water, 95% ethanol, or 50% ethanol at 40°C. 73

Figure 2.18 Thermodegradation mechanisms of PLA. "Reprinted from: Poly(lactic acid). Synthesis, structure, properties, processing, and applications, Nishida, Thermal degradation, 401-412, Copyright (2010), with permission from John Wiley & Sons, Inc." [286]. 75

Figure 2.19 Photodegradation of PLA via Norrish II mechanism, adapted from Tsuji *et al.* [302]. 78

Figure 2.20 Mechanisms of photodegradation of PLA, adapted from Janokar *et al.* [303]. 79

Figure 2.21 Radicals generated during photodegradation of PLA from cleavage of C-C bonds, adapted from Copinet *et al.* [263]. 80

Figure 2.22 Radicals generated during photodegradation of PLA (a) from C-O and (b) ester bond cleavage, adapted from Copinet <i>et al.</i> [263].	80
Figure 2.23 Diagram of solid waste management, adapted from the U.S. Environmental Protection Agency in Advancing Sustainable Materials Management [314].	82
Figure 2.24 Large-scale commercial composting process. “Reprinted from Polymer International, 57, Kijchavengkul <i>et al.</i> , Compostability of polymers, 793-804, Copyright (2008), with permission from Wiley” [329].	87
Figure 2.25 Schematic of polymer biodegradation mechanism, adapted from Leejarkpai <i>et al.</i> [332].	88
Figure 2.26 a) Amount of CO ₂ evolved from blank, cellulose, and PLA film; b) Percentage mineralization of cellulose and PLA film.	90
Figure 2.27 Calorific values of selected materials, adapted from Laußmann <i>et al.</i> [340].	92
Figure 2.28 Cradle-to-gate, cradle-to-grave, and cradle-to-cradle representations of production, consumption, and disposal of bio-based polymers from renewable resource via composting. “Reprinted from Polymer International, 57, Kijchavengkul <i>et al.</i> , Compostability of polymers, 793-804, Copyright (2008), with permission from Wiley” [329].	94
Figure 2.29 Carbon cycle of fossil-based polymers and bio-based polymers. Renewable resource pathway (green arrows); fossil resource pathway (black arrows); and pathway for both renewable and fossil resources (gray arrow), adapted from Kijchavengkul <i>et al.</i> [329].	96
Figure 2.30 GWP, primary energy of non-renewable resources expressed as higher heating values (HHV), and net water uptake for the production system of Ingeo™ resin, adapted from Vink and Davies [5].	97
Figure 2.31 Climate change, non-renewable energy, water depletion for 1 kg of PLA and other commercial polymers as available in Ecoinvent 3.2 and reported using Simapro 8.0.5 with Recipe (E) Midpoint Indicator considering the World as the geographical region, and Ingeo™ adapted from Vink and Davies [5].	99
Figure 2.32 PLA life cycle and boundary of the studied system. Adapted from Rossi <i>et al.</i> [315].	101
Figure 2.33 Comparison of dynamically-assessed global warming impacts over 100 years associated with the six end-of-life treatments for PLA. The bars on the left side present production impacts of the resin (cradle-to-gate) for comparison purposes, adapted from Rossi <i>et al.</i> [315].	102

Figure 2.34 Comparison of end-of-life options for PLA for each midpoint category, adapted from Rossi *et al.* [315].....103

Figure 3.1 Example of biodegradation test parameters as a function of time. Fitted lines ($y=\beta x+\alpha$) are included for visual guidance only. Air flow rate, temperature, moisture and pH monitored as a function of time in the May13 test during the first 60 days of testing. 157

Figure 3.2 Cumulative CO₂ evolution of blank bioreactors in the different biodegradation tests showing large variation of the CO₂ evolved although they were run under the same experimental conditions..... 158

Figure 3.3 Cumulative CO₂ evolution (a) and mineralization (b) of cellulose bioreactors in the different biodegradation tests. While similar or different CO₂ values were observed, the % mineralization is highly driven by the evolved CO₂ values for the blank test. 159

Figure 3.4 Cumulative CO₂ evolution (a) and mineralization (b) of CS in the different biodegradation tests. Biodegradation tests show a fast increase in the mineralization during the first 10 days of testing. 160

Figure 3.5 Cumulative CO₂ evolution and mineralization of LDPE (a & b) and PE (c & d) bioreactors in different biodegradation tests. Negative values of mineralization are observed in many tests. 163

Figure 3.6 Cumulative CO₂ evolution (a) and mineralization (b) of PLA bioreactors in the different biodegradation tests; solid, dashed and dotted lines represent PLA1 (93.5 kDa), PLA2 (82.9 kDa), and PLA3 (72.6 kDa), respectively..... 164

Figure 3.7 Cumulative CO₂ evolution and mineralization of CP and PLA tested in inoculated vermiculite in the Jan14 test. Lower values of evolved CO₂ are seen when compared with compost tests, as expected..... 166

Figure 3.8 Cumulative CO₂ (a) and mineralization (b) of CP, PLA1, PLA2, and PLA3 in the Nov15 test. Solid line, dashed line, and dotted line represent compost, inoculated vermiculite and uninoculated vermiculite, respectively. Large difference in CO₂ production can be observed between evolved CO₂ in inoculated and uninoculated vermiculite... 167

Figure 3.9 Cumulative CO₂ of blank and cellulose and % mineralization of cellulose of two different tests Sep12 test (a & b) and Nov15 test (c & d), respectively. The biodegradation process of cellulose was more homogeneous and more efficient in the test in which water was added twice a week seeing as a high % mineralization in a short period of time. 173

Figure 3.10 C/N of the compost as a function of time during the Nov14 test. The fitted line ($y=\beta x+\alpha$) is included for visual guidance only. 179

Figure 3.11 Microbial activity of the compost measured as the production of CO₂ per gram of VS. Variation between 30 and 80 mg of CO₂ per gram of VS is seen at 10 d. 180

Figure 3.12 Cumulative CO₂ evolution (a) and mineralization (b) of CP, CS, and GC in the Jan14 test. Mineralization values larger than 100% are observed for GC. 184

Figure 3.13 CO₂ evolution (a) and mineralization (b) of different materials in the Jun14 test. Large difference of % Mineralization is observed for the different materials. 185

Figure 3.14 Cumulative CO₂ (a) and mineralization (b) of CP, PLA2, and PLA4 in the Nov14 test. PLA 4032D shows faster and larger mineralization than PLA 2003D. 187

Figure 3.15 Cumulative CO₂ and % mineralization of CP and PLA pellets with two different concentrations: 5% and 15%, in the Jan14 test. % Mineralization was not affected regardless of the initial amount of PLA. 189

Figure 3.16 Cumulative CO₂ evolution (a) and mineralization (b) of CP and of PLA provided in different forms: pellet and film, in the Jan14 test. % Mineralization was not extensively different regardless of the shape of the material. 190

Figure 3.17 Comparison of the mineralization values obtained for PLA1 in the Jun14 and the Nov15 tests (a), and the mineralization values obtained for PLA2 in the Nov14 and the Nov15 tests (b). The mineralization ratio when adjusting the time span of the test seems to be similar when comparing the same test material 191

Figure 3.18 Biodegradation of CP (a) and PLA2 (b) during the Nov14 test. The black, red, blue, and green lines represent cumulative CO₂, mineralization, evolved CO₂ per measurement, and M_n reduction, respectively. The dashed blue line represents the evolved CO₂ per measurement of the blank bioreactors. The green line indicates a fitting of an equation of the form $M_n = M_{n0} \exp(-kt)$, where M_{n0} is the initial M_n , k is the rate constant and t is the time. The black dash-dot lines are used as reference to indicate the beginning and end of the biodegradation phase, and the M_n at which the biodegradation phase gets started. Different lag phases and biodegradation phases were observed for CP and PLA2. 192

Figure 3.19 Cumulative CO₂ (a) and mineralization (b) of CP, PLA1, PLA2, and PLA3 in the Nov15 test. Solid lines and dotted lines represent inoculated vermiculite and uninoculated vermiculite, respectively. 195

Figure 3.20 Molecular weight reduction as a function of time for PLA1, PLA2, and PLA3 in compost (solid line), inoculated vermiculite (dashed line), and uninoculated vermiculite (dotted line), in the Nov15 test. Lines indicate fitting of a first order reaction of the form $M_n = M_{n0} \exp(-kt)$, where M_{n0} is the initial M_n , k is the rate constant and t is the time.. 196

Figure 3E.1 Schematic diagram of a direct measurement respirometric system, reproduced from Castro-Aguirre, E. [40]. CO₂ from the incoming air is scrubbed by passing through a series of canisters containing soda lime. This CO₂-free air enters a

water tank, located inside the environmental chamber at 58°C, to get humidified; then, CO₂-free water-saturated air is provided to the bioreactors with an upward flow direction. The respired air stream exits the bioreactors and the environmental chamber passing through a water trap, a mass flow controller (MFC) and a NDIR-CO₂ sensor for CO₂ concentration measurement. Temperature, relative humidity (RH), air flow rate, time and CO₂ concentration are measured and recorded by a data acquisition system (DAS). 206

Figure 3F.1 Time vs. Concentration Plot, reproduced from Castro-Aguirre, E. [40] ... 209

Figure 3G.1 Calibration curve at 58 ± 2°C and 55 ± 5% RH. A linear relationship of the form $[C] = c \cdot k$ was fitted to the data, where $[C]$ is the actual CO₂ concentration, c the response CO₂ concentration as measured by the NDIR analyzer, and k the calibration factor. 212

Figure 3G.2 Response CO₂ concentration obtained when using different injection volumes and air flow rates. The maximum concentration can be achieved in each case regardless the air flow rate used. Fitted lines of the form $y = \beta x + \alpha$ are included for visual guidance only, with $\beta = 0$, and $\alpha = 507, 2535, 5070$, and 10140 , corresponding to the different injection volumes used. 213

Figure 3G.3 Time to reach the maximum CO₂ concentration when using different air flow rates. The longest time to reach the maximum concentration was observed when using the lowest air flow rate..... 214

Figure 3G.4 Response concentration and time required for a selected bioreactor to reach the peak concentration for different injection volumes and air flow rates. The longest time was observed with the highest CO₂ concentration and the lowest air flow rate..... 215

Figure 3I.1 Concentration of NO₃⁻ (left-black axis) and NH₄⁺ (right-red axis) as a function of time of the compost in blank bioreactors (a) and CP bioreactors (b) during the Nov14 test. 217

Figure 4.1 XRD spectra of the different nanoclays, PLA1, and (a) OMMT, (b) HNT, and (c) LRD bio-nanocomposite films. 244

Figure 4.2 TEM micrographs of (a) PLA-OMMT5, (b) PLA-HNT5, and c) PLA-LRD5 bio-nanocomposites at 10kx. The bar in the left bottom represents 1 μm. 244

Figure 4.3 CO₂ evolution of the three different nanoclays (Test I in compost)..... 247

Figure 4.4 (a) CO₂ evolution and (b) % Mineralization of PLA and PLA-OMMT5 films (Test I in compost)..... 249

Figure 4.5 (a) CO₂ evolution and (b) % Mineralization of PLA and PLA-OMMT films with three different levels of loading (1, 5, and 7.5%) (Test II in compost) 251

Figure 4.6 CO₂ evolution of OMMT nanoclay and QAC surfactant (Test II in compost) 252

Figure 4.7 CO ₂ evolution and % Mineralization of PLA-OMMT films (a & b) and PLA-QAC films (c & d) (Test III in compost).....	253
Figure 4.8 (a) CO ₂ evolution and (b) % Mineralization of PLA-HNT films (Test III in compost)	254
Figure 4.9 (a) CO ₂ evolution and (b) % Mineralization of PLA-LRD films (Test III in compost)	255
Figure 4.10 (a) CO ₂ evolution and (b) % Mineralization of PLA and PLA-OMMT5 films (Test IV in compost).....	256
Figure 4.11 (a) CO ₂ evolution and (b) % Mineralization of PLA, PLA-OMMT5, and PLA-QAC0.4 (Test IV in inoculated vermiculite (dashed lines) and uninoculated vermiculite (dotted lines))	257
Figure 4.12 Initial molecular weight of PLA and BNCs	258
Figure 4.13 Change in molecular weight of PLA2 film (Test III in compost)	259
Figure 4.14 Change in molecular weight of (a) PLA2, (b) PLA-OMMT1, (c) PLA-OMMT5, (d) PLA-QAC0.4, (e) PLA-QAC1.5, (f) PLA-HNT1, (g) PLA-HNT5, (h) PLA-LRD1, and (i) PLA-LRD5 films (Test III in compost).	261
Figure 4.15 Absorbance (600 nm) of (a) PA at 23°C, and (b) CE at 58°C for second biofilm test. Columns with the same letter within a group (<i>i.e.</i> , wells, films, or total) are not significantly different at $p \leq 0.05$ (Tukey test)	265
Figure 4.16 SEM micrographs of (a) PLA and (b) PLA-LRD at 1000x before incubation, (c) PLA and (d) PLA-LRD5 after incubation for 48 h at 58°C with compost extract in R2B.	266
Figure 4B.1 DSC of the PLA and BNCs films (1 st cycle)	272
Figure 4B.2 TGA of the PLA and PLA-OMMT films.....	272
Figure 4B.3 Moisture sorption isotherms of the nanoclays, PLA and BNCs films	273
Figure 4D.1 Deconvolution of the PLA2 peaks at days (a) 7, (b) 14, (c) 21, and (d) 28 (Test III in compost).....	280
Figure 4D.2 (a) M_n and (b) area fraction as function of time for PLA2 film (Test III in compost)	281
Figure 4D.3 Molecular weight reduction as function of time for PLA2 and (a) PLA-OMMT, (b) PLA-QAC, (c) PLA-HNT, and (d) PLA-LRD films (Test III in compost). Dashed lines indicate fitting of a first order reaction of the form $M_n/M_{n0} = \exp(-kt)$, where M_{n0} is the initial M_n , k is the rate constant and t is the time.....	282

Figure 4E.1 Absorbance (600 nm) of (a) PA at 23°C, and (b) CE at 58°C first iteration	284
Figure 5.1 (a) CO ₂ evolution and (b) % Mineralization of cellulose, PLA, and PLA-OMMT5, and PLA-QAC0.4 in compost (solid lines), inoculated vermiculite with mixed culture (dashed lines), and uninoculated vermiculite (dotted lines); adapted from Castro-Aguirre et al. [3].	308
Figure 5.2 (a) CO ₂ evolution and (b) % Mineralization of cellulose, PLA, and PLA-OMMT5 in compost without <i>Geobacillus</i> (solid lines) and with <i>Geobacillus</i> (dashed lines).	309
Figure 5.3 % Mineralization of (a) Cellulose, (b) PLA, and (c) PLA-OMMT5 in vermiculite with different levels of inoculation.....	311
Figure 5.4 % Mineralization of cellulose, PLA, and PLA-OMMT5 in (a) compost (same as Figure 5.2b), (b) vermiculite inoculated with mixed culture, and (c) uninoculated vermiculite. Solid lines represent samples without <i>Geobacillus</i> while dashed lines represent samples inoculated with <i>Geobacillus</i>	311
Figure 5.5 Molecular weight reduction as function of time for (a) PLA and (b) PLA-OMMT5 in vermiculite with different levels of inoculation. Lines represent the fitting of the equation $M_n = M_{n0} \exp(-kt)$, where M_{n0} is the initial M_n , k is the rate constant and t is the time.	312
Figure 5.6 <i>MWD</i> of PLA samples in vermiculite with different levels of inoculation (a) uninoculated, (b) <i>Geobacillus</i> only, (c) mixed culture, (d) mixed culture and <i>Geobacillus</i>	315
Figure 5B.1 <i>MWD</i> of PLA-OMMT5 samples in vermiculite with different levels of inoculation (a) uninoculated, (b) <i>Geobacillus</i> only, (c) mixed culture, (d) mixed culture and <i>Geobacillus</i>	323
Figure 5C.1 Absorbance (600 nm) of (a) PA at 23°C, and (b) <i>Geobacillus</i> at 58°C of biofilm formation samples. Bars with the same letter within a group (<i>i.e.</i> , wells, films, or total) are not statistically significantly different at $p \leq 0.05$ with Tukey-Kramer test.....	324
Figure 5C.2 Absorbance (600 nm) of (a) PA at 23°C, and (b) mixed culture at 58°C for biofilm test. Bars with the same letter within a group (<i>i.e.</i> , wells, films, or total) are not significantly different at $p \leq 0.05$ (Tukey-Kramer test). Adapted from Castro-Aguirre et al. [1].	324

KEY TO SYMBOLS AND ABBREVIATIONS

A	area under the curve in equation 3F.4
AATCC	American Association of Textile Chemists and Colorists
ABS	acrylonitrile butadiene styrene
AD	anaerobic digestion
A_{film}	surface area of the film
ANOVA	analysis of variance
APR	Association of Postconsumer Plastic Recyclers
ASTM	American Society for Testing and Materials
ATBC	acetyl- <i>tri-n</i> -butyl citrate
Biopol	poly(hydroxy butyrate)/poly(hydroxy valerate) blend
BNC	bio-nanocomposite
C	compost
C	concentration of CO ₂ evolved during the measurement interval in equation 3F.3
<i>c</i>	response concentration of CO ₂ as measured by the NDIR analyzer in equation 3F.1
$(\text{CO}_2)_B$	average cumulative mass of CO ₂ evolved from the blank in equation 3F.7
$(\text{CO}_2)_T$	average cumulative mass of CO ₂ evolved from the sample in equation 3F.7
$[C]$	actual concentration of CO ₂ of each sample in equation 3F.1
$[C]_n$	concentration of CO ₂ at time t_n in equation 3F.4
$[C]_{n-1}$	concentration of CO ₂ at time t_{n-1} in equation 3F.4
$C(\text{CO}_2)$	cumulative mass of CO ₂ in equation 3F.5

$C(\text{CO}_2)_H$	cumulative mass of CO_2 at time t_H in equation 3F.6
$C(\text{CO}_2)_L$	cumulative mass of CO_2 at time t_L in equation 3F.6
$C(\text{CO}_2)_{n-1}$	cumulative mass of CO_2 until time t_{n-1} in equation 3F.5
C/N	carbon-nitrogen ratio
CA	cellulose acetate
CAB	cellulose acetate butyrate
CCD	charge-coupled device
CD	complete disintegration
CE	compost extract
CFA	chemical foaming agent
CHN	elemental analysis
CMR	cumulative measurement respirometry
CNT	carbon nanotube
CP	cellulose powder
CS	cassava starch
C_{TOT}	proportion of total organic carbon in the total mass of test material in equation 3F.7
DAS	data acquisition system
DFS	direct fuel substitution
D-LA	D-Lactic acid
DMR	direct measurement respirometry
DNA	deoxyribonucleic acid
DS	dry solids
DSC	differential scanning calorimetry
$E(\text{CO}_2)$	mass of evolved carbon dioxide in equation 3F.3

$E(\text{CO}_2)_n$	mass of CO ₂ evolved from the sample at time t_n in equation 3F.5
E_{act}	average energy of activation
EFP	environmental footprint
EG	ethylene glycol
EGMA	poly(ethylene-glycidyl methacrylate)
EIS	electrochemical impedance spectroscopy
EPA	Environmental Protection Agency
EPS	exopolymeric substances
Eq.	equation
eq.	equivalent
ESIMS	electrospray ionization-mass spectrometry
ESR	electron spin resonance
EU	European Union
EVA	ethylene vinyl acetate
EVOH	ethylene vinyl alcohol
F	air flow rate in equation 3F.3
FDA	Food and Drug Administration
GC	gas chromatography
GC	glycerol
GHG	greenhouse gas
GMR	gravimetric measurement respirometry
GPC	gel permeation chromatography
GRAS	generally recognized as safe
GWP	global warming potential

HA	hydroxyapatite
HDPE	high-density polyethylene
HDT	heat deflection temperature
HHV	higher heating values
HNT	halloysite nanotubes
HPLC	high-performance liquid chromatography
HRC	hydrogen release compound
$I(\text{CO}_2)$	interpolated cumulative mass of CO_2 at time t_i in equation 3F.6
IC	industrial composting
IR	infrared
ISBM	injection stretch blow molding
ISO	International Organization for Standardization
IV	inoculated vermiculite
k	rate constant
k	calibration factor in equation 3F.1
L/D	ratio of flight length of the screw to its outer diameter
LA	lactic acid
LCA	life cycle assessment
LDPE	low-density polyethylene
LF	landfilling
L-LA	L-Lactic acid
LLDPE	linear low-density polyethylene
LRD	Laponite® RD
MA	malonic acid

MA	maleic anhydride
MCC	microcrystalline cellulose
MD	machine direction
MFC	mass flow controller
MFI	melt flow index
MFR	melt flow rate
MIC	minimum inhibitory concentration
% Mineralization	percent carbon molecules converted to CO ₂ in equation 3F.7
MMT	montmorillonite
M_n	number average molecular weight
M_{n0}	initial number average molecular weight
MR	mechanical recycling
MSU	Michigan State University
MSW	municipal solid waste
MSWI	municipal solid waste incineration
M_{TOT}	mass of test material in equation 3F.7
M_w	weight average molecular weight
MWCNT	multi-wall carbon nanotube
MWD	molecular weight distribution
NAPCOR	National Association for PET Container Resources
NCBI	National Center for Biotechnology Information
NCI	non-inhibitory concentration
NDIR	non-dispersive infrared gas analyzer
OM	organic matter

OMMT	organo-modified montmorillonite
PA	polyamide
PA	<i>Pseudomonas aeruginosa</i>
PAE	polyamide elastomer
PBAT	poly(butylene adipate-co-terephthalate)
PBS	polybutylene succinate
PBSA	poly(butylene succinate-co-adipate)
PBSL	poly(butylene succinate-co-L-lactate)
PC	polycarbonate
PCDI	polycarbodiimide
PCL	poly(ϵ -caprolactone)
PCR	post-consumer recycled
PDI	polydispersity index
PDLA	poly(D-lactic acid)
PDLLA	poly(D,L-lactic acid)
PE	polyethylene
PEG	poly(ethylene glycol)
PENNR	primary energy from nonrenewable resources
PEO	poly(ethylene oxide)
PET	poly(ethylene terephthalate)
PEVA	poly(ethylene-co-vinyl acetate)
PFA	physical foaming agent
PGA	polyglycolic acid
PGS	poly(glycerol sebacate)
pH	potential of hydrogen

PHAs	poly(hydroxyalkanoates)
PHB	poly(hydroxybutyrate)
PHBHxx	poly[(3-hydroxybutyrate)-co-(3-hydroxyhexanoate)]
PHBV	poly(3-hydroxybutyrate-co-3-hydroxyvalerate)
PI	polydispersity index
PIP	poly(<i>cis</i> -1,4-isoprene)
PLA	poly(lactic acid)
PLLA	poly(L-lactic acid)
PP	polypropylene
PPC	poly(propylene carbonate)
ppm	parts per million
PS	polystyrene
PTAT	poly(tetramethylene adipate-co-terephthalate)
PTFE	polytetrafluoroethylene
PTT	poly(trimethylene terephthalate)
PU	poly(ether)urethane
PVC	polyvinyl chloride
PVOH	polyvinyl alcohol
QAC	Tomamine™ (methyl, tallow, bis-2-hydroxyethyl, quaternary ammonium)
R2B	R2 broth
RDP	Ribosomal Database Project
RH	relative humidity
RIC	resin identification code
ROP	ring-opening polymerization

rRNA	ribosomal ribonucleic acid
RTSF	Research Technology Support Facility
SA	succinic acid
sccm	standard cubic centimeters per minute
SCE	sterile compost extract
SCORIM	shear-controlled orientation in injection molding
SEC	size exclusion chromatography
SEM	scanning electron microscopy
SF	silk fibroin
SIC	solvent induced crystallization
SoP	School of Packaging
SPC	soy protein concentrate
SPI	soy protein isolate
STP	standard temperature and pressure
t	time
T	measurement interval in equation 3F.3
TCD	thermal conductivity detector
T_d	decomposition temperature
$T_{d,0}$	initial decomposition temperature
$T_{d,1/2}$	half decomposition temperature
TEM	transmission electron microscopy
T_g	glass transition temperature
TGA	thermal gravimetric analysis
t_H	immediate higher value of the time interval in equation 3F.6

THF	tetrahydrofuran
t_i	time at which the measurement was taken
t_l	time interval in equation 3F.6
TKGM	thermoplastic konjac glucomannan
t_L	immediate lower value of the time interval in equation 3F.6
T_m	melting temperature
T_{mc}	melt crystallization temperature
t_n	time at which each measurement was done in equation 3F.2
t_{n-1}	time in which the previous measurement was done in equation 3F.4
TNPP	tris(nonylphenyl) phosphite
TOC	total organic carbon
TPDAS	thermoplastic dialdehyde starch
TPO	thermoplastic polyolefin elastomer
TPS	thermoplastic starch
T-RFLP	terminal restriction fragment length polymorphism
t_{sn}	time stamp at time t_n in equation 3F.2
t_{so}	time stamp at time to corresponding to the time at which the experiment started in equation 3F.2
t_T	total time of the test
US	United States
USA	United States of America
UV	ultraviolet light/radiation
V	volume

V	uninoculated vermiculite
V_c	molar volume of semicrystalline polymer
V_g	molar volume of glassy amorphous
VS	volatile solids
V_w	Van der Waals volume
wt.	weight
$\%X_c$	percentage crystallinity
XRD	X-ray diffraction
Z	impedance
ΔH_m	enthalpy
δ_p	solubility parameter

CHAPTER 1

INTRODUCTION

1.0 Background and motivation

Plastics represent 12.9% of the 258 million tons of municipal solid waste (MSW) generated in the United States in 2014, from which only 9.5% was recovered, mostly polyethylene (PE) and polyethylene terephthalate (PET). Hence, most plastic waste (25.1 million tons) ended up accumulating in landfills, creating a major environmental concern and representing a missing environmental opportunity to reduce greenhouse gases emissions [1].

Biodegradable polymers like poly(lactic acid) (PLA), poly(butylene adipate-co-terephthalate) (PBAT), and thermoplastic starch (TPS) represent a promising way to divert plastic waste from landfills, with composting as an alternative disposal route, and to replace conventional fossil-based plastics for some applications, especially in cases where the plastic waste is highly contaminated and/or difficult to recover through recycling [2].

Disposable products like packaging would greatly benefit from the biodegradable features of these materials, but such benefit is only realized if biodegradable products are disposed in an appropriate waste management system. Ideally, biodegradable plastics could be treated together with other organic wastes in composting facilities and produce compost, a valuable soil conditioner and fertilizer [3].

In the last two decades, there has been extensive research focusing on ways to overcome some of the performance limitations of biodegradable and bio-based plastics, and to expand their applications. Polymer bio-nanocomposites (BNCs) have gained

great attention for developing new materials with improved and/or tailored performance properties. One particularly useful class of inorganic layered materials that has been used to produce bio-nanocomposites is inorganic layered silicate minerals, or nanoclays, due to their availability, low cost, significant enhancements and relative simple processability [4].

Natural nanoclays, such as montmorillonite (MMT), and synthetic nanoclays, such as Laponite® RD (LRD) and halloysite nanotubes (HNT), offer a unique route for enhancing the mechanical, physical and barrier properties of polymers like PLA at low levels of loading (<5% wt.), especially when the nanoclay particles are well dispersed in the polymer matrix [5,6]. For example, organically-modified montmorillonite (OMMT), has already been proven to be an effective nanofiller to improve properties of biodegradable materials [4,6,7].

Some researchers reported that PLA-OMMT bio-nanocomposites have improved storage modulus, flexural, and tensile modulus, flexural strength, and elongation at break when compared to pristine PLA [8–10]. Similarly, PLA-HNT bio-nanocomposites have exhibited improvement in properties like tensile strength, Young and storage modulus, impact and flexural properties [11–14]. PLA-LRD bio-nanocomposites have also shown improvement in thermal stability, tensile strength and hydrophilicity [15–17].

Besides performance limitations, one of the drawbacks of some biodegradable polymers, like PLA, is that they do not biodegrade as fast as other organic wastes during composting, which in turn affects their general acceptance in industrial composting facilities [18]. Therefore, increasing their biodegradation rate in the

composting environment should facilitate and encourage their disposal through these facilities by degrading in a time frame comparable with other organic materials.

Several researchers studied the effect of OMMT on the biodegradation of biodegradable polymers like polycaprolactone (PCL) [19], poly(3-hydroxybutyrate-co-3-hydroxyvalerate) (PHBV) [20], TPS [21], and PLA [10,18,22–30]. Their results indicated that, in general, these BNCs biodegraded faster than their respective pristine polymer. Therefore, the incorporation of nanoclays into a biodegradable polymer matrix represents a promising approach not only for enhancing the polymer performance but also for increasing its biodegradation rate in composting conditions.

However, the effect of different nanoclays and organo-modifiers, on the abiotic and biotic degradation of PLA is still unclear and needs further investigation. Even though it is well known that the biodegradation mechanism of PLA involves chemical hydrolysis, the role of microorganisms and how they are affected by the presence of nanoparticles is still not well understood [29].

Bioaugmentation is another promising technique that can be studied to accelerate the biodegradation of compostable plastics. Some researchers have identified most of the microbial consortia present in the compost environment [31–33], and some have reported the isolation and identification of several species capable of biodegrading PLA [34–42], and other polymers [43–51] by 16S ribosomal ribonucleic acid (rRNA) sequence analysis. These isolated microbial strains can be potentially used to investigate the effect of bioaugmentation in the biodegradation rate of PLA and PLA bio-nanocomposites.

Thus, this study seeks to understand the biodegradation mechanisms of bio-nanocomposites made of PLA and the main factors contributing to their biodegradation rate such as those related to the polymer structure and also those related to the soil/compost environments or to the microbial populations that could be impacted by the presence of nanoparticles.

1.1 Overall goal and objectives

The overall goal of this research is to obtain fundamental knowledge and unique understanding about the biodegradation mechanisms of PLA, to evaluate the biodegradation rate of PLA in simulated composting conditions, and to propose and to test different mechanisms able to accelerate and/or to tailor this process, which could greatly benefit the general use of PLA and its acceptance in industrial composting facilities.

As consequence, if more solid wastes can be disposed through composting, the amount of waste reaching landfills could be reduced along with the social and environmental impacts associated with landfilling, for example soil and water contamination and generation of greenhouse gases like methane.

To accomplish the overall goal, PLA and three different nanoclays (OMMT, LRD, and HNT) will be used in this study as model systems for testing biodegradation in simulated composting conditions. The following specific objectives have been outlined:

Objective 1: To evaluate the effect of nanoclays on the aerobic biodegradation and biodegradation rate of PLA in composting conditions and their impact on the microbial community of the compost.

Some researchers have reported an accelerated degradation of PLA after addition of nanoclays. Therefore, the biodegradation rate of pristine PLA and PLA bio-nanocomposites (PLA-OMMT, PLA-LRD, PLA-HNT) will be evaluated in composting conditions. This objective should provide the necessary evidence to understand if the presence of nanoclay modifies the biodegradation rate of polymers like PLA.

Objective 2: To evaluate the effect of introducing microbial strains capable of degrading PLA during the composting process on the biodegradation rate of PLA and PLA bio-nanocomposites.

Preliminary studies indicate that certain microbial strains are capable of assimilating PLA. Therefore, the biodegradation rate of PLA and PLA-OMMT is evaluated in composting conditions with bioaugmentation, meaning that an isolated microbial strain capable of degrading PLA is introduced in the composting system. This objective provides the necessary evidence to understand if the addition of these microorganisms into the bioreactors helps increasing the biodegradation rate of PLA in solid environments like compost. This approach also allows to further understand the abiotic and biotic contributions on the biodegradation process.

1.2 Dissertation overview

To answer the objectives of this dissertation, this document is organized as follows: Chapter 2 provides an extensive literature review on PLA, including resin production, processing techniques, properties and applications. This chapter also covers the main degradation reactions, the different end-of-life scenarios, and the environmental footprint of PLA.

Chapter 3 provides a critical literature review about the biodegradation testing of polymers by analysis of evolved carbon dioxide in simulated composting conditions. This chapter not only provides insights on the biodegradation testing but also experiment-relevant information about the biodegradation mechanisms and the different abiotic and biotic factors controlling the biodegradation rate of PLA.

Chapter 4 is a version of a published article that first provides a critical review on PLA bio-nanocomposites and then presents the results about the impact of nanoclays on the biodegradation of PLA and BNCs in simulated composting conditions. This chapter also presents the results of a biofilm formation assay and scanning electron microscopy that were used to evaluate the effect of nanoclays on the microbial attachment on the surface of PLA and BNCs.

Chapter 5 investigates bioaugmentation, in which PLA-degrading bacteria were isolated from compost and identified as *Geobacillus* using 16S rRNA gene sequencing. These isolates were further used to study the effect of bioaugmentation on the biodegradation rate of PLA and BNCs in solid environments. This chapter also presents the results of a biofilm formation assay performed to assess the *Geobacillus* attachment on the surface of PLA and BNCs.

Chapter 6 summarizes all the work in this dissertation and concludes with future work recommendations.

REFERENCES

REFERENCES

- [1] EPA, Advancing Sustainable Materials Management: 2014 Tables and Figures, (2016) 1–65.
- [2] E. Castro-Aguirre, F. Iñiguez-Franco, H. Samsudin, X. Fang, R. Auras, Poly(lactic acid)—Mass production, processing, industrial applications, and end of life, *Adv. Drug Deliv. Rev.* 107 (2016) 333–366. doi:10.1016/j.addr.2016.03.010.
- [3] T. Kijchavengkul, R. Auras, Compostability of polymers, *Polym. Int.* 57 (2008) 793–804. doi:10.1002/pi.2420.
- [4] H.M.C. De Azeredo, Nanocomposites for food packaging applications, *Food Res. Int.* 42 (2009) 1240–1253. doi:10.1016/j.foodres.2009.03.019.
- [5] D.A.P. De Abreu, P.P. Losada, I. Angulo, J.M. Cruz, Development of new polyolefin films with nanoclays for application in food packaging, *Eur. Polym. J.* 43 (2007) 2229–2243. doi:10.1016/j.eurpolymj.2007.01.021.
- [6] J.M. Lagaron, Nanotechnology for bioplastics: opportunities , challenges and strategies, *Trends Food Sci. Technol.* 22 (2011) 611–617. doi:10.1016/j.tifs.2011.01.007.
- [7] M. Murariu, P. Dubois, PLA composites: From production to properties, *Adv. Drug Deliv. Rev.* (2016). doi:10.1016/j.addr.2016.04.003.
- [8] S.S. Ray, P. Maiti, M. Okamoto, K. Yamada, K. Ueda, New Polylactide/ Layered Silicate Nanocomposites. 1. Preparation, Characterization, and Properties, *Macromolecules.* 35 (2002) 3104–3110.
- [9] S.S. Ray, K. Yamada, M. Okamoto, K. Ueda, New polylactide-layered silicate nanocomposites. 2. Concurrent improvements of material properties, biodegradability and melt rheology, *Polymer (Guildf).* 44 (2003) 857–866.
- [10] S.S. Ray, K. Yamada, M. Okamoto, A. Ogami, K. Ueda, New polylactide/ layered silicate nanocomposites, 4. Structure, properties and biodegradability, *Compos. Interfaces.* 10 (2003) 435–450. doi:10.1163/156855403771953687.
- [11] M. Murariu, A.-L. Dechief, Y. Paint, S. Peeterbroeck, L. Bonnaud, P. Dubois, Polylactide (PLA)— Halloysite Nanocomposites: Production , Morphology and Key-Properties, *J. Polym. Environ.* 20 (2012) 932–943. doi:10.1007/s10924-012-0488-4.
- [12] K. Prashantha, B. Lecouvet, M. Sclavons, M.F. Lacrampe, P. Krawczak, Poly (lactic acid)/ Halloysite Nanotubes Nanocomposites: Structure, Thermal, and Mechanical Properties as a Function of Halloysite Treatment, *J. Appl. Polym. Sci.*

- (2013) 1895–1903. doi:10.1002/app.38358.
- [13] W. Wu, X. Cao, Y. Zhang, G. He, Poly lactide/ Halloysite Nanotube Nanocomposites: Thermal , Mechanical Properties, and Foam Processing, *J. Appl. Polym. Sci.* (2013) 443–452. doi:10.1002/app.39179.
- [14] Y. Chen, L.M. Geever, J.A. Killion, J.G. Lyons, C.L. Higginbotham, D.M. Devine, Halloysite Nanotube Reinforced Polylactic Acid Composite, (2015) 1–8. doi:10.1002/pc.
- [15] G.X. Zhou, M.W. Yuan, L. Jiang, M.L. Yuan, H.L. Li, The Preparation and Property Research on Laponite-Poly (L-Lactide) Composite Film, *Adv. Mater. Res.* 750 (2013) 1919–1923.
- [16] H.L. Li, G.X. Zhou, Y.K. Shan, M.L. Yuan, The Mechanical Properties and Hydrophilicity of Poly (L-Lactide)/Laponite Composite Film, *Adv. Mater. Res.* 706 (2013) 340–343.
- [17] X. Tang, S. Alavi, Structure and Physical Properties of Starch/Poly Vinyl Alcohol/ Laponite RD Nanocomposite Films, *J. Agric. Food Chem.* 60 (2012) 1954–1962.
- [18] P. Stloukal, S. Pekařová, A. Kalendova, H. Mattausch, S. Laske, C. Holzer, L. Chitu, S. Bodner, G. Maier, M. Slouf, M. Koutny, Kinetics and mechanism of the biodegradation of PLA/clay nanocomposites during thermophilic phase of composting process, *Waste Manag.* 42 (2015) 31–40. doi:10.1016/j.wasman.2015.04.006.
- [19] T. Wu, T. Xie, G. Yang, Preparation and characterization of poly (ϵ -caprolactone)/ Na + -MMT nanocomposites, *Appl. Clay Sci.* 45 (2009) 105–110. doi:10.1016/j.clay.2009.02.009.
- [20] M.C.S. Correa, M.C. Branciforti, E. Pollet, J.A.M. Agnelli, P.A.P. Nascente, L. Averous, Elaboration and Characterization of Nano-Biocomposites Based on Plasticized Poly (Hydroxybutyrate-Co-Hydroxyvalerate) with Organo-Modified Montmorillonite, *J. Polym. Environ.* 20 (2012) 283–290. doi:10.1007/s10924-011-0379-0.
- [21] N.F. Magalhães, C.T. Andrade, Thermoplastic corn starch/ clay hybrids: Effect of clay type and content on physical properties, *Carbohydr. Polym.* 75 (2009) 712–718. doi:10.1016/j.carbpol.2008.09.020.
- [22] S.-R. Lee, H. Park, H. Lim, T. Kang, X. Li, W.-J. Cho, C.-S. Ha, Microstructure, tensile properties, and biodegradability of aliphatic polyester/ clay nanocomposites, *Polymer (Guildf)*. 43 (2002) 2495–2500.
- [23] M.A. Paul, C. Delcourt, M. Alexandre, P. Degee, F. Monteverde, P. Dubois, Poly lactide/ montmorillonite nanocomposites: study of the hydrolytic degradation, *Polym. Degrad. Stab.* 87 (2005) 535–542.

doi:10.1016/j.polymdegradstab.2004.10.011.

- [24] Y.H. Lee, J.H. Lee, I. An, C. Kim, D.S. Lee, Y.K. Lee, J. Nam, Electrospun dual-porosity structure and biodegradation morphology of Montmorillonite reinforced PLLA nanocomposite scaffolds, *Biomaterials*. 26 (2005) 3165–3172. doi:10.1016/j.biomaterials.2004.08.018.
- [25] K. Fukushima, C. Abbate, D. Tabuani, M. Gennari, G. Camino, Biodegradation of poly (lactic acid) and its nanocomposites, *Polym. Degrad. Stab.* 94 (2009) 1646–1655. doi:10.1016/j.polymdegradstab.2009.07.001.
- [26] P.K. Roy, M. Hakkarainen, A. Albertsson, Nanoclay effects on the degradation process and product patterns of polylactide, *Polym. Degrad. Stab.* 97 (2012) 1254–1260. doi:10.1016/j.polymdegradstab.2012.05.032.
- [27] S. Molinaro, M.C. Romero, M. Boaro, A. Sensidoni, C. Lagazio, M. Morris, J. Kerry, Effect of nanoclay-type and PLA optical purity on the characteristics of PLA-based nanocomposite films, *J. Food Eng.* 117 (2013) 113–123. doi:10.1016/j.jfoodeng.2013.01.021.
- [28] P.M.S. Souza, A.R. Morales, M.A. Marin-Morales, L.H.I. Mei, PLA and Montmorillonite Nanocomposites: Properties , Biodegradation and Potential Toxicity, *J. Polym. Environ.* 21 (2013) 738–759. doi:10.1007/s10924-013-0577-z.
- [29] A. V. Machado, A. Araújo, M. Oliveira, Assessment of polymer-based nanocomposites biodegradability, (2014).
- [30] M.P. Balaguer, C. Aliaga, C. Fito, M. Hortal, Compostability assessment of nano-reinforced poly(lactic acid) films, *Waste Manag.* 48 (2016) 143–155. doi:10.1016/j.wasman.2015.10.030.
- [31] M. Kumar, A. Kumar, J. Khan, P. Singh, J.W.C. Wong, A. Selvam, Evaluation of thermophilic fungal consortium for organic municipal solid waste composting, *Bioresour. Technol.* 168 (2014) 214–221. doi:10.1016/j.biortech.2014.01.048.
- [32] C. Song, M. Li, X. Jia, Z. Wei, Y. Zhao, B. Xi, C. Zhu, D. Liu, Comparison of bacterial community structure and dynamics during the thermophilic composting of different types of solid wastes: anaerobic digestion residue, pig manure and chicken manure, *Microb. Biotechnol.* 7 (2014) 424–433. doi:10.1111/1751-7915.12131.
- [33] D. Liu, M. Li, B. Xi, Z. Wei, C. Song, C. Zhu, Metaproteomics reveals major microbial players and their biodegradation functions in a large-scale aerobic composting plant, *Microb. Biotechnol.* 8 (2015) 950–960. doi:10.1111/1751-7915.12290.
- [34] M.N. Kim, W.G. Kim, H.Y. Weon, S.H. Lee, Poly (L-lactide)-Degrading Activity of a Newly Isolated Bacterium, *J. Appl. Polym. Sci.* 109 (2008) 234–239.

doi:10.1002/app.26658.

- [35] M.N. Kim, S.T. Park, Degradation of Poly (L -lactide) by a Mesophilic Bacterium, *J. Appl. Polym. Sci.* 117 (2010) 67–74. doi:10.1002/app.31950.
- [36] M. Karamanlioglu, A. Houlden, G.D. Robson, Isolation and characterisation of fungal communities associated with degradation and growth on the surface of poly (lactic) acid (PLA) in soil and compost, *Int. Biodeterior. Biodegradation.* 95 (2014) 301–310. doi:10.1016/j.ibiod.2014.09.006.
- [37] T. Apinya, N. Sombatsompop, B. Prapagdee, Selection of a *Pseudonocardia* sp . RM423 that accelerates the biodegradation of poly (lactic) acid in submerged cultures and in soil microcosms, *Int. Biodeterior. Biodegradation.* 99 (2015) 23–30. doi:10.1016/j.ibiod.2015.01.001.
- [38] S. Sukkhum, S. Tokuyama, T. Tamura, V. Kitpreechavanich, A novel poly (L-lactide) degrading actinomycetes isolated from Thai forest soil , phylogenic relationship and the enzyme characterization, *J. Gen. Appl. Microbiol.* 55 (2009) 459–467. doi:10.2323/jgam.55.459.
- [39] N.R. Nair, V.C. Sekhar, K.M. Nampoothiri, Augmentation of a Microbial Consortium for Enhanced Polylactide (PLA) Degradation, *Indian J. Microbiol.* 56 (2016) 59–63. doi:10.1007/s12088-015-0559-z.
- [40] K. Tomita, H. Tsuji, T. Nakajima, Y. Kikuchi, Degradation of poly (D-lactic acid) by a thermophile, *Polym. Degrad. Stab.* 81 (2003) 167–171. doi:10.1016/S0141-3910(03)00086-7.
- [41] K. Tomita, T. Nakajima, Y. Kikuchi, N. Miwa, Degradation of poly (L -lactic acid) by a newly isolated thermophile, *Polym. Degrad. Stab.* 84 (2004) 433–438. doi:10.1016/j.polymdegradstab.2003.12.006.
- [42] E. Castro-Aguirre, R. Auras, M. Rubino, S.E. Selke, T. Marsh, Effect of Montmorillonite and Organo-modifier on the Aerobic Biodegradation of Poly(lactic acid) Bio-nanocomposites in composting conditions, in: 31st Polym. Degrad. Discuss. Gr. Conf., 2015.
- [43] S. Boonchan, M.L. Britz, G.A. Stanley, Degradation and Mineralization of High-Molecular-Weight Polycyclic Aromatic Hydrocarbons by Defined Fungal-Bacterial Cocultures, *Appl. Environ. Microbiol.* 66 (2000) 1007–1019. doi:10.1128/AEM.66.3.1007-1019.2000.
- [44] Z. Saadi, A. Rasmont, G. Cesar, Fungal Degradation of Poly (L-lactide) in Soil and in Compost, *J. Polym. Environ.* 20 (2012) 273–282. doi:10.1007/s10924-011-0399-9.
- [45] T. Teeraphatpornchai, M. Nakayama, Isolation and characterization of a bacterium that degrades various polyester-based biodegradable plastics,

Biotechnol. Lett. 25 (2003) 23–28. doi:10.1023/A:1021713711160.

- [46] N. Hayase, H. Yano, E.M.I. Kudoh, C. Tsutsumi, K. Ushio, Y. Miyahara, S. Tanaka, Isolation and Characterization of Poly (Butylene Succinate-co-Butylene Adipate) -Degrading Microorganism, *J. Biosci. Bioeng.* 97 (2004) 131–133. doi:10.1016/S1389-1723(04)70180-2.
- [47] K. Tomita, N. Hayashi, N. Ikeda, Y. Kikuchi, Isolation of a thermophilic bacterium degrading some nylons, *Polym. Degrad. Stab.* 81 (2003) 511–514. doi:10.1016/S0141-3910(03)00151-4.
- [48] K. Tomita, K. Kojoh, A. Suzuki, Isolation of Thermophiles Assimilating Poly (Ethylene-co-Vinyl Alcohol), *J. Ferment. Bioeng.* 84 (1997) 400–402. doi:10.1016/S0922-338X(97)81998-8.
- [49] M.N. Kim, M.G. Yoon, Isolation of strains degrading poly (Vinyl alcohol) at high temperatures and their biodegradation ability, *Polym. Degrad. Stab.* 95 (2010) 89–93. doi:10.1016/j.polymdegradstab.2009.09.014.
- [50] A. Esmaeili, A.A. Pourbabaee, H.A. Alikhani, F. Shabani, E. Esmaeili, Biodegradation of Low-Density Polyethylene (LDPE) by Mixed Culture of *Lysinibacillus xylanilyticus* and *Aspergillus niger* in Soil, *PLoS One.* 8 (2013) 1–10. doi:10.1371/journal.pone.0071720.
- [51] F. Muroi, Y. Tachibana, Y. Kobayashi, T. Sakurai, K. Kasuya, Influences of poly(butylene adipate- co -terephthalate) on soil microbiota and plant growth, *Polym. Degrad. Stab.* 129 (2016) 338–346. doi:10.1016/j.polymdegradstab.2016.05.018.

CHAPTER 2

POLY(LACTIC ACID) – MASS PRODUCTION, PROCESSING, INDUSTRIAL APPLICATIONS, AND END OF LIFE

A version of this chapter is published as:

Castro-Aguirre, E., Iniguez-Franco, F., Samsudin, H., Fang, X., Auras, R. Poly(lactic acid) – Mass production, processing, industrial applications, and end of life, *Advanced Drug Delivery Reviews Journal*, 107 (2016) 333 – 366.

2.0 Abstract

Global awareness of material sustainability has increased the demand for bio-based polymers like poly(lactic acid) (PLA), which are seen as a desirable alternative to fossil-based polymers because they have less environmental impact. PLA is an aliphatic polyester, primarily produced by industrial polycondensation of lactic acid and/or ring-opening polymerization of lactide. Melt processing is the main technique used for mass production of PLA products for the medical, textile, plasticulture, and packaging industries. To fulfill additional desirable product properties and extend product use, PLA has been blended with other resins or compounded with different fillers such as fibers, and micro and nanoparticles. This paper presents a review of the current status of PLA mass production, processing techniques and current applications, and also covers the methods to tailor PLA properties, the main PLA degradation reactions, PLA products' end-of-life scenarios and the environmental footprint of this unique polymer.

2.1 Introduction

Poly(lactic acid) (PLA) is a biodegradable and bio-based aliphatic polyester derived from renewable sources such as corn sugar, potato, and sugar cane. PLA has played a central role in replacing fossil-based polymers for certain applications [1, 2]. As a compostable polymer, PLA is considered a promising alternative to reduce the municipal solid waste (MSW) disposal problem by offering additional end-of-life scenarios [3]. High weight average molecular weight (M_w) PLA is generally produced by polycondensation and/or ring-opening polymerization (ROP) [4]. NatureWorks LLC is the major producer of PLA, with a capacity of 150,000 metric ton year in its U.S. manufacturing facility (in Blair, Nebraska) [2, 5]. Due to great market penetration,

worldwide attention, and the rise of PLA production [6], the number of published research studies and reports about PLA have exponentially increased in the last 25 years, as shown in **Figure 2.1**.

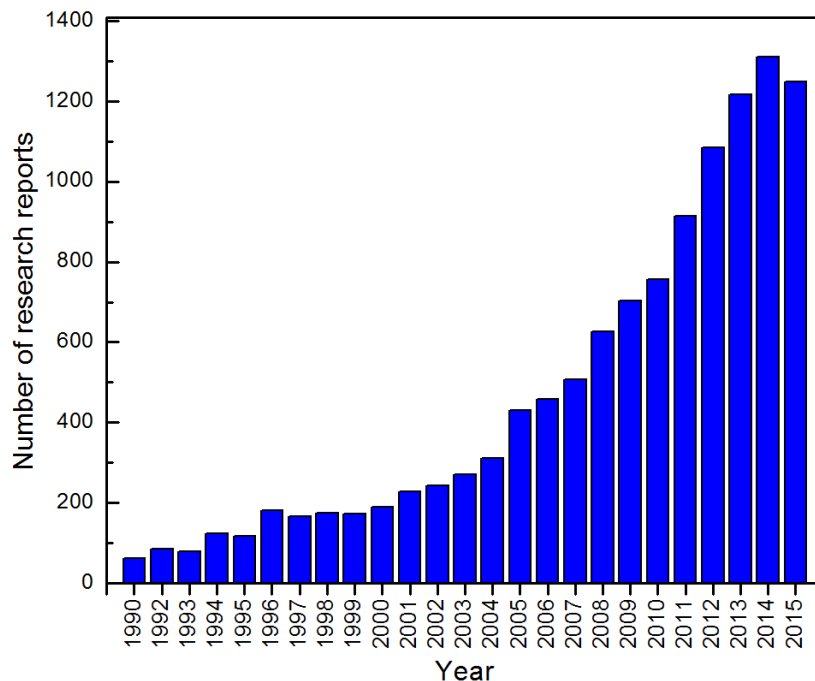


Figure 2.1 Number of research reports published since 1990 based on the Web of Science search using keywords "PLA", "PLLA", "PDLA", "polylactic acid", "polylactide", and "poly(lactic acid)" [7].

The use of PLA was initially limited to medical applications due to its high cost and low availability, but high M_w PLA now can be processed by injection molding, sheet and film extrusion, blow molding, foaming, fiber spinning, and thermoforming. Also, PLA provides comparable optical, mechanical, thermal, and barrier properties when compared with commercially available commodity polymers such as polypropylene (PP), poly(ethylene terephthalate) (PET), and polystyrene (PS), expanding its commercial range of applications [2, 5]. In the medical field, PLA is extensively used because of its biocompatibility with the human body, including for applications such as

medical implants, surgical sutures and medical devices [8-12]. In addition, PLA has been used for applications such as fibers, textiles, plasticulture, serviceware, packaging containers (*i.e.*, food packaging for short-life products), and environmental remediation films [13]. PLA is considered as a Generally Recognized as Safe (GRAS) material by the U.S. Food and Drug Administration (FDA). However, PLA has also some limitations (*e.g.*, poor toughness), so research efforts are centered on obtaining PLA products with particular desired properties by blending PLA with other biodegradable and non-biodegradable resins, and/or by compounding PLA with fillers such as fibers or micro and nanoparticles.

This critical review focuses on the status of PLA polymer regarding its mass production, the main processing techniques, and methods that have been used to extend PLA applications on the basis of its intrinsic properties. Furthermore, this review provides a panorama of the current main applications categorized according to PLA commercial usage, and an overview of different environments to which PLA products can be exposed during their lifetime that lead to their degradation, including hydrolysis in non-medical applications. Finally, the end-of-life scenarios of PLA products as well as the cradle-to-grave and cradle-to-cradle environmental footprint (EFP) are discussed.

2.2 PLA Resin Production

Lactic acid (LA), also named 2-hydroxy propionic acid, is the basic monomer of PLA. The monomer exists as two stereo isomers, L-LA and D-LA. **Figure 2.2** shows the different chemical structures of these two isomers [2].

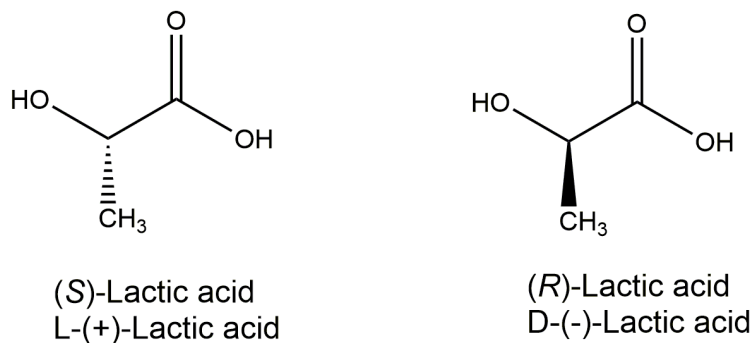


Figure 2.2 Chemical structure of L(+) and D(-) lactic acid.

The two main methods to produce LA are by bacterial fermentation of carbohydrates or by chemical synthesis [14]. Bacterial fermentation is the preferred industrial process used by NatureWorks LLC and Corbion®, the two major producers of PLA. Chemical synthesis has many limitations, including limited production capacity, inability to produce only the desired L-LA isomer, and high manufacturing costs [15].

The bacterial fermentation processes to produce LA can be classified as homofermentative or heterofermentative methods, depending on the bacteria used. In the heterofermentative method, 1 mole of hexose produces less than 1.8 moles of LA, along with significant levels of other metabolites such as acetic acid, ethanol, glycerol, mannitol, and carbon dioxide. However, in the homofermentative method, 1 mole of hexose can produce an average of 1.8 moles of LA, with minor levels of other metabolites, which means every 100 g of glucose could yield more than 90 g of LA. The homofermentative method is more frequently used by industry due to its greater production yields and lower levels of by-products in comparison with the heterofermentative method [16].

In the homofermentative method, species of the *Lactobacillus* genus, such as *L. delbrueckii*, *L. amylophilus*, *L. bulgaricus* and *L. leichmanii*, are used under conditions of

a pH range from 5.4 to 6.4, a temperature range from 38 to 42°C, and a low oxygen concentration. The nutrients used to feed the bacteria can be simple sugars, such as glucose and maltose from corn or potato or other sources such as vitamin-B, amino acids, and nucleotides provided by rich corn steep liquor. In general, batch production processes can yield 1 to 4.5 g.L⁻¹.h⁻¹ of LA, whereas continuous processes can achieve 3 to 9.0 g.L⁻¹.h⁻¹ of LA. On a larger scale, cell recycle reactors can produce up to 76 g.L⁻¹.h⁻¹ [16, 17]. After the initial production process, the LA must be purified by distillation if it will be used for pharmaceutical and food derivative purposes. NatureWorks LLC is currently using a lower pH process to produce LA, which reduces the amount of calcium hydroxide and sulfuric acid by-products, resulting in the lower production of calcium sulphate (gypsum) [5]. Corbion®, through a proprietary technology, produces LA in a gypsum-free process, which uses second generation feedstocks (*i.e.*, plant-based materials such as corn stover, bagasse, wheat straw, and wood chips) [18, 19].

LA can be used to produce PLA of variable molecular weights; however, usually only the high M_w PLA has major commercial value in the fiber, textile, plasticulture, and packaging industries. **Figure 2.3** shows the three main methods available to produce high M_w PLA from LA: (1) direct condensation polymerization; (2) direct polycondensation in an azeotropic solution; and (3) polymerization through lactide formation [17].

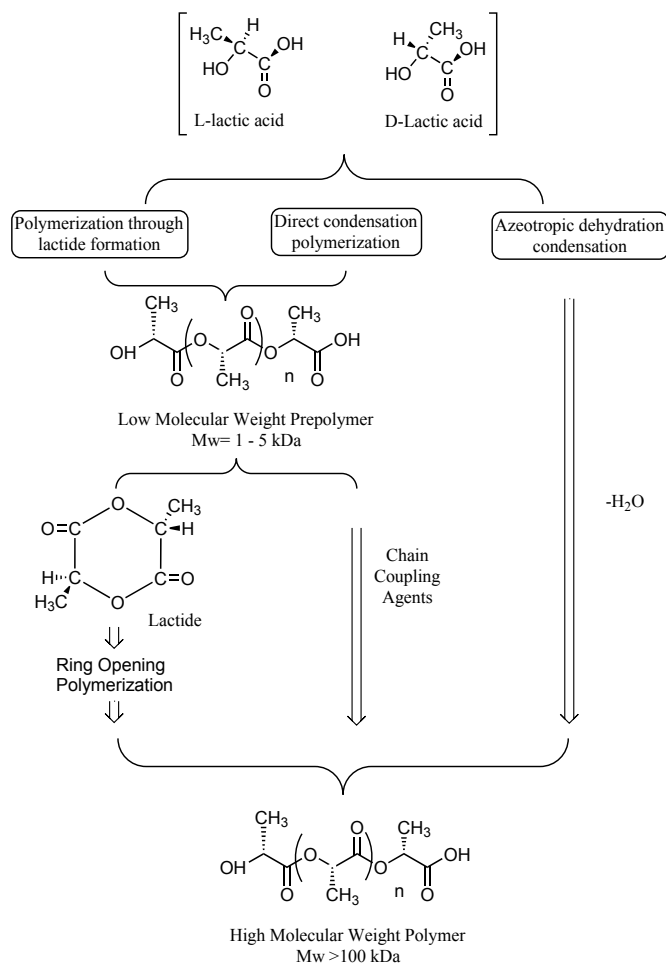


Figure 2.3 The manufacturing processes to produce high molecular weight PLA, adapted from Hartmann [17].

The direct condensation polymerization process involves three main steps: 1) free water removal, 2) oligomer polycondensation, and 3) melt polycondensation of high M_w PLA. A detailed description of this process can be found in Hartmann [17]. Direct condensation polymerization is generally considered the least expensive process to produce high M_w PLA. However, the necessity to use chain coupling agents and adjuvants to obtain a solvent-free PLA increases the costs of the products and the complexity of the process [14, 17, 20, 21].

Direct polycondensation in an azeotropic solution is the method applied by Mitsui Toatsu Chemicals, Inc. to produce high M_w PLA [22]. In the process, no chain extenders or adjuvants are used. The PLA is produced by a direct condensation while the condensation water is continuously removed by the azeotropic distillation. The process includes reduction of the distillation pressure of LA for 2–3 h at 130°C, and the majority of the condensation water is removed. Catalyst is added along with diphenyl ester. A tube packed with 3-Å molecular sieves is attached to the reaction vessel, and the solvent is returned to the vessel via the molecular sieves for an additional 30–40 h at 130°C. Finally, the polymer is isolated as is or it is dissolved and precipitated for further purification. The effect of different catalysts on the azeotropic dehydration of LA in diphenyl ether and additional details of the technique is reported elsewhere [17, 22].

NatureWorks LLC, the major producer of high M_w PLA based on the original Cargill-Dow patented process [23], combines a solvent-free process and a distillation process to produce PLA with controlled molecular weights in a multi-step process. The LA is first condensed to form low M_w prepolymer PLA. With controlled depolymerization, the cyclic dimer, also referred as lactide, is produced from the low M_w prepolymer PLA [24]. The lactide in the liquid form is purified by distillation. The PLA with controlled molecular weight is produced by the ring opening of lactide and then polymerization with catalyst [16, 17, 25, 26]. **Figure 2.4** shows the basic process design to produce high M_w PLA.

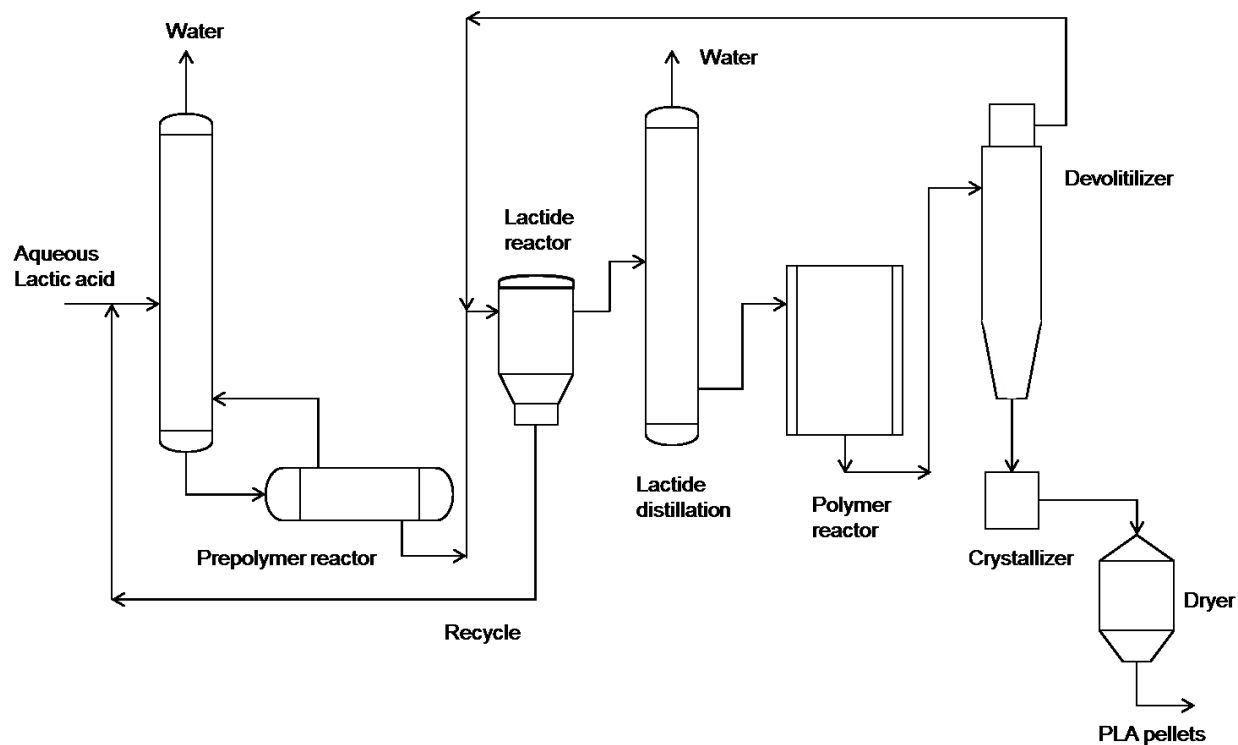


Figure 2.4 NatureWorks LLC commercial process for producing high molecular weight PLA, adapted from Auras *et al.* [2] and Vink *et al.* [5].

PLA produced from this process can be derived from different amounts of L- and D-lactide. The lactide reactor produces a combination of LA, LA oligomers, water, *meso*-lactide and impurities [18]. The mixture must be purified, in this case by vacuum distillation through a series of columns. Due to the difference in boiling points of lactide and *meso*-lactide (**Figure 2.5**), the highest M_w PLA is derived from L-lactide and a small amount of *meso*-lactide. The higher the stereochemical purity of the lactide mixture, the higher the stereochemical purity of the PLA. The NatureWorks LLC process results in a large amount of *meso*-lactide, so the properties of the PLA resin obtained through this process can vary according to the amount of *meso*-lactide in the mix. PLA with a large amount of 93% L-LA can crystallize.

Commonly used methods to perform separation of *meso*-lactide from either (S,S)-lactide or (R,R)-lactide are fractional distillation, melt crystallization and solvent recrystallization [29]; however, these methods pose some difficulties in separating *meso*-lactide from other impurities. NatureWorks LLC has patented a process in which *meso*-lactide can be separated from crude lactide efficiently by means of an enriched stream of a minimum 0.8-mole-fraction of *meso*-lactide and forming a purified (S,S)- and (R,R)-lactide stream. Futerra S.A., a joint venture company between Galactic and Total Petrochemicals, has also patented a method to produce *meso*-lactide, D-lactide, and L-lactide by back biting depolymerization of PLA. The process starts by employing a controlled temperature (200–290°C) and a reduced pressure in a presence of catalyst and co-catalyst to depolymerize PLA into its dimeric cyclic esters form. The resultant PLA components are depolymerized into a vaporized form in a reaction zone. This vaporized form is then condensed and the *meso*-lactide, D-lactide, and L-lactide produced are recovered separately or together. This invention, which is regarded as the second generation of PLA, can produce D-lactide and *meso*-lactide with high throughput for the production of poly(D-lactic acid) (PDLA) or co-polymers consisting of L- and D-LA enantiomers without the need to start off with LA [30].

Extensive research has also been conducted to produce lactide and PLA via low manufacturing and production costs and with enhanced properties [31, 32]. Various catalysts, ranging from metal, cationic, and organic, have been used during polymerization of PLA to achieve high M_w and high optical purity [33]. Metal complexes are reported to be one of the most efficient catalysts for the production of stereoblock isotactic PLA via ROP of *rac*-lactide due to its ability to control parameters such as

molecular and chain microstructure [34]. Dusselier *et al.* [35] reported the production of lactide through a direct Brønsted acidic zeolite-based catalytic process, which obtains considerably larger lactide yields than with the controlled ROP of low M_w PLA. Yang *et al.* [34] investigated the production of PLA by *rac*-lactide using monoanionic aminophenolate ligands with metal complexes in the presence of solvents such as tetrahydrofuran and 2-propanol. Monomeric zinc silylamido complexes with acrylamine coordination ligands produced a low degree of heterotactic PLA, and similar complexes with alkylamine coordination ligands produced isotactic PLA. The stereoselectivity of the *rac*-lactide polymerization was affected by the pattern of the monoanionic aminophenolate ligands coordination. Moreover, complexes of tetrametallic lithium and sodium diamino-bis(phenolate) were investigated for their efficacy in the polymerization of *rac*-lactide, and these complexes were able to produce PLA with narrow M_w dispersities [36].

A recent study reported the use of a biodiesel fuel by-product, glycerol, to produce *rac*-lactide, a monomer for producing stereoblock PLA [37]. The method employed a hydrothermal reaction in the presence of alkaline catalyst to produce racemic lactide. The lactide was further purified by acidizing sodium lactate with sulfuric acid, and the resultant lactide was extracted with ethyl acetate to obtain refined lactide. A mixture of lactide isomers (crude lactide) containing both *rac*-lactide and *meso*-lactide were produced via dimerization of lactic acid (*i.e.*, reactive distillation at temperature of 210–230°C and a pressure of 5–10 mmHg). The levels of *rac*-lactide and *meso*-lactide in the crude lactide were reported to be 32.8 and 32.6%, respectively, with 34.6% impurities (*i.e.*, LA and oligomer). This crude lactide was then purified with ethyl acetate

in a N₂ atmospheric condition via three-time recrystallization to obtain a refined *rac*-lactide of 99.1% purity, with *meso*-lactide (0.2%) and other impurities (0.7%) [37].

Zhu and Chen [38] also reported a new approach to convert *meso*-lactide to *rac*-lactide. On the basis of the “frustrated Lewis pair” concept, this approach utilized the epimerization of *meso*-lactide to *rac*-lactide using 1,4-diazabicyclo [2.2.2] octane (DABCO)/ tris(pentafluorophenyl) borane 95% (B(C₆F₅)₃) at 2M in toluene, which resulted in 95.4% conversion. This study investigated different types of Lewis acids with different molar concentrations and different polar and non-polar solvents to find optimized conversion of *meso*-lactide to *rac*-lactide. The epimerization method used in this study is versatile since it was able to effectively convert lactide stereoisomers regardless of ratio into *rac*-lactide [38].

2.3 PLA Processing

The methods for processing PLA are well-established polymer-manufacturing techniques used for other commercial polymers such as PS and PET [39]. Melt processing is the main technique for mass production of high *M_w* PLA in which the PLA resin obtained (as shown in **Figure 2.4**) is converted into end products such as consumer goods, packaging, and other applications. Melt processing is characterized by heating the material above its melting temperature, shaping the molten polymer into desired shapes, and finally cooling to stabilize its final dimensions. Processing of PLA has been extensively reviewed [1, 40]. The main objectives of this section are to summarize the key methods used to process PLA and then to provide a short update of new research since our last review of PLA processing [1]. Additionally, we direct the

reader to a number of contributions that explain each processing technique in further detail.

The limiting factors for processing PLA are similar to those for fossil-based polymers: degradation at the upper limits of temperature and shear, and poor homogeneity at the lower limits [39]. However, understanding PLA's thermal, crystallinity, and melt rheological behaviors is critical to optimize its processing and component qualities. Detailed information about these properties is provided elsewhere [13]. PLA is a hygroscopic material and very sensitive to high relative humidity (RH) and temperature [39]. Before PLA can be processed, it should be dried to a water content less than 100 ppm (0.01%, w/w) to avoid hydrolysis (M_w reduction), as discussed in section 2.6.1. During industrial production, PLA is mostly dried to values below 250 ppm water (0.025%, w/w). If PLA is processed at temperatures higher than 240°C or with longer residence times, the PLA resin should be dried below 50 ppm water to avoid number average molecular weight (M_n) reduction [1, 41]. To achieve effective drying, the dew point of the drying air should be equal or lower than -40°C, with an airflow rate greater than 0.03 m³.h⁻¹.kg⁻¹ of resin throughput. After the PLA resin is properly dried, melt extrusion is the most important technique for continuous melt processing of high M_w PLA consumer goods.

2.3.1 Extrusion

Extrusion of PLA in a heated screw is the first step before any further processing of PLA, such as injection, thermoforming or spinning, takes place. Commercial PLA resins can be processed by using conventional screws equipped with a general-purpose screw of L/D ratio (ratio of flight length of the screw to its outer diameter) of 24 to 30. If PLA is

processed in extruders designed for polyolefins, and the extruder is working near to its maximum power, the extruder may not have enough torque to process PLA. So, it is recommended to process PLA in extruders regularly used for polyesters or PS, with similar performance profile. The recommended compression ratio (ratio of the flight depth in the feed section to the flight depth in the metering section) for PLA processing is in the range of 2 to 3. The extruder provides the heat to melt the resins by heater bands wrapped around the barrel; however, the majority of heat input is provided by the friction of the resin between the screw and the barrel. Thus, to ensure that all the crystalline domains of the semicrystalline PLA are melted, and to achieve an optimal melt viscosity for processing, the heaters are usually set at 40 to 50°C higher than the melting temperature (T_m). The melt rheological properties of PLA play an important role in how the polymer flows during extrusion. Melt viscosities of High M_w PLA melt viscosities are in the order of 5,000–10,000 P (500–1000 Pa.s) at shear rates of 10–50 s^{-1} ; these polymer grades are equivalent to M_w of ~100,000 Da for injection molding to ~300,000 Da for cast film extrusion applications [1]. Extruding PLA at high temperatures can cause thermal degradation (as explained in section 2.6.2), so the temperature profile during extrusion of PLA should be tightly controlled. The thermal degradation of PLA can be attributed to several factors: (a) hydrolysis by trace amounts of water; (b) zipper-like depolymerization; (c) oxidative, random main-chain scission; (d) intermolecular transesterification to monomer and oligomeric esters; and (e) intramolecular transesterification resulting in formation of monomer and oligomer lactides of low M_w [40]. Processing PLA above 200°C can degrade PLA through intra and intermolecular ester exchange, *cis*-elimination, and radical and concerted non-

radical reactions resulting in the production of CO, CO₂, acetaldehyde, and methyl ketone [42]. Depending on the rate of the degradation reaction, the end product can be lactide or acetaldehyde. Formation of lactide during extrusion can affect the optical purity of the final extruded PLA; reduce the melt viscosity; produce fuming of lactide (*i.e.*, lactide vapor produced during extrusion); and can condense on equipment surfaces, such as chilled rollers and molds, which is known as “plate out.” To avoid lactide fuming and condensation, the temperature of the surfaces should be increased. **Table 2.1** shows the recommended processing temperatures for a number of commercially available NatureWorks LLC PLA resins known as Ingeo™ PLA.

Table 2.1 Properties and processing temperatures of selected commercially available Ingeo™ PLA resins

	2500HP [43]	3001D [44]	4032D [45]	6060D [46]	7001D [47]	8052D [48]
Application	Extrusion - Crystalline sheets	Injection molding	Biaxially oriented films	Fiber melt spinning	Injection stretch blow molding	Foam
Specific gravity, ASTM D792	1.24	1.24	1.24*	1.24	1.24	1.24
MFR, g/10 min (210°C, 2.16 kg) ASTM D1238	8	22	N/A	8-10	6	14
Melt temperature, °C	210	200	210	N/A	200-220	200
Feed throat, °C	45	20	45	N/A	20	20
Feed temperature, °C	190	150/165**	180	N/A	180	165
Compression section, °C	200	195	190	N/A	210	195
Metering section, °C	210	205	200	N/A	210-220	205
Nozzle,	N/A	205	200	N/A	210-220	205
Adapter, °C	210	N/A	N/A	N/A	N/A	N/A
Die, °C	210	N/A	N/A	N/A	N/A	N/A
Mold, °C	N/A	25	200	N/A	21-38	25
Screw speed, rpm	20 - 150	100-175	20-100	N/A	N/A	100-175
Back pressure, MPa	N/A	0.345- 0.689	0.414- 0.483	N/A	0.689- 1.379	0.345- 0.689

Notes: * ASTM 1505, **150°C amorphous / 165°C crystalline. N/A: Not available

2.3.2 Injection molding

PLA is primarily injected on machines that have a reciprocating screw extruder, as shown in **Figure 2.6**. In this case, the screw is designed to reciprocate within the barrel to inject the molten polymer into the mold cavities. At the start, the molds close and the nozzle opens, and the screw moves forward, injecting the molten polymer into the mold cavity. Since the polymer shrinks during cooling, the screw is maintained in the injection position by holding pressure steady. Then, the nozzle is closed and the screw starts retracting. During the cooling cycle of the molds, the screw rotates and conveys the melt polymer forward; sufficient cooling time should be provided to produce stable parts. Cycle time of the injection part is extremely important to control shrinkage of the PLA injection-molded parts, which are generally brittle due to the accelerated physical aging of PLA, which is attributed to its low glass transition temperature (T_g). PLA parts produced with low M_n are subjected to faster aging. Likewise, PLA injection-molded parts could exhibit low crystallinity due to the slow crystallization rate of PLA. Furthermore, in order to avoid excessive shrinkage, processing parameters such as mold temperature, packing pressure, cooling rate, and post-mold cooling treatment should be properly controlled. A complete explanation of how to optimize the cycling time for PLA injection-molded parts and reduce shrinkage is provided elsewhere [1].

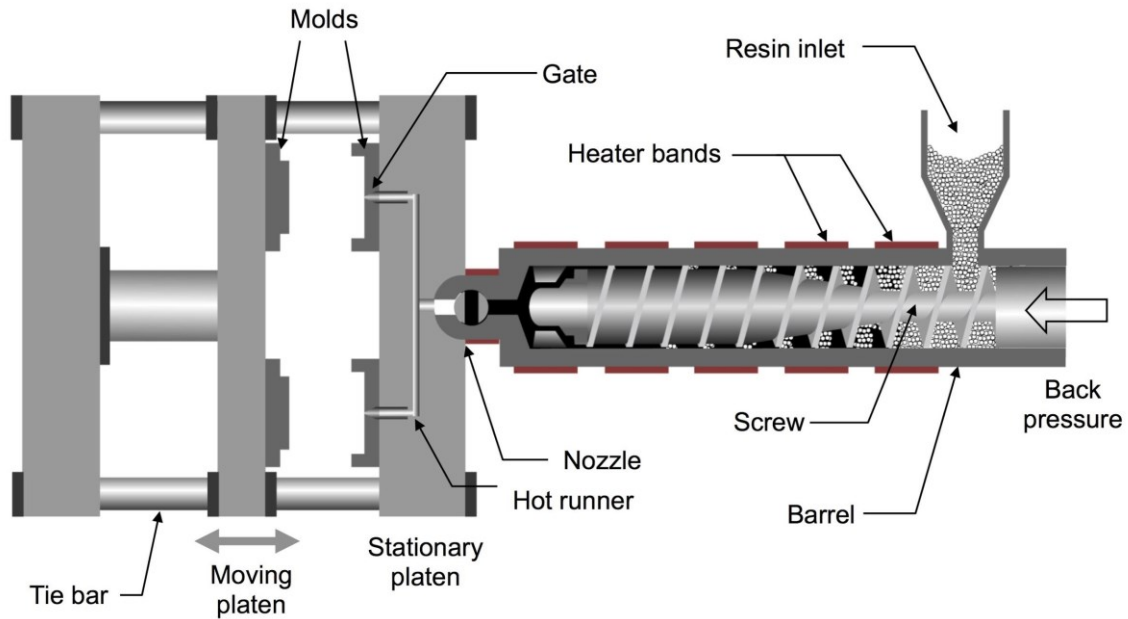


Figure 2.6 Major components of an injection molding machine showing the extruder (reciprocating screw) and clamp units. “Reprinted from *Progress in Polymer Science*, 33, Lim *et al.*, Processing technologies for poly (lactic acid), 820-852, Copyright (2008), with permission from Elsevier” [1].

Shear-controlled orientation in injection molding (SCORIM) is a technique that allows the enhancement of mechanical properties of semicrystalline polymers, like PLA, by tailoring the morphology of the solidifying polymer melt using an in-mold shearing action that is externally controlled [39]. As in conventional injection molding, the processing cycle begins with the filling of the cavity. The SCORIM unit, which has two cylinders with their own melt flow path and three operation modes (A, B and C), then can manipulate the melt. Mode-A consists of an out of phase reciprocation of the two pistons; Mode-B consists of an in-phase operation to pump more melt into the cavity; and Mode-C consists of applying hydrostatic pressure by two cylinders for offsetting volumetric shrinkage [3].

2.3.3 Injection stretch blow molding

Injection stretch blow molding (ISBM) is primarily used to produce bottles. **Figure 2.7** shows a general ISBM process for making PLA bottles. ISBM requires the initial production of a parison or preform by injection molding. Then, the preform is transferred to a blow molding machine where it is heated at around 90°C, and the preform is stretched in both the axial and hoop directions to achieve biaxial orientation, which improves the physical and barrier properties of PLA bottles. Additives are added to the PLA resins to optimize the absorption of energy by the preform from the infrared lamps, so that optimal stretching is achieved. PLA preforms tend to shrink after reheat in regions near the neck and the end cap (*i.e.*, regions where the residual injection stresses are largest.) Residual stresses can be minimized by properly designing the preform. ISBM can be conducted in one or two stages where the preform is produced during the same step as blowing or it is just produced in two consecutive steps [1]. PLA resins show strain-hardening when stretched to a high strain ratio. Therefore, stretching of PLA should be programmed to obtain PLA bottles with optimal sidewall orientation and thickness. Under-stretched preforms result in bottles with large wall thickness variation and lower mechanical properties. Over-stretched preforms result in stress whitening due to the formation of micro-cracks on the bottle surface that diffract light. Preform axial stretch ratios of 2.8–3.2 and hoop stretch ratios of 2–3, with the desirable planar stretch ratio of 8–11, are recommended [1]. Introducing standard features in the bottle design, such as transition shape, step changes, and pinch points on the core and cavity, may help to improve PLA bottle performance. Preform designs are also important for obtaining bottles with good clarity and physical properties, which usually

depends on the bottle design and the blow mold equipment; however, there is little information about that in the literature due to the proprietary nature of this information.

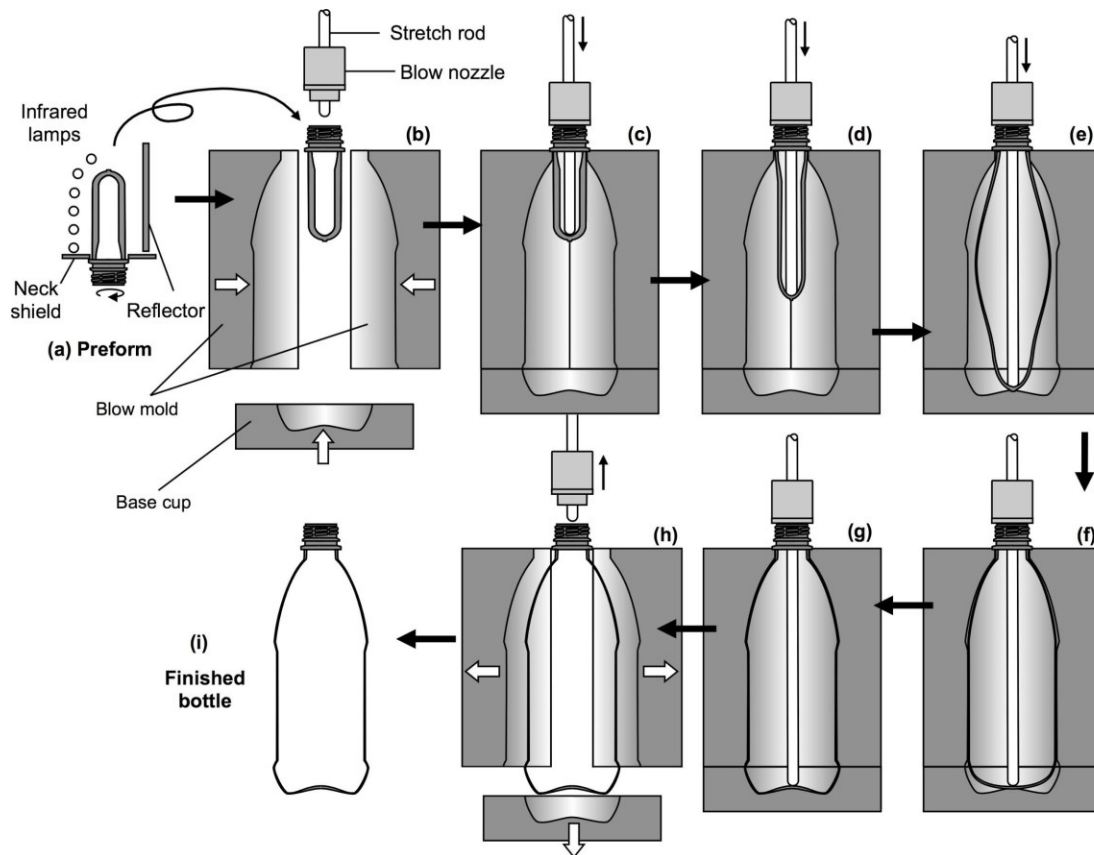


Figure 2.7 Injection stretch blow molding (ISBM) of PLA bottle. “Reprinted from Progress in Polymer Science, 33, Lim *et al.*, Processing technologies for poly (lactic acid), 820-852, Copyright (2008), with permission from Elsevier” [1].

2.3.4 Cast film and sheet

Cast is the main method to produce films with thickness ≤ 0.076 mm and sheets with thickness typically ≥ 0.25 mm. During the production of cast films, molten PLA is extruded through a lip die and quenched on polished chrome rollers refrigerated with cooled water. Cast films usually have a low crystallinity and transparent appearance due to the rapid cooling provided by the chilled rolls. Cast film extrusion has the

advantages of providing good optical properties, high production rate, and good control of film thickness [39]. Deckle systems to control film and sheet edge trimming are generally avoided to reduce the effect that the degraded molten PLA introduces in the edge instability. The gap of the die is set to around 10% higher than the thickness of the film and/or sheet to obtain the right film and sheet dimensions. **Table 2.1** shows the recommended temperatures to extrude PLA films and sheets (PLA 4032D and 2500HP). Horizontal roll stacks are used to produce PLA films and sheets due to the polymer's low melt strength. Roller temperature between 25–50°C is recommended to avoid lactide condensation, and by using an exhaust system around the die, lactide buildup can be controlled. Additionally, good contact between the web and the rolls is recommended to minimize lactide buildup. Slitting and web handling of PLA is similar to that for PS. Rotary shear knives are recommended for trimming the edge of PLA web since razor knives could yield rough edges and break the web. Orientation between 2 and 10 times its original length will improve PLA thermal and impact sheet properties. PLA films produced from 98% L-lactide can be subjected to 2 to 3 times machine direction (MD) stretch ratios, and 2 to 4 times transverse stretch ratios. When a larger amount of D-lactide is present in PLA, more amorphous sheet or film is produced, and larger stretch ratios can be obtained. Extruded PLA films and sheets have excellent optical properties and high Young's modulus, but low elongation at break and toughness [40]. **Table 2.2** shows the main optical, physical, thermal, mechanical, and barrier properties of PLA films. **Figure 2.8** shows the production of biaxially oriented PLA extrusion cast film.

Production of PLA film by blown film technologies is rarely done since PLA has weaker melt strength, and so formation of a stable bubble during extrusion is challenging. Attempts to create PLA blown film have been conducted by using viscosity enhancers. Most of the additives used to increase the melt strength of the PLA are proprietary [40]. Besides low melt strength, PLA is stiff, so when collapsing the bubble during blown film production, permanent wrinkles may be produced. The problem of dead-fold properties can be overcome by also introducing additives.

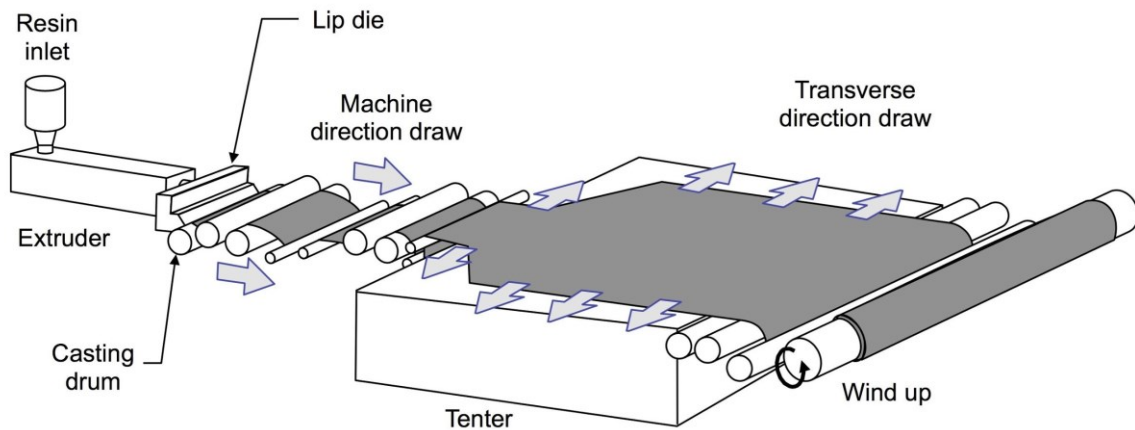


Figure 2.8 Biaxial oriented extrusion cast film machine, adapted from “Reprinted from Progress in Polymer Science, 33, Lim *et al.*, Processing technologies for poly (lactic acid), 820-852, Copyright (2008), with permission from Elsevier” [1].

Table 2.2 Selected average optical, physical, mechanical, and barrier properties of PLA films reported from a number of studies using different grades of PLA, adapted and modified from Auras [49].

Optical	
Refractive index ^{(a), [50]}	1.35-1.45
Clarity	Clear - yellow
Thermo-Physical	
Density amorphous, ^[51] kg.m ⁻³	1250
Density 100 % crystalline, ^{(b), [50]} , kg.m ⁻³	1490
Van der Waals volume (V _W), ^{(c), [50]} , cm ³ .mol ⁻¹	34.45
Molar volume of glassy amorphous (V _g), ^{(c), [50]} , cm ³ .mol ⁻¹	55.12
Molar volume of semicrystalline polymer (V _c), ^{(c), [50]} , cm ³ .mol ⁻¹	49.44
Solubility parameter (δ_p), 25°C, ^[2] , MPa ^{0.5}	19-20.5
T _g , ^[52] , °C	50-80
T _m , ^[52] , °C	130-180
Initial decomposition temperature (T _{d,0}), ^[53] , °C	335
Half decomposition temperature (T _{d,1/2}), ^[53] , °C	395
Average energy of activation (E _{act}), ^[53] , kJ.mol ⁻¹	205-297
Enthalpy (ΔH_m), ^[54] 100%, J.g ⁻¹	93
Crystallinity, ^[53] , %	0 – 40
Heat deflection temperature, ^[55] , °C	55 – 65
Vicat penetration temperature, ^[55] , °C	59
Thermal conductivity x10 ⁻⁴ , ^[1] , cal.cm ⁻¹ .s ⁻¹ . °C ⁻¹	2.9
Heat capacity, ^[1] , cal.g ⁻¹ .°C ⁻¹	0.39
Thermal expansion coefficient x10 ⁻⁶ , ^[1] , °C ⁻¹	70
Surface tension, ^[2] , dyn.cm ⁻¹	42.0
Friction coefficient, ^[2]	0.37

Table 2.2 (cont'd)

Thermo-Physical	
Melt flow Index, ^{d, [2]} , g. min ⁻¹	0.85
Rheological	
Mark-Houwink constants	
K , ^{(e), [56]} , mL.g ⁻¹	0.0174
a ^{(e), [56]}	0.736
Mechanical	
Tensile strength @ yield, ^[2] , MPa	0.88
Elastic modulus, ^[2] , GPa	8.6
Elongation at break, ^[2] , %	3-30
Flexural strength, ^[55] , MPa	70
Flexural modulus, ^[55] , GPa	3.8
Unnotch Izod Impact, ^[55] , J.m ⁻¹	106
Notched Izod Impact, ^[55] , J. m ⁻¹	26
Rockwell hardness, ^[55]	88
Impact strength	Poor
Barrier	
Oxygen permeability $\times 10^{-18}$, ^{(f), [52, 54]} , kg.m.m ⁻² .s ⁻¹ .Pa ⁻¹ @25°C	1.21 ± 0.07
Oxygen activation energy, ^{(f), [52, 54]} , kJ.mol ⁻¹ [25-45°C]	41.43 ± 3.5
Carbon dioxide permeability $\times 10^{-17}$, ^{(g), [52]} , kg.m.m ⁻² .s ⁻¹ .Pa ⁻¹ @25°C	2.77 ± 0.05
Carbon dioxide activation energy, ^{(g), [52]} , kJ.mol ⁻¹	15.65 ± 0.63
Nitrogen permeability $\times 10^{-19}$, ^[57] , kg.m.m ⁻² .s ⁻¹ .Pa ⁻¹	468
Nitrogen activation energy, ^[57] , kJ.mol ⁻¹	11.2
Water permeability $\times 10^{-14}$, ^{(h), [52, 54]} , kg.m.m ⁻² .s ⁻¹ .Pa ⁻¹ @25°C	1.75 ± 0.05
Water activation energy, ^{(h), [52, 54]} , kJ.mol ⁻¹	-9.73 ± 0.27
d-limonene permeability $\times 10^{-19}$, ^{(i), [58, 59]} , kg.m.m ⁻² .s ⁻¹ .Pa ⁻¹	<1.0

Table 2.2 (cont'd)

Barrier	
Ethyl acetate permeability $\times 10^{-19}$, (i), [58, 59], $\text{kg.m.m}^{-2}.\text{s}^{-1}.\text{Pa}^{-1}$	5.34*
Methane permeability $\times 10^{-18}$, [57], $\text{m}^3(\text{STP}).\text{m.m}^{-2}.\text{s}^{-1}.\text{Pa}^{-1}$	7.50
Methane activation energy, [57], kJ.mol^{-1}	13
Helium transmission rate $\times 10^{-6}$, (j), [60], $\text{cm}^3.\text{cm.m}^{-2}.\text{s}^{-1}.\text{kPa}^{-1}$	10.30

N/A: Not available

Note: (a) Refractive index values for PLA were calculated by Gladstone and Dale, Vogel, and Lloyenga methods; (b) density of 100% PLA was calculated according to the group contribution method; (c) PLA value was calculated using the group contribution method; (d) PLA value measured at 200°C and 5 kg according ASTM D1238; (e) PLA value was measured according to ASTM D445 and D446 (PLA values were determined in tetrahydrofuran at 30°C); (f) oxygen activation energy is reported for temperatures between 25-45°C; (g) carbon dioxide activation energy is reported for temperatures between 25-45°C; (h) water activation energy is reported for temperatures between 10-37.8°C; (i) ethyl acetate values of PLA at 3030 Pa and 30°C and 9435 Pa and 30°C, respectively; d-limonene values of PLA at 245 Pa and 45°C and 45 Pa and 23°C, respectively; (j) value of amorphous PLA at 23°C and 0% RH.

2.3.5 Thermoforming

Thermoforming is a standard method to produce PLA containers, such as clamshell, cups, and food trays, extensively used for short–shelf-life product packaging applications. Thermoforming is a process in which a pliable plastic is pressed into a final shape by vacuum or air pressure. **Figure 2.9** shows the steps to produce a thermoformed PLA part. Generally, a PLA sheet (thickness >10 mil or 254 μm) is extruded as previously described, heated, introduced to a mold where it is pre-stretched and then formed (assisted or not by a plunger) to obtain the final PLA container. Initial heating of the PLA film is by infrared (IR) lamps; the IR wavelength should match the

maximum absorbance of the polymer being thermoformed. PLA sheets are thermoformed at temperatures around 80–110°C. Aluminum molds are recommended for thermoforming PLA. As in the case of ISBM, orientation improves toughness of PLA containers; therefore, thermoformed parts are less brittle than PLA sheet, especially in regions highly stretched during the forming operations rather than flanges and lips. Clamshells produced from PLA sheets show better drop-impact properties at freezing temperature (-20°C) than PET and PS clamshells [61]. PLA sheets produced with 100% recycled PLA flakes showed a reduction of M_n of around 5% compared with the original PLA samples; however, this reduction did not affect the production of PLA containers with 100% post-consumer recycled (PCR) PLA content [62].

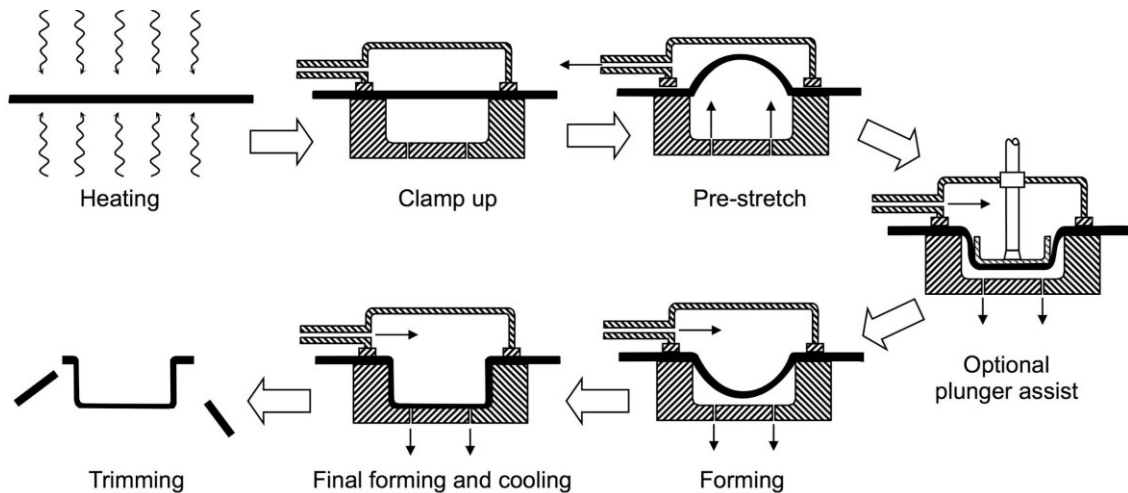


Figure 2.9 Production of a thermoforming part, reproduced “Reprinted from Progress in Polymer Science, 33, Lim *et al.*, Processing technologies for poly (lactic acid), 820-852, Copyright (2008), with permission from Elsevier” [1].

2.3.6 Other processes – Foaming and fibers

PLA resins are used in foam and textile applications. Although methodologies for these applications are well established for other commercial polymers, until now the amount of commercial PLA (by weight) marketed in these forms has been minor. Obtaining lightweight materials with improved cushioning, insulation, and structural performance is a major reason to produce PLA foam parts. Initially, PLA foams were extensively used for medical applications (sutures, implants, and screws), but it is also a promising bioplastic for use in relatively short-lived applications like transport packaging (loose-fill packaging, insulation, and cushioning) or disposable cutlery. In this context, PLA would allow an alternative disposal route and replace fossil-based foams since the polymer is biodegradable and based on renewable resources [63].

Most commercial foaming of PLA is obtained by batch or continuous processes. In these processes, a physical or chemical foaming agent (PFA or CFA) is introduced in the PLA matrix. PFAs are dissolved in the molten PLA matrix and undergo a physical change, such as volatilization of a liquid or release of compressed gas, during foaming. Examples of PFAs are hydrocarbons and halogenated hydrocarbons and gases such as N₂, CO₂, and Ar. CFAs are chemical compounds which are stable at room temperature, such as sodium bicarbonate, azodicarbonamide, *p,p'*-oxybis(benzene) sulfonyl hydrazide, *p*-toluene sulfonyl semicarbazide, and 5-phenyltetrazole, but after a set change of temperature and pressure conditions these compounds convert to gas by undergoing a chemical reaction that provides gas to nucleate bubbles inside the PLA matrix and create the foam structure. CFAs can react endothermically (*i.e.*, absorption of heat during decomposition), or exothermically (*i.e.*, release of heat during

decomposition) [64]. Generally, CFAs are selected to be used at temperatures close to the processing temperature of the polymer. In the case of PLA, a number of PFAs and CFAs have been used such as CO₂, N₂, and BIH40 (a CFA produced by Boehringer Ingelheim Chemicals) [64].

During the batch process, a gas (N₂, CO₂ or a mixture) is saturated into the PLA matrix at a pressure below 800 MPa at room temperature in a chamber. Then, the saturated PLA sample is removed from the chamber, and the solubility of the blowing agents is suddenly reduced by increasing the temperature and/or reducing the pressure, so that bubbles can nucleate. Finally, the produced cells are vitrified by reducing the temperature below the T_g of the PLA matrix. **Figure 2.10a** shows a representation of a batch process.

The continuous microcellular foaming process was developed to overcome some of the drawbacks of the batch process, for example, the time required to saturate the samples. In a continuous process, a blowing agent, generally a gas, is introduced into the molten PLA matrix in a modified extruder (**Figure 2.10b**). After that, the saturated gas PLA matrix is solution mixed and transferred to a static mixer, which guarantees the single-phase solution. Finally, the microcellular nucleation occurs in the nozzle of the extruder unit due to the rapid pressure drop. PLA foaming is affected by a number of parameters such as initial crystallinity, melt rheology, fillers, amount of CFAs, and processing conditions. A detailed review of PLA microcellular foams can be found elsewhere PLA foam samples have been reported to increase Notched Izod impact strength by more than triple while reducing the specific density by almost half [64].

PLA's low melt strength is the main drawback of using it for foaming applications; however, new modifiers are being investigated to induce crosslinking, chain extension, or grafting to increase the molecular weight and the melt properties such as shear and elongational viscosity. Gottermann *et al.* [63] reported that the use of modifiers, such as organic peroxide, multifunctional epoxide, styrene maleic anhydride, isocyanurate + diisocyanate, and bisoxazoline + diisocyanate, helps to increase the M_w of commercially available PLA. In most cases the foam density decreased and cell size increased (except with multifunctional epoxide), and when modified with organic peroxide and multifunctional epoxide the elongational viscosity of PLA increased [63].

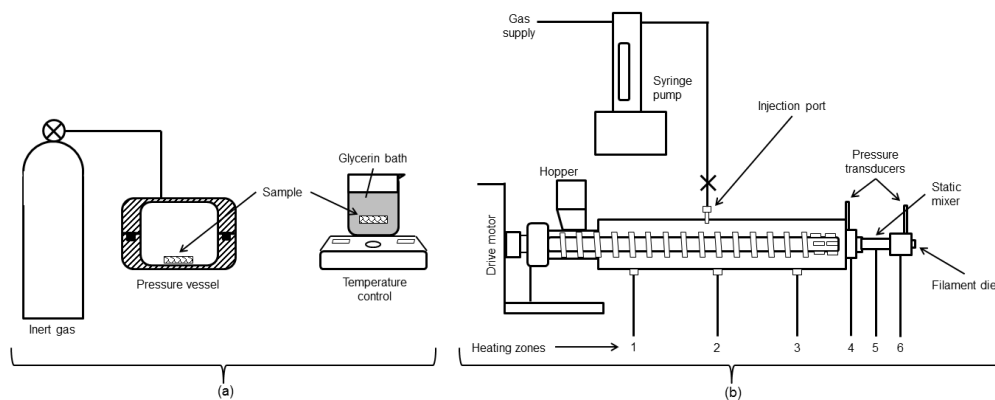


Figure 2.10 Schematic of microcellular foaming process: a) batch process, b) continuous process; 1 to 6 are the main regions of the extruder; adapted from Matuana [64].

Spinning of PLA fibers has been used to produce PLA fibers for suture applications. PLA fibers are gaining importance since they have lower water barrier properties. Conventional processes and finishing technologies can be used for processing PLA fabrics; PLA shows similar properties to other synthetic fibers, but requires modified dyeing and finishing techniques due to its low affinity to conventional

water-soluble dyes [65]. PLA fibers can be used to produce breathable garments. Among the important criteria to produce fibers are: *i*) to control moisture content to be less than 50 ppm to avoid any possible hydrolytic degradation, and *ii*) to achieve an optimum drawing temperature ($>T_g$ of PLA) and drawing speed (200–9000 m.min⁻¹) to obtain appropriate crystallinity and strong PLA fibers [66]. During spinning of PLA fibers, the microstructure of the polymer chains is oriented in the axis direction of the fiber, so a fiber with very high aspect ratio (length to diameter) and orientation can be produced. Spinning of fibers produces a controlled molecular orientation and spatial arrangement of the PLA structure. In modern spinning processes, a molten polymer or solution is extruded through a small orifice and is elongated by applying an external force. Then, the polymer filament is cooled and precipitated. Further processing of the polymer filament may take place, such as drawing, unidirectional stretching, and texture control. PLLA with a M_w around 0.5 to 3.5 x 10⁵ Da is used for melt spinning through a two-stage process that includes melt spinning and hot drawing [67]. A standard melt spinning process is represented in **Figure 2.11**. A typical melt temperature profile for PLA resin melt spinning is shown in **Table 2.2**. A general extrusion process, as described in section 2.3.1, is used to produce the fibers; however, the spin pack plays an extremely important role since it delivers the molten PLA previously filtered to remove impurities to the spinneret plate through the spinneret holes. The spinneret holes have a specific ratio of length to diameter to achieve the desirable shear flow mode. Spinneret plates can be monofilament or multifilament. Deniers, the unit used to quantify filaments, is defined as weight in grams of a 9,000-m long filament. For PLA, the recommended diameter of the spinneret holes range from 0.2–0.35 mm with a

typical ratio of 2 to 3. Larger hole diameters are necessary for filaments greater than 6 deniers. After the filament is produced, it is air cooled at temperatures about 15–30°C in an air quench zone or chamber, which cools the filament through its melt crystallization temperature (T_{mc}) and to its T_g . When the spun filament temperature is below the T_g , the spinning process is considered complete. Then, the spun filament needs to be finished and wound up. A detailed description of the production of melt spinning PLA fibers can be found elsewhere [67].

Solution spinning of PLA can also be carried out to avoid the substantial hydrolytic degradation that happens during melt spinning. During solution spinning, PLA is extruded as in melt spinning, but then the spinneret is submerged in a spinning bath, so that the PLA melting point is immediately depressed to below room temperature. After that, the solvent is removed by solvent-assisted coagulation or evaporation. Two main methods are used for solution spinning: wet and dry spinning. During wet spinning, PLA is dissolved in a solvent such as tetrahydrofuran, chloroform and/or dichloromethane, and then it is extruded in a submerged bath with a mixture of a solvent and a non-solvent (e.g., toluene at 110°C) to induce coagulation. Generally, PLLA with $M_w < 3 \times 10^5$ Da is not suitable for wet spinning. During dry spinning, after the PLLA dope solution (e.g., PLLA in chloroform) is extruded, and pumped through a multi-hole spinneret, it is introduced in a chamber with circulating heated air/gas, so that the solvent can evaporate. PLA fibers are used for textiles and medical applications; examples of these applications are presented in section 2.5.2.

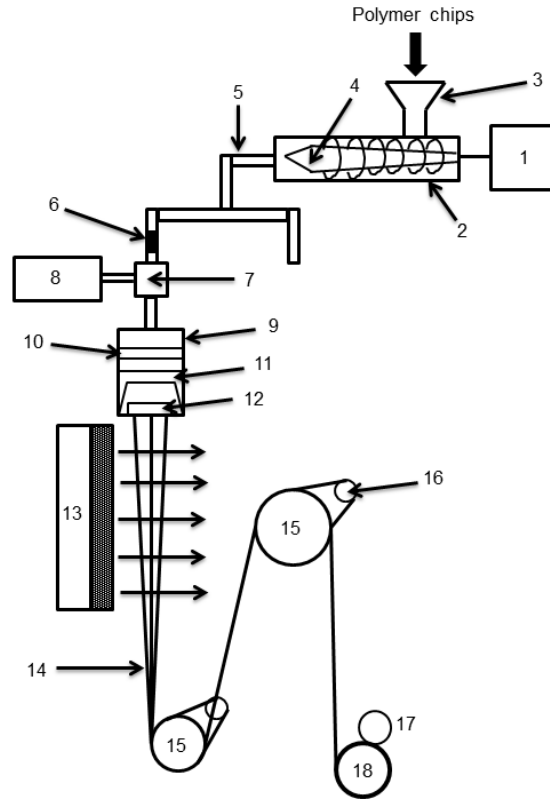


Figure 2.11 Schematic representation of melt spinning setup: (1) extruder drive, (2) single-extruder - 24 to 36:1 L/D ratio, (3) hopper, (4) screw, (5) manifold, (6) static mixer, (7) metering pump, (8) metering pump drive, (9) spin pack, (10) mesh filters, (11) distributor, (12) spinneret, (13) cross-flow quench chamber, (14) freshly spun yarn, (15) godet, (16) idler roller, (17) friction-driven winder, (18) yarn bobbin, adapted from Agrawal [67].

2.4 Tailoring PLA Properties

Although PLA has many desirable properties for consumer good applications, there are limitations for all-purpose use, as with any polymer. Researchers have been trying to expand PLA use and applications by blending PLA with a number of biodegradable and non-biodegradable resins, and/or by compounding PLA with a number of fillers such as fibers and micro and nanoparticles. Covering all of the blends and composites in a short

overview is a daunting task, and a number of review papers have been written to discuss the improvements of PLA properties [68-73]. Therefore, this section provides a summary of the main resins used to blend and/or compound with PLA, and it will direct the reader to the original work to obtain additional information.

Blending of PLA with biodegradable and non-biodegradable polymers has been extensively reported [71-73]. **Figure 2.12** shows the main biodegradable and non-biodegradable resins blended with PLA. PLA is considered a brittle polymer, so extensive research has been conducted to improve its toughness for different applications [74, 75]. In general, a rubbery polymer with low T_g (generally below 20°C of the use temperature) is blended with PLA at a low ratio to create small rubber domains between 0.1 and 1.0 μm with good interfacial adhesion to PLA, so that the rubber domains can dissipate the impact energy when PLA is failing through fracture [76]. Beside an improvement in toughness, different polymers have been blended to PLA to improve properties such as optical [75, 77], barrier [78-83], thermal [74], and biodegradation [84-88].

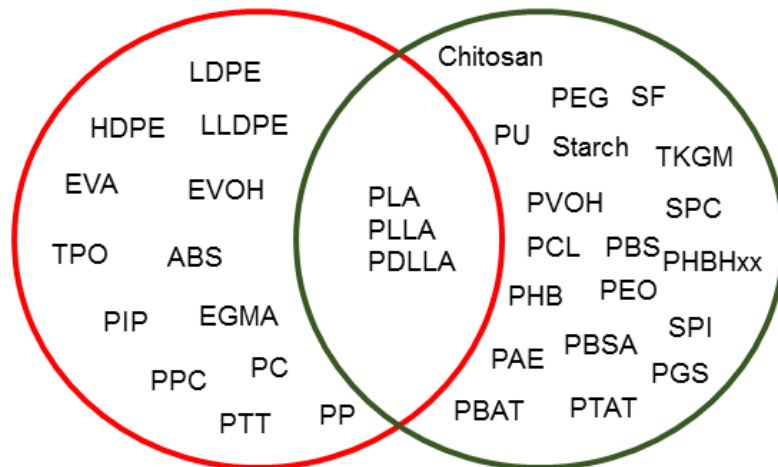


Figure 2.12 Selected biodegradable and non-biodegradable blends of PLA polymers: PLA-LDPE [89], PLA-LLDPE [90], PLLA-LLDPE [90-92], PLLA-HDPE [91], PLA-PS [93], PLLA-PEVA [94], PLLA-EVOH [95], PLA-TPO [96], PLLA-ABS [97], PLLA-PIP [98], PLA-PVOH [99], PLA-PHB [100] PLLA-PBS [101, 102], PLA-PBSA [103], PLA-PBAT [104, 105], PLLA-PTAT [106], PLA-PAE [107], PLA-PU [108], PLA-PEG [109], PLA-SPI [110], PLA-SPC [110], PLA-SF [111], PLA-TKGM [112], PLA-Chitosan [83, 113], PDLLA-Chitosan [114], PLLA-Chitosan [114], PLLA-PBSL [115], PLLA-PEO [116], PLLA-PCL [117-119], PDLLA-PCL [117], PLA-PCL [120], PLA-Starch [121-124], PLA-PHBHxx [125], PLA-PPC [126], PLA-PP [127], PLA-PC [128], PLA-PGS [129], PLA-PTT [130], and PLA-EGMA [131].

A polymer composite is defined as a material that has two or more distinct phases. One of the phases is a discontinuous phase considered as the reinforcement phase dispersed in a continuous or matrix phase. The reinforcement phase can be fibers and/or micro and nano particles. The main goal of adding a reinforcement phase to PLA is to tailor its properties, such as elongation at break [81, 132-141], heat resistance [138, 142, 143], dimensional stability [137, 144-147], barrier [132, 137, 140,

148, 149], and cost [150], to overcome some of PLA's shortcoming properties compared with fossil commodity polymers, as well as brittleness and low thermal stability [2]. Since the main engineering properties of a composite result from the discontinuous phase, PLA has been reinforced with natural and synthetic fibers, micro and nano fillers [73, 151].

Fibers with a larger length to diameter ratio can be used to carry load in fiber-PLA composites, and increase their applications [73]. Natural and synthetic fibers have been used to reinforce PLA. Dispersion and orientation of the fibers play a crucial role in obtaining PLA composites with the desired properties. Adhesion between the PLA matrix and the fibers is a strong controlling parameter of the final composite properties since enhancement of the composite performance is strongly attributed to the adhesion between the continuous and discontinuous phases. Wood and non-wood natural fibers, such as cotton, jute, flax, kenaf, sisal, and hemp, are extremely attractive to be compounded with PLA since they are 100% renewable and so a fully bio-based composite is obtained. Synthetic fibers, such as glass and carbon-based, are also commonly used to reinforce PLA parts since they have extremely high tensile strength, which improves the final mechanical properties of the composite [73].

Fillers in micro and nano sizes have played an increasing role in creating composites with lower cost and environmental footprint. Inorganic fillers, such as talc, mica, hydroxyapatite, carbon black, and gypsum, have been used for many decades to reinforce polymers since they can enhance PLA mechanical properties with a small amount of composite. Lately, the addition of nanoparticles has gained attention since adding nanoscale clay particles results in significant improvement of material

performance. Some of the specific nanocomposite properties that are enhanced through the exfoliation of these nanoparticles include mechanical [152-160], barrier [132, 137, 140, 148, 149, 160, 161], and thermal properties [156, 157, 160]. The mechanical property of polymers with a nanoclay loading of 3–6% can achieve equivalent mechanical properties (*i.e.*, tensile strength, impact strength, flexural modulus) to a polymer with up to 30 wt% fillers at the microscale (*i.e.*, glass and mineral fibers, etc.) [162, 163]. Since clay platelets are considered impermeable to small molecules (*e.g.*, gasses, liquids), and their presence in the polymer matrix extends the diffusion path of small molecules through a tortuous path, nanoclays can improve the barrier of the nanocomposite [164]. Although a recent study showed that in the case of organic compounds, it is the sorption of the compound to the surfactant added to the nanoclay that modifies the barrier property of PLA (*i.e.*, by modifying the solubility parameters) [165]. The high thermal stability of clays allows their use in polymers for heat-resistant and flame-retardant applications. Enhancement in polymer thermal stability is affected by the size of clay particles; nanoclays with an aspect ratio (lateral dimension vs thickness) greater than 100 are usually preferred [163]. Well-dispersed nanoclay particles in a polymer matrix can act as both a superior heat insulator [166] and mass transport barrier [167]. **Figure 2.13** shows the diameter or thickness of selective micro and nanofillers that have been added to PLA.

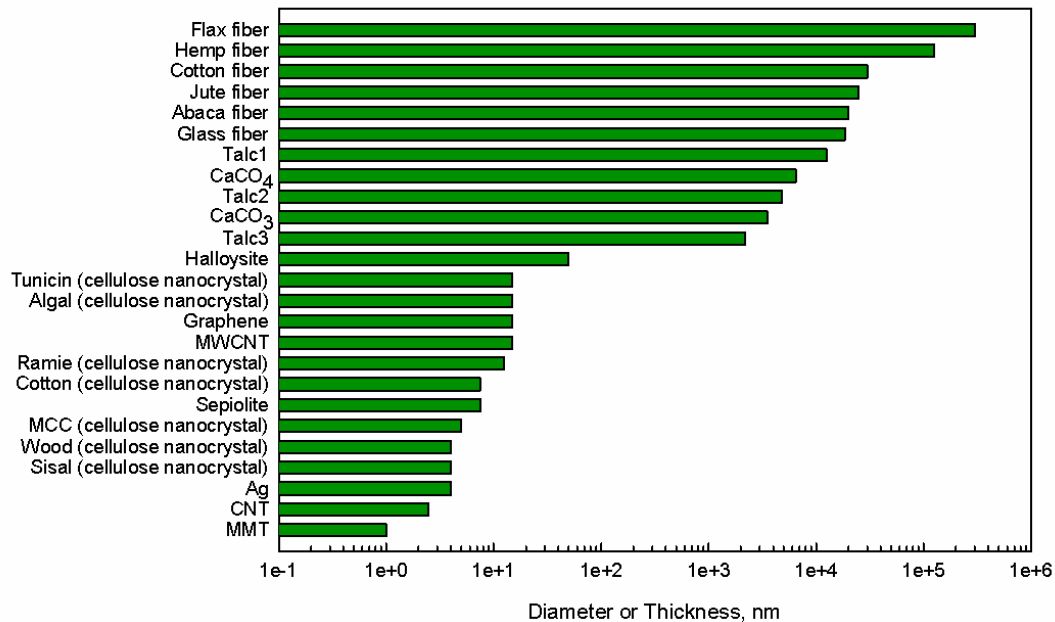


Figure 2.13 Average scale dimensions of selected fillers in PLA composites: MMT (montmorillonite) [168], CNT (carbon nanotube) [169], Ag [170], sisal [171], wood [168, 172, 173], MCC (microcrystalline cellulose) [174], sepiolite [168], cotton [175, 176], ramie [177, 178], MWCNT (multiwall carbon nanotube), graphene, algal [179, 180], tunicin [181], halloysite [148], talc3 [182], CaCO₃ [183], talc2 [182], CaSO₄ [184], talc1 [182], glass fiber [185, 186], abaca fiber [187], jute fiber [187], cotton fiber [187], hemp fiber [187], and flax fiber [186, 188].

2.5 PLA Industrial Applications

Production of PLA for industrial applications has risen steeply due to its competitive cost and the positive public perception of the polymer's environmental footprint. Industrial applications for PLA can be categorized into two main groups: consumer durable goods and consumer non-durable goods. From an economic perspective, consumer durable goods are commodity products with a lifetime of more than three years such as

appliances, cars, and medical products. Consumer non-durable goods are products having a lifetime up to three years such as packaging, short-term medical items, and serviceware [189]. In some cases these product categories may overlap, depending on the PLA design. The next section lays out the industrial applications for PLA according to commercial usage categories: medical, fibers and textiles, packaging and serviceware, environmental remediation, and others.

2.5.1 Medical

Since the early 1960s, PLA has been used for medical applications such as implants and medical devices. PLA found a favorable niche for medical implants since it degrades over time, therefore the removal step of an implant is not required. Also, LA is naturally produced by the body and has no known toxicity effect on humans. Various applications for PLA as medical implants include tissue growth, bone grafting, and fracture fixation devices. PLA is commonly used in combination with other polymers and/or proteins, such as polyglycolic acid (PGA), glass fiber, collagen, carbon fiber, and hydroxyapatite (HA) ceramic, to improve its functionality for stabilization of fractures, fixation of tendons and ligaments, and improvement of mechanical properties. On the other hand, degradation of PLA has been reported to lower the pH of cells/tissues due to the accumulation of LA, leading to inflammation of the in-contact tissue [190]. Zhou and Li [191] reported that a composite of PLA-chitosan could alleviate this inflammation issue, as the presence of chitosan neutralizes the PLA-induced pH sites [10, 191]. In addition, PLA composite implants may help treat any organ loss or malfunction by stimulating the growth of the natural cells around the polymer part. The American Society of Plastic Surgeons has recently promoted dermal fillers made of PLA. Such a

filler works by stimulating the production of collagen in the human body and is intended for facial improvement [192]. Although extensive documentation is available on the use of PLA composites as medical implants, reports on clinical practice using these implants are scarce, which could be due to possible compatibility issues between the human body and PLA implants. Fast or slow degradation of PLA implants may cause some defense reaction from the human host. Moreover, the toxicity effect may occur for long-term use [190].

The use of PLA medical devices to replace metallic medical devices has been researched for more than a decade. PLA has been sought as an alternative to solve issues associated with metal device implants such as possible corrosion and distortion of magnetic resonance images [192]. For example, Zimmer Biomet®, a musculoskeletal health solutions company, produced Bio-Statak®, a tissue attachment device made of PLLA that is resorbable and was reported to have comparable pullout strength to metal devices [193]. Researchers from the Fraunhofer Institute in Germany in 2010 developed PLA composite screws that are claimed to closely mimic real bone strength as an alternative to titanium surgical implants [194]. Other companies, such as Arthrex™, Phusis, Gunze, Takiron, and Linvatec, have commercialized PLA medical devices for use as interference screws, miniplates, rods, and suture anchors. Most of the aforementioned medical devices are made through a drawing process of PLLA with $M_w > 7.0 \times 10^4$ Da [190]. This process helps to strengthen the property of the devices to be as close as possible to real bones, and is achieved as a result of the orientation and crystallinity of PLA. The drawing process of PLLA also seems to affect the piezoelectricity property of the devices; this property is associated with stimulation of

bone growth [190]. PLA seems to be a better option than metal, but in the case of bone grafting, PLA has slower effect on bone resorption. Moreover, some mechanisms of PLA degradation in the human body are not fully understood. In 2005, Mitek Sports Medicine launched a biocomposite implant known as Biocryl[®] Rapide[®], with the claim of superior function over PLA. By 2013, this biocomposite had reportedly been used for knee and shoulder implants in more than 250,000 patients [195]. Additional examples of PLA use in medical applications are provided in the other reviews of this series. Advanced tailoring and molecular modification of PLA are still needed to expand PLA's function as medical implants.

2.5.2 Fibers and textiles

PLA can be processed into fibers by spinning, as explained in section 2.3.6. PLA is suitable for fiber applications due to its ability to absorb organic compounds and its wicking properties. Since the polymer is fairly polar, it can absorb moisture, which makes PLA a suitable candidate for wipes. For example, Biovation[®] developed a PLA single-use antimicrobial wipe. Fraunhofer UMSICHT and FKUR developed water filters based on PLA blend fibers (Bio-Flex[®] S 9533)—this blend is reported to contain adsorbent carbon made of coconut shells [196]. Since PLA has excellent wicking properties, the polymer also can be used for disposable products. For example, Biovation launched disposable antimicrobial blood pressure cuff shields called Bioarmour[™]—this product is composed of 74 wt% PLA and is intended to protect a patient's skin from being directly in contact with the cuff and provides comfort for patients due to its breathability [197]. Ahlstrom Corporation recently introduced a fine-

filament web filter for tea made from PLA fibers—the polymer’s wicking ability allows the infusion of the tea flavor into hot water [198].

PLA fibers also are of interest to the automotive industry. Approximately 10% of a vehicle compartment is made of plastic. Various companies, including Ford Motor Company, are looking into environmentally friendly polymer options for car interior parts such as carpets, floor mats, and trim parts. Some companies have started producing parts with different bio-products such as PLA, flax, jute, and cotton. A conference on bio-based materials for automotive applications (bio!CAR) was held in Stuttgart, Germany, in September 2015. However, some obstacles must be solved, such as emission of undesirable odors when the polymer is at high temperature, time span of degradation processes, and moisture effects towards materials, before PLA can be fully implemented for such applications [199]. Ford Motor Company performed a study comparing PET and PLA-based seat fabrics to investigate automotive requirement properties such as seam fatigue, flammability, resistance to abrasion and snagging. The study found that PLA met most of the requirements for automotive fabrics and had comparable performance to PET, but failed in the flammability and abrasion tests [200]. Other biopolymers, such as polyurethane and soy-based polymers, have been investigated for their use in the automotive industry by Daimler AG, Fiat, and the Toyota Motor Group. These major car producers are primarily concerned with the durability of the biopolymers [201]. Some improvements are needed before PLA can replace fossil-based polymers in the car industry.

The use of PLA to replace major synthetic polymers, such as nylon and PET, in the textile industry is increasing. PLA textiles are being used by garment industries (*i.e.*,

apparel, homeware). Although PET-cotton blends are a common combination in apparel for established brands like Nike®, Gap®, and Under Armour®, PLA itself is seen as a promising alternative due to its wicking properties and breathability, making PLA a comfortable material for apparel manufacturing. The Hohenstein Research Institute tested the use of PLA and PLA-cotton blends in garments, and found that PLA is suitable for sports apparel due to its thermal insulation and buffering capacity to sweat, among other specifications [202]. PLA had high resiliency when used for making jackets. Also, the ability of PLA to withstand laundry service with multiple washing was tested and was in accordance with the American Association of Textile Chemists and Colorists (AATCC) standards. However, some issues are associated with PLA textiles, such as the pressing and ironing temperatures, which are limited to temperatures lower than those acceptable for PET and cotton [202]. The dyeing and finishing processes for textiles often undergo conditions involving temperature, pH, and time, thus imposing a challenge for PLA since the polymer is susceptible to degradation under the aforementioned conditions [202]. PLA has good retention and crimp properties, so it is suitable for knitted and embroidered textiles. Another application for PLA textile is in homeware use such as curtains, pillowcases, and rugs [203]. Early in 2015, Kansai University and Teijin™ developed a new wearable piezoelectric device to detect "directional changes and arbitrary displacement"—this device is made of laminated PLLA and PDLA [204]. In summary, there is significant potential for PLA to be used by the fiber and textile industries, but its limitations remain an issue and more development and changes are needed for PLA to compete with existing fossil-based polymers.

2.5.3 Packaging and serviceware

The use of PLA in packaging and serviceware has largely increased over the last five years. Research is being performed by both academia and industry with collaborative works between the two to strengthen the green-packaging market to meet consumer demands for packaging derived from renewable resources. PLA has numerous challenges for commercial packaging applications due to its limited mechanical and barrier performance. However, PLA package performance has been improved significantly by tailoring polymer processing, blending with other polymers, and adding compounds, such as nucleating agents, antioxidants, and plasticizers, to meet the end needs [205].

For example, oriented and non-oriented PLA can be produced by tailoring PLA processing. Oriented PLA has considerable thermal resistance with good clarity over non-oriented PLA. Although oriented PLA films pose desirable characteristics, their brittleness is still of concern due to the fragility and loud noise produced by the packages. Frito Lay introduced a compostable PLA bag for their SunChips® brand in 2010, but this bag underwent major public scrutiny over the loud crinkling sounds during bag handling. The bags were later removed completely from the market [206, 207]. Oriented PLA films are also used for bakery packaging and gift cards [205]. Meanwhile, non-oriented PLA sheets are preferred for use as thermoformed clamshells to package fresh products [208] and other products with short shelf life. These clamshells are still being used to pack some Wal-Mart products. Other companies have claimed that the shelf life of the packaged fruits is 10–15% longer in PLA containers [209]. However, the low barrier properties of PLA towards moisture and gases may cause limitations in other

applications. **Table 2.3** shows examples of products that have been and/or continue to be packaged in PLA containers.

Major European markets showed early interest in the use of commercialized PLA. Danone®, for example, launched yogurt cups made of PLA for its Germany market, which accounted for 80% of the total volume of their Activia product line [210]. Other thermoformed PLA products also are available by various companies (**Table 2.3**). Packages produced from non-oriented PLA, however, are limited to non-heat applications. Some other commercial packaging applications for PLA include shrink films and shrink labels. For PLA to meet the requirements for these types of applications, it needs to exhibit shrinkage, which is commonly observed for oriented PLA at temperature above 60°C with a reported shrinkage ratio of 70% [205]. ConAgra Foods uses recycled PLA shrink film (produced and supplied by EarthFirst®) as tamper-evident seals for its three leading table spread brands: Fleischmann's®, Blue Bonnet®, and Parkay® [211] (**Table 2.3**). The use of oriented PLA as shrink labels does have a slight limitation since PLA's shrinkage ratio is low at around 70°C, which results in whitening of the label due to the crystallization process. Thus, lamination with other polyester films or blending other polymers with amorphous PLA are used to ameliorate PLA shrinkage properties [205]. Commercial use of PLA shrink labels was reported for soft drink products manufactured by S&B Foods, Nisshin Oilio, and Asahi [205].

PLA is used to produce bottles for water and juices; however, this market is not extensive. Common production for PLA bottles is ISBM, as previously explained. Application for PLA bottles is limited only to non-carbonated beverages due to the insufficient creep behavior of PLA and low barrier towards CO₂ (which results in product

with a lack of carbonation). Vitamore[®] carbonated drink in PLA was reported to have shelf life of about 6 months with a moderate loss of CO₂ [212]. Further improvements are needed to tailor the barrier properties of PLA for products with a longer shelf life to expand commercial applications. Some examples of PLA bottled products for the beverage market are listed in **Table 2.3**. Despite numerous efforts by manufacturers in introducing PLA-based bottles into the market, further development is needed to obtain PLA bottles with the required commercial properties to compete with the established fossil-based polymers. Nevertheless, Coca Cola[®] has shown interest in bio-based materials, such as high density poly(ethylene) (HDPE) made from sugarcane molasses, for their Odwalla juice beverage line [213]. Tetra Pak, one of the world's leading packaging companies, recently launched a new bio-based carton made of certified paperboard, and bio-based low-density poly(ethylene) (LDPE) films with bio-based HDPE caps named Tetra Rex[®]. Valio, a dairy producer in Finland, is currently using these Tetra Pak[®] cartons for Eila lactose-free semi skimmed milk drink for the Finnish market [214].

Production of PLA containers for serviceware applications, such as microwaveable containers and single-use disposable drinking cups, is challenging since PLA is susceptible to heat deformation. For such applications, a higher heat deflection temperature (HDT) is desirable as it allows the molten polymer to mold faster and to retain its dimensional shape once the formed polymer is removed from the mold. The HDT of PLA is reported to be between 55 and 65°C [1, 215], which is too low for producing thermally stable PLA containers for a non-refrigerated supply chain. Therefore, nucleating agents, such as alkylene bisamide [205], Ecopromote[®]—a

biodegradable nucleating agent by Nissan Chemical [216], talc, and PDLA, are often incorporated into the PLA [205]. The presence of a nucleating agent helps to induce faster crystallization of PLA, so an increase in HDT can be achieved. For example, Corbion Purac[®] produces PURALACT[®] lactide serviceware, which is microwaveable and has a comparable impact resistance to acrylonitrile butadiene styrene (ABS); production is achieved by manipulating the stereochemistry of PLA with D-lactide monomers, but no further process details have been disclosed by the company [217]. SelfEco, a company under VistaTek LLC, has produced party serviceware items from PLA and its blends [218]. Teknor Apex has developed a PLA series (Terraloy BP-34001) with improved impact strength and HDT of 135 J.m⁻¹ and 112°C, respectively, which are higher than those of standard PLA (impact strength = 33 J.m⁻¹; HDT = 55–65°C). Teknor Apex claimed that this new compound contains 78 wt% PLA and has the ability for rapid processing with shorter cycle times [219]. It is likely that thermal resistant food serviceware made of PLA will become more available in the coming years.

Table 2.3 Selected examples of packaging containers produced from PLA

Trademark/ Commerciali zed Brand	Year Active	Improved Functions	Applications	Remarks	Ref.
Tenova, Sweden	2003- current	None	Shopping bags	Bags composed of 45 wt% PLA and 55 wt% Ecoflex	[220]
Biota®, U.S.	2004-2006	None	Bottled waters	Advertised as biodegradable bottles No longer on market due to company bankruptcy	[221, 222]
Wal-Mart, U.S.	2005- current	None	Strawberries, Brussel sprouts	Advertised as biodegradable clamshells Among the first company to use commercialized PLA	[208]
Del-Monte, U.S.	2005- current	None	Fresh-cut produce	Advertised as biodegradable clamshells	[223]
SPAR, Austria	2005- current	None	Organic pears, apples, tomatoes	Advertised as biodegradable thermoformed with flexible PLA lid	[209]
Hypermarket chain Auchan, France	2005- current*	None	Fresh salads	Advertised as biodegradable containers	[224]
Newman's Own, U.S.	2005- current*	None	Organic salads	Advertised as biodegradable containers	[225]
Pacific Pre- Cut, U.S.	2005- current*	None	Freshly prepared salads	Advertised as biodegradable containers	[226]
Vitamore®, Ihr Platz (drugstore chain), Germany	2006- current	None	Bottled beauty, energy and memory drinks	Advertised as 100% bio-based bottles	[212]

Table 2.3 (cont'd)

Trademark/ Commercialized Brand	Year Active	Improved Functions	Applications	Remarks	Ref.
Huhtamaki, Finland	2006-current	None	Dessert cups	Advertised as biodegradable containers	[227]
Greenware®, Fabri-Kal, U.S.	2008-current	None	Cold drink cups, lids and portion containers	100% biodegradable	[228]
Noble Juice, U.S.	2008-current	None	Organic and non-organic citrus juice bottles	100% biodegradable	[229]
Apple Inc., U.S.	2008-current*	None	iTunes prepaid gift cards	Current status in market unknown	[230]
Sant' Anna, Italy	2008-current	None	Bottled water	100% biodegradable bottles with PE lids	[231]
Fleischmann's®, Blue Bonnet®, Parkay®, ConAgra Foods, U.S.	2009-current	Improved shrinkage performance	Tamper evident seals for tablespreads	Made of recycled PLA Claimed to reduce 20% of facility's energy consumption	[211]
Reddi-Wip®, PAM®, ConAgra Foods, U.S.	2009-current	Improved shrinkage performance	Shrink labels for cream whipped topping and cooking spray	Made of recycled PLA Claimed to reduce 20% of facility's energy consumption	[211]
Shiseido-Urara, China	2009-current	None	Bottled shampoo	Favorable reception in Chinese market as an environmentally friendly option Bottles are 50 wt% PLA and 50 wt% HDPE	[232]

Table 2.3 (cont'd)

Trademark/ Commercialized Brand	Year Active	Improved Functions	Applications	Remarks	Ref.
Wal-Mart; Sams-Club, Mexico	2010- current*	None	Small white onion	No longer on the market Advertised as biodegradable clamshells	[233]
Sunchips®, Frito Lay, U.S.	2010-2014	Thermal resistance	Potato chips bags	Bags withdrawn from the market within a year due to loud crinkling noise Original flavor was retained for a while after incident, but is no longer available Bags composed of 94 wt% PLA, 6 wt% adhesive and ink, 0.2 wt% aluminum liner	[206, 207]
Activia®, Danone, Germany	2010/2011- current	None	Yogurt	Improved carbon footprint by 25% 43% less fossil resource usage than original package	[210]
Stonyfield Farm®, U.S.	2010/2011- current	None	Organic yogurt multipack cups	Cups composed of 93 wt% PLA, 4 wt% titanium dioxide and 3 wt% compounded additives 48% reduction of greenhouse gas emissions	[234]

Table 2.3 (cont'd)

Trademark/ Commercialized Brand	Year Active	Improved Functions	Applications	Remarks	Ref.
Polenghi LAS, Italy	2010-current	None	Bottled lemon juice	Claimed to be first blown extrusion PLA bottle in EU market	[235, 236]
Ceramis®, Amcor's Swiss	2011-current	High barrier towards O ₂ , moisture, aroma compounds	Snacks (pouches) Fruits and vegetables (thermoformed) Breads	Silicon oxide coating provides excellent barrier for PLA	[237]
Track & Field, Brazil	2011-current*	None	Capsules for athletic apparel	Current status in market is unknown	[238]
PURALACT®, Netherlands	2013-current	Thermoformed containers able to tolerate boiling temperature	Single-use hot beverage cups	Conversion to PLA packaging line is feasible by using an existing PS line	[239]
PURALACT®, Netherlands	2013-current	Comparable impact resistance to ABS	Serviceware	Safe food contact application, and the containers are microwavable	[217]

* Current (2016) market availability could not be confirmed.

2.5.4 Plasticsulture

Plasticsulture is the use of plastics for agricultural applications. Plastics are used for applications such as *i*) to protect soils from erosion and plants from weed, insects, and birds via mulch films, *ii*) to function as drip irrigation tubing, and *iii*) to cover tunnels of greenhouses (**Figure 2.14** and **Figure 2.15**). The use of plastics for agricultural applications started in the 1950s to improve and increase the growth and production of agricultural products [240]. Conventional non-renewable plastics are the default choice

in the plasticulture industry, and poly(ethylene) (PE) is the main polymer in use. However, various issues regarding the use of non-renewable plastics are of increasing concern among agricultural personnel and consumers. Among these issues are cost of waste management, end-of-life options, and consumer demands for more environmentally friendly options. Waste management handling is expensive, due to the additional labor cost for the removal of conventional plastics after use and associated transportation costs. Also, the end-of-life option is not feasible since landfill soil may become contaminated with pesticide residues from the used plastics. Similarly, recycling is not an option and open burning is illegal in several states in the U.S. [241]. Therefore, biodegradable plastics, such as PLA, poly(hydroxyalkanoates) (PHAs), starch, and poly(butylene adipate-co-terephthalate) (PBAT), are seen as attractive options to help solve these issues [242].

The implementation of biodegradable plastics in the plasticulture industry is still at the early stage and is mostly done at the research level due to the high per-pound cost of the polymers. The most promising outcome to be expected from the use of biodegradable plastics for plasticulture is that they are able to biodegrade after use.



Figure 2.14 (left) tomato plots covered with mulch films; (right) high tunnel or overwintering house.

Although, as discussed above, PLA has considerable potential for various industrial applications, the use of homopolymer PLA in the plasticulture industry has been limited due to its poor mechanical and thermal properties. Mulch films (**Figure 2.15**) made with PLA alone are deemed insufficient to protect soils and plants due to brittleness. The relatively high T_g of PLA and less available amorphous region limit the food sources for microorganisms to initiate the biodegradation process at low temperatures [240]. Consequently, PLA is blended with other biodegradable polyesters to produce commercialized PLA-based mulch films [240]. Commercialized PLA-based mulch films are commonly made with plasticizers, and those that incorporate LA derivatives or oligomers demonstrate an accelerated biodegradation process [243, 244]. The accelerated biodegradation of plasticized PLA-based mulch films could be attributed to the introduction of free volume in the PLA polymer matrix, allowing the diffusion of surrounding water into the polymer, thus promoting hydrolysis and, in turn, increasing the accessibility of microorganisms to their food sources. This described

phenomenon is called bulk erosion. Another phenomenon involved in the biodegradation process is known as surface erosion [2]. Details on hydrolysis of PLA-based films in non-medical environments are provided in section 2.6.1.

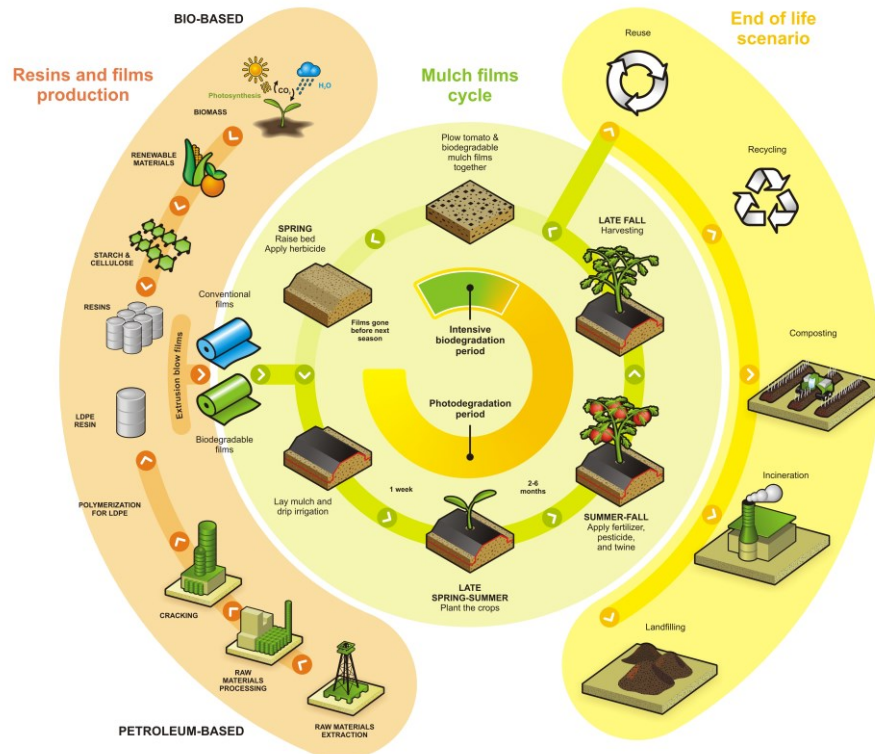


Figure 2.15 Cradle to gate, grave, and cradle life cycle flowchart of plastic mulch films. After removal of conventional mulch films, they can be reused, recycled, incinerated, and/or landfilled. Biodegradable mulch provides the same end-of-life scenario routes and also can be composted.

2.5.5 Environmental remediation

Removal of contaminants from the environment is known as environmental remediation or bioremediation. Remediation is one waste management method available today to treat water and wastewater by employing mostly sorption and denitrification mechanisms. Theoretically, it is believed that the efficiency of these mechanisms relies

on Van der Waals interaction and electronic affinity between contaminants and sorption/source media [245]. The sorption/source media may be adsorbents such as activated carbon, zeolite, and polymers. Biodegradable polymers, such as PCL, PBS, poly(3-hydroxybutyrate-co-3-hydroxyvalerate) (PHBV), and PLA, have the potential to be used for environmental remediation [246]. These polymers act either by absorbing the contaminants from any contaminated system (sorption mechanism) or by supplying carbon and energy to microorganisms to facilitate the denitrification mechanism.

PLA, among other biodegradable polymers, is being investigated for possible use in environmental remediation due to its availability as a raw material and its relatively lower price. One example of commercialized PLA used for environmental remediation is Hydrogen Release Compound (HRC[®]), produced by Regenesis Bioremediation Products (San Clemente, CA). This product is manufactured in a liquid and a gel-like form intended for controlled-release of LA for certain durations [247]. However, to a certain extent, PLA characterization and research for environmental applications are limited. The efficiency of biodegradable polymers for environmental applications relies on their T_g . In the case of PLA, its ability to adsorb contaminants would be limited to conditions $>60^\circ\text{C}$ [246]. In addition, PLA has more resistance to microbial activity than that of other biodegradable polymers like PCL [248]. The resistance of PLA toward microbial activity is mainly due to the high molecular weight of PLA ($\geq 2.0 \times 10^5$ Da). Thus, microorganisms need more time to use PLA as their food source; hydrolysis should reduce the M_w to be manageable for the microorganisms to use it. Consequently, lower molecular weight PLA is likely a better candidate for the denitrification mechanism. Studies on PLA with $M_w < 1.0 \times 10^4$ Da showed a significantly

greater removal rate of nitrogen than for PLAs of higher molecular weight [246]. Meanwhile, the focus for environmental remediation applications seems to lie with other aforementioned biodegradable polymers (*i.e.*, PCL, PBS, PHBV) due to their effectiveness in adsorbing contaminants, such as chlorophenols, at room temperature [246].

2.5.6 Other applications

Some other commercialized or potential applications of PLA include paints, cigarette filters, 3D printing, and parts for space exploration [249]. A 3D portable on-board printer was developed by collaborative work of Altran Italia, Thales Alenia Space, and the Italian Institute of Technology for use in space; the printer was produced with approximately 5.5 kg of PLA. PLA characteristics, such as glossiness and multicolor appearance, make PLA one of the main choices for 3D printing. A high accuracy for dimensional parts can be achieved with PLA because it poses less warp behavior than commonly used printing filament materials like ABS [249]. PLA has been used to develop tow fibers for cigarette filters by D.M. Enterprises Pvt. Limited (Hong Kong) to replace cellulose acetate tow, an invention that may help to reduce cigarette litter. Although cellulose acetate is a natural product, its degradation is relatively slow; the addition of acid may improve the degradation rate. However, concentrated acid worked better to accelerate the degradation process of cellulose acetate, thus it is not a safe choice for such applications [250]. Therefore, the use of biodegradable polymers like PLA may alleviate the current degradation issue associated with cigarette filters.

Another newly developed application of PLA is as a water-based paint: Fujitsu Laboratories Ltd. developed this product to reduce the level of volatile organic

compounds commonly found in solvent-based paints. Isocyanate reactant was used to improve the stability of PLA emulsion and, in turn, the quality for its final application as water-based paint [251]. Additionally, Fujitsu in collaboration with Toray Industries, Inc. in 2005, developed a PLA alloy that had high heat resistance and flame retardant used to mass produce the Fujitsu's FMV-BIBLO notebook models [252]. Similarly, PEGA D&E of PEGATRON Corp. collaborated with the Plastic Industry Development Center (Taichung, Taiwan) to produce an alloy consisting of both PLA and medical recycled PC for use in consumer electronics [253].

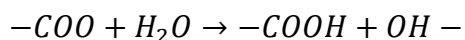
Many newer applications of PLA surfaced with the help of existing and newly developed technologies. Most of these applications were achieved through a fundamental understanding of the physicochemical, mechanical, stereo-chemical, and morphological properties of PLA.

2.6 PLA Degradation

PLA polymeric parts can be exposed to different environments during their lifetime, which may promote their degradation. Degradation leads to irreversible changes of the polymer until it gradually fails due to the loss of various properties. Such loss of properties can occur under different mechanisms, including chemical hydrolysis, microbial, photochemical, thermal, and enzymatic degradation, which mainly occur by main chain scission or side chain scission [2, 254, 255]. Depending on the application, degradation of PLA can be an advantage or a disadvantage. In the case of mulch films or contaminated packages, degradation through different mechanisms is one of the advantages of PLA. In this section, the main mechanisms of PLA degradation in commercial applications are discussed.

2.6.1 Hydrolysis

Hydrolytic degradation takes place when PLA is exposed to moisture: the ester groups of the main chain of the polymer are cleaved, resulting in a decrease of molecular weight and the release of soluble oligomers and monomers. The products of the hydrolysis self-catalyze the reaction [256-258]. Thus, hydrolysis of PLA starts by the diffusion of water molecules into the amorphous regions, which in turn initiates the cleavage of the ester bonds. Then, degradation continues in the boundary layer of the crystalline domains [259, 260]. The following reaction shows the hydrolysis of the ester groups of aliphatic polyesters, as in PLA, in the presence of water:



Information regarding PLA hydrolysis in non-medical applications, such as in food packaging, plasticulture, and environmental remediation, is scarce. Only a few studies have been done in different environments and media (other than in medical settings) in which PLA can be in contact with water during its use, leading to hydrolysis reactions.

For example, PLA has been used in plasticulture as mulch films (as shown in section 2.5.4) where PLA can be affected by a number of abiotic factors, such as temperature, pH, soil moisture, and UV radiation, which all play relevant roles in the degradation. During abiotic degradation, the mulch films are fragmented, the tensile strength of the material weakens, and a slight reduction of M_w occurs [240], then PLA is converted into CO_2 , water, and inorganics. Hydrolysis is one of the mechanisms that helps degrade PLA in this environment. Furthermore, in other agriculture applications, for example during controlled release of herbicides for stimulating the plant growth and

improving yield, hydrolysis of PLA takes place since the material is exposed to high RH or put in direct contact with water [8, 261, 262].

In packaging applications, when PLA is used for fresh produce or beverage containers, it is exposed to humid environments that can trigger hydrolysis reactions. Copinet *et al.* reported that at high RH the rate of hydrolysis increases due to absorption of water molecules into PLA. As a result, a decrease of the M_w was observed, leading to a reduction in T_g from 60 to 19.4°C when exposed to 100% RH, and a 50% reduction of the initial percent elongation at break at 30°C in 15 and 10 weeks when PLA films were exposed to 50 and 100% RH, respectively [263].

PLA containers have been developed to be in contact with water, cold-chain dairy, and juices, so the PLA is in contact with different environments at different pH and polarity. The medium pH influences the rate of hydrolysis of PLA-based materials. In strong acidic and basic media, polymer chains are more easily degraded since the hydrolysis reactions are catalyzed by the presence of hydronium and hydroxide ions (**Figure 2.16**) [264-267]. For example, if PLA is used for a citrus juice bottle, the PLA will be exposed to an acidic medium (pH <4) making the hydrolysis mechanism proceed via chain-end scission [257, 268].

In PLA containers used for alcoholic products, ethanol will swell the PLA matrix, act as plasticizer, and increase the chain mobility; as a result, the PLA will be subjected to solvent induced crystallization (SIC) [269-271]. To certify polymers for food contact applications, common food simulants are used for migration studies, including 95% ethanol, 50% ethanol, and water for fatty, alcoholic, and aqueous liquid products, respectively [272, 273]. PLA films exposed to alcohol solutions at 40°C undergo

hydrolysis, in turn causing a large reduction of M_n , especially when PLA films are exposed to 50% ethanol [274] (**Figure 2.17**).

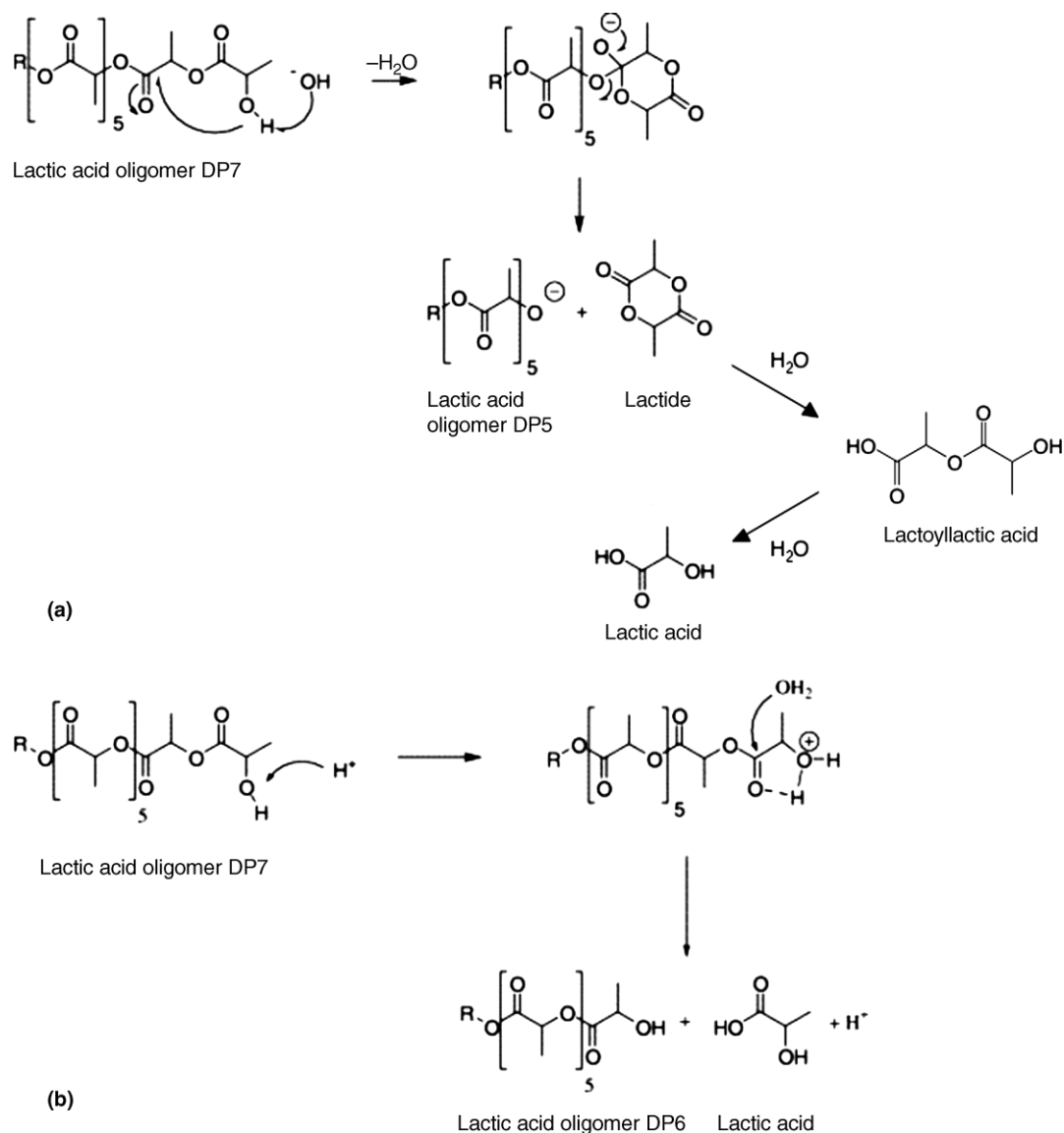


Figure 2.16 Hydrolytic chain cleavage mechanisms of PLA in alkaline (a) and acidic (b) media. “Reprinted from Polymer, 42, Jong *et al.*, New insights into the hydrolytic degradation of poly(lactic acid): participation of the alcohol terminus, 2795-2802, Copyright (2001), with permission from Elsevier” [257].

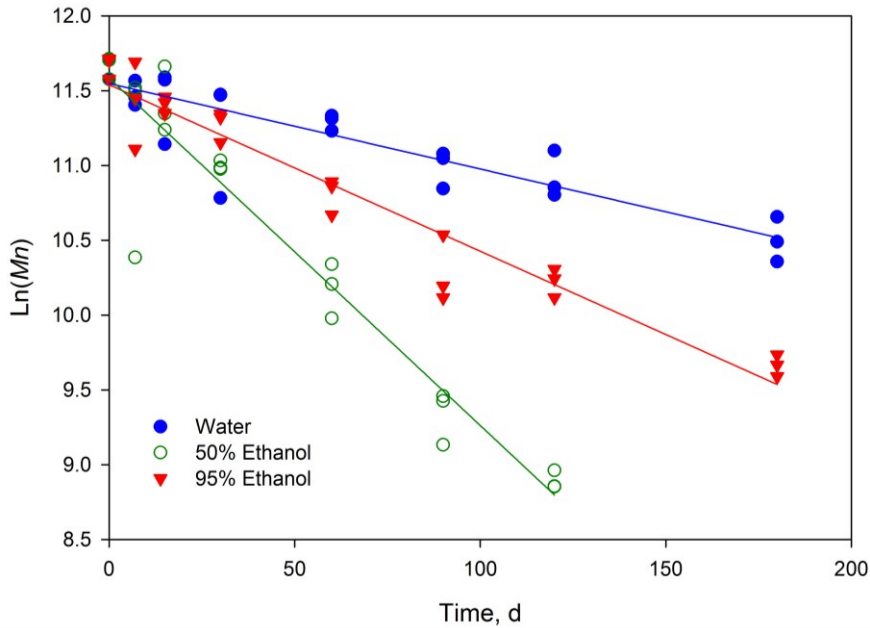


Figure 2.17 $\ln(M_n)$ as a function of time during hydrolysis of PLA films into water, 95% ethanol, or 50% ethanol at 40°C.

Temperature also plays a crucial role in the hydrolysis of PLA in non-medical applications. The rate of degradation of PLA increases with temperature, resulting in faster cleavage of the ester bonds [258, 263, 275, 276]. When PLA is immersed in water at 30, 40, and 50°C, chain scission is accelerated as temperature increases, and an increment of carbonyl index attributed to the formation of carboxyl groups during hydrolysis is also expected [277].

2.6.2 Thermal degradation

PLA is susceptible to thermal degradation during processing, leading to a decrease in M_w and the rheological and mechanical properties of processed PLA parts. Thermal degradation of PLA can be attributed to the hydrolysis initiated by residuals of water during processing, unzipping depolymerization reaction, random main-chain scission,

and intramolecular and intermolecular transesterification (**Figure 2.18**) [278]. Therefore, drying PLA resins before processing is highly recommended.

A number of studies have addressed the complex mechanism of the thermal degradation of PLA. Kopinke *et al.* [279, 280] proposed that the dominant pathway of the PLA thermal degradation above 200°C is intra- and intermolecular ester exchange, *cis*-elimination, radical and concerted nonradical reactions. McNeill and Leiper [281] stated that the mechanism is based upon a hydroxyl end-initiated ester interchange, non-radical process. Aoyagi *et al.* [282] and Abe *et al.* [283] proposed that PLA not only follows one mechanism during pyrolysis but this thermodegradation also involves more than two pathways, such as random scission, unzipping depolymerization, and intermolecular transesterification. Furthermore, changes of activation energies of the thermal degradation process have been reported, with increasing weight loss using isothermal methods going from 103 to 72 kJ.mol⁻¹, 80 to 160 kJ.mol⁻¹ and 170 to 190 kJ.mol⁻¹ involving complex kinetic mechanisms [282, 284, 285].

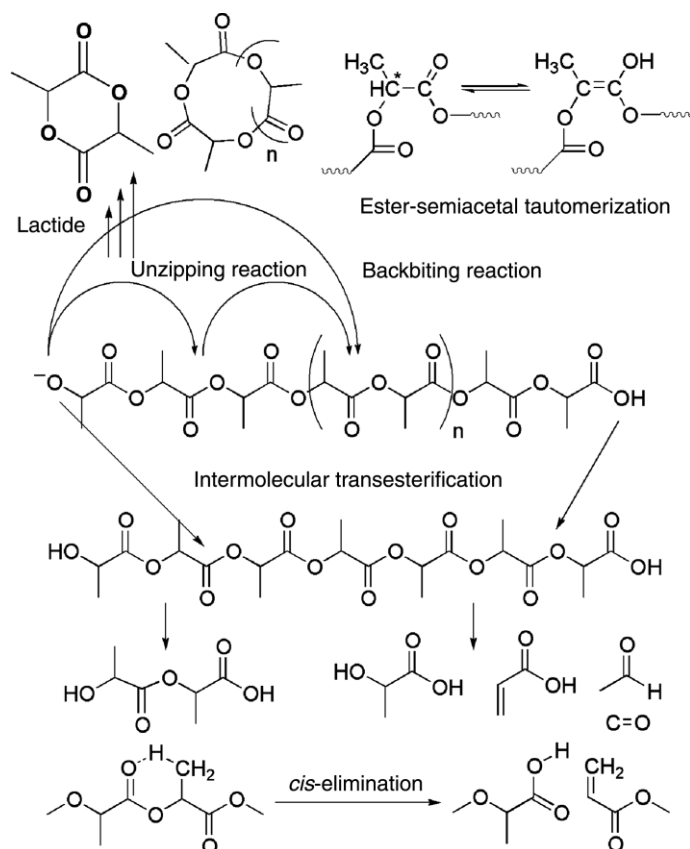


Figure 2.18 Thermodegradation mechanisms of PLA. “Reprinted from: Poly(lactic acid).

Synthesis, structure, properties, processing, and applications, Nishida, Thermal degradation, 401-412, Copyright (2010), with permission from John Wiley & Sons, Inc.” [286].

Thermal degradation of PLA is a complex phenomenon leading to the appearance of different compounds such as low molecular weight molecules and linear and cyclic oligomers with different M_w and lactide. Other degradation products have been detected such as CO, CO₂, acetaldehyde, and methyl ketone [280, 281, 285]. Kopinke *et al.* [280] found that temperatures above 270°C lead to degradation of PLA and that the formation of acetaldehyde increases with temperature. However, McNeill and Leiper [281] showed that during degradation temperatures in the range of 230–440°C, acetaldehyde was formed in the highest concentration at 230°C and then a

decreasing effect was observed at 440°C. The decrease in proportion can be explained by the thermal degradation of acetaldehyde, involving chain reactions to obtain the by-products CH₄ and CO.

PLA thermal degradation is influenced by several factors such as initial M_w , moisture, and residual polymerizing catalysts [287, 288]. Moisture in the resin, temperature, and residence time in the extruder during processing contribute to the decrease in M_n and stress and strain at break due to the dependency of these parameters on M_w [289, 290]. The presence of residual metals is a parameter that also causes drastic thermal degradation of PLA. Kopinke *et al.* [280] showed that PLA in the presence of residual Sn from the polymerization process leads to a selective depolymerization step producing lactide. Cam and Marucci [291] observed that the presence of residual metals assists thermal degradation in PLA, affecting the onset temperature in the order of Fe > Al > Zn > Sn. Furthermore, the presence of stannous octoate catalyst (Sn(Oct)₂) in a proportion of 0.5, 1, and 5 wt%, accelerated the degradation of PLA. The presence of 5 wt% of Sn(Oct)₂, even at the low temperature of 160°C, accelerates PLA degradation [278, 292]. Abe *et al.* [283] found that Zn catalyzes intermolecular transesterification to produce linear PLA oligomers, and selective unzipping depolymerization of cyclic PLA oligomers to produce lactides.

Improving the thermal stability of PLA to avoid the degradation of the polymer during processing, via end-protection or using chain extenders, has been studied. End-protection of the hydroxyl group has been assessed due to the mechanism of pyrolysis in PLA by a back-biting reaction, which causes an unzipping depolymerization starting from the hydroxyl ends of the chains [280, 281, 284]. One method is by the acetylation

process, which not only achieves end protection, but also is capable of removing residual metals that accelerate degradation of PLA [283, 288, 291, 293]. Fan *et al.* [293] studied the relationship between the effects of the acetylation and metal content by acetic anhydride where the stabilization was due to the elimination of residual Sn. On the other hand, chain extenders, such as tris (nonylphenyl) phosphite (TNPP), polycarbodiimide (PCDI) and Joncryl[®], have been used where the onset temperature of degradation is increased due to the reduction of active sites on the chain end per mass by the production of longer polymer chains [273, 294, 295].

2.6.3 Photodegradation

PLA is exposed to sunlight during its lifetime for applications in plasticulture, packaging containers, or films, thereby inducing plastic degradation due to the low wavelength and high-energy UV radiation. Other applications involve the use of UV irradiation for sterilization of biomedical and pharmaceutical products. The carbonyl group presence in the PLA chemical structure absorbs UV radiation at about 280 nm via $n-\pi^*$ electron transition, thus increasing the susceptibility of PLA to photodegradation [296].

Aliphatic polyesters, including PLA, photodegrade under UV and sunlight exposure via the Norrish II mechanism (**Figure 2.19**) whereby chain scission of the main chain occurs and the formation of C=C double bonds takes place along with carboxyl end groups and where the reaction is triggered by the electron transition at C=O [297-300]. The main-chain scission of PLA during photodegradation occurs randomly; the photodegradability is higher in the amorphous regions than in crystalline regions, resulting in the reduction of M_w where anhydride groups are formed and decreasing the rate of crystallization [299, 301, 302]. When UV radiation penetrates the polymer, the

degradation proceeds via bulk erosion where the light penetrates the polymer without a significant reduction in its intensity regardless of the chemical structure and the crystallinity of the polymer [302].

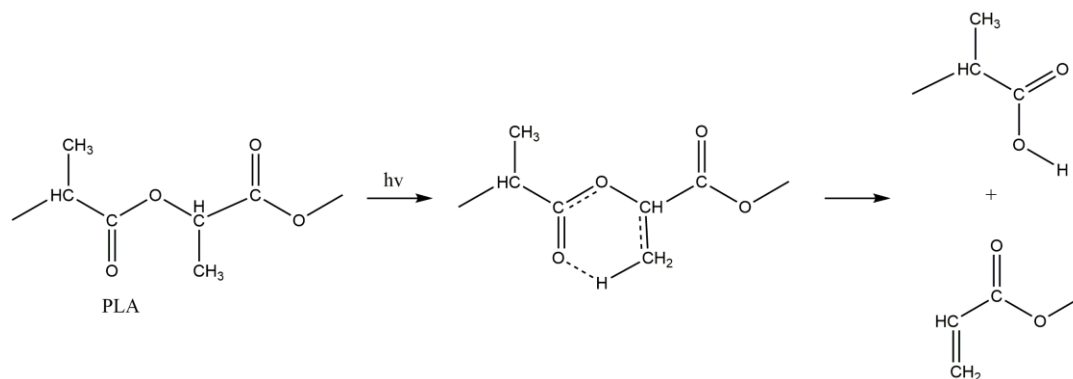


Figure 2.19 Photodegradation of PLA via Norrish II mechanism, adapted from Tsuji *et al.* [302].

Other basic mechanisms have been proposed to predict the degradation of PLA products by UV irradiation. Janokar *et al.* [303], studying the effect of wavelength on PLA photodegradation at a range of 232–500 nm, concluded that photodegradation mainly occurs between 200–300 nm and proposed two mechanisms. One mechanism leads to breakage of the main chain C-O by a photolysis reaction (**Figure 2.20a**), and the other leads to the formation of hydroperoxide derivatives and subsequent degradation compounds containing carboxylic acid and diketone end groups by photooxidation (**Figure 2.20b**).

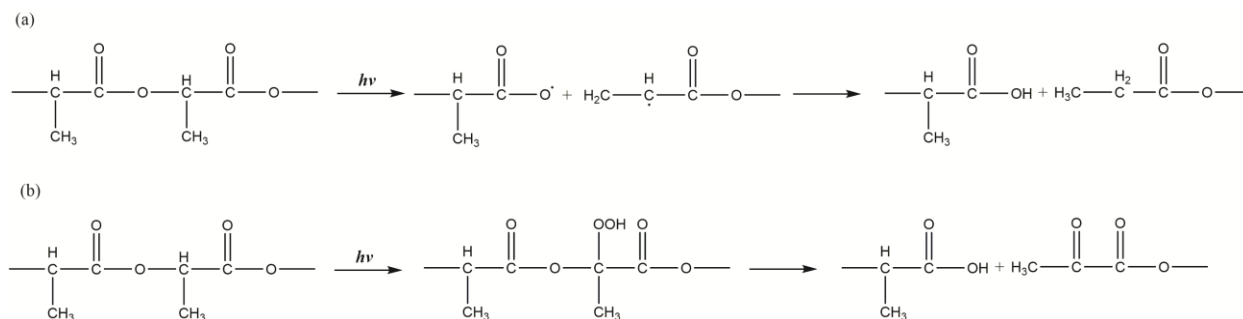


Figure 2.20 Mechanisms of photodegradation of PLA, adapted from Janokar *et al.*

[303].

UV irradiation can have different effects in PLA. UV irradiation can cause a decrease in M_w of PLA; UV also causes an increase in M_w distribution, which has an effect on mechanical properties, such as the decrease in stress and strain at break, where PLA becomes brittle over time [302-305]. Furthermore, a faster degradation takes place when exposure time to UV light increases [301].

The combination of different factors can affect the degradation of PLA. Copinet *et al.* [263] studied the effect of temperature and humidity of PLA exposed to UV irradiation at 315 nm, where the UV light accelerated the reduction of molecular weight, T_g , percentage of elongation at break, and crystallinity at different temperatures and RH. During this study, from the cleavage of C-C bonds of the main chain, two radicals were supposed to be produced (**Figure 2.21**), and two others from cleavage at C-O of the main chain (**Figure 2.22a**), and from cleavage of ester bonds (**Figure 2.22b**).

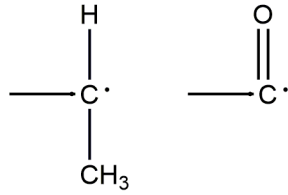


Figure 2.21 Radicals generated during photodegradation of PLA from cleavage of C-C bonds, adapted from Copinet *et al.* [263].

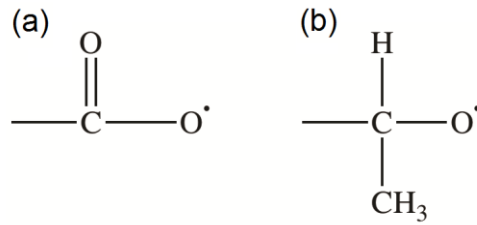


Figure 2.22 Radicals generated during photodegradation of PLA (a) from C-O and (b) ester bond cleavage, adapted from Copinet *et al.* [263].

Besides UV light, PLA can be exposed to different kinds of radiation such as γ -irradiation when the material undergoes a γ -sterilization process. The effect of γ -radiation has been studied by Balbanalbi *et al.* [306] using electron paramagnetic resonance (ESR) spectroscopy, where the radicals formed during degradation were the result from the scission of the ester bonds and hydrogen abstraction from the methane groups of PLA main chain. Birkinshaw *et al.* [307] examined the effect of γ -radiation on the molded poly-D,L-lactide, where changes in mechanical properties and reduction in M_w were observed, making the sample brittle due to random chain scission of the polymer. γ -radiation occurs mainly in the amorphous region of the polymer [308].

2.7 End-of-life Scenarios for PLA

According to the 2015 Global Sustainable Development Report, the increasing global awareness of sustainability is noticeably changing consumer preferences, and producers have to adapt to meet those preferences [309], along with the need of tools that allow the assessment of environmental impacts of materials [310]. Consequently, there is increasing demand for bio-based polymers to replace traditional fossil-based polymers, as the latter are perceived to have higher environmental footprints [3, 5, 311].

PLA is likely the most popular bio-based polymer. It is recyclable and biodegradable under industrial composting (IC) conditions through an initial hydrolysis process [2], and it has been proposed to be used especially in cases where plastics become highly contaminated and are difficult to recover through recycling such as food packaging and agricultural mulch films. While PLA is derived from renewable resources and offers an alternative disposal route (*i.e.*, composting), there are limitations to its implementation due to the lack of suitable infrastructure for sorting, recycling, and/or composting PLA products at their end of life [3].

The European Commission introduced a five-level waste hierarchy in the European Waste Directive 2008/98/EC, which includes: 1) prevention, 2) reuse, 3) recycling, 4) other recovery, and 5) disposal [312]. Likewise, the U.S. Environmental Protection Agency (EPA) has a four-level integrated waste management hierarchy, including: 1) source reduction (including reuse), 2) recycling (including composting), 3) combustion with energy recovery, and 4) disposal through landfill [313, 314]. The four components are important within the integrated waste management system as shown in **Figure 2.23**.

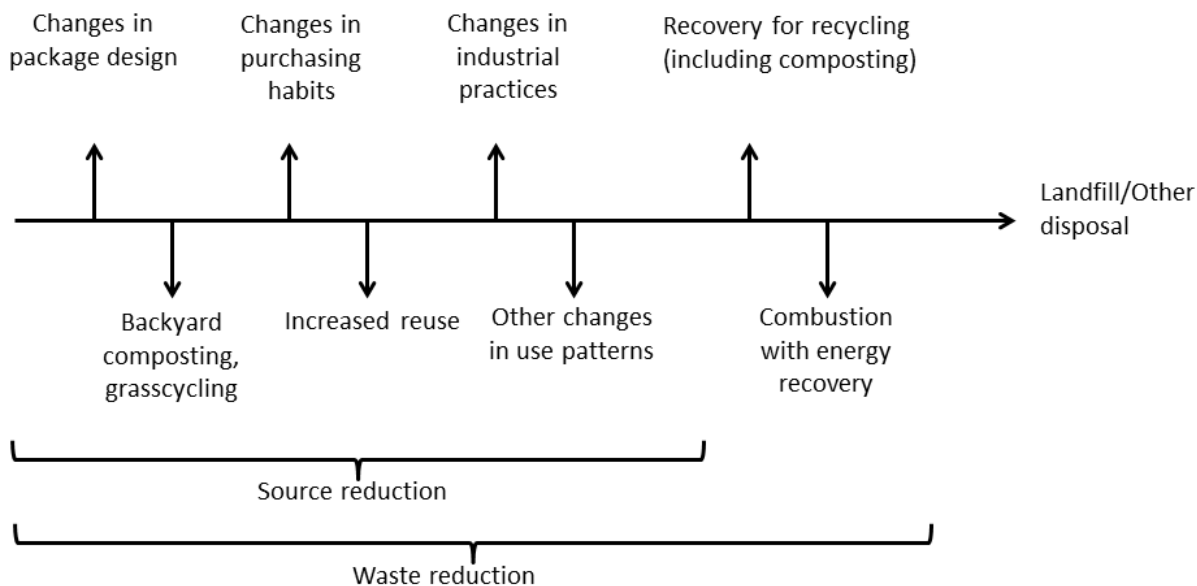


Figure 2.23 Diagram of solid waste management, adapted from the U.S. Environmental Protection Agency in *Advancing Sustainable Materials Management* [314].

PLA is a special polymer since it can be treated in all levels of the hierarchy, including composting as an end-of-life scenario [315]. However, according to *U.S. EPA Advancing Sustainable Materials Management: Facts and Figures 2013* [314], about 254,110 thousands of tons of MSW were generated in the U.S. in 2013, from which about 25.5% was recycled, 8.8% was composted, 12.9% was combusted with energy recovery, and 52.8% was discarded in landfills. Packaging and containers comprised the biggest portion (29.8%) of the MSW, from which only about 5.2% of plastic packaging was recovered, mostly PET (24.8%) and HDPE (16%). On the other hand, from the 50 thousand tons of PLA waste that was generated (mostly for plates and cups, packaging, and other non-durable goods), only a negligible amount (less than 5 thousand tons, 10%) was recovered through recycling and/or composting [313, 314].

2.7.1 Source reduction (reuse)

For new applications of PLA to enter the market, it is important to analyze in more detail the preferred end-of-life scenarios [315]. Waste management hierarchy emphasizes source reduction by designing products, especially packaging, to achieve material reduction (lightweighting), longer product life, and reuse [313, 314, 316].

Lightweighting of PLA has been of great interest not only for its economic value but also for waste reduction. Nevertheless, with this approach one must consider the possibility of reduced mechanical functionality of the PLA. Efforts made over the years to produce lightweight PLA materials with good physical and mechanical properties include producing reinforced PLA with fibers/fillers, PLA composites, and foamed PLA, to name a few. PLA–sugar-beet composite materials produced by compression-heating techniques have reduced density compared with PLA; however, the mechanical properties of the composite materials were affected negatively with increasing amounts of sugar beet pulp [317]. Peinado *et al.* [318] fabricated PLA reinforced with functionalized sepiolite-aminosilane grafted filler and CFA to produce lightweight PLA with improved mechanical properties. Although the addition of CFA significantly reduced the material density, its mechanical properties were compromised in the absence of the functionalized sepiolite filler. A synergistic effect of the CFA and the functionalized sepiolite was reported, where the density of the material was significantly reduced with an improved modulus. Additionally, the application of lightweight PLA-cellulose fiber composite was extended to the automotive industry for use as floor-load materials [319]. The composite with 50 wt% fiber fraction demonstrated the highest tensile strength due to the ability of this fiber to form hydrogen bonding networks within PLA matrices. The

composites with 50 wt% fiber fraction with fixed nominal density of 0.2, 0.3, and 0.4 g/cm³ met the flexural stress and stiffness for the supportable load floor weight of vehicle specifications [319]. As the market for PLA parts increase, we expect additional research of technologies to lightweight PLA.

In the case of retail packaging, a wide-scale reuse system for materials has restricted potential due to the logistics and cost involved in returning empty containers to suppliers [320]. PLA packaging is not the exception. On a much smaller scale, PLA products and packaging could be reused (whether for its primary purpose or not) by households, assuming the PLA products and packaging maintain the desired properties, functionality, and safety.

2.7.2 Recycling

Following the hierarchy, the next preferable disposal route of PLA would be recycling, which can be either chemical or mechanical [62, 321, 322]. PLA packaging, such as water bottles or blisters, usually has low contamination, making recycling a viable route to recover the material [62]. However, as previously mentioned, the lack of infrastructure to collect PLA and the logistics required to recover make it challenging to collect and recycle PLA. The economic cost involved in recycling at the post-consumer level does not usually favor the recovery and recycling of plastics other than HDPE and PET (mostly bottles); these two post-consumer resins have a big market demand since they can be used to form new bottles or other products like fibers, clothes, carpets, and textiles [62, 323].

During chemical recycling, PLA is hydrolyzed at a high temperature to yield LA, which can be readily polymerized to high M_w PLA [62, 321, 322]. The disadvantage of

chemical recycling is that it is still complex and expensive [62]. NatureWorks LLC have successfully recycled off-grade Ingeo™ by using chemical recycling [324].

Mechanical recycling (MR) would be the easiest and cheapest way to recycle post-consumer PLA, and it involves recovering, sorting, regrinding, and reprocessing (*i.e.*, melt processing) the PLA waste [62]. However, there is a debate on whether PLA can be successfully recycled in the current plastics recycling infrastructure due to the contamination of the recycling stream. According to Cornell [323], for PLA to be mechanically recycled, it must be either completely fungible with existing recycled resins or be available in sufficient quantity to achieve the needed critical mass. On one hand, there are some initiatives to facilitate the recycling of PLA through the existing infrastructure for recovery and sorting. One initiative is to improve the material identification by establishing a new resin identification code (RIC) exclusive to PLA since it currently falls in the category of “7-OTHER” according to the ASTM D7611 – Standard Practice for Coding Plastic Manufactured Articles for Resin Identification; this category is shared with other uncoded materials such as polycarbonate, ethylene vinyl alcohol, to name a few. Other initiatives are focused on the use of technologies like near-infrared or black light illumination to facilitate the sorting of PLA from the waste stream [325]. Thus, if there are sufficient PLA containers entering the waste stream, recycling entrepreneurs may explore means of recovering and recycling PLA in a cost-effective fashion. Various organizations, such as the Bioplastics Recycling Consortium and Greenplastics Inc., were formed to develop solutions for post-consumer bioplastic materials [326, 327]. On the other hand, the National Association for PET Container Resources (NAPCOR) and the Association of Postconsumer Plastic Recyclers (APR)

have refuted the idea of mixing biopolymers like PLA into the existing stream of recycled containers, expressing concerns regarding the cost of separation and processing, increased contamination, and reduced quality of the recycled material [323, 328].

2.7.3 Composting

Biodegradation is considered to be nature's way of recycling [4, 329]. PLA is biodegradable under IC conditions starting with an hydrolysis process, in which ultimate PLA degradation results from the action of naturally occurring microorganisms at a high temperature (58°C) and 50% RH [329]. **Figure 2.24** shows a typical large-scale composting process in which biodegradable materials decompose, resulting in compost, CO₂, H₂O, and minerals. There are three indispensable factors for polymer biodegradation to take place: substrate (chemical structure and conformation), environment (temperature, oxygen, and moisture) and microorganisms (metabolic pathways and enzymes) [330, 331].

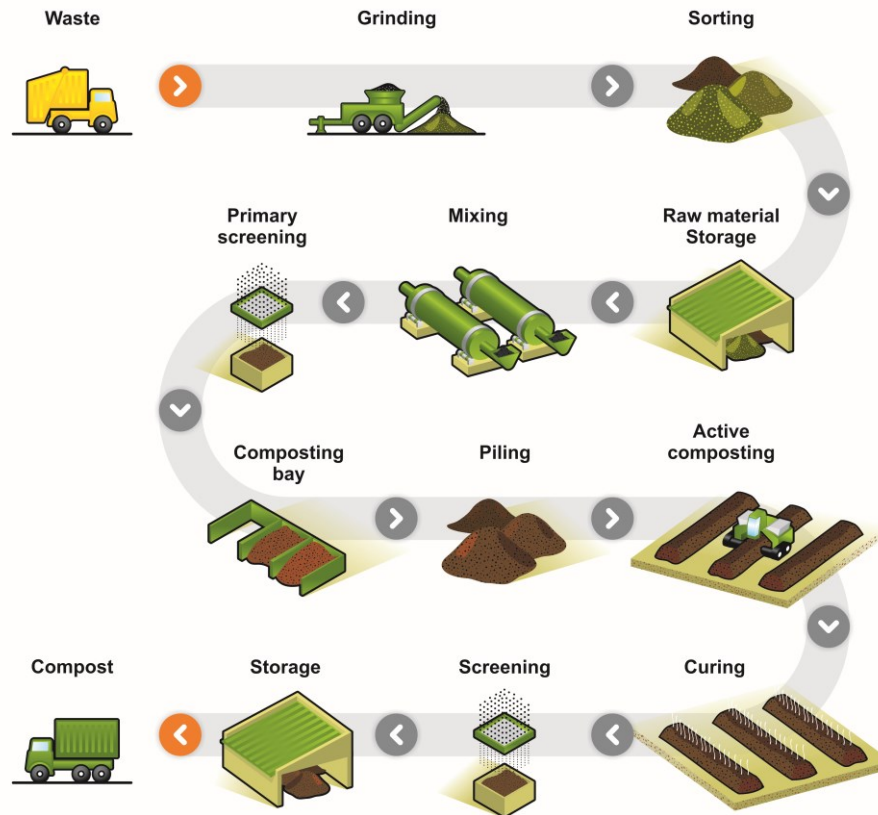


Figure 2.24 Large-scale commercial composting process. “Reprinted from Polymer International, 57, Kijchavengkul *et al.*, Compostability of polymers, 793-804, Copyright (2008), with permission from Wiley” [329].

Biodegradation of polymers (including PLA) usually takes place in two main steps: primary degradation, in which fragmentation of the polymer chain occurs due to hydrolysis or another oxidative reaction, and ultimate biodegradation, in which the microorganisms assimilate the low M_w chains formed (**Figure 2.25**) [330-332].

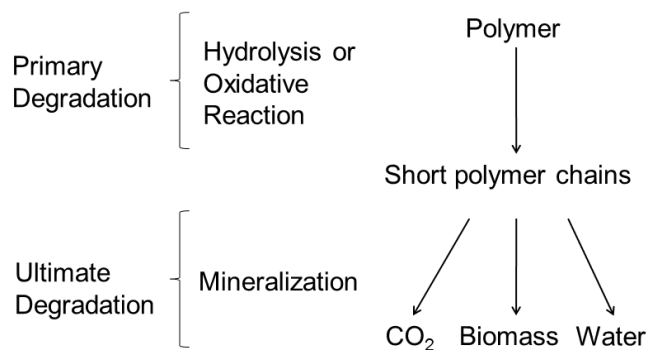


Figure 2.25 Schematic of polymer biodegradation mechanism, adapted from Leejarkpai *et al.* [332].

Biodegradation can be evaluated by different analytical techniques, either in a direct or an indirect approach [333], but respirometric methods are usually preferred to evaluate biodegradation of polymers in laboratory settings [330]. Respirometric methods directly measure the consumption of oxygen or the evolution of CO₂ [333]. A number of standards have been developed to define the requirements and the methodologies to assess the biodegradability of plastic materials [4]. ASTM D5338 and ISO 14855 are the main standards describing the measurement of an aerobic biodegradation of plastic materials under composting conditions by analysis of evolved CO₂ [334, 335]. **Table 2.4** shows a basic comparison between these two standards.

Table 2.4 General requirements to test biodegradation under laboratory conditions and comparison between ASTM D5338 and ISO 14855 standards [334, 335], reproduced from Castro-Aguirre, E. [336].

Requirement		ASTM D5338	ISO 14855
Apparatus	Number of bioreactors	At least 12	At least 9
	Volume of bioreactors	2 to 5 L (sufficient headspace)	2 L or higher (sufficient headspace)
	Aeration	Water saturated CO ₂ -free	Dry or water saturated CO ₂ -free
	Sensor	Accurate flow rate Specific sensors or appropriate gas chromatographs	At pre-set flow rate Infrared analyzer Gas chromatograph
Compost Inoculum	Age	2-4 months old	2-4 months old
	Homogeneity	Sieved on a screen <10 mm Allows addition of structural material	Sieved on a screen of about 0.5 to 1 cm Allows addition of structural material
	Dry solids	Between 50 and 55%	Between 50 and 55%
	Volatile solids	Ash content <70%	No more than 15% of wet or 30% of dry solids
	pH	Between 7 and 8.2	Between 7 and 9
	Production of carbon dioxide	Between 50 and 150 mg of CO ₂ per gram of volatile solids over the first 10 days	Between 50 and 150 mg of CO ₂ per gram of volatile solids over the first 10 days
	C/N ratio	Between 10 and 40	Between 10 and 40
Substrate	Shape	Granules, powder, film, simple shapes	Granules, powder, film, simple shapes
	Surface area	2×2 cm max.	2×2 cm max.
	Positive control	Cellulose (particle size <20 μm)	Cellulose (particle size <20 μm)
	Negative control	Polyethylene	Not required
Other	Temperature	58 ± 2°C	58 ± 2°C
	Water content	About 50%	About 50%
	Ratio of mixture	6:1 sample (dry solids)	6:1 sample (dry solids)
	Frequency of measurement	At least daily	At least twice per day
	Test period	At least 45 days	Not exceeding 6 months
	Incubation	Dark or diffused light	Dark or diffused light
	Oxygen concentration	6% or higher	6% or higher

The aerobic biodegradation of PLA film (Ingeo™ 2003D) in compost was evaluated by using an in-house-built direct measurement respirometer (DMR) following the methodology described by Selke *et al.* [337], in which bioreactors containing PLA, blank (compost only), and cellulose (positive reference) were tested. **Figure 2.26a** shows that the PLA film produced a significantly higher amount of CO₂ than the blank, meaning that microorganisms were able to use the carbon from the polymer for their metabolic processes. The amount of CO₂ produced by the PLA film is comparable with that for the positive reference in the same time period. **Figure 2.26b** shows that the PLA film mineralized above 70% after two months of composting. PLA also presented a lag time during the first 3 weeks of the test, which is related to the primary degradation where the M_w of the polymer should be reduced to around 9.0×10^3 Da (data not shown) for the microorganisms to start the ultimate degradation or mineralization.

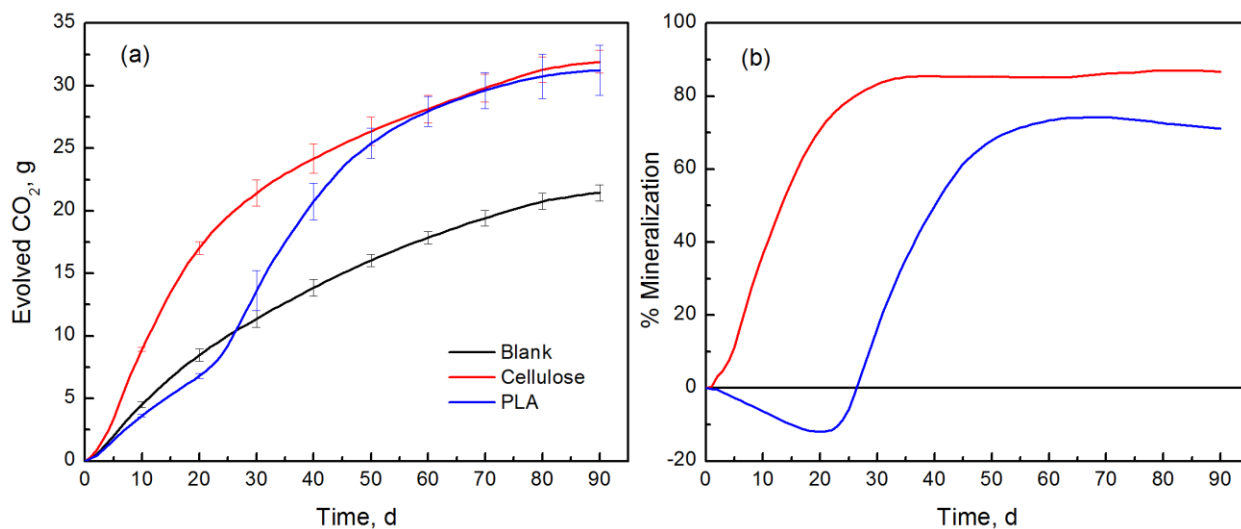


Figure 2.26 (a) Amount of CO₂ evolved from blank, cellulose, and PLA film; (b) Percentage mineralization of cellulose and PLA film.

Composting would be the optimal end-of-life option for contaminated PLA. However, there are only few existing composting facilities that accept biodegradable

plastic materials since most are concerned that biodegradable plastics are not easily distinguishable from conventional plastics and that quality control is difficult [315].

Similar to recycling, there is a big challenge for collecting and sorting PLA waste from other MSW so that the PLA can be sent to the composting facilities. Hence, the benefit provided by PLA of offering an additional disposal route (biodegradation or composting) is only realized if PLA is disposed in an appropriate waste management system that uses their biodegradable features [320]; otherwise, the PLA would accumulate like other plastic materials in the landfill.

2.7.4 Incineration with energy recovery

The incineration of waste is not only a volume-reduction practice, but it has evolved to waste-to-energy plants in which energy is recovered from waste materials to produce heat or electricity, followed by the disposal of the fly and bottom ashes. Incineration of waste with energy recovery also reduces the dependency of using fossil resources and other fuel sources. Even though air pollution is often the main concern about incineration, the improvements in gas cleaning technology allow the reduction of pollutants released to the atmosphere [338, 339].

Thus, some of the energy content of plastics can be recovered by incineration, and reasonable energy efficiency can be achieved through various approaches such as co-fuelling of kilns [320]. Disposing PLA waste via incineration recovers the energy embedded in PLA, representing a CO₂-neutral method of energy production, and it contributes to the conservation of fossil resources [340]. However, energy recovery does not reduce the demand for raw material used in plastic production [320], and it is also important to consider the composition of the emitted combustion gases [340].

NatureWorks LLC reported that Ingeo™ resin heat content is about 19.5 MJ.kg⁻¹ [341]. This value is in agreement with the calorific values reported by Laußmann *et al.* [340] (**Figure 2.27**), who carried out comparative experiments between biopolymers, fossil-based polymers, and fuels. They concluded that biopolymers, including PLA, are suitable for thermal energy recovery since they have calorific values comparable to cellulosic-based materials, and they do not produce additional toxicologically critical substances during combustion [340].

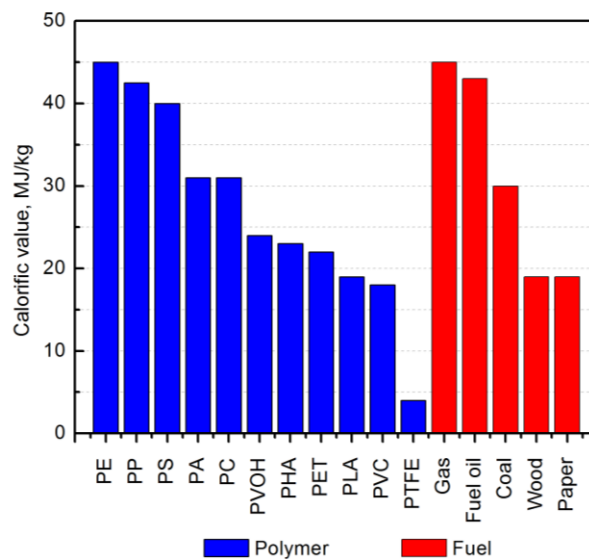


Figure 2.27 Calorific values of selected materials, adapted from Laußmann *et al.* [340].

2.7.5 Landfill

The less preferable option to dispose PLA is landfilling (LF). According to the U.S. EPA, although disposal of MSW to landfill decreased from 145.3 million tons in 1990 to 134.3 million tons in 2013, landfill remains the most economic and attractive method for handling MSW [313, 314]. LF has some environmental impacts primarily due to gas and leachate formation, including health hazards, fires and explosions, vegetation damage, unpleasant odors, landfill settlement, ground water pollution, air pollution, and global

warming [342]. The drawback of disposing plastics in landfills lies in the fact that most plastic materials do not degrade in a practical period of time and end up accumulating [343]. Landfills usually do not provide the appropriate environment to promote degradation, and their conditions vary considerably by geography [344]. On the other hand, PLA biodegradation is highly dependent on temperature and moisture, since these two factors promote hydrolysis of the polymer chains, and in turn accelerate biodegradation. At mesophilic temperatures little or no degradation of PLA is observed [344].

According to NatureWorks LLC, their resin Ingeo™ is stable in landfill conditions with no statistically significant quantity of methane released. Studies performed under accelerated landfill conditions at different temperatures and moisture levels found that the amorphous PLA did generate a small amount of methane in the test at 35°C, but no methane was generated in the test at ambient temperature. Semicrystalline PLA did not generate a significant amount of methane in any of the tests. The company also pointed out that it is likely that any degradation of PLA in a landfill would require a chemical hydrolysis step prior to any biodegradation [344].

2.8 Environmental Footprint of PLA

The increasing global awareness of sustainability is changing the perceptions and preferences of consumers; therefore, environmental assessment tools are being used to evaluate the EFP of systems and products [310]. An EFP is a quantitative measurement describing how human activities can inflict different impacts on global sustainability considering the environmental, social, and economic indicators [345].

Life cycle assessment (LCA) can be used to evaluate the EFP of PLA. LCA is a method to assess the environmental performance of products and/or potential impacts of a system considering raw materials acquisition, production, use, and disposal [346, 347]. LCA is conventionally thought of as a “cradle-to-grave” approach; however, in the last few years a “cradle-to-cradle” approach has been introduced [345].

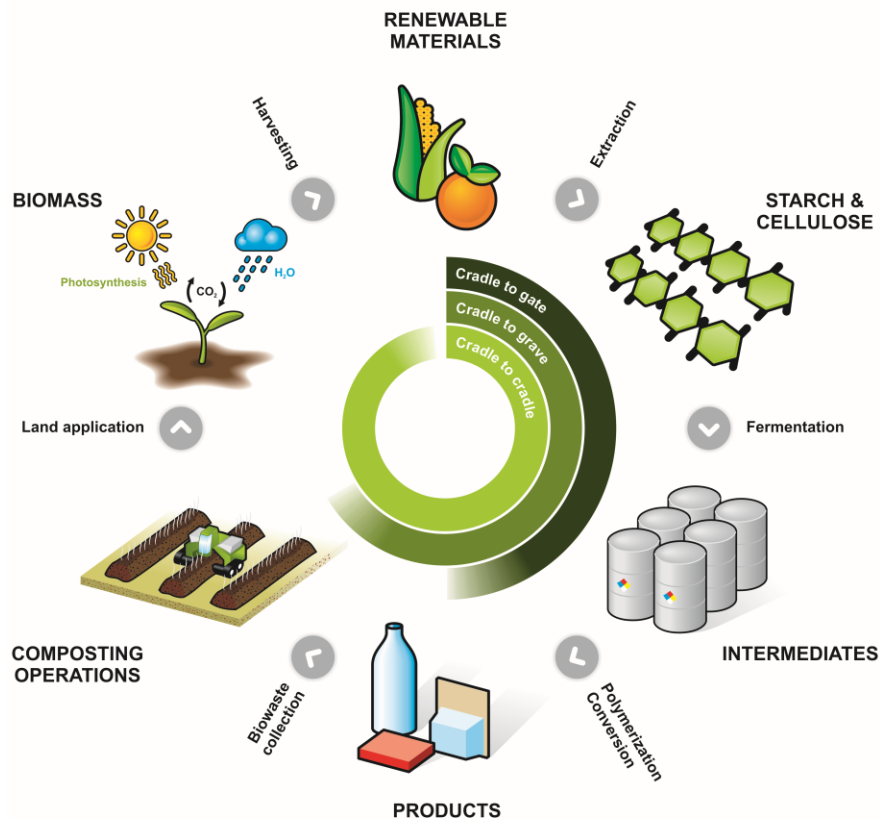


Figure 2.28 Cradle-to-gate, cradle-to-grave, and cradle-to-cradle representations of production, consumption, and disposal of bio-based polymers from renewable resource via composting. “Reprinted from Polymer International, 57, Kijchavengkul *et al.*, Compostability of polymers, 793-804, Copyright (2008), with permission from Wiley” [329].

In other words, LCA systematically evaluates each of the life stages of a product or product system, in which environmental inputs (resources) and environmental outputs (emission and waste) are produced and the impacts to human health and environment are calculated. LCA results are interpreted in relation to the objectives of the study [346, 347]. LCA studies are mostly conducted under the framework of the international standards ISO 14040 and 14044 [348, 349], which provide requirements, recommendations, and guidelines about methods and techniques for quantifying inputs and outputs, and impact characterization [346, 347].

The EFP of PLA resins and/or PLA products can be evaluated using midpoint impact categories [350]. Additionally, measuring key indicators such as greenhouse gases (GHG) emissions and non-renewable energy use, and comparing the data between PLA and traditional polymers (e.g., PET and PS) can give insights about PLA environmental performance.

In 2003, NatureWorks LLC published the first cradle-to-gate life cycle inventory data (ecoprofile) for its PLA (Ingeo™) based on the 140,000-t/y plant design, in which they provided some information regarding the production technology [351]. In 2007, the company provided an updated eco-profile based on the actual data collected from its production facilities, and also provided a more accurate description of the manufacturing system and LCA calculation procedure [352]. In 2010, NatureWorks LLC published an updated eco-profile based on the production technology improvements and also benchmarked the results for energy requirements and GHG emissions with data for a selection of fossil-based polymers [353]. Recently (2015), the company published an updated PLA eco-profile providing a detailed description of the production of its resin

(now 150,000-t/y plant) and focused on the corn feedstock used to produce Ingeo™ and on the PLA intrinsic zero material carbon footprint, as explained below [5, 345].

One of the advantages of using bio-based biodegradable polymers like PLA is to help replenish the carbon cycle (**Figure 2.29**) [329]. When using renewable carbon feedstock to manufacture plastic materials instead of fossil carbon feedstock, there is an intrinsic zero material carbon footprint value proposition; in other words, the carbon footprint reduction arises from the material itself and not necessarily from the process of converting the feedstock to products (process carbon footprint) [354].

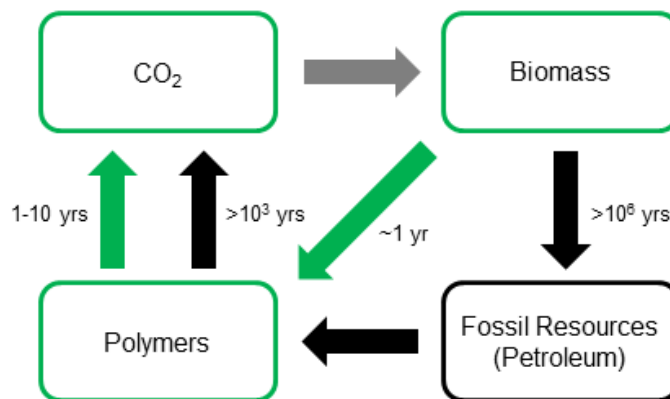


Figure 2.29 Carbon cycle of fossil-based polymers and bio-based polymers. Renewable resource pathway (green arrows); fossil resource pathway (black arrows); and pathway for both renewable and fossil resources (gray arrow), adapted from Kijchavengkul *et al.* [329].

Fossil resources could be considered renewable, but it takes more than a million years for biomass to be converted into fossil fuels. Since the rate of consumption is much greater than the rate of replenishment, mass imbalance occurs in the carbon cycle. In contrast, biodegradable polymers made from bio-based materials, such as corn and corn starch, can be produced and converted into biomass in similar time

frames [329]. **Figure 2.30** shows the global warming potential (GWP), primary energy from nonrenewable resources (PENNR), such as oil, gas, coal, and uranium, and water uptake for 1 kg of Ingeo™ PLA resin [5]. One of the main value propositions for using PLA to replace other fossil-based polymers, is the lower GWP due to carbon sequestration during the corn-growing stage.

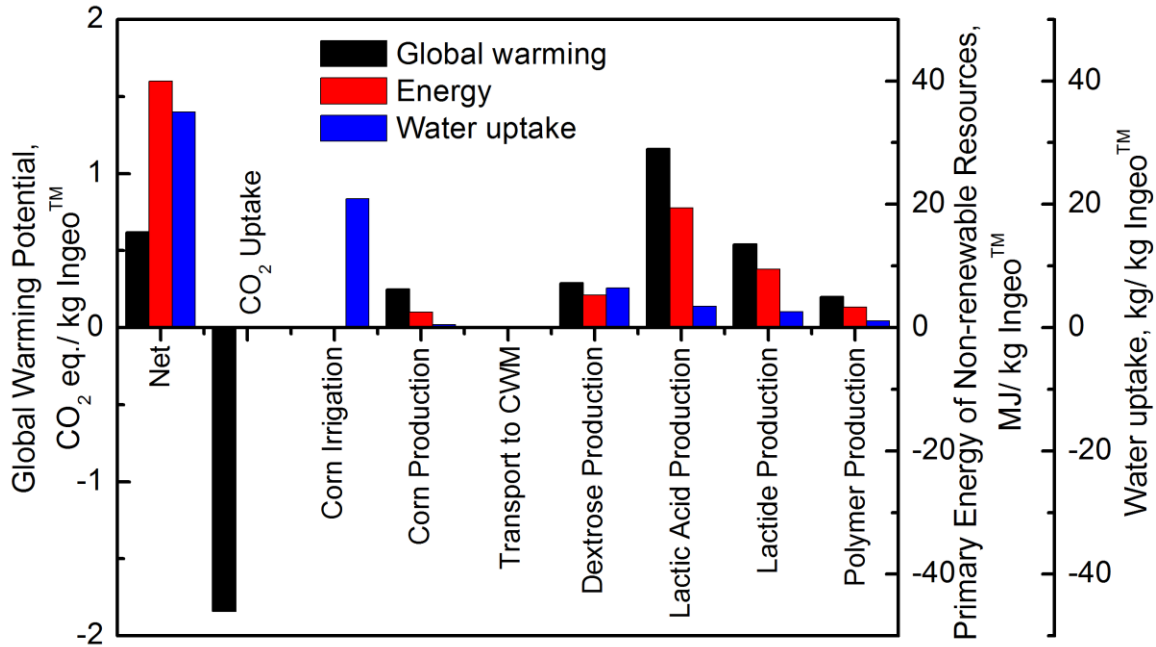


Figure 2.30 GWP, primary energy of non-renewable resources expressed as higher heating values (HHV), and net water uptake for the production system of Ingeo™ resin, adapted from Vink and Davies [5].

Several authors have done LCAs regarding the performance of PLA in comparison with other materials like PET and PS for different applications, in which PLA could be a good substitute for clamshell containers, trays, and water bottles [311, 355-358]. **Table 2.5** and **Figure 2.31** show general information about the EFP of PLA in comparison with other polymers.

Table 2.5 Environmental footprint of 1 kg of selected commercial polymer resins as available in Ecoinvent 3.2 and reported using Simapro 8.0.5 with ReCiPe (E) Midpoint Indicator considering the World as the geographical region.

Impact category	PLA	Nylon 6-6	PET	HDPE	LLDPE	LDPE	PP	PS
Climate change, kg CO ₂ eq.	2.7907	7.0460	2.4813	1.6815	1.6055	1.8154	1.7666	2.9690
Ozone depletion, kg CFC ⁻¹¹ eq.	2.18E-07	2.61E-09	1.48E-07	1.18E-09	4.75E-08	1.13E-09	8.85E-10	5.46E-09
Terrestrial acidification, kg SO ₂ eq.	0.0218	0.0295	0.0121	0.0064	0.0057	0.0078	0.0062	0.0112
Freshwater eutrophication, kg P eq.	0.0004	0.0003	0.0001	1.23E-06	9.03E-07	1.42E-06	4.33E-05	3.56E-06
Marine eutrophication, kg N eq.	0.0065	0.0091	0.0002	0.0001	0.0001	0.0002	0.0002	0.0003
Human toxicity, kg 1,4-DB eq.	9.4123	1.7760	4.6504	0.4946	0.2917	0.6967	0.4113	0.6617
Photochemical oxidant formation, kg NMVOC	0.0115	0.0205	0.0087	0.0086	0.0065	0.0093	0.0076	0.0096
Particulate matter formation, kg PM10 eq.	0.0063	0.0082	0.0040	0.0020	0.0021	0.0023	0.0019	0.0033
Terrestrial ecotoxicity, kg 1,4-DB eq.	0.0089	0.0002	0.0018	1.51E-05	1.13E-05	2.04E-05	1.21E-05	0.0003
Freshwater ecotoxicity, kg 1,4-DB eq.	0.0090	0.0037	0.0021	0.0004	0.0002	0.0005	0.0003	0.0009
Marine ecotoxicity, kg 1,4-DB eq.	3.5355	2.5132	2.9761	0.2391	0.1561	0.3246	0.1915	0.9059
Ionizing radiation, kBq U235 eq.	0.1398	0.0006	0.0785	0.0002	0.0002	0.0003	0.0002	0.0004
Agricultural land occupation, m ² a	1.1321	0.0009	0.1035	0.0004	0.0003	0.0003	0.0003	0.0006
Urban land occupation, m ² a	0.0674	0.0006	0.0147	0.0002	0.0001	0.0002	0.0002	0.0004
Natural land transformation, m ²	0.0004	-2.04E-06	0.0004	-3.77E-07	-4.39E-08	-7.27E-07	-3.98E-07	-1.25E-06
Water depletion, m ³	0.2726	0.2262	0.0714	0.0136	0.0443	0.0176	0.0156	0.0524
Metal depletion, kg Fe eq.	0.1538	0.0046	0.1646	0.0015	0.0019	0.0029	0.0015	0.0108
Fossil depletion, kg oil eq.	0.8246	2.6814	1.5455	1.5908	1.5628	1.5684	1.5716	1.8711
Non-renewable energy, MJ primary	41.739	135.86	73.182	76.398	74.090	78.223	74.636	87.542

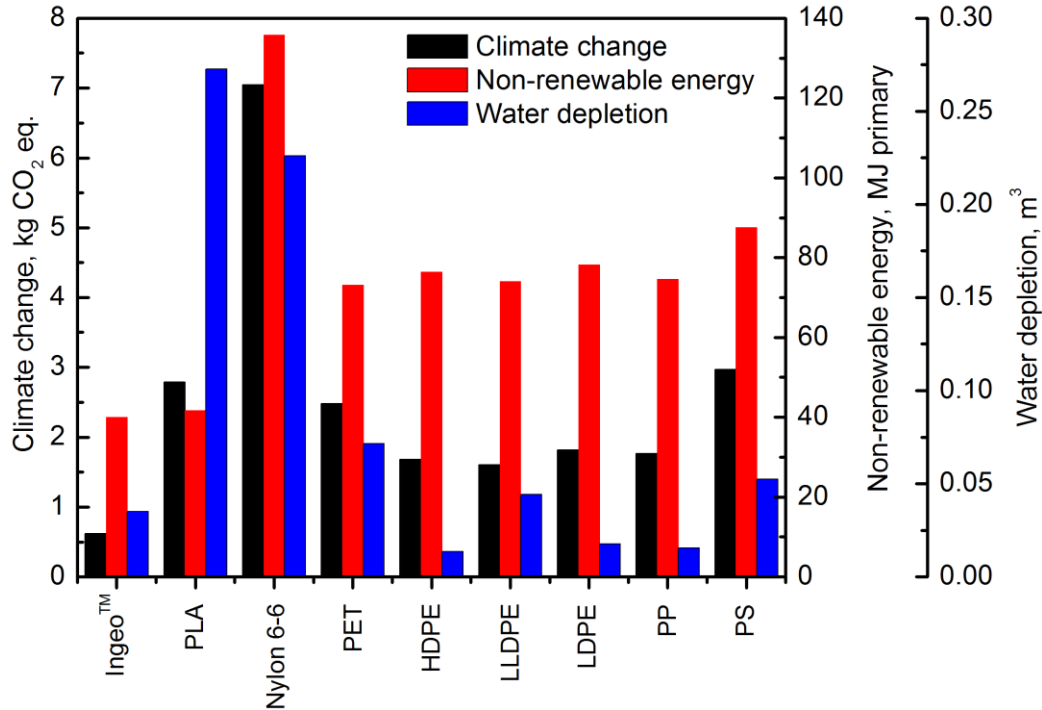


Figure 2.31 Climate change, non-renewable energy, water depletion for 1 kg of PLA and other commercial polymers as available in Ecoinvent 3.2 and reported using Simapro 8.0.5 with Recipe (E) Midpoint Indicator considering the World as the geographical region, and Ingeo™ adapted from Vink and Davies [5].

Such a comparison is effective only if: a) polymer weights in the studied applications are quite similar; b) contributions to impact categories are dominated by the polymer-pellet production; c) energy requirements for converting the polymer into product are relatively small or relatively similar; d) use phase is similar; e) the same recycling or end-of-life routes are employed; f) the same level of detail in the life cycle inventory data-collection process was used; g) the same LCA methodology was used; h) the same database for upstream inventory data was used; and i) the same life cycle impact assessment methodology, indicators, and characterization factors (+version) were used [5]. Given the above, the climate change of Ingeo™ and PLA have large

differences since carbon sequestration has not been accounted for in PLA. If this factor is taken into consideration, a global warming potential of PLA would be 0.9 kg CO₂ eq per kg of resin vs 0.62 kg CO₂ eq per kg of resin for Ingeo™. Thus a large benefit is obtained using the new reported data for Ingeo™ [5]. In the case of non-renewable energy, similar values are reported by Vink and Davies and the current data are available in Ecoinvent 3.2. In the case of water depletion, the new values reported by Vink and Davies make sure to properly account for water uptake from river and ground for the Blair manufacturing plant, excluding the water for hydropower installations and rainwater. So, a much lower water EFP is reported for Ingeo™, provided that water consumption is similar to that for polyolefins.

A large controversy exists regarding the use of the arable food land for plastic materials [359-361]. Vink and Davies reported, based on Carus [362], that 0.00046% of the 5 billion hectares of agricultural land available will be required to supply the corn needed for the 150,000 t/y Ingeo™ production in Blair, and if we imagine a scenario where the 300 million tons of plastics annually produced in the world were to be replaced by bio-based polymers with the same land use per kg of PLA, 0.9% of the 5 billion hectares of agricultural land available will be required [5, 362, 363].

An LCA study has been done recently regarding the end-of-life options for PLA [315]. In their study, Rossi *et al.* performed an LCA of the end-of-life options for biodegradable packaging based on the waste hierarchy mentioned in section 2.7. **Figure 2.32** shows the system boundary, which covers the primary material production and end-of-life treatment processes such as MR, IC, anaerobic digestion (AD), direct fuel substitution in industrial facility (DFS), incineration with heat recovery in MSW

incinerator (MSWI), and LF. Details of the life cycle inventory for each scenario can be found elsewhere [315].

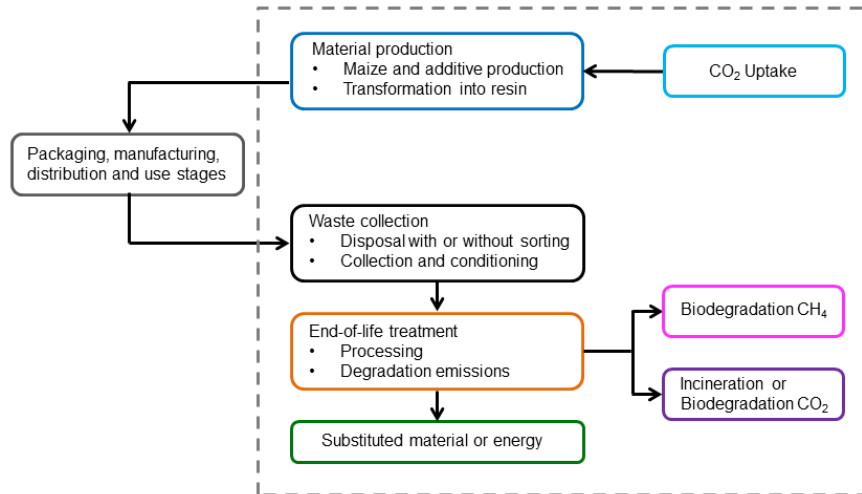


Figure 2.32 PLA life cycle and boundary of the studied system. Adapted from Rossi *et al.* [315].

Rossi *et al.* [315] used IMPACT 2002+ LCIA method to evaluate the environmental impacts for the different end-of-life scenarios complemented by water withdrawal and turbinated water indicators. Global warming impacts for PLA dynamically assessed over a 100-year time horizon are presented in **Figure 2.33**, in which IC has the highest net impact (measured in kg of CO₂ eq. per kilogram of dry PLA packaging without food contamination after deduction of the treatment credits) and MR has the lowest net impact.

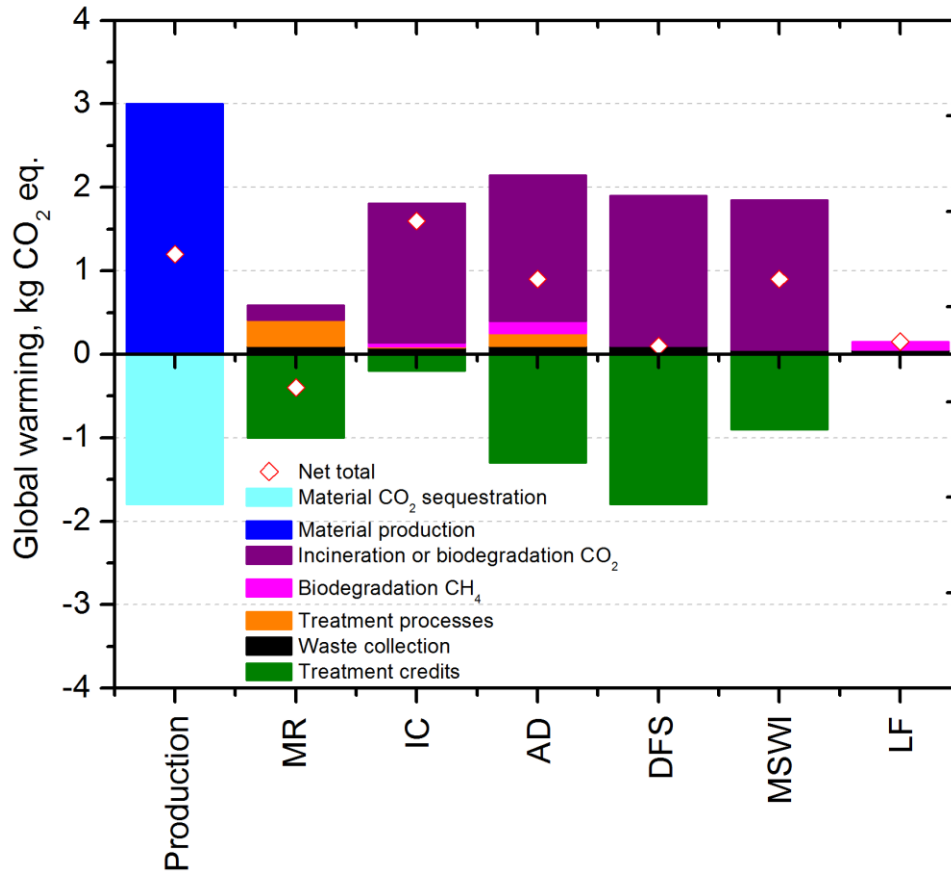


Figure 2.33 Comparison of dynamically-assessed global warming impacts over 100 years associated with the six end-of-life treatments for PLA. The bars on the left side present production impacts of the resin (cradle-to-gate) for comparison purposes, adapted from Rossi *et al.* [315].

Likewise, **Figure 2.34** shows the non-weighted scores of the PLA production and end-of-life scenarios for each midpoint category, in which for most impact categories MR was the least-burdening option. On the other hand, IC and LF were the least favorable options for most impact categories.

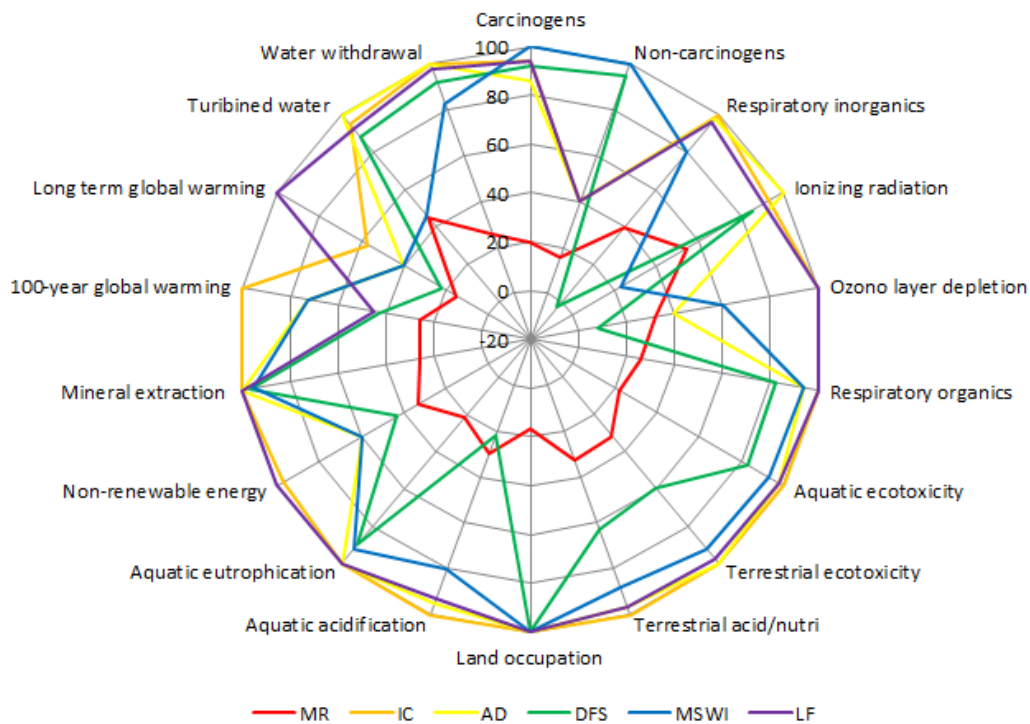


Figure 2.34 Comparison of end-of-life options for PLA for each midpoint category, adapted from Rossi *et al.* [315].

However, the authors emphasize that those conclusions are only valid under the stated hypotheses since other factors may lead to different conclusions. Additional studies are needed to ensure that this preliminary finding can be translated to other boundary conditions and can be applied to other regions.

2.9 Final Remarks

The range of PLA applications for consumer durable and non-durable goods has increased significantly since industrial methodologies, such as polycondensation and ROP, allowed the production of high M_w PLA to reach the market. At present, the main producer of the commercially available high M_w PLA derived from corn is NatureWorks LLC. Additional producers (*e.g.*, Corbion®) are expected to reach the market with PLA

derived from plant-based materials and/or biomass waste, which should increase its availability and further commercial applications.

Additional research has been focused on understanding and enhancing the physical and mechanical properties of PLA by, for example, deriving commercial PLA from *rac*-lactide. Extensive work has been conducted on blending PLA with biodegradable and non-biodegradable polymers and on using fillers at the micro and nano scales to create blends and composites with optimal properties, lower cost, and less environmental footprint. All these new variations of PLA-based materials target enhanced performance of PLA while sometimes at the expense of losing the biodegradability of the polymer matrix and reducing its industrial commercial recovery. Thus, new materials should be produced while keeping in mind that they need to be recovered by the more preferred routes of the waste management hierarchy (*i.e.*, source reduction, recycling, composting, incineration with energy recovery, and landfill).

The methods used for PLA mass production are well-established polymer-manufacturing techniques (*i.e.*, extrusion, injection molding, blow molding, thermoforming, foaming, and spinning). Therefore, PLA has found extended applications such as fibers, textiles, plasticulture, serviceware, and packaging containers via established processing technologies. However, use of different PLA structures may complicate the performance and/or use of these methods. Additional research may be needed in the production of the new *rac*-lactide derived PLA.

One of the main value propositions for PLA is its intrinsic degradation, which can be triggered when PLA is exposed to different environments. Thus, degradation of PLA can be seen as an advantage or disadvantage depending on the application. Extensive

research has been conducted on the degradation of PLA in human, processing, and composting environments. However, additional research is needed to assess the degradation of PLA and its modification when in contact with different solvents and simulants.

Furthermore, the increasing awareness of sustainability is highly influencing consumer preferences towards bio-based polymers, and PLA has the potential to become one of the major commercialized polymers. PLA can be derived from renewable resources, such as regular crops, plant-based materials, and biomass waste, and it could be treated in all levels of the waste management hierarchy. In this regard, however, there are still limitations due to the lack of suitable infrastructure for sorting, recycling, and/or composting PLA products at their end of life. So, efforts should be centered on working with industries, commodity groups, industry associations, and government groups to improve the recovery rate of PLA.

Finally, life cycle assessment has been used to evaluate the environmental footprint of PLA, providing useful information about the environmental impacts that PLA may have during raw material acquisition, production, use, and disposal. Robust data exists about the PLA resin production from one producer, NatureWorks LLC. However, sufficient information is missing regarding the use and end-of-life scenarios of PLA parts.

In conclusion, PLA has transcended from a minor bio-based polymer player in the market of commercial fossil-based polymers to be considered as part of a new solution for an increasingly recognized new bio-based economy. Present and future

efforts in developing PLA for an array of applications should secure PLA's status as one of the major new bio-based polymers.

REFERENCES

REFERENCES

- [1] L.-T. Lim, R. Auras, M. Rubino, Processing technologies for poly (lactic acid), *Prog. Polym. Sci.* 33 (2008) 820-852.
- [2] R. Auras, B. Harte, S. Selke, An overview of polylactides as packaging materials, *Macromolecular Bioscience* 4 (2004) 835-864.
- [3] J. Ren, *Biodegradable poly (lactic acid): synthesis, modification, processing and applications*, Springer Science & Business Media, 2011.
- [4] E. Rudnik, *Compostable polymer materials*, Elsevier, 2010.
- [5] E.T. Vink, S. Davies, Life Cycle Inventory and Impact Assessment Data for 2014 Ingeo™ Polylactide Production, *Industrial Biotechnology* 11 (2015) 167-180.
- [6] A.S. Mirabal, L. Scholz, M. Carus, Market study on bio-based polymers in the word-capacities, production and applications: status quo and trends towards 2020, Nova-Institute, GmbH (2013).
- [7] Web of Science. Available: http://apps.webofknowledge.com.proxy1.cl.msu.edu/WOS_GeneralSearch_input.do?product=WOS&search_mode=GeneralSearch&SID=4A6KOlgZ3TGlfH8Fk9&preferencesSaved=. Access date December 7th, 2015.
- [8] K.M. Nampoothiri, N.R. Nair, R.P. John, An overview of the recent developments in polylactide (PLA) research, *Bioresour. Technol.* 101 (2010) 8493-8501.
- [9] A.J. Lasprilla, G.A. Martinez, B.H. Lunelli, A.L. Jardini, R. Maciel Filho, Poly-lactic acid synthesis for application in biomedical devices—A review, *Biotechnol. Adv.* 30 (2012) 321-328.
- [10] R.P. Pawar, S.U. Tekale, S.U. Shisodia, J.T. Totre, A.J. Domb, Biomedical Applications of Poly (Lactic Acid), *Recent. Pat. Regen. Med.* 4 (2014) 40-51.
- [11] M. Vert, Aliphatic polyesters: great degradable polymers that cannot do everything, *Biomacromolecules* 6 (2005) 538-546.
- [12] M. Vert, G. Schwarch, J. Coudane, Present and future of PLA polymers, *J. Macromol. Sci., Pure Appl. Chem.* 32 (1995) 787-796.
- [13] R. Auras, L.T. Lim, S. Selke, H. Tsuji, *Poly(lactic acid). Synthesis, Structures, Properties, Processing, and Applications*, John Wiley & Sons, Inc., New Jersey, 2010.

- [14] H.R. Kricheldorf, I. Kreiser-Saunders, C. Jürgens, D. Wolter, Polylactides-synthesis, characterization and medical application, *Macromol. Symp.* 103 (1996) 85-102.
- [15] R. Datta, M. Henry, Lactic acid: recent advances in products, processes and technologies—a review, *J. Chem. Technol. Biotechnol.* 81 (2006) 1119-1129.
- [16] G. Kharas, F. Sanchez-Riera, D. Severson, Polymers of lactic acid, in: D.P. Mobley (Ed.), *Plastics from microbes: microbial synthesis of polymers and polymer precursors*, Hanser Publishers, Munich, 1994, pp. 93-137.
- [17] M.H. Hartmann, High molecular weight polylactic acid polymers, in: D.L. Kaplan (Ed.), *Biopolymers from renewable resources*, Springer, Heidelberg/Berling, 1998, pp. 367-411.
- [18] W. Groot, J.v. Krieken, O. Sliekersl, S. de Vos, Production and purification of lactic acid and lactide, in: R. Auras, L.T. Lim, S. Selke, H. Tsuji (Eds.), *Poly(lactic acid). Synthesis, Structures, Properties, Processing, and Applications*, John Wiley & Sons, Inc., New Jersey, 2010, pp. 3-16.
- [19] Corbion. Available: <http://www.corbion.com/about-corbion/innovation>. Access date December 14th, 2015,
- [20] S.-H. Hyon, K. Jamshidi, Y. Ikada, Synthesis of polylactides with different molecular weights, *Biomaterials* 18 (1997) 1503-1508.
- [21] Y. Zhao, Z. Wang, J. Wang, H. Mai, B. Yan, F. Yang, Direct synthesis of poly (D, L-lactic acid) by melt polycondensation and its application in drug delivery, *J. Appl. Polym. Sci.* 91 (2004) 2143-2150.
- [22] M. Ajioka, K. Enomoto, K. Suzuki, A. Yamaguchi, The basic properties of poly (lactic acid) produced by the direct condensation polymerization of lactic acid, *J. Environ. Polym. Degr.* 3 (1995) 225-234.
- [23] P. Gruber, M. O'Brien, Polylactides “Natureworks® PLA”, *Biopolymers Online* (2005).
- [24] A.C. Albertsson, I.K. Varma, Recent developments in ring opening polymerization of lactones for biomedical applications, *Biomacromolecules* 4 (2003) 1466-1486.
- [25] R.E. Drumright, P.R. Gruber, D.E. Henton, Polylactic acid technology, *Adv. Mater.* 12 (2000) 1841-1846.
- [26] S. Jacobsen, H.-G. Fritz, P. Degée, P. Dubois, R. Jérôme, New developments on the ring opening polymerisation of polylactide, *Ind. Crop. Prod.* 11 (2000) 265-275.

- [27] S. Inkinen, M. Hakkarainen, A.-C. Albertsson, A. Södergård, From lactic acid to poly (lactic acid)(PLA): characterization and analysis of PLA and its precursors, *Biomacromolecules* 12 (2011) 523-532.
- [28] NatureWorks, NatureWorks Introduces Its Next Generation Polymer Grade Lactide, in: Ingeo™ M700, the meso-lactide stereoisomer delivers higher performance than prior alternatives in a host of industrial applications, NatureWorks, Minnetonka, MN, 2013.
- [29] R.D. Benson, E.S. Sumner, J.D. Schroeder, Methods for Producing Lactide with Recycle of Meso-Lactide, in, NatureWorks LLC, 2010.
- [30] C.B. Penu, B., Production of meso-lactide, d-lactide and l-lactic by back biting of polylactide, in, Futerra S.A., 2014.
- [31] P. Hornmair, E.L. Marshall, V.C. Gibson, R.I. Pugh, A.J. White, Study of ligand substituent effects on the rate and stereoselectivity of lactide polymerization using aluminum salen-type initiators, *Proc. Natl. Acad. Sci. U. S. A.* 103 (2006) 15343-15348.
- [32] T.M. Ovitt, G.W. Coates, Stereochemistry of lactide polymerization with chiral catalysts: new opportunities for stereocontrol using polymer exchange mechanisms, *J. Am. Chem. Soc.* 124 (2002) 1316-1326.
- [33] K. Masutani, Y. Kimura, PLA Synthesis. From the Monomer to the Polymer, in: A. Jimenez, M. Peltzer, R. Ruseckaite (Eds.), *Poly(lactic acid) Science and Technology: Processing, Properties, Additives and Applications*, The Royal Society of Chemistry, 2014, pp. 3-31.
- [34] Y. Yang, H. Wang, H. Ma, Stereoselective Polymerization of rac-Lactide Catalyzed by Zinc Complexes with Tetradentate Aminophenolate Ligands in Different Coordination Patterns: Kinetics and Mechanism, *Inorg. Chem.* 54 (2015) 5839–5854.
- [35] M. Dusselier, P. Van Wouwe, A. Dewaele, P.A. Jacobs, B.F. Sels, Shape-selective zeolite catalysis for bioplastics production, *Science* 349 (2015) 78-80.
- [36] D. Alhashmialameer, N. Ikpo, J. Collins, L.N. Dawe, K. Hattenhauer, F.M. Kerton, Ring-opening polymerization of rac-lactide mediated by tetrametallic lithium and sodium diamino-bis (phenolate) complexes, *Dalton Trans.* 44 (2015) 20216-20231.
- [37] T. Hasegawa, N. Nomura, T. Moriya, H. Nishikawa, S. Yamaguchi, H. Kishida, Synthesis of Racemic Lactide Using Glycerol By-product from Biodiesel Fuel Production Process as Feedstock, *Energy Procedia* 56 (2014) 195-200.

- [38] J.-B. Zhu, E.Y.-X. Chen, From meso-Lactide to Isotactic Polylactide: Epimerization by B/N Lewis Pairs and Kinetic Resolution by Organic Catalysts, *J. Am. Chem. Soc.* 137 (2015) 12506-12509.
- [39] M. Jamshidian, E.A. Tehrany, M. Imran, M. Jacquot, S. Desobry, Poly-Lactic Acid: production, applications, nanocomposites, and release studies, *Compr. Rev. Food Sci. Food Saf.* 9 (2010) 552-571.
- [40] L.-T. Lim, K. Cink, Vanyo, Processing of Poly(lactic acid), in: R. Auras, L.T. Lim, S. Selke, H. Tsuji (Eds.), *Poly(lactic acid). Synthesis, Structures, Properties, Processing, and Applications*, John Wiley & Sons, Inc., New Jersey, 2010, pp. 191-215.
- [41] NatureWorks. Crystallizing and Drying Ingeo™ Biopolymer. Available: http://www.natureworkslc.com/~media/Technical_Resources/Processing_Guides/ProcessingGuide_Crystallizing-and-Drying_pdf.pdf. Access date December 9th, 2015.
- [42] F.-D. Kopinke, M. Remmler, K. Mackenzie, M. Möder, O. Wachsen, Thermal decomposition of biodegradable polyesters—II. Poly (lactic acid), *Polym. Degrad. Stab.* 53 (1996) 329-342.
- [43] NatureWorks. Ingeo™ Biopolymer 2500HP Technical Data Sheet. Available: http://www.natureworkslc.com/~media/Technical_Resources/Technical_Data_Sheets/TechnicalDataSheet_2500HP_extrusion_pdf.pdf?la=en. Access date December 9th, 2015.
- [44] NatureWorks. Ingeo™ Biopolymer 3001D Technical Data Sheet. Available: http://www.natureworkslc.com/~media/Technical_Resources/Technical_Data_Sheets/TechnicalDataSheet_3001D_injection-molding_pdf.pdf. Access date December 9th, 2015.
- [45] NatureWorks. Ingeo™ Biopolymer 4032D Technical Data Sheet. Available: http://www.natureworkslc.com/~media/Technical_Resources/Technical_Data_Sheets/TechnicalDataSheet_4032D_films_pdf.pdf. Access date December 9th, 2015.
- [46] NatureWorks. Ingeo™ Biopolymer 6060D Technical Data Sheet. Available: http://www.natureworkslc.com/~media/Technical_Resources/Technical_Data_Sheets/TechnicalDataSheet_6060D_fiber-melt-spinning_pdf.pdf. Access date December 9th, 2015.
- [47] NatureWorks. Ingeo™ Biopolymer 7001D Technical Data Sheet. Available: http://www.natureworkslc.com/~media/Technical_Resources/Technical_Data_Sheets/TechnicalDataSheet_7001D_bottles_pdf.pdf. Access date December 9th, 2015.

- [48] NatureWorks. Ingeo™ Biopolymer 8052D Technical Data Sheet. Available: http://www.natureworkslc.com/~media/Technical_Resources/Technical_Data_Sheets/TechnicalDataSheet_8052D_foam_pdf.pdf. Access date December 9th, 2015.
- [49] R. Auras, Poly (lactic acid), in: K. Yam (Ed.) Encyclopedia Of Polymer Science and Technology, John Wiley & Sons, Inc., New Jersey, 2010, pp. 967-983.
- [50] K.D. Van, P. Krevelen, Properties of polymers: Their estimation and correlation with chemical structure, third ed., Elsevier, Amsterdam, 1997.
- [51] D. Witzke, Introduction to properties, engineering, and prospects of polylactide polymers, in, Thesis, Michigan State Univ, Michigan, 1997.
- [52] R.A. Auras, B. Harte, S. Selke, R. Hernandez, Mechanical, physical, and barrier properties of poly (lactide) films, *J. Plast. Film Sheet.* 19 (2003) 123-135.
- [53] G. Kale, R. Auras, S.P. Singh, Comparison of the degradability of poly (lactide) packages in composting and ambient exposure conditions, *Packag. Technol. Sci.* 20 (2007) 49-70.
- [54] R. Auras, B. Harte, S. Selke, Effect of water on the oxygen barrier properties of poly (ethylene terephthalate) and polylactide films, *J. Appl. Polym. Sci.* 92 (2004) 1790-1803.
- [55] R. Bhardwaj, A.K. Mohanty, Advances in the properties of polylactides based materials: a review, *J. Biobased Mater. Bio.* 1 (2007) 191-209.
- [56] J.R. Dorgan, Rheology of Poly(lactic acid), in: R. Auras, L.T. Lim, S. Selke, H. Tsuji (Eds.), Poly(lactic acid). Synthesis, Structures, Properties, Processing, and Applications, John Wiley & Sons, Inc., New Jersey, 2010, pp. 125-139.
- [57] H.J. Lehermeier, J.R. Dorgan, J.D. Way, Gas permeation properties of poly (lactic acid), *J. Membr. Sci.* 190 (2001) 243-251.
- [58] R.A. Auras, Solubility of gases and vapors in polylactide polymers, in: T.M. Letcher (Ed.), Thermodynamics, Solubility and Environmental Issues, Elsevier, Amsterdam, 2007, pp. 343-368.
- [59] R. Auras, B. Harte, S. Selke, Sorption of ethyl acetate and d-limonene in poly (lactide) polymers, *J. Sci. Food Agric.* 86 (2006) 648-656.
- [60] G. Colomines, S. Domenek, V. Ducruet, A. Guinault, Influences of the crystallisation rate on thermal and barrier properties of polylactide acid (PLA) food packaging films, *Int. J. Mater. Form.* 1 (2008) 607-610.
- [61] R. Auras, S.P. Singh, J. Singh, Performance evaluation of PLA against existing PET and PS containers, *J. Test. Eval.* 34 (2006) 530.

- [62] C. Chariyachotilert, S.E. Selke, R.A. Auras, S. Joshi, Assessment of the properties of poly (L-lactic Acid) sheets produced with differing amounts of post-consumer recycled poly (L-lactic Acid), *J. Plast. Film Sheet.* 28 (2012) 314-335.
- [63] S. Gottermann, S. Weinmann, C. Bonten, Foams made from modified standard PLA, in: *Bioplastics*, Polymedia Publisher GmbH, Germany, 2015, pp. 38-40.
- [64] L.M. Matuana, Foaming, in: R. Auras, L.T. Lim, S. Selke, H. Tsuji (Eds.), *Poly(lactic acid). Synthesis, Structures, Properties, Processing, and Applications*, John Wiley & Sons, Inc., New Jersey, 2010, pp. 273-291.
- [65] O. Avinc, A. Khoddami, Overview of poly (lactic acid)(PLA) fibre, *Fibre Chem.* 42 (2010) 68-78.
- [66] M. Mathur, M.A. Hira, Specialty Fibres-IV: Poly Lactic Acid Fibres, *Man-Made Textiles in India* 51 (2008) 232-237.
- [67] A.K. Agrawal, Spinning of Poly(lactic acid) Fibers, in: R. Auras, L.T. Lim, S. Selke, H. Tsuji (Eds.), *Poly(lactic acid). Synthesis, Structures, Properties, Processing, and Applications*, John Wiley & Sons, Inc., New Jersey, 2010, pp. 323-341.
- [68] H. Liu, J. Zhang, Research progress in toughening modification of poly (lactic acid), *J. Polym. Sci., Part B: Polym. Phys.* 49 (2011) 1051-1083.
- [69] H. Balakrishnan, A. Hassan, M. Imran, M.U. Wahit, Toughening of polylactic acid nanocomposites: A short review, *Polym. Plast. Technol. Eng.* 51 (2012) 175-192.
- [70] L. Natureworks, Technology Focus Report: Toughened PLA, Available online at: http://www.natureworkslc.com/~media/Technical_Resources/Properties_Documents/PropertiesDocument_Toughened-Ingeo_pdf.pdf (2007).
- [71] S. Detyothin, A. Kathuria, W. Jaruwattanayon, S.E.M. Selke, R. Auras, Poly(lactic acid) Blends, in: R. Auras, L.T. Lim, S. Selke, H. Tsuji (Eds.), *Poly(lactic acid). Synthesis, Structures, Properties, Processing, and Applications*, John Wiley & Sons, Inc., New Jersey, 2010, pp. 227-266.
- [72] L. Yu, E. Petinakis, K. Dean, H. Liu, Poly(lactic acid)/Starch Blends, in: R. Auras, L.T. Lim, S. Selke, H. Tsuji (Eds.), *Poly(lactic acid). Synthesis, Structures, Properties, Processing, and Applications*, John Wiley & Sons, Inc., New Jersey, 2010, pp. 217-225.
- [73] S.B. Ghosh, S. Bandyopadhyay-Ghosh, M. Sain, Composites, in: R. Auras, L.T. Lim, S. Selke, H. Tsuji (Eds.), *Poly(lactic acid). Synthesis, Structures, Properties, Processing, and Applications*, John Wiley & Sons, Inc., New Jersey, 2010, pp. 293-307.

- [74] V. Mittal, T. Akhtar, N. Matsko, Mechanical, Thermal, Rheological and Morphological Properties of Binary and Ternary Blends of PLA, TPS and PCL, *Macromol. Mater. Eng.* 300 (2015) 423-435.
- [75] B. Meng, J. Deng, Q. Liu, Z. Wu, W. Yang, Transparent and ductile poly(lactic acid)/poly(butyl acrylate) (PBA) blends: Structure and properties, *Eur. Polym. J.* 48 (2012) 127-135.
- [76] Natureworks, Technology Focus Report: Toughened PLA, Available online at: http://www.natureworkslc.com/~media/Technical_Resources/Properties_Documents/PropertiesDocument_Toughened-Ingeo_pdf.pdf (2007).
- [77] W. Zhang, Z. Gui, C. Lu, S. Cheng, D. Cai, Y. Gao, Improving transparency of incompatible polymer blends by reactive compatibilization, *Mater. Lett.* 92 (2013) 68-70.
- [78] H. Abdillahi, E. Chabrat, A. Rouilly, L. Rigal, Influence of citric acid on thermoplastic wheat flour/poly(lactic acid) blends. II. Barrier properties and water vapor sorption isotherms, *Ind. Crop. Prod.* 50 (2013) 104-111.
- [79] I. Armentano, Processing and characterization of plasticized PLA/PHB blends for biodegradable multiphase systems, *Express Polym. Lett.* 9 (2015) 583-596.
- [80] V. Jost, R. Kopitzky, Blending of polyhydroxybutyrate-co-valerate with polylactic acid for packaging applications--reflections on miscibility and effects on the mechanical and barrier properties, *Chem. Biochem. Eng. Q.* 29 (2015) 221.
- [81] M. Boufarguine, A. Guinault, G. Miquelard-Garnier, C. Sollogoub, PLA/PHBV Films with Improved Mechanical and Gas Barrier Properties, *Macromol. Mater. Eng.* 298 (2013) 1065-1073.
- [82] S.M. Razavi, S. Dadbin, M. Frounchi, Oxygen-barrier properties of poly(lactic acid)/poly(vinyl acetate-co-vinyl alcohol) blends as biodegradable films, *J. Appl. Polym. Sci.* 125 (2012) E20-E26.
- [83] N.E. Suyatma, A. Copinet, L. Tighzert, V. Coma, Mechanical and barrier properties of biodegradable films made from chitosan and poly (lactic acid) blends, *J. Polym. Environ.* 12 (2004) 1-6.
- [84] R. Kwiatkowski, P. Dacko, SAXS Studies of Heating/Cooling Cycle Behavior of Biodegradable BTA/PLA-b Blends, *Macromol. Symp.* 296 (2010) 478-486.
- [85] J.M. Onyari, F. Mulaa, J. Muia, P. Shiundu, Biodegradability of Poly (lactic acid), Preparation and Characterization of PLA/Gum Arabic Blends, *J. Polym. Environ.* 16 (2008) 205-212.

- [86] Y.-X. Weng, L. Wang, M. Zhang, X.-L. Wang, Y.-Z. Wang, Biodegradation behavior of P(3HB,4HB)/PLA blends in real soil environments, *Polym. Test.* 32 (2013) 60-70.
- [87] M. Zhang, N.L. Thomas, Blending polylactic acid with polyhydroxybutyrate: The effect on thermal, mechanical, and biodegradation properties, *Adv. Polym. Tech.* 30 (2011) 67-79.
- [88] Q. Zhao, S. Wang, M. Kong, W. Geng, R.K.Y. Li, C. Song, D. Kong, Phase morphology, physical properties, and biodegradation behavior of novel PLA/PHBHHx blends, *J. Biomed. Mater. Res. B.* 100B (2012) 23-31.
- [89] Y.F. Kim, C.N. Choi, Y.D. Kim, K.Y. Lee, M.S. Lee, Compatibilization of immiscible poly (l-lactide) and low density polyethylene blends, *Fiber. Polym.* 5 (2004) 270-274.
- [90] K.S. Anderson, S.H. Lim, M.A. Hillmyer, Toughening of polylactide by melt blending with linear low-density polyethylene, *J. Appl. Polym. Sci.* 89 (2003) 3757-3768.
- [91] K.S. Anderson, M.A. Hillmyer, The influence of block copolymer microstructure on the toughness of compatibilized polylactide/polyethylene blends, *Polymer* 45 (2004) 8809-8823.
- [92] Y. Wang, M.A. Hillmyer, Polyethylene-poly (L-lactide) diblock copolymers: Synthesis and compatibilization of poly (L-lactide)/polyethylene blends, *J. Polym. Sci., Part A: Polym. Chem.* 39 (2001) 2755-2766.
- [93] G. Biresaw, C. Carriere, Compatibility and mechanical properties of blends of polystyrene with biodegradable polyesters, *Composites Part A* 35 (2004) 313-320.
- [94] J.-S. Yoon, S.-H. Oh, M.-N. Kim, I.-J. Chin, Y.-H. Kim, Thermal and mechanical properties of poly (l-lactic acid)-poly (ethylene-co-vinyl acetate) blends, *Polymer* 40 (1999) 2303-2312.
- [95] C.M. Lee, E.S. Kim, J.S. Yoon, Reactive blending of poly (L-lactic acid) with poly (ethylene-co-vinyl alcohol), *J. Appl. Polym. Sci.* 98 (2005) 886-890.
- [96] C.-H. Ho, C.-H. Wang, C.-I. Lin, Y.-D. Lee, Synthesis and characterization of TPO-PLA copolymer and its behavior as compatibilizer for PLA/TPO blends, *Polymer* 49 (2008) 3902-3910.
- [97] Y. Li, H. Shimizu, Improvement in toughness of poly (l-lactide)(PLLA) through reactive blending with acrylonitrile-butadiene-styrene copolymer (ABS): morphology and properties, *Eur. Polym. J.* 45 (2009) 738-746.
- [98] H.-J. Jin, I.-J. Chin, M.-N. Kim, S.-H. Kim, J.-S. Yoon, Blending of poly (L-lactic acid) with poly (cis-1, 4-isoprene), *Eur. Polym. J.* 36 (2000) 165-169.

- [99] H. Tsuji, H. Muramatsu, Blends of aliphatic polyesters: V non-enzymatic and enzymatic hydrolysis of blends from hydrophobic poly (l-lactide) and hydrophilic poly (vinyl alcohol), *Polym. Degrad. Stab.* 71 (2001) 403-413.
- [100] L. Zhang, C. Xiong, X. Deng, Miscibility, crystallization and morphology of poly (β -hydroxybutyrate)/poly (d, l-lactide) blends, *Polymer* 37 (1996) 235-241.
- [101] G.-X. Chen, H.-S. Kim, E.-S. Kim, J.-S. Yoon, Compatibilization-like effect of reactive organoclay on the poly (L-lactide)/poly (butylene succinate) blends, *Polymer* 46 (2005) 11829-11836.
- [102] R. Wang, S. Wang, Y. Zhang, C. Wan, P. Ma, Toughening modification of PLLA/PBS blends via in situ compatibilization, *Polym. Eng. Sci.* 49 (2009) 26.
- [103] Y. Wang, J.F. Mano, Biodegradable poly (L-lactic acid)/poly (butylene succinate-co-adipate) blends: Miscibility, morphology, and thermal behavior, *J. Appl. Polym. Sci.* 105 (2007) 3204-3210.
- [104] C. Ludvik, G. Glenn, A. Klamczynski, D. Wood, Cellulose fiber/bentonite clay/biodegradable thermoplastic composites, *J. Polym. Environ.* 15 (2007) 251-257.
- [105] N. Zhang, Q. Wang, J. Ren, L. Wang, Preparation and properties of biodegradable poly (lactic acid)/poly (butylene adipate-co-terephthalate) blend with glycidyl methacrylate as reactive processing agent, *J. Mater. Sci.* 44 (2009) 250-256.
- [106] T.-Y. Liu, W.-C. Lin, M.-C. Yang, S.-Y. Chen, Miscibility, thermal characterization and crystallization of poly (l-lactide) and poly (tetramethylene adipate-co-terephthalate) blend membranes, *Polymer* 46 (2005) 12586-12594.
- [107] W. Zhang, L. Chen, Y. Zhang, Surprising shape-memory effect of polylactide resulted from toughening by polyamide elastomer, *Polymer* 50 (2009) 1311-1315.
- [108] Y. Li, H. Shimizu, Toughening of polylactide by melt blending with a biodegradable poly (ether) urethane elastomer, *Macromol. Biosci.* 7 (2007) 921-928.
- [109] Y. Hu, Y. Hu, V. Topolkaraev, A. Hiltner, E. Baer, Aging of poly (lactide)/poly (ethylene glycol) blends. Part 2. Poly (lactide) with high stereoregularity, *Polymer* 44 (2003) 5711-5720.
- [110] J. Zhang, L. Jiang, L. Zhu, J.-I. Jane, P. Mungara, Morphology and properties of soy protein and polylactide blends, *Biomacromolecules* 7 (2006) 1551-1561.
- [111] H. Zhu, X. Feng, H. Zhang, Y. Guo, J. Zhang, J. Chen, Structural characteristics and properties of silk fibroin/poly (lactic acid) blend films, *J. Biomater. Sci., Polym. Ed.* 20 (2009) 1259-1274.

- [112] C. Xu, X. Luo, X. Lin, X. Zhuo, L. Liang, Preparation and characterization of polylactide/thermoplastic konjac glucomannan blends, *Polymer* 50 (2009) 3698-3705.
- [113] M. Peesan, P. Supaphol, R. Rujiravanit, Preparation and characterization of hexanoyl chitosan/polylactide blend films, *Carbohydr. Polym.* 60 (2005) 343-350.
- [114] Y. Wan, H. Wu, A. Yu, D. Wen, Biodegradable polylactide/chitosan blend membranes, *Biomacromolecules* 7 (2006) 1362-1372.
- [115] M. Shibata, Y. Inoue, M. Miyoshi, Mechanical properties, morphology, and crystallization behavior of blends of poly (L-lactide) with poly (butylene succinate-co-L-lactate) and poly (butylene succinate), *Polymer* 47 (2006) 3557-3564.
- [116] S. Ghosh, J.C. Viana, R.L. Reis, J.F. Mano, Development of porous lamellar poly (l-lactic acid) scaffolds by conventional injection molding process, *Acta Biomater.* 4 (2008) 887-896.
- [117] Y.-H. Na, Y. He, X. Shuai, Y. Kikkawa, Y. Doi, Y. Inoue, Compatibilization effect of poly (ϵ -caprolactone)-b-poly (ethylene glycol) block copolymers and phase morphology analysis in immiscible poly (lactide)/poly (ϵ -caprolactone) blends, *Biomacromolecules* 3 (2002) 1179-1186.
- [118] C.-C. Chen, J.-Y. Chueh, H. Tseng, H.-M. Huang, S.-Y. Lee, Preparation and characterization of biodegradable PLA polymeric blends, *Biomaterials* 24 (2003) 1167-1173.
- [119] N. López-Rodríguez, A. López-Arraiza, E. Meaurio, J. Sarasua, Crystallization, morphology, and mechanical behavior of polylactide/poly (ϵ -caprolactone) blends, *Polym. Eng. Sci.* 46 (2006) 1299-1308.
- [120] L. Wang, W. Ma, R. Gross, S. McCarthy, Reactive compatibilization of biodegradable blends of poly (lactic acid) and poly (ϵ -caprolactone), *Polym. Degrad. Stab.* 59 (1998) 161-168.
- [121] T. Ke, X. Sun, Effects of moisture content and heat treatment on the physical properties of starch and poly (lactic acid) blends, *J. Appl. Polym. Sci.* 81 (2001) 3069-3082.
- [122] T. Ke, X. Sun, Thermal and mechanical properties of poly (lactic acid) and starch blends with various plasticizers, *T. ASAE* 44 (2001) 945-953.
- [123] T. Ke, X. Sun, Melting behavior and crystallization kinetics of starch and poly (lactic acid) composites, *J. Appl. Polym. Sci.* 89 (2003) 1203-1210.
- [124] T. Ke, S.X. Sun, P. Seib, Blending of poly (lactic acid) and starches containing varying amylose content, *J. Appl. Polym. Sci.* 89 (2003) 3639-3646.

- [125] R.M. Rasal, D.E. Hirt, Toughness decrease of PLA-PHBHHx blend films upon surface-confined photopolymerization, *J. Biomed. Mater. Res. Part A* 88 (2009) 1079-1086.
- [126] W. Ning, Z. Xingxiang, Y. Jiugao, F. Jianming, Partially miscible poly (lactic acid)-blend-poly (propylene carbonate) filled with carbon black as conductive polymer composite, *Polym. Int.* 57 (2008) 1027-1035.
- [127] T.W. Yoo, H.G. Yoon, S.J. Choi, M.S. Kim, Y.H. Kim, W.N. Kim, Effects of compatibilizers on the mechanical properties and interfacial tension of polypropylene and poly (lactic acid) blends, *Macromol. Res.* 18 (2010) 583-588.
- [128] J.B. Lee, Y.K. Lee, G.D. Choi, S.W. Na, T.S. Park, W.N. Kim, Compatibilizing effects for improving mechanical properties of biodegradable poly (lactic acid) and polycarbonate blends, *Polym. Degrad. Stab.* 96 (2011) 553-560.
- [129] Z.-y. Gui, C. Lu, Y.-f. Li, S.-j. Cheng, Preparation and Characterization of PGS-PLA Blend Composite [J], *Journal of East China University of Science and Technology (Natural Science Edition)* 1 (2009) 012.
- [130] H. Zou, C. Yi, L. Wang, W. Xu, Crystallization, hydrolytic degradation, and mechanical properties of poly (trimethylene terephthalate)/poly (lactic acid) blends, *Polym. Bull.* 64 (2010) 471-481.
- [131] H.T. Oyama, Super-tough poly (lactic acid) materials: Reactive blending with ethylene copolymer, *Polymer* 50 (2009) 747-751.
- [132] M.P. Arrieta, E. Fortunati, F. Dominici, E. Rayón, J. López, J.M. Kenny, PLA-PHB/cellulose based films: Mechanical, barrier and disintegration properties, *Polym. Degrad. Stab.* 107 (2014) 139-149.
- [133] N. Graupner, Application of lignin as natural adhesion promoter in cotton fibre-reinforced poly(lactic acid) (PLA) composites, *J. Mater. Sci.* 43 (2008) 5222-5229.
- [134] N. Graupner, A.S. Herrmann, J. Müssig, Natural and man-made cellulose fibre-reinforced poly(lactic acid) (PLA) composites: An overview about mechanical characteristics and application areas, *Composites Part A* 40 (2009) 810-821.
- [135] Y. Hu, Q. Wang, M. Tang, Preparation and properties of Starch-g-PLA/poly(vinyl alcohol) composite film, *Carbohydr. Polym.* 96 (2013) 384-388.
- [136] I.S.M.A. Tawakkal, R.A. Talib, K. Abdan, C.N. Ling, Mechanical and physical properties of kenaf-derived cellulose (KDC)-filled polylactic acid (PLA) composites, *BioResources* 7 (2012) 1643-1655.
- [137] E. Jalalvandi, R. Majid, T. Ghanbari, H. Ilbeygi, Effects of montmorillonite (MMT) on morphological, tensile, physical barrier properties and biodegradability of

- polylactic acid/starch/MMT nanocomposites, *J. Thermoplast. Compos. Mater.* 28 (2015) 496-509.
- [138] A.K. Mohapatra, S. Mohanty, S.K. Nayak, Study of Thermo-Mechanical and Morphological Behaviour of Biodegradable PLA/PBAT/Layered Silicate Blend Nanocomposites, *J. Polym. Environ.* 22 (2014) 398-408.
- [139] K. Nuñez, C. Rosales, R. Perera, N. Villarreal, J.M. Pastor, Nanocomposites of PLA/PP blends based on sepiolite, *Polym. Bull.* 67 (2011) 1991-2016.
- [140] J.-W. Rhim, S.-I. Hong, C.-S. Ha, Tensile, water vapor barrier and antimicrobial properties of PLA/nanoclay composite films, *LWT-Food Sci. Technol.* 42 (2009) 612-617.
- [141] G.-X. Zou, X. Zhang, C.-X. Zhao, J. Li, The crystalline and mechanical properties of PLA/layered silicate degradable composites, *Polym. Sci. Ser. A* 54 (2012) 393-400.
- [142] M. Sabzi, L. Jiang, M. Atai, I. Ghasemi, PLA/sepiolite and PLA/calcium carbonate nanocomposites: A comparison study, *J. Appl. Polym. Sci.* 129 (2013) 1734-1744.
- [143] S. Siengchin, Reinforced Flax Mat/Modified Polylactide (PLA) Composites: Impact, Thermal, and Mechanical Properties, *Mech. Compos. Mater.* 50 (2014) 257-266.
- [144] A. Araújo, G. Botelho, M. Oliveira, A.V. Machado, Influence of clay organic modifier on the thermal-stability of PLA based nanocomposites, *Appl. Clay Sci.* 88-89 (2014) 144-150.
- [145] L. Basilissi, G. Di Silvestro, H. Farina, M.A. Ortenzi, Synthesis and characterization of PLA nanocomposites containing nanosilica modified with different organosilanes II: Effect of the organosilanes on the properties of nanocomposites: Thermal characterization, *J. Appl. Polym. Sci.* 128 (2013) 3057-3063.
- [146] B.-K. Chen, C.-C. Shih, A.F. Chen, Ductile PLA nanocomposites with improved thermal stability, *Composites Part A* 43 (2012) 2289.
- [147] M. Iturrondobeitia, A. Okariz, T. Guraya, A.M. Zaldua, J. Ibarretxe, Influence of the processing parameters and composition on the thermal stability of PLA/nanoclay bio-nanocomposites, *J. Appl. Polym. Sci.* 131 (2014) 9120-9127.
- [148] G. Gorrasi, R. Pantani, M. Murariu, P. Dubois, PLA/halloysite nanocomposite films: water vapor barrier properties and specific key characteristics, *Macromol. Mater. Eng.* 299 (2014) 104-115.
- [149] E. Picard, E. Espuche, R. Fulchiron, Effect of an organo-modified montmorillonite on PLA crystallization and gas barrier properties, *Appl. Clay Sci.* 53 (2011) 58-65.

- [150] P.M.S. Souza, A.R. Morales, M.A. Marin-Morales, L.H.I. Mei, PLA and montmorillonite nanocomposites: Properties, biodegradation and potential toxicity, *J. Polym. Environ.* 21 (2013) 738-759.
- [151] S.S. Ray, Nanocomposites, in: R. Auras, L.T. Lim, S. Selke, H. Tsuji (Eds.), *Poly(lactic acid). Synthesis, Structures, Properties, Processing, and Applications*, John Wiley & Sons, Inc., New Jersey, 2010, pp. 311-321.
- [152] R.T. De Silva, P. Pasbakhsh, S.M. Lee, A.Y. Kit, ZnO deposited/encapsulated halloysite–poly (lactic acid) (PLA) nanocomposites for high performance packaging films with improved mechanical and antimicrobial properties, *Appl. Clay Sci.* 111 (2015) 10-20.
- [153] H. Ebadi-Dehaghani, H.A. Khonakdar, M. Barikani, S.H. Jafari, Experimental and theoretical analyses of mechanical properties of PP/PLA/clay nanocomposites, *Composites Part B* 69 (2015) 133-144.
- [154] M.R. Kamal, V. Khoshkava, Effect of cellulose nanocrystals (CNC) on rheological and mechanical properties and crystallization behavior of PLA/CNC nanocomposites, *Carbohydr. Polym.* 123 (2015) 105-114.
- [155] S.-M. Lai, S.-H. Wu, G.-G. Lin, T.-M. Don, Unusual mechanical properties of melt-blended poly(lactic acid) (PLA)/clay nanocomposites, *Eur. Polym. J.* 52 (2014) 193.
- [156] Q.K. Meng, M. Hetzer, D. De Kee, PLA/clay/wood nanocomposites: nanoclay effects on mechanical and thermal properties, *J. Compos. Mater.* 45 (2011) 1145-1158.
- [157] G. Ozkoc, S. Kemaloglu, Morphology, biodegradability, mechanical, and thermal properties of nanocomposite films based on PLA and plasticized PLA, *J. Appl. Polym. Sci.* 114 (2009) 2481-2487.
- [158] S.I. Pirani, P. Krishnamachari, R. Hashaikh, Optimum loading level of nanoclay in PLA nanocomposites: Impact on the mechanical properties and glass transition temperature, *J. Thermoplast. Compos. Mater.* 27 (2014) 1461-1478.
- [159] Q. Shi, C. Zhou, Y. Yue, W. Guo, Y. Wu, Q. Wu, Mechanical properties and in vitro degradation of electrospun bio-nanocomposite mats from PLA and cellulose nanocrystals, *Carbohydr. Polym.* 90 (2012) 301.
- [160] M. Yourdkhani, T. Mousavand, N. Chapleau, P. Hubert, Thermal, oxygen barrier and mechanical properties of polylactide-organoclay nanocomposites, *Compos. Sci. Technol.* 82 (2013) 47.
- [161] M. Farmahini-Farahani, H. Xiao, Y. Zhao, Poly lactic acid nanocomposites containing modified nanoclay with synergistic barrier to water vapor for coated paper, *Journal of Applied Polymer Science* 131 (2014) n/a-n/a.

- [162] H.A. Patel, R.S. Somani, H.C. Bajaj, R.V. Jasra, Nanoclays for polymer nanocomposites, paints, inks, greases and cosmetics formulations, drug delivery vehicle and waste water treatment, *Bull. Mater. Sci.* 29 (2006) 133-145.
- [163] F. Uddin, Clays, nanoclays, and montmorillonite minerals, *Metall. Mater. Trans. A* 39 (2008) 2804-2814.
- [164] S.S. Ray, M. Okamoto, Polymer/layered silicate nanocomposites: a review from preparation to processing, *Prog. Polym. Sci.* 28 (2003) 1539-1641.
- [165] X. Fang, S. Domenek, V. Ducruet, M. Réfrégiers, O. Vitrac, Diffusion of aromatic solutes in aliphatic polymers above glass transition temperature, *Macromolecules* 46 (2013) 874-888.
- [166] M.W. Noh, D.C. Lee, Synthesis and characterization of PS-clay nanocomposite by emulsion polymerization, *Polym. Bull.* 42 (1999) 619-626.
- [167] M. Zanetti, S. Lomakin, G. Camino, Polymer layered silicate nanocomposites, *Macromol. Mater. Eng.* 279 (2000) 1-9.
- [168] J.-M. Raquez, Y. Habibi, M. Murariu, P. Dubois, Polylactide (PLA)-based nanocomposites, *Prog. Polym. Sci.* 38 (2013) 1504-1542.
- [169] D. Wu, L. Wu, M. Zhang, Y. Zhao, Viscoelasticity and thermal stability of polylactide composites with various functionalized carbon nanotubes, *Polym. Degrad. Stab.* 93 (2008) 1577-1584.
- [170] K. Shameli, M.B. Ahmad, W.M.Z.W. Yunus, N.A. Ibrahim, R.A. Rahman, M. Jokar, M. Darroudi, Silver/poly (lactic acid) nanocomposites: preparation, characterization, and antibacterial activity, *Int. J. Nanomedicine* 5 (2010) 573.
- [171] N.L.G. De Rodriguez, W. Thielemans, A. Dufresne, Sisal cellulose whiskers reinforced polyvinyl acetate nanocomposites, *Cellulose* 13 (2006) 261-270.
- [172] J. Araki, M. Wada, S. Kuga, T. Okano, Influence of surface charge on viscosity behavior of cellulose microcrystal suspension, *J. Wood Sci.* 45 (1999) 258-261.
- [173] S. Beck-Candanedo, M. Roman, D.G. Gray, Effect of reaction conditions on the properties and behavior of wood cellulose nanocrystal suspensions, *Biomacromolecules* 6 (2005) 1048-1054.
- [174] I. Kvien, B.S. Tanem, K. Oksman, Characterization of cellulose whiskers and their nanocomposites by atomic force and electron microscopy, *Biomacromolecules* 6 (2005) 3160-3165.
- [175] J. Araki, M. Wada, S. Kuga, T. Okano, Birefringent glassy phase of a cellulose microcrystal suspension, *Langmuir* 16 (2000) 2413-2415.

- [176] X.M. Dong, J.-F. Revol, D.G. Gray, Effect of microcrystallite preparation conditions on the formation of colloid crystals of cellulose, *Cellulose* 5 (1998) 19-32.
- [177] Y. Habibi, L. Foulon, V. Aguié-Béghin, M. Molinari, R. Douillard, Langmuir–Blodgett films of cellulose nanocrystals: Preparation and characterization, *J. Colloid Interface Sci.* 316 (2007) 388-397.
- [178] Y. Habibi, L.A. Lucia, O.J. Rojas, Cellulose nanocrystals: chemistry, self-assembly, and applications, *Chem. Rev.* 110 (2010) 3479-3500.
- [179] S.J. Hanley, J. Giasson, J.-F. Revol, D.G. Gray, Atomic force microscopy of cellulose microfibrils: comparison with transmission electron microscopy, *Polymer* 33 (1992) 4639-4642.
- [180] J.-F. Revol, On the cross-sectional shape of cellulose crystallites in *Valonia ventricosa*, *Carbohydr. Polym.* 2 (1982) 123-134.
- [181] C. Gauthier, Nanocomposite materials from latex and cellulose whiskers, *Polym. Adv. Technol.* 6 (1994) 351355.
- [182] M. Huda, L. Drzal, A. Mohanty, M. Misra, The effect of silane treated-and untreated-talc on the mechanical and physico-mechanical properties of poly (lactic acid)/newspaper fibers/talc hybrid composites, *Composites Part B* 38 (2007) 367-379.
- [183] H.S. Kim, B.H. Park, J.H. Choi, J.S. Yoon, Mechanical properties and thermal stability of poly (L-lactide)/calcium carbonate composites, *J. Appl. Polym. Sci.* 109 (2008) 3087-3092.
- [184] M. Murariu, L. Bonnaud, P. Yoann, G. Fontaine, S. Bourbigot, P. Dubois, New trends in polylactide (PLA)-based materials:“Green” PLA–Calcium sulfate (nano) composites tailored with flame retardant properties, *Polym. Degrad. Stab.* 95 (2010) 374-381.
- [185] M. Bühler, P.-E. Bourban, J.-A.E. Månson, Cellular composites based on continuous fibres and bioresorbable polymers, *Composites Part A* 39 (2008) 1779-1786.
- [186] G. Koronis, A. Silva, M. Fontul, Green composites: a review of adequate materials for automotive applications, *Composites Part B* 44 (2013) 120-127.
- [187] A. Bledzki, A. Jaszkiwicz, Mechanical performance of biocomposites based on PLA and PHBV reinforced with natural fibres–A comparative study to PP, *Compos. Sci. Technol.* 70 (2010) 1687-1696.
- [188] A. Le Duigou, P. Davies, C. Baley, Seawater ageing of flax/poly (lactic acid) biocomposites, *Polym. Degrad. Stab.* 94 (2009) 1151-1162.

- [189] Consumer Good, in: E. Britannica, 2015.
- [190] S. Suzuki, Y. Ikada, Medical Applications, in: R. Auras, L.T. Lim, S. Selke, H. Tsuji (Eds.), Poly(lactic acid). Synthesis, Structures, Properties, Processing, and Applications, Wiley Publishers, New Jersey, 2010, pp. 443-456.
- [191] C.R.L. Zhou, L.H., Application of Novel PLA/Chitosan Composite Materials on Bone Tissue Scaffolds, Australasian Society for Biomaterials and Tissue Engineering 8 (2004) 1572.
- [192] D.M. Inc., Biocryl Rapide: TCP/PLGA Composite, in, DePuy Mitek, Raynham, MA, 2005.
- [193] Z. Inc. Zimmer(R) Bio-Statak(R) Soft Tissue Attachment Device. Available: <http://www.zimmer.com/content/dam/zimmer-web/documents/en-US/pdf/surgical-techniques/trauma/Zimmer-Biostatak-Soft-Tissue-Attachment.pdf>. Access date Sept 15, 2015, 2015.
- [194] T. Deligio, PLA Composite Screws Replace Titanium in Surgical Implants, in: Plastics Today, 2010.
- [195] A. Hamilton, Mitek Sports Medicine Introduces New Interference Screw Design For Faster, Easier Insertion, in, PR Newswire, Chicago, 2013.
- [196] S.M.A. Bianca, Award-winning Water Filter Made from Bioplastic, in, Fraunhofer Institute UMSICHT, 2014.
- [197] K. Seitz, Biovation Launches Bioarmour™ Blood Pressure Cuff Shield, in: Biovation Launches Bioarmour™ Blood Pressure Cuff Shield, An Infectious Disease Barrier Product For Hospitals And Healthcare Facilities, Biovation, 2015.
- [198] Ahlstrom. Ahlstrom BioWeb® Ultrasonic and Heatseal Teabags. Available: <http://www.ahlstrom.com/en/Products/Food-and-Beverage/Tea-bags/BioWeb-Ultrasonic--heatsealable-teabags/>. Access date September 2nd, 2015.
- [199] Ford researchers aim to create greener, lighter plastics. Available: <http://www.reliableplant.com/Read/20034/ford-researchers-aim-to-create-greener,-lighter-plastics>. Access date Sept 2nd, 2015.
- [200] S.K. Ghosh, S., Application of Poly(lactic acid) Fibres in Automotive Interior, Indian J. Fibre Text. 32 (2007) 119-121.
- [201] K. So, Automotive Giants Turn to Bioplastics Worldwide, in, Plastics News, Brussel, 2012.
- [202] D. Farrington, J. Lunt, S. Davies, R. Blackburn, Poly (lactic acid) fibers, in: R. Blackburn (Ed.), Biodegradable and sustainable fibres, Woodhead Publishing Limited, Cambridge, England, 2005, pp. 191-220.

- [203] M. Mochizuki, Textile Applications, in: R. Auras, L.T. Lim, S. Selke, H. Tsuji (Eds.), Poly (Lactic Acid): Synthesis, Structures, Properties, Processing, and Applications, John Wiley & Sons, Inc., New Jersey, 2010, pp. 469-476.
- [204] T. Limited, Kansai Univ., Teijin Develop World's First Piezoelectric Fabrics for Wearable Devices, in, BioSpace, Tokyo, Japan, 2015.
- [205] S. Obuchi, S. Ogawa, Packaging and other commercial applications, in: R. Auras, L.T. Lim, S. Selke, H. Tsuji (Eds.), Poly (lactic acid): Synthesis, Structures, Properties, Processing, and Applications, John Wiley & Sons, Inc., New Jersey, 2010, pp. 457-467.
- [206] D. Sullivan. Chipmaker's All-Or-Nothing Claim Sets The Bar In Big And Bold. Available: <http://www.biocycle.net/2010/08/17/chipmakers-all-or-nothing-claim-sets-the-bar-in-big-and-bold/>. Access date September 2nd, 2015.
- [207] K. Siranosian. New SunChips Bag: 90% Plant-based, 100% Compostable. Available: <http://www.triplepundit.com/2010/02/new-sunchips-bag-compostable/>. Access date Sept 2nd, 2015.
- [208] M. Rosenthal, SAM'S CLUB Partners with NatureWorks PLA to Help the Environment, in, NatureWorks LLC, 2005.
- [209] NatureWorks, SPAR Austria Enhances Freshness of Produce with NatureWorks PLA, in, NatureWorks, Linz, Austria, 2005.
- [210] A.M. Mohan. Danone First to Switch to PLA for Yogurt Cup in Germany. Available: http://www.greenerpackage.com/bioplastics/danone_first_switch_pla_yogurt_cup_germany. Access date September 2nd, 2015.
- [211] J. Mochal, ConAgra Foods' New, Renewable Shrink Film Technology to Reduce Impact on the Environment, in, ConAgra Foods, Omaha, NE, 2009.
- [212] Bioplastics, First PLA Bottle in Germany, in: Bioplastics, Bioplastics, 2006, pp. 20-21.
- [213] R. Cernansky. Odwalla Juice Transitioning to 'PlantBottles' - HDPE Plastic From Plant-Based Materials. Access date September 2nd, 2015.
- [214] T. Pak, Fully Renewable Carton Package Now on the Shelves, in: A world first for Valio and Tetra Pak, Tetra Pak, 2015.
- [215] A. Mohanty, M. Misra, L. Drzal, Sustainable bio-composites from renewable resources: opportunities and challenges in the green materials world, J. Polym. Environ. 10 (2002) 19-26.

- [216] Y. Kasai, Nucleating Agents for inducing the Crystallization of PLA-Ecopromote(R), in: Innovation Takes Root Conference, Orlando, FL, 2012.
- [217] C. Purac, Bioplastics Product Profile: PLA Injection Molded Serviceware, in: C. Purac (Ed.), Corbion, 2013.
- [218] K. Jansen, Serving Up Plant-Based Plastics, in, Plastic News, Rosement, IL, 2015.
- [219] D. Smock, New Bioplastic Feature Higher HDT, Impact Strength, in, DesignNews, 2011.
- [220] Compostable Grocery Bags. Available: <http://advantage-environment.com/livsmedel/compostable-grocery-bags/>. Access date September 2nd, 2015.
- [221] B. Bregar, PLA Bottle Maker Biota Enters Bankruptcy, in, PlasticNews, 2007.
- [222] R. Lingle, PLA Makes Splash in Bottled Water, in: Packaging World, Packaging World, 2004.
- [223] A. ElAmin. Wal-Mart Signals Move to Natural Packaging. Available: <http://www.foodproductiondaily.com/Packaging/Wal-Mart-signals-move-to-natural-packaging>. Access date September 2nd, 2015.
- [224] Delhaize Expands Biodegradable Packaging Switch. Access date Sept 2nd, 2015.
- [225] NatureWorks, Nature-Based Packaging for Fresh Cut Produce in High Demand, in: NatureWorks(R) PLA Offereing Brand Owners and reatilers a Solution Consumers Desire, NatureWorks, Minnetonka, MN, 2005.
- [226] NatureWorks, Pacific Pre-Cut Enhance The Freshness of Its Brand with NatureWorks PLA Packaging for Fresh-Packed Salads., in, NatureWorks, Minnetonka, MN, 2005.
- [227] Bioplastics, Huhtamaki Awarded Silver: Huhtamaki's PLA Dessert Cup Successful in the Annual UK Starpack Competition, in: Bioplastics, Bioplastics, 2006, pp. 7.
- [228] Fabri-Kal. Fabri-Kal Announces Addition to Greenware Product Family. Available: <http://www.fabri-kal.com/fabri-kal-announces-addition-to-greenware-product-family/>. Access date October 10, 2015.
- [229] NatureWorks, Award, in: IngeoNews, 2008.
- [230] R. Thompson, Packaging, PLA, in, Sustainable Is Good, 2007.
- [231] PLA Bottles Soon To Be Released in Italy, in: Packaging Europe, Packaging Europe, 2008.

- [232] Shiseido, Shiseido to Commercialize Polylactic Acid Containers with Low Environmental Load: To Be Introduced to URARA Brand Exclusively for the Chinese Market, in, Shiseido, 2009.
- [233] H. Soto-Valdez, PLA clamshells, in: H. Samsudin (Ed.), 2011.
- [234] A.M. Mohan. Stonyfield Farm Makes Studied Switch to PLA for Yogurt Multipacks. Available:
http://www.greenerpackage.com/regulations/stonyfield_farm_makes_studied_switch_pla_yogurt_multipacks. Access date September 2nd, 2015.
- [235] Polenghi. Bio Bottle. Available: <http://www.polenghigroup.it/en/sostenibilita/>. Access date October 10, 2015.
- [236] P. Strategies, Bio Bottle Is First in Europe, in: Packaging Strategies, 2010.
- [237] M. Beune. Barrier Films: SiOx Barrier Benefits. Available: <http://www.pffc-online.com/coat-lam/coatings/8832-siox-barrier-benefits-1001>. Access date October 24th, 2015.
- [238] Bioplastics, PLA Capsules for Athletic Apparel, in: Bioplastics, Bioplastics, 2011.
- [239] C. Purac, Bioplastics Product Profile: PLA Thermoformed Single-Use Hot Beverage Cups, in: C. Purac (Ed.), Corbion, 2013.
- [240] D.G. Hayes, S. Dharmalingam, L.C. Wadsworth, K.K. Leonas, C. Miles, D. Inglis, Biodegradable agricultural mulches derived from biopolymers, in: C.S. Kishan Khemani (Ed.), Degradable polymers and materials: Principles and practice, American Chemical Society, Washington, DC, 2012, pp. 201-223.
- [241] S. Kasirajan, M. Ngouajio, Polyethylene and biodegradable mulches for agricultural applications: a review, *Agron. Sustain. Dev.* 32 (2012) 501-529.
- [242] T. Kijchavengkul, Design of biodegradable aliphatic aromatic polyester films for agricultural applications using response surface methodology, in: Packaging, Michigan State University, Michigan, 2010.
- [243] M. Hakkarainen, S. Karlsson, A.C. Albertsson, Influence of low molecular weight lactic acid derivatives on degradability of polylactide, *J. Appl. Polym. Sci.* 76 (2000) 228-239.
- [244] S.R. Andersson, M. Hakkarainen, A.-C. Albertsson, Tuning the polylactide hydrolysis rate by plasticizer architecture and hydrophilicity without introducing new migrants, *Biomacromolecules* 11 (2010) 3617-3623.
- [245] Y. Matsuzawa, Z.-I. Kimura, Y. Nishimura, M. Shibayama, A. Hiraishi, Removal of Hydrophobic Organic Contaminants from Aqueous Solutions by Sorption onto Biodegradable Polyesters, *J. Water Resour. Prot.* 2 (2010) 214-221.

- [246] A. Hiraishi, Environmental Applications, in: R. Auras, L. Lim, S. Selke, H. Tsuj (Eds.), Poly(Lactic Acid), John Wiley & Sons, Inc., Hoboken, NJ, 2010, pp. 469-476.
- [247] S.S. Koenigsberg, Hydrogen Release Compound (HRC): A Novel Technology for the Bioremediation of Chlorinated Hydrocarbons, in: Proceedings of the 1999 Conference on Hazardous Waste Research, St. Louis, MO, 1999.
- [248] G. Caruso, Plastic Degrading Microorganisms as a Tool for Bioremediation of Plastic Contamination in Aquatic Environments, J. Pollut. Eff. Cont. 3 (2015) e112.
- [249] L. Chilson. The Difference between ABS and PLA for 3D Printing. Available: <http://www.protoparadigm.com/news-updates/the-difference-between-abs-and-pla-for-3d-printing/>. Access date November 30th, 2015.
- [250] R.M. Robertson, W.C. Thomas, J.N. Suthar, D.M. Brown, Accelerated degradation of cellulose acetate cigarette filters using controlled-release acid catalysis, Green Chem. 14 (2012) 2266-2272.
- [251] F.L. Ltd. Fujitsu Laboratories Develops Industry's First Bio-Derived, Water-based Paint. Available: <http://www.fujitsu.com/global/about/resources/news/press-releases/2014/1210-01.html>. Access date November 30th 2015.
- [252] Fujitsu, Fujitsu and Toray Develop World's First Environmentally-Friendly Large-Size Plastic Housing for Notebook PCs. Available: <http://www.fujitsu.com/global/about/resources/news/press-releases/2005/0113-01.html>. Access date February 28th, 2016.
- [253] PEGA. Available: <http://www.pegadesign.com/en/portfolio-pla.html>. Access date February 28th, 2016.
- [254] W.L. Hawkins, Polymer Degradation and Stabilization, Springer-Verlag, Berlin, 1984.
- [255] R. Muller, Biodegradability of polymers: Regulations and methods of testing. , in: A. Steinbuchel (Ed.), Biopolymer, General Aspects and Special Application, Wiley Publishers, 2008, pp. 366-388.
- [256] H. Tsuji, Hydrolytic Degradation, in: R. Auras, L.T. Lim, S. Selke, H. Tsuji (Eds.), Poly(lactic acid). Synthesis, Structures, Properties, Processing, and Applications, John Wiley & Sons, Inc., New Jersey, 2010, pp. 345-381.
- [257] S. De Jong, E.R. Arias, D. Rijkers, C. Van Nostrum, J. Kettenes-Van den Bosch, W. Hennink, New insights into the hydrolytic degradation of poly (lactic acid): participation of the alcohol terminus, Polymer 42 (2001) 2795-2802.

- [258] S. Lyu, J. Schley, B. Loy, D. Lind, C. Hobot, R. Sparer, D. Untereker, Kinetics and time-temperature equivalence of polymer degradation, *Biomacromolecules* 8 (2007) 2301-2310.
- [259] E. Fischer, H.J. Sterzel, G. Wegner, Investigation of the structure of solution grown crystals of lactide copolymers by means of chemical reactions, *Kolloid Z. Z. Polym.* 251 (1973) 980-990.
- [260] C. Chu, Hydrolytic degradation of polyglycolic acid: tensile strength and crystallinity study, *J. Appl. Polym. Sci.* 26 (1981) 1727-1734.
- [261] Y.-N. Chang, R.E. Mueller, E.L. Iannotti, Use of low MW polylactic acid and lactide to stimulate growth and yield of soybeans, *Plant Growth Regul.* 19 (1996) 223-232.
- [262] C. Xiang, A.G. Taylor, J.P. Hinestroza, M.W. Frey, Controlled release of nonionic compounds from poly (lactic acid)/cellulose nanocrystal nanocomposite fibers, *J. Appl. Polym. Sci.* 127 (2013) 79-86.
- [263] A. Copinet, C. Bertrand, S. Govindin, V. Coma, Y. Couturier, Effects of ultraviolet light (315 nm), temperature and relative humidity on the degradation of polylactic acid plastic films, *Chemosphere* 55 (2004) 763-773.
- [264] J.H. Jung, M. Ree, H. Kim, Acid-and base-catalyzed hydrolyses of aliphatic polycarbonates and polyesters, *Catal. Today* 115 (2006) 283-287.
- [265] K. Makino, H. Ohshima, T. Kondo, Mechanism of hydrolytic degradation of poly (L-lactide) microcapsules: effects of pH, ionic strength and buffer concentration, *J. Microencapsulation* 3 (1986) 203-212.
- [266] H. Tsuji, Y. Ikada, Properties and morphology of poly (L-lactide). II. Hydrolysis in alkaline solution, *J. Polym. Sci., Part A: Polym. Chem.* 36 (1998) 59-66.
- [267] Y. Ikada, H. Tsuji, Biodegradable polyesters for medical and ecological applications, *Macromol. Rapid Commun.* 21 (2000) 117-132.
- [268] H.S. Burdurlu, N. Koca, F. Karadeniz, Degradation of vitamin C in citrus juice concentrates during storage, *J. Food Eng.* 74 (2006) 211-216.
- [269] H. Tsuji, K. Sumida, Poly (L-lactide): v. effects of storage in swelling solvents on physical properties and structure of poly (L-lactide), *J. Appl. Polym. Sci.* 79 (2001) 1582-1589.
- [270] S. Sato, D. Gondo, T. Wada, S. Kanehashi, K. Nagai, Effects of various liquid organic solvents on solvent-induced crystallization of amorphous poly (lactic acid) film, *J. Appl. Polym. Sci.* 129 (2013) 1607-1617.

- [271] J. Gao, L. Duan, G. Yang, Q. Zhang, M. Yang, Q. Fu, Manipulating poly (lactic acid) surface morphology by solvent-induced crystallization, *Appl. Surf. Sci.* 261 (2012) 528-535.
- [272] FDA. Guidance for Industry: Preparation of Premarket Submissions for Food Contact Substances: Chemistry Recommendations. Food and Drug Administration. Available: <http://www.fda.gov/Food/GuidanceRegulation/GuidanceDocumentsRegulatoryInformation/IngredientsAdditivesGRASPackaging/ucm081818.htm> - iid1a. Access date September 15th, 2015.
- [273] 10/2011/EU Commission regulation on plastic materials and articles intended to come into contact with food. The European Commission., *Official Journal of the European Union* 12 (2011) 15.11.2011.
- [274] F. Iñiguez-Franco, G. Burgessa, D. Holmes, X. Fanga, M. Rubino, H. Soto-Valdez, R. Auras, Concurrent induced solvent crystallization and hydrolytic degradation of PLA by water-ethanol solutions, *Polymer*. 99 (2016) 315-323.
- [275] M.K. Mitchell, D.E. Hirt, Degradation of PLA fibers at elevated temperature and humidity, *Polym. Eng. Sci.* 55 (2015) 1652-1660.
- [276] K. Fukushima, D. Tabuani, M. Dottori, I. Armentano, J. Kenny, G. Camino, Effect of temperature and nanoparticle type on hydrolytic degradation of poly (lactic acid) nanocomposites, *Polym. Degrad. Stab.* 96 (2011) 2120-2129.
- [277] W. Tham, Z.M. Ishak, W. Chow, Water absorption and hygrothermal aging behaviors of SEBS-g-MAH toughened poly (lactic acid)/halloysite nanocomposites, *Polym. Plast. Technol. Eng.* 53 (2014) 472-480.
- [278] K. Jamshidi, S.-H. Hyon, Y. Ikada, Thermal characterization of polylactides, *Polymer* 29 (1988) 2229-2234.
- [279] F.-D. Kopinke, K. Mackenzie, Mechanistic aspects of the thermal degradation of poly (lactic acid) and poly (β -hydroxybutyric acid), *J. Anal. Appl. Pyrolysis* 40 (1997) 43-53.
- [280] F.-D. Kopinke, M. Remmler, K. Mackenzie, Thermal decomposition of biodegradable polyesters—I: Poly (β -hydroxybutyric acid), *Polym. Degrad. Stab.* 52 (1996) 25-38.
- [281] I. McNeill, H. Leiper, Degradation studies of some polyesters and polycarbonates—2. Polylactide: degradation under isothermal conditions, thermal degradation mechanism and photolysis of the polymer, *Polym. Degrad. Stab.* 11 (1985) 309-326.

- [282] Y. Aoyagi, K. Yamashita, Y. Doi, Thermal degradation of poly [(R)-3-hydroxybutyrate], poly [ϵ -caprolactone], and poly [(S)-lactide], *Polym. Degrad. Stab.* 76 (2002) 53-59.
- [283] H. Abe, N. Takahashi, K.J. Kim, M. Mochizuki, Y. Doi, Thermal degradation processes of end-capped poly (L-lactide) s in the presence and absence of residual zinc catalyst, *Biomacromolecules* 5 (2004) 1606-1614.
- [284] A. Babanalbandi, D.J.T. Hill, D.S. Hunter, L. Kettle, Thermal stability of poly (lactic acid) before and after γ -radiolysis, *Polym. Int.* 48 (1999) 980-984.
- [285] H. Zou, C. Yi, L. Wang, H. Liu, W. Xu, Thermal degradation of poly (lactic acid) measured by thermogravimetry coupled to Fourier transform infrared spectroscopy, *J. Therm. Anal. Calorim.* 97 (2009) 929-935.
- [286] H. Nishida, Thermal degradation, in: R. Auras, L.T. Lim, S. Selke, H. Tsuji (Eds.), *Poly(lactic acid). Synthesis, Structures, Properties, Processing, and Applications*, Wiley Publishers, New Jersey, 2010, pp. 401-412.
- [287] P. Degée, P. Dubois, R. Jérôme, Bulk polymerization of lactides initiated by aluminium isopropoxide, 3. Thermal stability and viscoelastic properties, *Macromol. Chem. Phys.* 198 (1997) 1985-1995.
- [288] O. Wachsen, K. Platkowski, K.-H. Reichert, Thermal degradation of poly-L-lactide—studies on kinetics, modelling and melt stabilisation, *Polym. Degrad. Stab.* 57 (1997) 87-94.
- [289] V. Taubner, R. Shishoo, Influence of processing parameters on the degradation of poly (L-lactide) during extrusion, *J. Appl. Polym. Sci.* 79 (2001) 2128-2135.
- [290] H. Tsuji, I. Fukui, Enhanced thermal stability of poly (lactide) s in the melt by enantiomeric polymer blending, *Polymer* 44 (2003) 2891-2896.
- [291] D. Cam, M. Marucci, Influence of residual monomers and metals on poly (L-lactide) thermal stability, *Polymer* 38 (1997) 1879-1884.
- [292] A. Södergård, J. Näsman, Stabilization of poly (L-lactide) in the melt, *Polym. Degrad. Stab.* 46 (1994) 25-30.
- [293] Y. Fan, H. Nishida, Y. Shirai, Y. Tokiwa, T. Endo, Thermal degradation behaviour of poly (lactic acid) stereocomplex, *Polym. Degrad. Stab.* 86 (2004) 197-208.
- [294] N. Najafi, M. Heuzey, P. Carreau, P.M. Wood-Adams, Control of thermal degradation of polylactide (PLA)-clay nanocomposites using chain extenders, *Polym. Degrad. Stab.* 97 (2012) 554-565.

- [295] R. Al-Itry, K. Lamnawar, A. Maazouz, Improvement of thermal stability, rheological and mechanical properties of PLA, PBAT and their blends by reactive extrusion with functionalized epoxy, *Polym. Degrad. Stab.* 97 (2012) 1898-1914.
- [296] W. Sakai, N. Tsutsumi, Photodegradation and radiation degradation, in: R. Auras, L.-T. Lim, S. Selke, H. Tsuji (Eds.), *Poly(lactic acid): Synthesis, Structures, Properties, Processing, and Applications*, John Wiley & Sons, Inc., New Jersey, 2010, pp. 413-421.
- [297] E. Ikada, M. Ashida, Promotion of photodegradation of polymers for plastic waste treatment, *J. Photopolym. Sci. Technol.* 4 (1991) 247-254.
- [298] E. Ikada, Role of The Molecular Structure in The Photodecomposition of Polymers, *J. Photopolym. Sci. Technol.* 6 (1993) 115-122.
- [299] E. Ikada, Photo-and bio-degradable polyesters. Photodegradation behaviors of aliphatic polyesters, *J. Photopolym. Sci. Technol.* 10 (1997) 265-270.
- [300] E. Ikada, Relationship between Photodegradability and Biodegradability of Some Aliphatic Polyesters, *J. Photopolym. Sci. Technol.* 12 (1999) 251-256.
- [301] L. Santonja-Blasco, A. Ribes-Greus, R. Alamo, Comparative thermal, biological and photodegradation kinetics of polylactide and effect on crystallization rates, *Polym. Degrad. Stab.* 98 (2013) 771-784.
- [302] H. Tsuji, Y. Echizen, Y. Nishimura, Photodegradation of biodegradable polyesters: A comprehensive study on poly (l-lactide) and poly (ϵ -caprolactone), *Polym. Degrad. Stab.* 91 (2006) 1128-1137.
- [303] A.V. Janorkar, A.T. Metters, D.E. Hirt, Degradation of poly (L-lactide) films under ultraviolet-induced photografting and sterilization conditions, *J. Appl. Polym. Sci.* 106 (2007) 1042-1047.
- [304] K.-L.G. Ho, A.L. Pometto III, Effects of electron-beam irradiation and ultraviolet light (365 nm) on polylactic acid plastic films, *J. Environ. Polym. Degr.* 7 (1999) 93-100.
- [305] K.-L.G. Ho, A.L. Pometto III, P.N. Hinz, Effects of temperature and relative humidity on polylactic acid plastic degradation, *J. Environ. Polym. Degr.* 7 (1999) 83-92.
- [306] A. Babanalbandi, D. Hill, J. O'Donnell, P. Pomery, A. Whittaker, An electron spin resonance study on γ -irradiated poly (l-lactic acid) and poly (d, l-lactic acid), *Polym. Degrad. Stab.* 50 (1995) 297-304.
- [307] C. Birkinshaw, M. Buggy, G. Henn, E. Jones, Irradiation of poly-D, L-lactide, *Polym. Degrad. Stab.* 38 (1992) 249-253.

- [308] J. Collett, L. Lim, P. Gould, Gamma-irradiation of biodegradable polyesters in controlled physical environments, *Polymer Prepr. Am. Chem. Soc.* 30 (1989) 468-469.
- [309] Global Sustainable Development Report. Briefs Available: <https://sustainabledevelopment.un.org/content/documents/1870GSDR%202015%20Briefs.pdf> Access date October 24th, 2015.
- [310] M.A. Curran, Life cycle assessment: a review of the methodology and its application to sustainability, *Curr. Opin. Chem. Eng.* 2 (2013) 273-277.
- [311] S. Madival, R. Auras, S.P. Singh, R. Narayan, Assessment of the environmental profile of PLA, PET and PS clamshell containers using LCA methodology, *J. Clean Prod.* 17 (2009) 1183-1194.
- [312] Directive 2008/98/EC of the European Parliament and of the Council of 19 November 2008 on waste and repealing certain directives. Available: <http://eur-lex.europa.eu/legal-content/EN/TXT/PDF/?uri=CELEX:32008L0098&from=EN> Access date October 26th, 2015.
- [313] EPA, Advancing Sustainable Materials Management: 2013 Fact Sheet Available: http://www3.epa.gov/epawaste/nonhaz/municipal/pubs/2013_advncng_smm_fs.pdf. Access date September 14th, 2015.
- [314] EPA, Advancing Sustainable Materials Management: Facts and Figures 2013 Available: http://www3.epa.gov/epawaste/nonhaz/municipal/pubs/2013_advncng_smm_rpt.pdf. Access date September 14th, 2015.
- [315] V. Rossi, N. Cleeve-Edwards, L. Lundquist, U. Schenker, C. Dubois, S. Humbert, O. Jolliet, Life cycle assessment of end-of-life options for two biodegradable packaging materials: sound application of the European waste hierarchy, *J. Clean Prod.* 86 (2015) 132-145.
- [316] E. Kosior, R.M. Braganca, P. Fowler, Lightweight compostable packaging: literature review, *The Waste & Resources Action Programme* 26 (2006) 1-48.
- [317] L. Liu, M.L. Fishman, K.B. Hicks, C.-K. Liu, Biodegradable composites from sugar beet pulp and poly (lactic acid), *J. Agric. Food. Chem.* 53 (2005) 9017-9022.
- [318] V. Peinado, L. García, Á. Fernández, P. Castell, Novel lightweight foamed poly (lactic acid) reinforced with different loadings of functionalised Sepiolite, *Compos. Sci. Technol.* 101 (2014) 17-23.
- [319] Y. Du, N. Yan, M.T. Kortschot, Novel lightweight sandwich-structured bio-fiber-reinforced poly (lactic acid) composites, *J. Mater. Sci.* 49 (2014) 2018-2026.

- [320] R.C. Thompson, C.J. Moore, F.S. Vom Saal, S.H. Swan, Plastics, the environment and human health: current consensus and future trends, *Phil. Trans. R. Soc. B* 364 (2009) 2153-2166.
- [321] A. Jarerat, Y. Tokiwa, H. Tanaka, Production of poly (L-lactide)-degrading enzyme by *Amycolatopsis orientalis* for biological recycling of poly (L-lactide), *Appl. Microbiol. Biotechnol.* 72 (2006) 726-731.
- [322] V. Piemonte, S. Sabatini, F. Gironi, Chemical recycling of PLA: a great opportunity towards the sustainable development?, *J. Polym. Environ.* 21 (2013) 640-647.
- [323] D.D. Cornell, Biopolymers in the existing postconsumer plastics recycling stream, *J. Polym. Environ.* 15 (2007) 295-299.
- [324] NatureWorks. End-of-life options. Feedstock Recycling. Available: <http://www.natureworkslc.com/The-Ingeo-Journey/End-of-Life-Options/Feedstock-Recycling>. Access date October 13th, 2015.
- [325] NatureWorks. End-of-life options. Recycling. Available: <http://www.natureworkslc.com/The-Ingeo-Journey/End-of-Life-Options/Recycling>. Access date October 13th, 2015.
- [326] D. Bellm. New business buys post-consumer PLA for use in packaging. Available: <http://www.packagingdigest.com/smart-packaging/new-business-buys-post-consumer-pla-use-packaging> Access date October 13th, 2015.
- [327] D. Bellm. Sustainable packaging: First new company formed to recycle PLA. Available: <http://www.packagingdigest.com/smart-packaging/sustainable-packaging-first-new-company-formed-recycle-pla>. Access date October 13th, 2015.
- [328] NAPCOR refutes claims that PLA can be recycled with PET. Available: <http://www.packagingdigest.com/smart-packaging/napcor-refutes-claims-pla-can-be-recycled-pet> Access date October 13th, 2015.
- [329] T. Kijchavengkul, R. Auras, Compostability of polymers, *Polym. Int.* 57 (2008) 793-804.
- [330] A.A. Shah, F. Hasan, A. Hameed, S. Ahmed, Biological degradation of plastics: a comprehensive review, *Biotechnol. Adv.* 26 (2008) 246-265.
- [331] S. Grima, V. Bellon-Maurel, P. Feuilloley, F. Silvestre, Aerobic biodegradation of polymers in solid-state conditions: a review of environmental and physicochemical parameter settings in laboratory simulations, *J. Polym. Environ.* 8 (2000) 183-195.
- [332] T. Leejarkpai, U. Suwanmanee, Y. Rudeekit, T. Mungcharoen, Biodegradable kinetics of plastics under controlled composting conditions, *Waste Manage. (Oxford)* 31 (2011) 1153-1161.

- [333] V. Mittal, *Characterization techniques for polymer nanocomposites*, John Wiley & Sons, Weinheim, Germany, 2012.
- [334] ASTM Standard D5338-11, *Standard Test Method for Determining Aerobic Biodegradation of Plastic Materials Under Controlled Composting Conditions. Incorporating Thermophilic Temperatures*, West Conshohocken, PA, 2011.
- [335] International Standard ISO 14855-1:2005(E), *Determination of the ultimate aerobic biodegradability of plastic materials under controlled composting conditions - Method by analysis of evolved carbon dioxide - Part 1: General Method*, in, Geneva, Switzerland, 2005.
- [336] E. Castro Aguirre, *Design and construction of a medium-scale automated direct measurement respirometric system to assess aerobic biodegradation of polymers*, in: *School of Packaging*, Michigan State University, Michigan, 2013.
- [337] S. Selke, R. Auras, T.A. Nguyen, E. Castro Aguirre, R. Cheruvathur, Y. Liu, *Evaluation of Biodegradation-Promoting Additives for Plastics*, *Environ. Sci. Technol.* 49 (2015) 3769-3777.
- [338] M. Grosso, A. Motta, L. Rigamonti, *Efficiency of energy recovery from waste incineration, in the light of the new Waste Framework Directive*, *Waste Manage. (Oxford)* 30 (2010) 1238-1243.
- [339] A. Damgaard, C. Riber, T. Fruergaard, T. Hulgaard, T.H. Christensen, *Life-cycle-assessment of the historical development of air pollution control and energy recovery in waste incineration*, *Waste Manage. (Oxford)* 30 (2010) 1244-1250.
- [340] C. Laußmann, U. Land, B. Münster, G.H.-J. Endres, F. Hannover, G.U. Giese, A.-S. Kitzler, A. Papierveredelung, *Disposal of Bio-Polymers via Energy Recovery*, in: *Bioplastics magazine* 2010, pp. 42-43.
- [341] NatureWorks. *End-of-life options. Incineration.* Available: <http://www.natureworkslc.com/The-Ingeo-Journey/End-of-Life-Options/Incineration>. Access date October 13th, 2015.
- [342] M. El-Fadel, A.N. Findikakis, J.O. Leckie, *Environmental impacts of solid waste landfilling*, *J. Environ. Manage.* 50 (1997) 1-25.
- [343] S.E. Selke, *Plastics recycling and biodegradable plastics: The Complete Guide to Properties and Performance*, McGraw-Hill, New York, 2006.
- [344] J.J. Kolstad, E.T. Vink, B. De Wilde, L. Debeer, *Assessment of anaerobic degradation of Ingeo™ polylactides under accelerated landfill conditions*, *Polym. Degrad. Stab.* 97 (2012) 1131-1141.
- [345] L. Čuček, J.J. Klemeš, Z. Kravanja, *A review of footprint analysis tools for monitoring impacts on sustainability*, *J. Clean Prod.* 34 (2012) 9-20.

- [346] J. Potting, How to Approach the Assessment?, in: M.A. Curran (Ed.), Life Cycle Assessment Handbook: A Guide for Environmentally Sustainable Products John Wiley & Sons, Inc., Cincinnati, OH, USA, 2012, pp. 391-412.
- [347] K.A. Weitz, Life Cycle Assessment and End of Life Materials Management, in: M.A. Curran (Ed.), Life Cycle Assessment Handbook: A Guide for Environmentally Sustainable Products John Wiley & Sons, Inc., Cincinnati, OH, USA, 2012, pp. 249-266.
- [348] International Standard ISO 14040. Environmental Management – Life Cycle Assessment – Principles and Framework, in, Geneva, Switzerland, 2010.
- [349] International Standard ISO 14044. Environmental Management – Life Cycle Assessment – Requirements and Guidelines, in, Geneva, Switzerland, 2006.
- [350] O. Jolliet, M. Margni, R. Charles, S. Humbert, J. Payet, G. Rebitzer, R. Rosenbaum, IMPACT 2002+: a new life cycle impact assessment methodology, *Int. J. Life. Cycle. Assess.* 8 (2003) 324-330.
- [351] E.T. Vink, K.R. Rabago, D.A. Glassner, P.R. Gruber, Applications of life cycle assessment to NatureWorks™ polylactide (PLA) production, *Polym. Degrad. Stab.* 80 (2003) 403-419.
- [352] E.T. Vink, D.A. Glassner, J.J. Kolstad, R.J. Wooley, R.P. O'Connor, Original research: the eco-profiles for current and near-future NatureWorks® polylactide (PLA) production, *Industrial Biotechnology* 3 (2007) 58-81.
- [353] E.T. Vink, S. Davies, J.J. Kolstad, ORIGINAL RESEARCH: The eco-profile for current Ingeo® polylactide production, *Industrial Biotechnology* 6 (2010) 212-224.
- [354] R. Narayan, Carbon footprint of bioplastics using biocarbon content analysis and life-cycle assessment, *MRS Bull.* 36 (2011) 716-721.
- [355] S. Paping, P. Malakul, R. Trungkavashirakun, P. Wenunun, T. Chom-in, M. Nithitanakul, E. Sarobol, Comparative assessment of the environmental profile of PLA and PET drinking water bottles from a life cycle perspective, *J. Clean Prod.* 65 (2014) 539-550.
- [356] M. Joo, N. Lewandowski, R. Auras, J. Harte, E. Almenar, Comparative shelf life study of blackberry fruit in bio-based and petroleum-based containers under retail storage conditions, *Food Chem.* 126 (2011) 1734-1740.
- [357] F. Gironi, V. Piemonte, Life cycle assessment of polylactic acid and polyethylene terephthalate bottles for drinking water, *Environ. Prog. Sustain. Energy* 30 (2011) 459-468.

- [358] U. Suwanmanee, T. Leejarkpai, Y. Rudeekit, T. Mungcharoen, Life cycle energy consumption and greenhouse gas emissions of polylactic acid (PLA) and polystyrene (PS) trays, *Nat. Sci.* 44 (2010) 703-716.
- [359] N. Peelman, P. Ragaert, B. De Meulenaer, D. Adons, R. Peeters, L. Cardon, F. Van Impe, F. Devlieghere, Application of bioplastics for food packaging, *Trends Food Sci. Tech.* 32 (2013) 128-141.
- [360] M. Carus, S. Piotrowski, Land use for bioplastics, *Bioplastics Magazine* 4 (2009) 4.
- [361] V. Piemonte, F. Gironi, Land-use change emissions: How green are the bioplastics?, *Environ. Prog. Sustain. Energy* 30 (2011) 685-691.
- [362] M. Carus, Agricultural resources for bioplastics, in: *Bioplastics Magazine* 2011, pp. 44-46.
- [363] European Bioplastics. Bioplastics Facts and Figures. Available: <http://european-bioplastics.org> Access date December 14th, 2015.

CHAPTER 3

INSIGHTS ON THE AEROBIC BIODEGRADATION OF POLYMERS BY ANALYSIS OF EVOLVED CARBON DIOXIDE IN SIMULATED COMPOSTING CONDITIONS

A version of this chapter is published as:

Castro-Aguirre, E., Auras R., Selke S., Rubino M., Marsh T. Insights on the aerobic biodegradation of polymers by analysis of evolved carbon dioxide in simulated composting conditions, *Polymer Degradation and Stability*, 137 (2017) 251 – 271.

3.0 Abstract

The development of novel biodegradable polymers as a way to create sustainable materials has required the development of methodologies to evaluate and understand their biodegradation. In this work, we first provide a critical summary of selected biodegradation tests performed in the last fifteen years for a number of biodegradable materials, providing relevant information about the materials tested, characteristics of the compost used and the method for testing. Then, we report a comparative analysis of the results obtained from eight different biodegradation tests performed in simulated composting conditions by analysis of evolved CO₂ and carried out in an in-house built direct measurement respirometer. The materials evaluated for biodegradation were cellulose, starch, glycerol, polyethylene, and poly(lactic acid). Our results along with the information provided in the literature allowed us to identify that one of the main issues of biodegradation testing is the low reproducibility due to the number of variables involved in the biodegradation process. It is difficult to provide fair comparisons of samples that are not within the same test. Therefore, we provide a critical overview of the different factors affecting the biodegradability, biodegradation rate, and biodegradation mechanisms of polymeric materials. Furthermore, we share the experiences and insights gained during the performance of the different biodegradation tests and identify areas of opportunity for improving biodegradation testing through evolved CO₂. This information should create a common knowledge platform for people interested in studying the biodegradation of materials.

3.1 Introduction

Biodegradable polymers represent a promising way to reduce the amount of plastic waste disposed in landfills, with composting the preferred alternative for their disposal. Many biodegradable polymers have been developed in the last two decades with the desired performance properties [1–7] for replacing conventional polymers for applications where plastics are highly contaminated and are difficult to recover through recycling such as agricultural films and single-use products like packaging and disposable cutlery [8,9]. Thus, along with the development of these novel materials, evaluation and understanding of their biodegradation performance and their environmental impacts have become germane [8–11].

Different analytical techniques have been used to evaluate biodegradation of polymers in composting using a direct or an indirect approach. Even though techniques like visual observations, weight loss measurements, changes in mechanical properties, and changes in molecular weight, can provide insights into the degradation process of a polymer, they do not necessarily demonstrate biodegradation [12]. Therefore, respirometric methods, in which the consumption of oxygen and/or the evolution of carbon dioxide (CO₂) is measured, have become the preferred technique for such assessment.

During aerobic biodegradation, microorganisms use the polymer as a source of carbon for growth and their metabolic processes yield CO₂. The amount of CO₂ produced during metabolic reactions and the fraction of carbon that is incorporated into biomass is a function of the substrate type and concentration, physical attributes of the environment, species-specific characteristics of the degradative microbial populations,

and population dynamics within a complex community of microbes [8,10,13,14]. In respirometric methods, the evolved CO₂ can be measured in either a discrete or a continuous way by using different techniques.

In cumulative measurement respirometry (CMR), the evolved CO₂ is trapped in a solution, *e.g.*, sodium hydroxide (NaOH), throughout the test and then quantified by titration [8]. Similarly, in gravimetric measurement respirometry (GMR), CO₂ is captured in absorption columns filled with pellets of NaOH, and the amount of CO₂ is quantified by the weight increase in the columns [8]. When direct measurement respirometry (DMR) is used, the output air is directly analyzed using either a non-dispersive infrared (NDIR) sensor or a gas chromatograph (GC) coupled with a thermal conductivity (TCD) detector to quantify the amount of evolved CO₂ [8].

In this context, several respirometric systems have been designed and built by different research groups around the world [15–20] following international standards such as ASTM D5338 and ISO 14855 [21,22]. A detailed list and information about different available standards is provided elsewhere [23,24]. However, performing biodegradation tests is not an easy task; it is costly, time-consuming, and requires constant attention to the proper functioning of the equipment. Moreover, due to the biological nature of the process, there are many variables that must be properly controlled and/or monitored.

Table 3.1 shows the results of selected tests found in the literature using different methods for assessing biodegradation of materials in compost. The majority of these tests used CO₂ evolution to track the biodegradation of the materials, but some authors have used visual inspection and weight loss for estimating biodegradation. **Table 3.1**

also provides information relevant for biodegradation tests such as the material shape and thickness, molecular weight, and the physicochemical characteristics of the compost used for testing - whenever provided by the authors. However, when comparing the same materials, *e.g.*, cellulose or PLA, there is large variation in biodegradation and the time to reach similar levels of biodegradation among tests. This variation makes it difficult to compare biodegradation values between and within tests. Therefore, further understanding and review of the different factors affecting biodegradation would be useful for conducting future biodegradation tests in which the key factors could be more strictly monitored and controlled, reducing such variability.

In this work, we report a comparative analysis of the results obtained from eight biodegradation tests of different materials (*i.e.*, cellulose powder (CP), glycerol (GC), cassava starch (CS), poly(lactic acid) (PLA), polyethylene powder (PE), and a blend of linear low density polyethylene (LLDPE) and low density polyethylene (LDPE)) performed in simulated composting conditions by the analysis of evolved CO₂ using the same DMR system. The data from published work is critically reviewed and compared with the data from our eight biodegradation tests performed by the evolved CO₂ approach. Finally, we share insights gained from the different biodegradation tests in an attempt to identify areas in need of improvement and to establish more standardized procedures for researchers interested in studying aerobic biodegradation of polymers by analysis of evolved CO₂.

Table 3.1 Selected biodegradation tests in composting conditions reported in the literature and presented in reverse chronological order for 2015 through 1990, including information about the samples, compost and the main methods for assessing biodegradation

Sample Materials	Form	Thickness, mm	M_n , kDa	M_w , kDa	PI	% Biodegradation	Time, d	Method for assessing biodegradation	Characterization of the compost					Ref.
									Dry solids, %	Volatile solids, %	pH	C/N	Temperature, °C	
PLA 4042D	Film	0.04 - 0.06	150		1.7	CD	30	Visual inspection	45-60		4-8		45-70	[2]
CAB 500-5	Film	0.04 - 0.06	57			CD	>90							
PLA/CAB 80/20	Film	0.04 - 0.06				CD	9							
PLA/CAB 50/50	Film	0.04 - 0.06				CD	>90							
PLA/CAB/PEG 80/20/20	Film	0.04 - 0.06				CD	90							
PLA 4032D	Film	0.2	217		2	100	28	Weight loss			6.5		58	[25]
PLA-PEG	Film	0.2				100	28							
PLA-ATBC	Film	0.2				100	28							
PLA-PHB-PEG	Film	0.2				100	35							
PLA-PHB-ATBC	Film	0.2				100	35							
Cellulose	Paper	0.35				78	115	CO ₂ evolution (DMR-NDIR)	24.3	88.9	7.9	20	55	[26]
Plastarch	Sheet	0.48				51	115							
Paper pulp + soy wax	Sheet	2.14				12	115							
PET + additive	Sheet	0.36				1	115							

Table 3.1 (cont'd)

PLA				15		71	110	CO ₂ evolution (CMR-Titration)	50.5	29	7.7	3.9	58	[27]
LA-EG-MA			10.3			53	110							
LA-EG-SA			10.8			51	110							
Cellulose	Powder					76	45							
PHBV-3	Film	0.01 - 0.08	404			80	110	CO ₂ evolution (DMR-NDIR)	52.4	14.5	8.2	14.2	58	[3]
PHBV-20	Film	0.01 - 0.08	324			89	110							
PHBV-40	Film	0.01 - 0.08	324			91	110							
PHB	Film	0.01 - 0.09	240			80	110							
P(3HB, 4HB)	Powder		446			90	110							
Cellulose	Powder					83	110							
PBAT (Manure compost)	Film	0.04				67	45	CO ₂ evolution (DMR-NDIR)				22.9	58	[28]
PBAT (Yard compost)	Film	0.04				34	45							
PBAT (Food waste compost)	Film	0.04				45	45							
PLA 7000 D	Sheet	3				60	80	CO ₂ evolution (DMR-NDIR)	46.4		8.4		58	[29]
Cellulose	Powder					78	80							
PLA60/St arch40	Sheet	3				>80	80							
PLA90/St arch10	Sheet	3				~60	80							
PLA90/Wood-flour10	Sheet	3				~50	80							

Table 3.1 (cont'd)

Microcrystalline cellulose	Powder					>70	45	CO ₂ evolution (CMR-Titration)	42-52	48	7.6	32	[30]
Industrial recycled cellulose	Particle size < 2.8 mm					>70	45						
PLA (Biomer L 9000)	Particle size < 2.8 mm			174.2	1.9	>60	80						
Wheat straw	Particle size < 2.8 mm					>70	45						
Soy straw	Particle size < 2.8 mm					>70	45						
PLA-Wheat straw (50:50)	Particle size < 2.8 mm			132.9	1.8	>60	60						
PLA-Soy straw (50:50)	Particle size < 2.8 mm			158.3	1.8	>60	60						
PCL	Particle size < 2.8 mm			171.7	1.6	>60	120						
Soy meal	Particle size < 2.8 mm					>70	45						
DDGS	Particle size < 2.8 mm					>70	45						
PCL-DDGS (70:30)	Particle size < 2.8 mm			162.3	1.6	>60	100						
PCL-Soy meal (70:30)	Particle size < 2.8 mm			168.2	1.6	>60	100						

Table 3.1 (cont'd)

Cellulose	Powder					72.4 - 82.5	45	CO ₂ evolution (DMR-NDIR)	51	45	7.2		58	[17]
Potato starch-based tray						80		Weight loss - home composting						[31]
Starch-based tray with a starch/PC L laminate						80								
Pressed wood pulp plate						40								
Pressed silvergrass pulp crate						80								
Molded coconut fiber tray						40								
Moulded recycled paper pulp tray						40								
PLA tray						<5								
Starch/PC L-extrudate sample						<5								
PP with biodegradability additive						<5								

Table 3.1 (cont'd)

PP compound ed with starch granules						<5		Weight loss - home composting							[31]
EPI						0	72	Weight loss	45	91.7	6.2 - 8.5	27.9	>50	[32]	
Mater-Bi						27	72								
Cellulose filter paper	Paper					100	72								
Microcrystalline cellulose	Powder					74	45	CO ₂ evolution (CMR-Titration)	49	28.4	7.2	14.1	58	[4]	
TPS	Powder					73	56								
TPDAS6	Powder					66	56								
TPDAS30	Powder					56	56								
TPDAS50	Powder					45	56								
TPDAS70	Powder					26	56								
TPDAS95	Powder					6	56								
PLA (2002 D)	Sheet	1				55	90	CO ₂ evolution (CMR-Titration)	48	45.4	7.1	10.4	58	[5]	
TPS	Sheet	1				87	90								
PLA/TPS 75/25	Sheet	1				61	90								
PLA/TPS/Coir 52/17/30	Sheet	1				59	90								
PLA/TPS/MA 75/25/1	Sheet	1				57	90								
PLA/TPS/Coir/MA 52/17/30/1	Sheet	1				54	90								

Table 3.1 (cont'd)

PBAT 25w (white)	Film	0.03	86.3			>60	120	CO ₂ evolution (DMR-NDIR)	40-50				58	[6]
PBAT 35w (white)	Film	0.04	89.3			>60	120							
PBAT B (black)	Film	0.04	84.4			>60	120							
Corn starch	Powder					>70	120							
PLA	Sheet	0.3				86	120	CO ₂ evolution (CMR-Titration)	52.5	28.2	8.5		58	[33]
Cellulose	Powder					87	120							
PLA bottle (96% L-lactide)				209.3	1.7	84	58	CO ₂ evolution (CMR-Titration)					58	[34]
Cellulose	Powder					86	58							
PLA bottle (96% L-lactide)				209.3	1.7	81	58	CO ₂ evolution (GMR-MODA)					58	[34]
Cellulose	Powder					70	55							
PLA bottle (96% L-lactide)				209.3	1.7	CD	30	Visual inspection	37		8.5		65	[35]
PLA tray (94% L-lactide)				222.7	1.7	CD	30							
Cellulose	Paper					72	45	CO ₂ evolution (DMR-NDIR)	95	63	8.7	10	58	[36]
Kraft paper	Paper					62	45							
Mirel bag						64	45							
PLA straws						61	45							

Table 3.1 (cont'd)

Sugar cane plate						60	45	CO ₂ evolution (DMR-NDIR)	95	63	8.7	10	58	[36]
Corn-based trash bag						60	45							
Ecoflex bag						60	45							
Polyethylene	Sheet					2	45							
Oxodegradable bag						2	45							
PCL	Particle size <10 mesh				50	52	45	CO ₂ evolution (CMR-Titration)	52		7.4	43	58	[7]
CA	Particle size <10 mesh					22	45							
LDPE	Particle size <10 mesh				36.4	8	45							
Cellulose	Powder					70	45							
PCL/CA 60/40	Particle size <10 mesh					56	45							
PCL/CA 40/60	Particle size <10 mesh					65	45							
PLA bottle						64	63	CO ₂ evolution (DMR-NDIR)	40-50				58	[18]
PET bottle						3	63							
Corn starch						72	63							

Table 3.1 (cont'd)

PLA bottle (96% L-lactide)				209.3	1.7	CD	<30	Visual inspection	37		8.5	65	[37]	
PLA tray (94% L-lactide)				176.8	2	CD	<30							
PLA container (94% L-lactide)				215.5	1.7	CD	<30							
PLA/Starch/PLA	Sheet	2.19				78	45	CO ₂ evolution (NS)	52.7	65.8	8	28.9	58	[38]
Microcrystalline cellulose	Powder					90	45	CO ₂ evolution (DMR-NDIR)				10-40	52	[19]
Starch-polyester						87	45							
Starch-PVOH						72	45							
Biopol						88	45	CO ₂ evolution (NS)	50-55	30	7-9	10-40	58	[39]
Kraft paper	Paper					80	45							
Microcrystalline cellulose	Powder					84	45							

Table 3.1 (Cont'd)

Notes: Cells without values indicate that the authors did not report or calculate these values, films are samples with thickness ≤ 0.254 mm, sheets are samples with thickness > 0.254 mm. M_n : number average molecular weight, M_w : weight average molecular weight, CD: complete disintegration, NS: not specified, PLA: poly(lactic acid), CAB: cellulose acetate butyrate, PEG: poly(ethylene glycol), PHB: poly(hydroxybutyrate), ATBC: acetyl-*tri-n*-butyl citrate, LA: lactic acid, EG: ethylene glycol, SA: succinic acid, MA: malonic acid, PHBV: poly(hydroxybutyrate-co-hydroxyvalerate), PBAT: poly(butylene adipate-co-terephthalate), PCL: poly(caprolactone), DDGS: distillers dried grains with solubles, PP: poly(propylene), EPI: environmental product Inc. containing 3% of totally degradable plastic additive, Mater-Bi: starch/hydrophilic-biodegradable resin blend, TPDAS: thermoplastic dialdehyde starch, TPS: thermoplastic starch, MA: maleic anhydride, CA: cellulose acetate, LDPE: low-density polyethylene, PET: poly(ethylene terephthalate), Biopol: poly(hydroxy butyrate)/ poly(hydroxy valerate) blend, PVOH: poly(vinyl alcohol).

3.2 Materials and Methods

3.2.1 Materials

Cellulose powder (CP) with particle size $\sim 20 \mu\text{m}$ and glycerol (GC) 99+% was purchased from Sigma-Aldrich (St. Louis, MO) and cassava starch (CS) containing $25 \pm 6\%$ amylose content from Erawan Marketing Co., LTD (Bangkok, Thailand). Polyethylene powder (PE), low density polyethylene resin (LDPE 501I) and linear low density polyethylene resin (DOWLEX 2045G) were obtained from Dow Chemical (Houston, TX), and poly(lactic acid) resin (Ingeo™ 2003D and 4032D) from NatureWorks LLC. (Minnetonka, MN). Materials were used as received unless specified and the same batch of a compound was used for all the tests.

3.2.1.1 Material processing and characterization

A 70% wt. LDPE- 30% wt. LLDPE blend film (hereafter referred to as LDPE) was produced by blown extrusion with an overall thickness of $0.023 \pm 0.005 \text{ mm}$. The number average molecular weight (M_n), weight average molecular weight (M_w) and polydispersity (PI) of LDPE was 20.6 kDa, 92.6 kDa, and 4.5, respectively; and for PE 2.9 kDa, 22.0 kDa, and 7.6, respectively. Three Ingeo™ 2003D films with different molecular weights (PLA1>PLA2>PLA3) were obtained by cast extrusion, varying the temperature of processing, with an overall thickness of 0.031 ± 0.006 , 0.022 ± 0.003 , and $0.034 \pm 0.009 \text{ mm}$, respectively. Additionally, a PLA sheet (PLA4) was produced with Ingeo™ 4032D having an overall thickness of $0.255 \pm 0.021 \text{ mm}$. The M_n , M_w , and PI of the different PLA samples are presented in **Table 3.2**. The carbon, hydrogen, and nitrogen content of the different test materials were determined by elemental analysis.

More details regarding the film processing, molecular weight determination and elemental analysis are provided in the appendices 3A, 3B, and 3C, respectively.

Table 3.2 Initial M_n , M_w , and PI of the PLA samples

Sample Material	M_n, kDa	M_w, kDa	PI
PLA pellet	95.1 ± 5.8	180.2 ± 6.2	1.9 ± 0.1
PLA1	93.5 ± 15.6	188.9 ± 17.3	2.0 ± 0.2
PLA2	82.9 ± 6.7	170.5 ± 16.8	2.1 ± 0.1
PLA3	72.6 ± 5.7	139.7 ± 2.8	1.9 ± 0.2
PLA4	75.0 ± 1.4	134.8 ± 0.4	1.8 ± 0.03

3.2.2 Biodegradation test

The aerobic biodegradation of the materials was evaluated under controlled composting conditions by analysis of evolved CO₂ using an in-house built DMR system, which uses a non-dispersive infrared gas analyzer (NDIR) for measuring the concentration of CO₂ evolved from the bioreactors. Detailed information about the equipment and the calculation method is provided in the Appendices 3F and 3G, and elsewhere [40]. Besides compost, CP and PLA pellets were also tested in inoculated vermiculite in the Jan14 test. Similarly, in the Nov15 test, CP, PLA1, PLA2, and PLA3 were evaluated in three different media: compost, inoculated vermiculite and uninoculated vermiculite. Additionally, analysis of the reduction of molecular weight of PLA was performed in these experiments. **Table 3.3** shows a summary of the different tests performed, the materials that were evaluated in each test and the type of media used for testing.

Table 3.3 Biodegradation test, materials, and media used for testing

Test ID ^a	Materials tested	Media for testing
Sep12	Blank, CP, LDPE	Commercial compost
Feb13	Blank, CP, LDPE	MSU compost (A) ^b
May13	Blank, CP, CS, LDPE	MSU compost (A)
Jul13	Blank, CP, LDPE	MSU compost (A)
Jan14	Blank, CP, CS, GC, PE, PLA1, PLA pellets	MSU compost (B), inoculated vermiculite
Jun14	Blank, CP, CS, PE, LDPE, PLA1	MSU compost (C)
Nov14	Blank, CP, PLA2, PLA4	MSU compost (C)
Nov15	Blank, CP, PLA1, PLA2, PLA3	MSU compost (C), inoculated vermiculite, uninoculated vermiculite

^a Test ID refers to the month and year in which the test was performed

^b The compost ID (A, B, C) indicates that the initial compost was obtained from the same compost batch

3.2.2.1 Compost source

For the Sep12 test, Earthgro[®] organic humus and manure from Scotts Miracle-Gro (Marysville, OH) was used. For all the other tests, manure-straw compost prepared at the MSU Composting Facility (East Lansing, MI) was used. Detailed information about the preparation of this compost is provided in the Appendix 3E.

In all cases, the compost was sieved on a 10 mm screen and preconditioned at 58°C for a period of 3 days before use. Deionized water was added to increase the moisture content to about 50%. Saturated vermiculite premium grade (Sun Gro Horticulture Distribution Inc., Bellevue, WA) was added to the compost (1:4 parts, dry wt. compost) to provide better aeration.

3.2.2.2 Compost characterization

Samples of the compost from the different tests were sent to the Soil and Plant Nutrient Laboratory at Michigan State University (East Lansing, MI, USA) for determination of the physicochemical parameters. The dry solids (DS) were obtained after drying the compost sample at about 105°C to constant mass. The volatile solids (VS) were obtained by the loss-on-ignition method, in which the residues after incineration at 550°C are subtracted from the total DS. The pH was determined in a 1:5 compost-to-water suspension. The total organic carbon (TOC) was determined by calculation from the VS since carbon is typically considered to comprise about 58% of the VS [41]. The total nitrogen content was obtained by the Dumas method [42], the ammonium (NH_4^+) concentration by the salicylate method [43], and the nitrate (NO_3^-) concentration by the cadmium reduction method [44]. Subsequent moisture content measurements were done in a moisture analyzer, model MX-50 from A&D Engineering, Inc. (San Jose, CA).

3.2.2.3 Preparation of inoculum solution

The solution used for inoculation of vermiculite was prepared by combining compost extract with a mineral solution (**Table 3.4**) at a 1:1 ratio [22]. Compost extract was prepared by mixing dry compost with deionized water (20% wt./vol.), stirring and letting sit for 30 minutes followed by filtration through a sieve with 1 mm mesh.

Table 3.4 Detailed composition of 1 L of mineral solution

1 L of Mineral solution	
KH ₂ PO ₄ , g	1
MgSO ₄ , g	0.5
CaCl ₂ (10% sol), mL	1
NaCl (10% sol), mL	1
Trace-element solution, mL	1

1 L of trace-element solution, mg	
H ₃ BO ₃	500
KI	100
FeCl ₃	200
MnSO ₄	400
(NH ₄) ₆ Mo ₇ O ₂₄	200
FeSO ₄	400

3.2.2.4 Biodegradation in compost

The bioreactors were loaded with either 500 g (wet wt.) of compost (first experiment) or 400 g of compost (subsequent experiments) and mixed thoroughly with 8 g of polymer sample. Film samples were cut to 1 cm² pieces and triplicates of each test material were analyzed. Additionally, triplicates of blank bioreactors (with compost only) were evaluated. To simulate composting conditions, the bioreactors were placed in an environmental chamber set at a constant temperature of 58 ± 2°C. Water-saturated CO₂-free air was provided to each bioreactor with a flow rate of 40 ± 2 sccm (cm³/min at standard temperature and pressure). The bioreactors were incubated in the dark for at least 45 d or until the evolved CO₂ reached a plateau.

3.2.2.5 Biodegradation in vermiculite

Biodegradation tests were also carried out with inoculated and uninoculated vermiculite during the Nov15 test in an attempt to avoid the priming effect, which is discussed in section 3.3.3.6, and to decouple biotic and abiotic degradation during the

biodegradation test of PLA. In this case, vermiculite was mixed in a proportion of 1:4 (wt.) with the inoculum solution described in section 3.2.2.3, and with distilled water, respectively. The bioreactors were loaded with 400 g (wet wt.) of either inoculated or uninoculated vermiculite and mixed thoroughly with 8 g of the polymer. The bioreactors were then subjected to the testing conditions described in section 3.2.2.4.

3.3 Results and Discussion

This section first presents the physicochemical characteristics of the media (compost and vermiculite) that are relevant for the biodegradation test in composting conditions. Then, it provides a comparison of the results obtained by the analysis of evolved CO₂ approach in the eight tests with the different sample materials. To better understand and interpret the results of the biodegradation tests, a discussion of each of the factors affecting the biodegradation rate and the biodegradability of the materials is also presented. Likewise, some recommendations based on the literature and on our own experiences gained during the performance of these eight different biodegradation tests and more than 10 years of testing biodegradation of samples are provided to inform future testing. Finally, a case study is presented to gain additional understanding on the biodegradation mechanism of PLA, one of the most popular commercial compostable biobased polymers.

3.3.1 Biodegradation: CO₂ evolution and mineralization

An in-house built DMR system (as shown in **Figure 3.21**) was used to perform the eight different biodegradation tests in which temperature, RH, air flow rate, CO₂ concentration, and time were continuously monitored and measured (**Figure 3.1**). Temperature and pH were stable at 58°C and 7, respectively. The flow rate of air

passing in each bioreactor was adjusted to 40 sccm throughout the testing period. Moisture content was measured periodically in a control bioreactor to determine the amount of water required for adjustment. Detailed discussion of the effect of each physical parameter is presented in section 3.3.2.

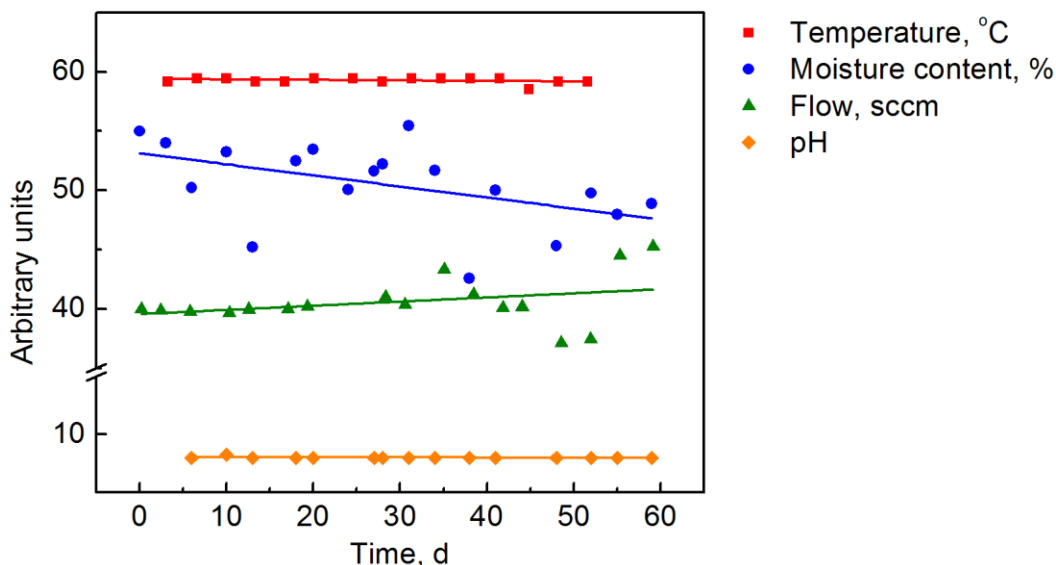


Figure 3.1 Example of biodegradation test parameters as a function of time. Fitted lines ($y=\beta x+\alpha$) are included for visual guidance only. Air flow rate, temperature, moisture and pH monitored as a function of time in the May13 test during the first 60 days of testing.

3.3.1.1 Biodegradation in compost

The cumulative CO₂ and % mineralization curves obtained from the different biodegradation tests in compost are presented in **Figure 3.2** to **Figure 3.6**. For the data analysis (Appendix 3F), the amount of CO₂ evolved from each bioreactor was calculated first (Eq. 3F.3); subsequently, the average cumulative CO₂ (Eq. 3F.5) and % mineralization (Eq. 3F.7) of each test material was determined and plotted as a function of time. The % mineralization represents the relationship between the amount of CO₂ evolved from the test material and the theoretical amount of CO₂ that can be evolved

from the same test material; e.g., in the case of CP, with a 42.5% carbon content (**Table 3.8**) and the introduction of 8 g into a bioreactor, the theoretically possible CO₂ evolution from this material is 12.5 g (denominator of Eq. 3F.7). Looking at the CO₂ evolution plots of the different materials, it seems that in general, the samples from the May13, Jul13, and Jun14 tests produced the highest amount of CO₂ and the samples from the Sep12 and Jan14 tests produced the least amount of CO₂ over time.

The blank bioreactors produced an amount of CO₂ ranging from 9.7 to 23.9 g after 60 days of testing, with the Jun14 test having the highest variability (**Figure 3.2**). Even though all tests were performed under the same conditions, and in most of the cases using the same type of compost (except Sep12), there is significant difference in the production of CO₂ between some of the tests. The compost of the Sep12 test produced the lowest amount since it was a different kind of compost and due to the experienced drying conditions as explained in section 3.3.2.4.

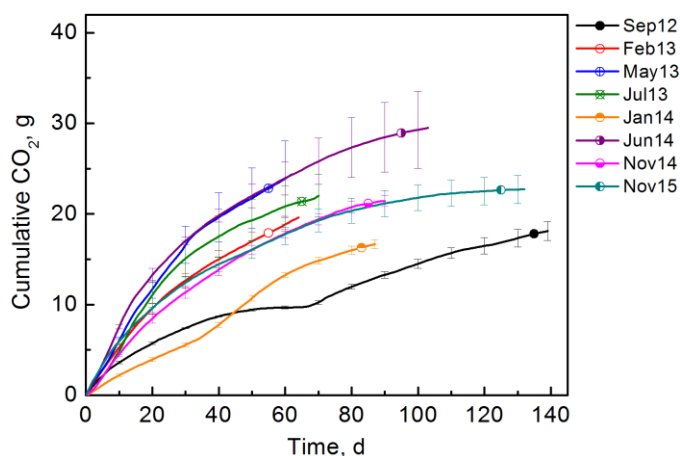


Figure 3.2 Cumulative CO₂ evolution of blank bioreactors in the different biodegradation tests showing large variation of the CO₂ evolved although they were run under the same experimental conditions.

The CO₂ evolved from the blank bioreactors represents the background, so their average is later subtracted from the amount of CO₂ produced by the test sample bioreactors to determine the mineralization, as shown in Eq. 3F.7 of the Appendix 3F. The background and the variability value of evolved CO₂ between the blank replicates have a large influence on the final mineralization values.

For example, looking at the average values of the CO₂ evolution and % mineralization of cellulose (**Figure 3.3**), the May13 and the Jul13 tests produced almost the same amount of CO₂; but the calculated mineralization in the Jul13 test was much higher than in the May13 test due to the CO₂ evolution from the blank. Similarly, the cellulose in the Jun14 test produced a much greater amounts of CO₂ than in the Jan14 test, but the average mineralization values were not very different from each other.

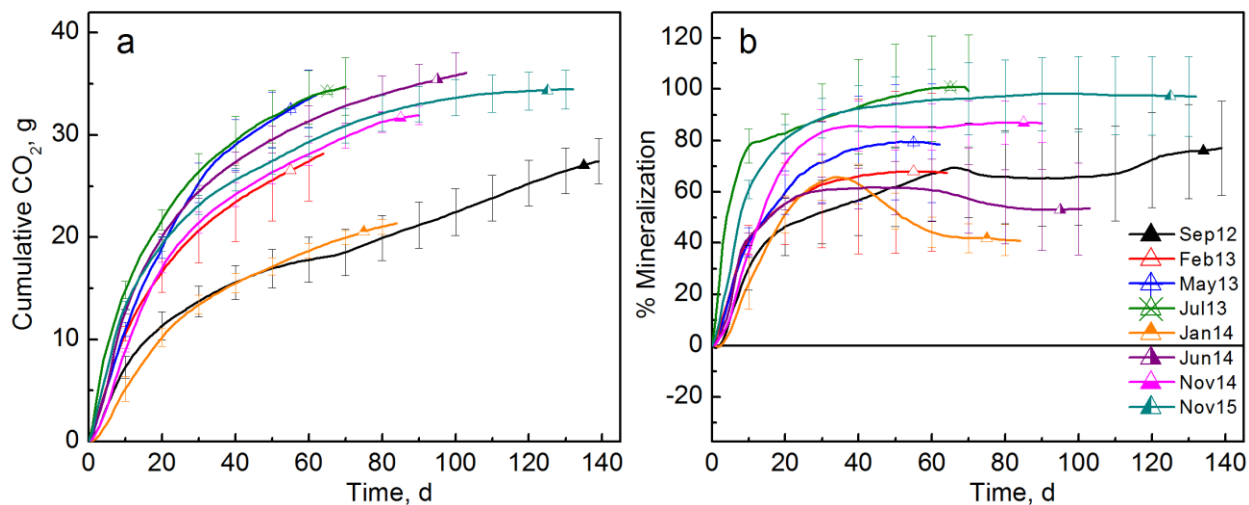


Figure 3.3 Cumulative CO₂ evolution (a) and mineralization (b) of cellulose bioreactors in the different biodegradation tests. While similar or different CO₂ values were observed, the % mineralization is highly driven by the evolved CO₂ values for the blank test.

Overall, we can also state that except for the Sep12 and the Jan14 tests the behavior and amount of CO₂ evolved from most of the blank bioreactors is fairly similar (27.5 – 33.7 g at day 60). When accounting for the total background production, the % mineralization varied from 61.8 to 100.8%. These results are comparable to the ones reported in the literature (**Table 3.1**) with % mineralization of cellulose ranging 70 – 100% between 45 – 120 days.

The decrease in the mineralization curves of the Jan14 and the Jun14 tests indicates that the cellulose bioreactors were no longer producing more CO₂ than the blank bioreactors; a similar behavior was observed with the CS, being even more pronounced (**Figure 3.4**).

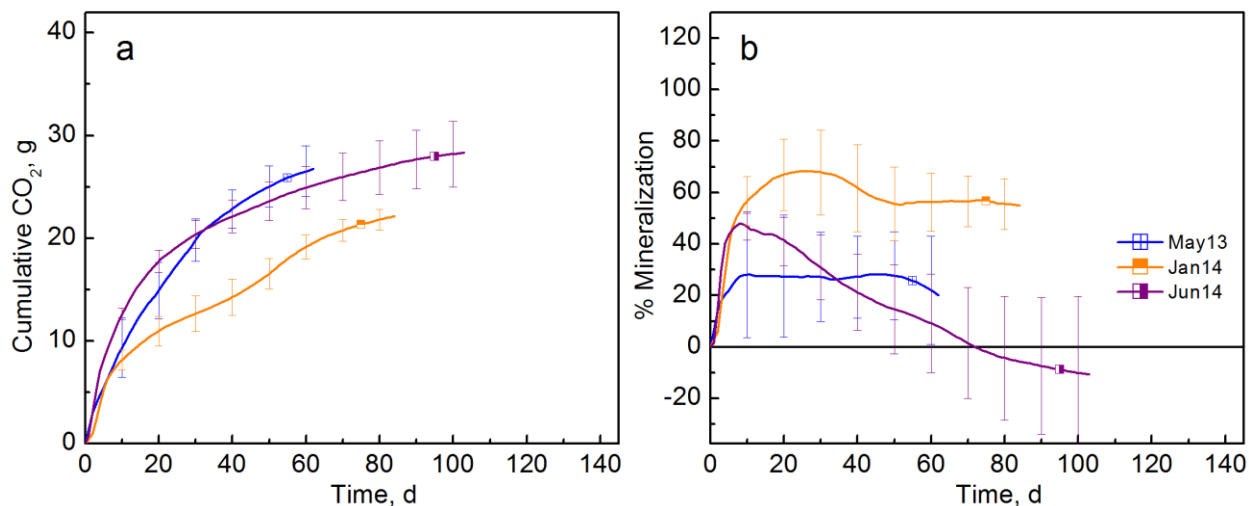


Figure 3.4 Cumulative CO₂ evolution (a) and mineralization (b) of CS in the different biodegradation tests. Biodegradation tests show a fast increase in the mineralization during the first 10 days of testing.

A possible explanation of the behavior observed in the mineralization curve of starch (**Figure 3.4b**) is that at the beginning of the test there is a rapid large increase in the microbial population since materials like starch are readily or easily available for

microbial assimilation, but once these resources are depleted and/or limited, a decrease in the mineralization curve is observed. It should be considered that microorganisms do not only use carbon for generation of energy but also for growing [13].

Figure 3.4 shows that the CO₂ evolved from the CS bioreactors ranged from 19.1 to 26.5 g at day 60, while the % mineralization varied from 28.1 to 68.3. **Table 3.1** shows results for two corn starch tests (70 and 72% mineralization after 120 and 63 days, respectively) [6,18], and two for TPS tests (73 and 87% mineralization after 56 and 90 days, respectively) [4,5]; however, those samples did not show the decline in the mineralization curve behavior, as reported in **Figure 3.4**, based on the figures presented in the respective papers.

In some cases, especially in polymers that are not biodegradable like LDPE, negative mineralization values have been reported (**Figure 3.5**). Physically these values make no sense, but they are possible since they are generated as an artifact when the blank bioreactors produce more CO₂ than the LDPE bioreactors [14]. These negative mineralization values could be attributed to a physical barrier offered by the polymer film, which limits the availability and/or the distribution of carbon and other nutrients for basic microorganism functions.

In the Jan14 and Jun14 tests, PE was evaluated to determine if this material, which is in the form of powder and with $M_n = 2.9$ kDa, is more susceptible to biodegradation than the LDPE film. **Figure 3.5** shows that the amount of CO₂ evolved from the LDPE bioreactors varied from 8.9 to 25.1 g at day 60, while the maximum mineralization was $6.8 \pm 4.8\%$. The amount of CO₂ evolved from the PE bioreactors varied from 10.6 to 24.5 g at day 60, while the maximum mineralization was $3.7 \pm 2.5\%$.

Therefore, no significant increase in the biodegradability or mineralization of this material was found. The maximum mineralization of LDPE reported from the literature in **Table 3.1** was 8% after 45 days. Similarly, Esmaeili *et al.* (2013) reported a mineralization of 7.6% after 126 days in soil and 15.8% in soil inoculated with a mixed culture of *Lysinibacillus xylanilyticus* and *Aspergillus niger* after the same period of time [45]. However, these mineralization values may be attributed to the microbial assimilation of organic carbon present in the samples used to modify the material or degradation products formed during oxidation reactions [14]. The influence of the chemical structure, form, and molecular weight of the materials on biodegradation is further discussed in Section 3.3.4.

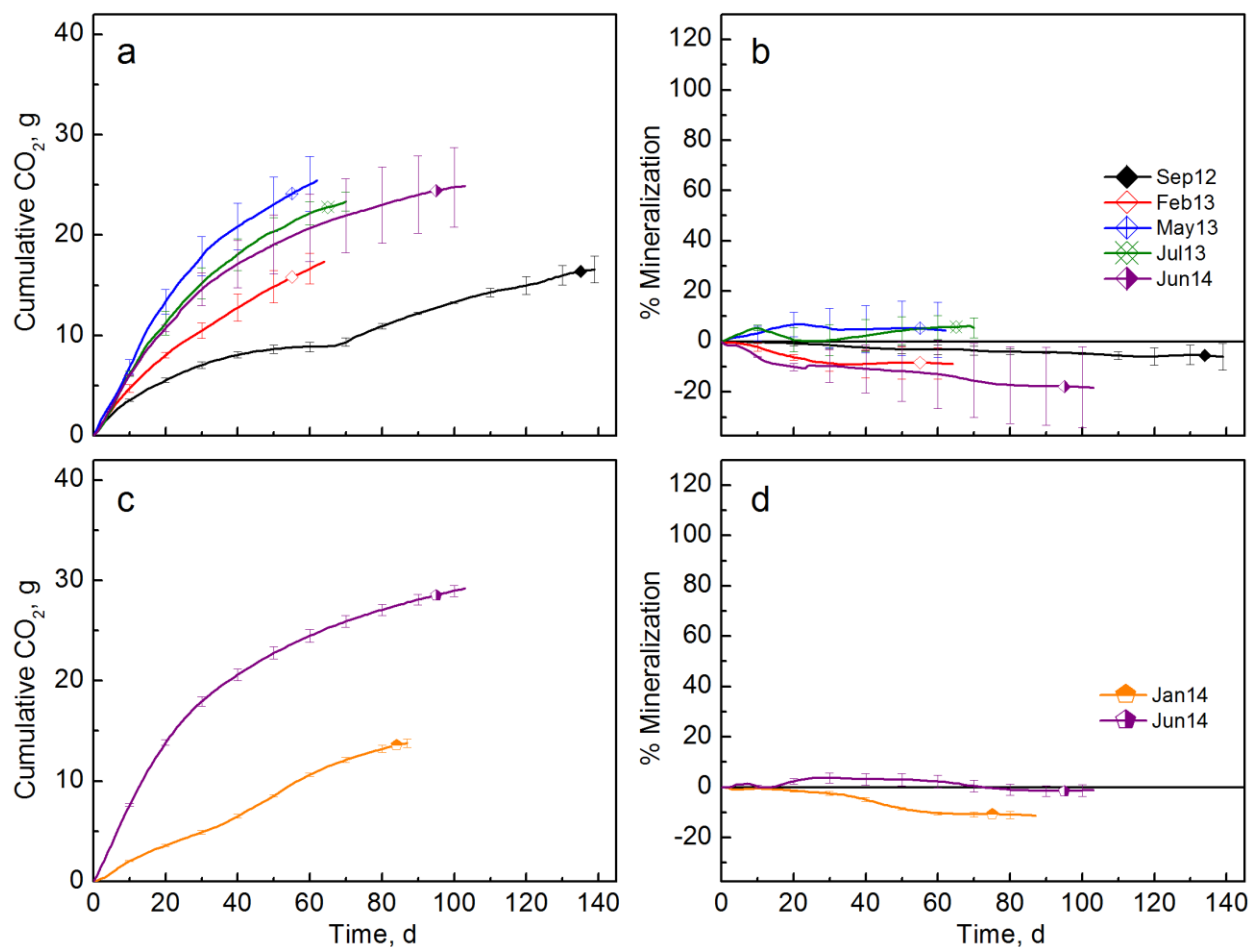


Figure 3.5 Cumulative CO₂ evolution and mineralization of LDPE (a & b) and PE (c & d) bioreactors in different biodegradation tests. Negative values of mineralization are observed in many tests.

Figure 3.6 shows the biodegradation results of the PLA1, PLA2, and PLA3 films, indicating that the initial molecular weight of biodegradable polymers is highly influential on the biodegradation of PLA. The amount of CO₂ evolved from the PLA1 bioreactors varied from 19.5 to 30.8 g at day 60, while the mineralization varied from 47.4 to 68%. However, the production of CO₂ and mineralization increased as the molecular weight of PLA decreased, reaching a maximum mineralization of 109.1% with the lowest molecular weight. Mineralization over 100% is an indication of the priming effect, which

is attributed to the over-degradation of the indigenous organic carbon present in the compost when testing materials like glucose and its polymers [46], further discussed in Section 3.3.3.6.

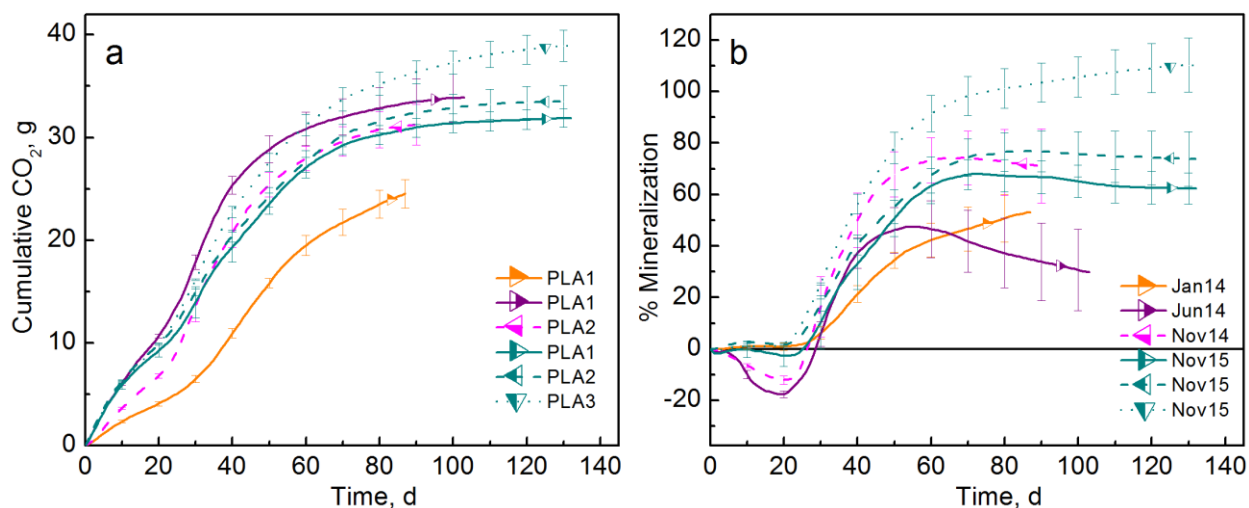


Figure 3.6 Cumulative CO₂ evolution (a) and mineralization (b) of PLA bioreactors in the different biodegradation tests; solid, dashed and dotted lines represent PLA1 (93.5 kDa), PLA2 (82.9 kDa), and PLA3 (72.6 kDa), respectively.

The zero mineralization (or negative in some cases) at the early stage of the PLA test corresponds to the lag time, *i.e.*, the period in which the polymer chains are hydrolyzed -cleaved by the presence of water- until a certain degree of degradation has been reached and the degradation products become water soluble and available for microbial assimilation [47]. The specific biodegradation mechanism of PLA will be discussed in more detail in section 3.3.5.

The results shown in this section indicate that the reproducibility between different tests is low, even if the tests were performed in the same equipment, using the same procedures, the same batches of materials, and excluding technical failures. The intrinsic variability in these biological tests makes it difficult to provide a fair comparison

of samples that are not within the same test, and therefore to compare the results obtained between and within research groups. Hoshino *et al.* (2007) performed a round robin test for studying the aerobic biodegradation of PCL and PLA by the gravimetric method in seven countries, and they found that even though the method is effective for testing compostability of materials on a laboratory scale test there is variation in the results which was mainly attributed to the compost [48].

Other researchers have reported that the inoculum quality is a source of variability that can affect the results of biodegradation tests [49]. Therefore, all the physicochemical characteristics of the compost must be reported since they may influence the efficiency and the rate of the biodegradation process. Based on the literature review and data provided in **Table 3.1**, we observed that in some papers, including previous papers from our research group, authors have reported only 3 or fewer parameters of the compost. Without a more extensive reporting of these parameters the final results and conclusions may be incomplete or misleading.

In this context, it would be relevant to further understand the different factors affecting the biodegradation rate and biodegradability of the sample materials, so in future biodegradation tests such factors can be strictly monitored and controlled in an attempt to improve the reproducibility of the test results. The physicochemical characteristics of the media used in the eight different biodegradation tests are shown and discussed in more detail in section 3.3.3.

3.3.1.2 Biodegradation in vermiculite

The biodegradation of CP and PLA samples was evaluated in inoculated vermiculite in the Jan14 and the Nov15 tests, and also uninoculated vermiculite in the Nov15 test. The

results are shown in **Figure 3.7** and **Figure 3.8**. The production of CO₂ from the blank bioreactors was very low, allowing better detection of the CO₂ signal from the sample bioreactors. During the Jan14 test (**Figure 3.7**), the mineral solution described in **Table 3.4** was not provided in the compost extract used for inoculation (sections 3.2.2.3 and 3.2.2.5), and PLA was tested in the form of pellets as received from NatureWorks LLC. The PLA pellet bioreactors produced 5.6 ± 0.4 g of CO₂ and reached $34.5 \pm 2.8\%$ mineralization after 60 days of testing, while in compost they produced 19.0 ± 0.8 g of CO₂ and reached $39.2 \pm 5.5\%$ mineralization in the same period of time. Similarly, cellulose bioreactors produced 4.9 ± 0.5 g of CO₂ and reached a mineralization of $35.3 \pm 3.9\%$ after 60 days of testing, while in compost cellulose produced 18.7 ± 0.7 g of CO₂ and reached $44.3 \pm 5.9\%$ mineralization in the same period of time.

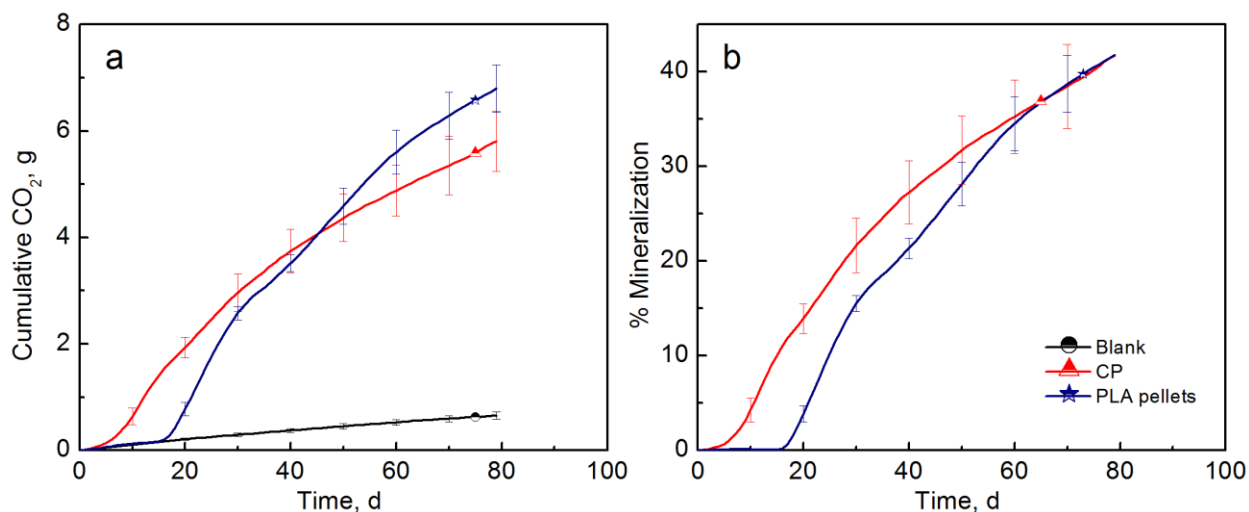


Figure 3.7 Cumulative CO₂ evolution and mineralization of CP and PLA tested in inoculated vermiculite in the Jan14 test. Lower values of evolved CO₂ are seen when compared with compost tests, as expected.

The PLA films with three different molecular weights (**Table 3.2**) were evaluated in the Nov15 test (**Figure 3.8**) in which the inoculation of vermiculite was performed as

described in sections 3.2.2.3 and 3.2.2.5. In this case, the cellulose bioreactors produced 7.3 ± 0.4 g of CO_2 and reached a mineralization of $60.2 \pm 3.3\%$ after 60 days of testing, while in compost they reached $95.7 \pm 12.1\%$ mineralization in the same period of time. PLA1, PLA2, and PLA3 produced 5.2 ± 0.6 , 8.6 ± 0.9 , and 7.2 ± 0.3 g of CO_2 , and reached mineralization of 34.6 ± 4.4 , 58.3 ± 5.8 , and $48.5 \pm 1.8\%$, respectively, after 60 days of testing. The mineralization in compost of these test materials was found to be 63.3 ± 6.7 , 67.6 ± 7.1 , and $91.5 \pm 7.0\%$ at day 60. No significant CO_2 evolution was found from the samples tested in uninoculated vermiculite, as expected.

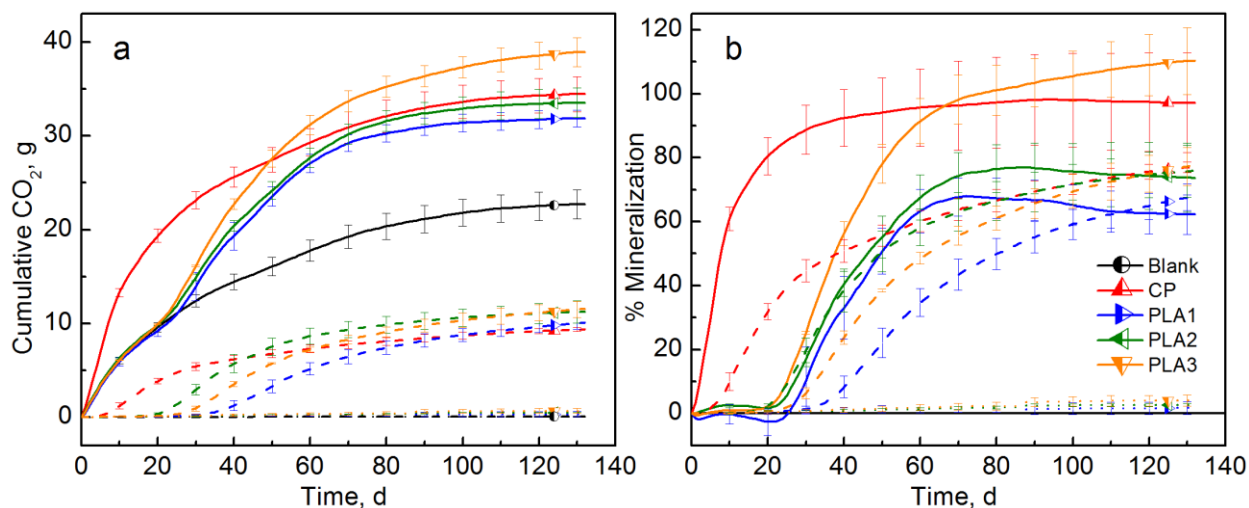


Figure 3.8 Cumulative CO_2 (a) and mineralization (b) of CP, PLA1, PLA2, and PLA3 in the Nov15 test. Solid line, dashed line, and dotted line represent compost, inoculated vermiculite and uninoculated vermiculite, respectively. Large difference in CO_2 production can be observed between evolved CO_2 in inoculated and uninoculated vermiculite.

Even though the biodegradation in inoculated vermiculite seems to be slower, the evolved CO_2 from the background is much lower and more stable. The use of

inoculated vermiculite has proven to be an excellent way to test biodegradation although with unrealistic estimated biodegradation times. For example, the mineralization values of PLA1 and PLA2 (**Figure 3.8**) are basically the same in either compost or vermiculite towards the end of the test (130 d). The % mineralization of PLA3 in vermiculite looks more similar to that of PLA1 and PLA2; while in compost it was believed to exhibit a priming effect since the mineralization was over 100%.

Furthermore, the higher mineralization reached by cellulose in the Nov15 test when compared with Jan14, could be due to additional supplementation of a mineral solution in the Nov15 test, which provides the basic nutrients required by the microorganisms to grow and multiply efficiently. In the case of PLA, other factors like molecular weight also play a role in the biodegradation process as discussed in section 3.3.4.

3.3.2 Environment-related factors affecting biodegradation

The purpose of biodegradation as a disposal route of polymers is the total breakdown of their molecular structure and their complete assimilation back into the environment by the action of naturally occurring microorganisms like bacteria, fungi, and algae in a reasonable time frame (months to a few years) [14]. However, environmental conditions such as temperature, oxygen, and water availability play a crucial role in the biodegradation rate and biodegradation mechanism of a material.

3.3.2.1 Microorganisms

The amount and type of microorganisms present in the compost play a crucial role in the biodegradation of materials. As previously mentioned, environmental conditions like temperature, oxygen, water, pH, and nutrients can affect the kind of microorganisms

present in the media and strongly influence their metabolic pathways, growth and survival [50]. In industrial composting, the microorganisms that predominate are mesophiles and thermophiles depending on the composting stage [51], while in laboratory controlled composting conditions the microorganisms that prevail are mostly thermophiles since the temperature is usually kept constant at $58 \pm 2^\circ\text{C}$. The microbial community in the compost is mainly formed by bacteria, fungi and possibly archaea and viruses. Bacteria are thought to be the major microbial domain responsible for the biodegradation process and bacteria belonging to the *Bacillus* species are more predominant in the thermophilic stage of composting [51]. A number of studies have been conducted to identify the microbial consortia present in the compost environment [52–54], and some have reported the isolation and identification of several species capable of the biodegradation of PLA [55–63], and other polymers [45,64–71]. The isolation of these bacteria has been done using selective enrichment and clear zone formation, in which the specific polymer was provided as the sole source of carbon. Further classification and identification of the isolated microbial strains has been performed by 16S rRNA sequence analysis [72,73]. However, few studies have used molecular ecological techniques and next generation sequencing which allows the identification of the vast microbial diversity present in the compost including the uncultured microorganisms that may also play a crucial role in the biodegradation of polymers [72]. For example, terminal restriction fragment length polymorphism (T-RFLP), a cultivation independent technique used for comparative community analysis, can be used to monitor changes in complex microbial communities over time [74,75]. Recent studies have also shown the potential of metaproteomics to provide direct

information about the microbial activity and the metabolic pathways occurring during the composting process [54]. Therefore, these novel techniques could be used along with biodegradation tests to gain insight into polymer biodegradation mechanisms and metabolic pathways.

The structure and diversity of microbial communities present in the soil are not likely to be the same in different regions of the world [50], which in turn may lead to different results when testing biodegradation of materials. Guo et al. (2010) have suggested the use of a specific microbial community to evaluate material biodegradability in a shorter period of time and improve the reproducibility of the results; such a community containing 20 selected microbial strains capable of degrading at least 14 types of biodegradable materials including among them starch, PLA, PCL, PHBV, and PVOH [73]. However, further studies with solid media, e.g., vermiculite, in composting conditions are required to prove the improved reproducibility of the results.

3.3.2.2 Temperature

Depending on the temperature, the microbial populations present in the media can be predominantly mesophilic or thermophilic. Usually, temperatures in the range of 54-60°C are considered optimal for composting since this favors the thermophilic compost microorganisms. Moreover, elevated temperatures can accelerate reactions like hydrolysis. Temperatures above 60°C would kill several microbial species and contribute to a faster drying of the compost, limiting the biodegradation rate [51,76]. Even though some authors have performed biodegradation studies using temperature profiles to simulate real composting, the recommendation is to keep it constant at $58 \pm 2^\circ\text{C}$ if the purpose is to reduce the amount of time required for testing [39]. **Figure 3.1**

shows that the temperature is one of the simplest parameters to control in simulated composting tests.

3.3.2.3 Oxygen availability

Depending on the oxygen availability, biodegradation can be aerobic or anaerobic [23,76]. Composting is a predominantly aerobic process in which microorganisms use oxygen to oxidize the carbon from the organic materials and produce CO₂, water, compost and heat [12,23]. Therefore, a continuous flow of air must be provided to ensure that aerobic conditions are maintained within the bioreactors [22,77].

It is recommended to set the air provided to each bioreactor to an optimal value; if the air flow rate is too low, oxygen becomes a limiting factor slowing down the biodegradation process. Conversely, high air flow rates can also be problematic in that it contributes to faster drying and cooling of the compost that also slows down the biodegradation process by decreasing water availability and temperature [76,77]. To determine the optimal air flow rate, it should also be considered that increasing the air flow rate decreases the concentration of CO₂ in the respired air stream and therefore the air flow rate for the test should be established as the one that allows the CO₂ concentration to be within the limits of the NDIR sensor [17]. In our system, the optimal air flow rate was found to be 40 sccm, and it was determined after a series of trial tests in which different known concentrations of CO₂ were injected into the bioreactors and different air flow rates were used for measurement of CO₂ with the NDIR sensor, as shown in the Appendix 3G.

3.3.2.4 Water availability

Water availability is essential for the biodegradation process and usually moisture contents between 50 and 60% are preferable [51]. Water is a distribution medium for microorganisms and nutrients; it influences the microbial development and metabolic activity; and it is an important factor affecting the biodegradation rate [76]. For example in the Sep12 test (**Figure 3.9**) cellulose produced ~16 g of CO₂ (**Figure 3.9a**) and reached 59% mineralization (**Figure 3.9b**) after 45 days of composting, and in the Nov15 test the same amount of cellulose produced about 26 g of CO₂ (**Figure 3.9c**) and reached 93% mineralization (**Figure 3.9d**). The difference in the biodegradation rate of the samples tested in the Sep12 and the Nov15 tests was mainly attributed to the water availability, assuming that the type of compost did not greatly influence this particular behavior. The effect of the compost characteristics is explained in Section 3.3.3.

In the case of the Sep12 test (**Figure 3.9a** and **Figure 3.9b**), water was not added at the beginning of the test, *i.e.*, the moisture content depended only on the availability of water on the water-saturated air supplied to the bioreactors. After day 60, when the compost experienced considerable drying, distilled water was injected into each bioreactor every three days, clearly increasing the biodegradation rate and allowing the reestablishment of a healthy microbial population, as suggested by the Birch effect. Birch (1964) demonstrated that alternate drying and rewetting of soil results in stimulated mineralization of the soil organic matter (*i.e.*, higher release of CO₂) due to a rapid increase of the microbial activity in response to the water availability [78,79].

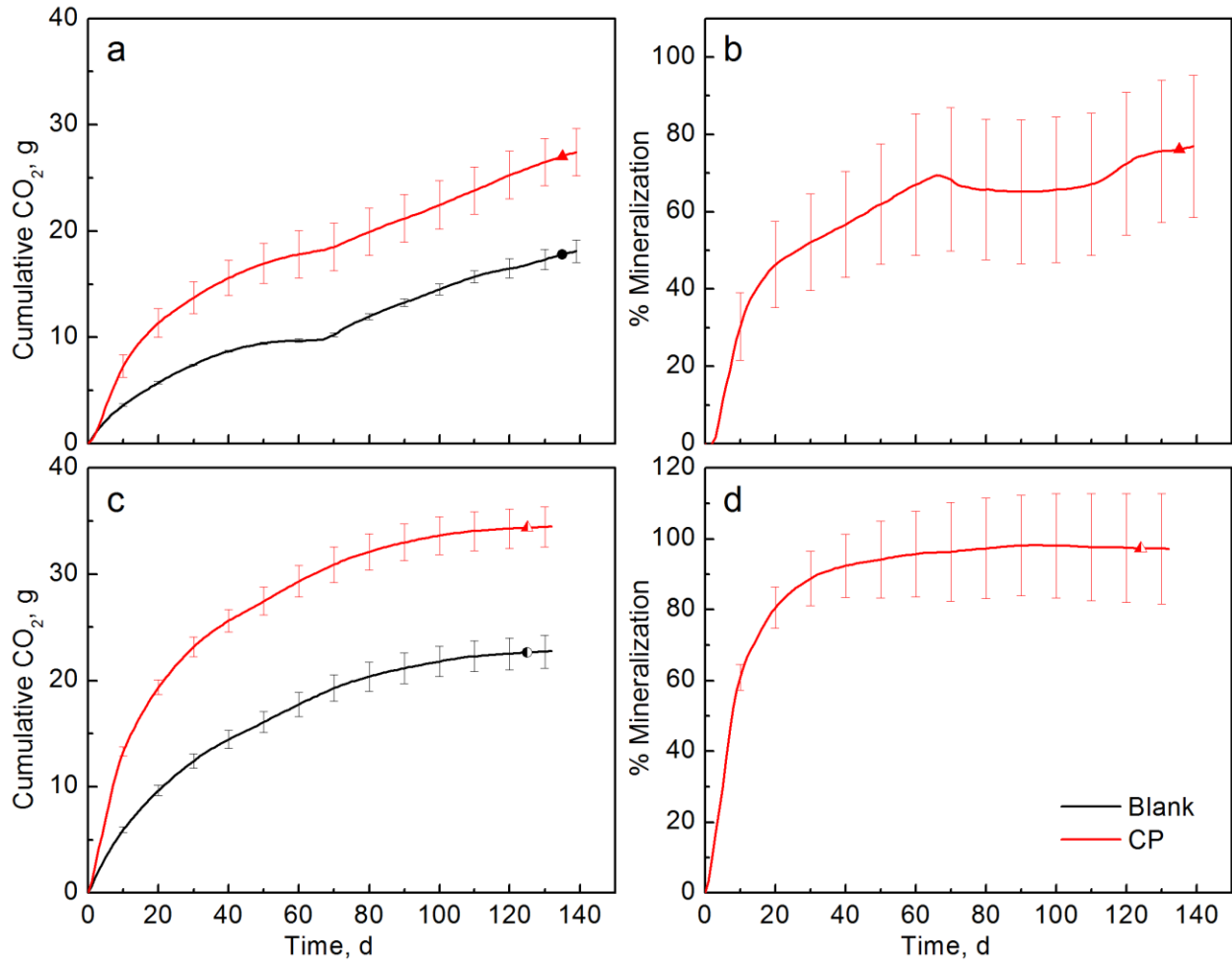


Figure 3.9 Cumulative CO₂ of blank and cellulose and % mineralization of cellulose of two different tests Sep12 test (a & b) and Nov15 test (c & d), respectively. The biodegradation process of cellulose was more homogeneous and more efficient in the test in which water was added twice a week seeing as a high % mineralization in a short period of time.

The addition of water is therefore necessary throughout the testing period; water-saturated air helps to prevent excessive drying of the compost, but it is in general not sufficient by itself to maintain the moisture content at the level required for the test. Thus, in the case of the Nov15 test (**Figure 3.9c** and **Figure 3.9d**), as well as all the other tests, water was added from the beginning of the test to each bioreactor every

three days. The amount of water added was determined by first measuring the moisture content of the compost in the control bioreactors with a moisture analyzer and then calculating the amount of water required to increase the moisture content to 50%, based on the initial dry weight of the compost. Currently, a soil moisture sensor has been integrated into a bioreactor for constant monitoring and easier determination of compost moisture.

Other researchers have determined the amount of water required by weighing each bioreactor and then adding enough water to restore the initial weight [15]. Likewise, other researchers have collected the water condensate from each bioreactor and returned it to the bioreactor to keep the moisture levels constant [17]. However, these methods can be complicated for some equipment settings or when there is a large number of bioreactors.

Water is vital for the function of the composting process; however, excessive water leads to a reduction of the airspace within the compost matrix causing oxygen limitation or anaerobiosis [77]. In this context, it has been recommended that inorganic structural materials like vermiculite to be added to the compost, to provide increased porosity and help maintain aerobic conditions [22].

Furthermore, it is recommended that bioreactors are regularly shaken (*e.g.*, every three days) to homogenize the contents and to prevent the compost sticking together and clogging [17,19]. For example, if water is added to a bioreactor without mixing, then it is likely to have moisture variability throughout the compost that would result in zones with limited water for the biodegradation process. Some authors have also found that the addition of water and shaking (material mixing) help restore

favorable conditions for biodegradation increasing the biological activity of the compost [80].

3.3.3 Inoculum-related factors affecting biodegradation

The composition of the compost plays an important role in the biodegradation rate since, besides the microorganisms, it should provide the essential nutrients required for the microorganisms to grow and efficiently multiply. Previous researchers have shown that different raw materials such as manure, yard, and food waste have different physicochemical parameters and also different microbial activity, consequently producing different amounts of evolved CO₂ [28,49,81–83]. The media used in the Sep12 test was commercial compost that according to the manufacturer was made of 90% organic materials (humus) and 10% manure, while the media for the other tests was taken from different piles at the MSU Composting Facility, comprised of a 1:1 mixture of manure and straw. Therefore, the lower evolved CO₂ in the Sep12 test (**Figure 3.2**) could also be attributed to the type of compost as previously demonstrated [28].

Table 3.5 shows the physicochemical characteristics of the several compost media used in the different biodegradation tests in comparison with the values recommended by the ISO 14855-1:2005 standard [22], which in turn are mostly based on quality standards and guidelines for compost maturity and stability found elsewhere [84,85].

Table 3.5 Characteristics of the compost samples for each test and requirements according to ISO 14855 standard

Parameters	ISO ^b	Sep12	Feb13	May13	Jul13	Jan14	Jun14	Nov14	Nov15
Dry solids, %	50-55	57.4	54.9	46.3	N/A	53.3	52.7	41.5	60.9
Volatile solids, %	<30	23.1	67.6	44.6	N/A	26.4	44.3	43.2	39.1
pH	7-9	7.6	8.9	9.1	N/A	7.8	7.9	8.5	7.4
Total Carbon, %	N/A ^a	13.4	39.2	25.9	N/A	15.3	25.7	25.1	22.7
Total Nitrogen, %	N/A ^a	1.1	2.3	1.1	N/A	0.9	2.4	2.4	2.1
C/N ratio	10-40	12.4	17.0	22.9	N/A	17.4	10.8	10.3	10.9
Compost activity ^c	50-150	49.6	35.7	73.2	N/A	39.0	81.1	63.0	62.5

^a Not applicable or not available

^b Values based on ISO 14855-1:2005 standard

^c Average values measured in mg of CO₂ per g of VS in the first 10 days

3.3.3.1 Dry solids and volatile solids

The DS of the compost used in the different tests varied from 41.5 to 60.9%, which means that in most of the cases the initial moisture content was within a reasonable range [51,86]. Likewise, the VS of the compost used in the different tests varied from 23.1 to 44.6% of the DS, except in the Feb13 test in which the VS were particularly higher (67.6%) perhaps because the compost was not mature enough at the time or because in this particular test the analysis of the compost was done before mixing with vermiculite. From **Table 3.1**, considering the tests in which the biodegradation of cellulose was more efficient and in which the physicochemical parameters of the compost were provided, the DS and VS ranged from 49-52% and 28-48%, respectively.

The VS are an indication of the organic matter (OM) present in the compost, considering that other non-organic compounds (e.g., carbonates and structural water) may be lost after ignition at 550°C; the portion of organic carbon is typically considered to be 50-58% of the VS [51,87,88]. The usual recommendation is to keep the VS low since a high amount of OM may favor the priming effect, or the microorganisms may

prefer it over the test material especially when testing more resistant materials like hydrophobic polyesters [49].

3.3.3.2 pH

In all of the tests, the pH was within the range 7-9 suggested by the ISO 14855 standard [22]. Other composting guidelines tolerate broader initial pH ranges (5.5 -9) due to the natural buffering capacity of the compost and the wide range of microorganisms involved in the process [51,86]. However, a neutral pH is preferred for the survival and full activity of the microorganisms [76]. Lauber et al. (2009), showed that the microbial community diversity is highest in soils with neutral pH [50]. An acidic pH can cause inhibition while an alkaline pH is usually associated with loss of nitrogen as ammonia (NH_3) and odor problems [51,88]. From **Table 3.1**, considering the tests in which the biodegradation of cellulose was more efficient and in which the physicochemical parameters of the compost were provided, the pH ranged from 7.2 to 7.7, mostly neutral.

3.3.3.3 C/N

The C/N of the compost used in our different biodegradation tests ranged from 10.3 to 22.9. The values reported in the literature (**Table 3.1**), considering also the tests in which the biodegradation of cellulose was more efficient and in which the physicochemical parameters of the compost were provided, varied between 14 and 43; which are basically within the wide range suggested by the ISO 14855 standard [22].

In our case, we obtained good results when using the compost piles with C/N of ~10 and ~23; however, other authors and composting guidelines have suggested different C/N, e.g., Bernal et al. suggested the C/N to be below 12 [89], Daryl et al.

below or equal to 25 [85], the Woods End Research Laboratory Incorporate below 17 [88], the Ontario Compost Quality Standard below 22 [86], the California Compost Quality Council below or equal to 25 but ideal of 10 [87], Stoffella et al. mentioned a reasonable range of 20-40 and a preferred range of 25-30 due to the large variation depending on the starting feedstock materials of the compost [51]. A list of the C/N of the different feedstock materials can be found elsewhere [51,82].

Despite the difference in C/N suggested by different sources, all agreed that high C/N slowed down the biodegradation rate since N was assumed to become a limiting factor for microbial growth while a low C/N caused excess N to be converted to NH_3 and to volatilize, which is also not desirable as discussed earlier [51,88]. Huang et al. studied the effect of C/N on composting and found that a pile with an initial C/N of 30 had a more efficient composting process by achieving maturity faster than one with C/N of 15 [90]. **Figure 3.10** shows that the C/N of the compost vs. time in the blank bioreactors of the Nov14 test slightly decreased, though not significantly.

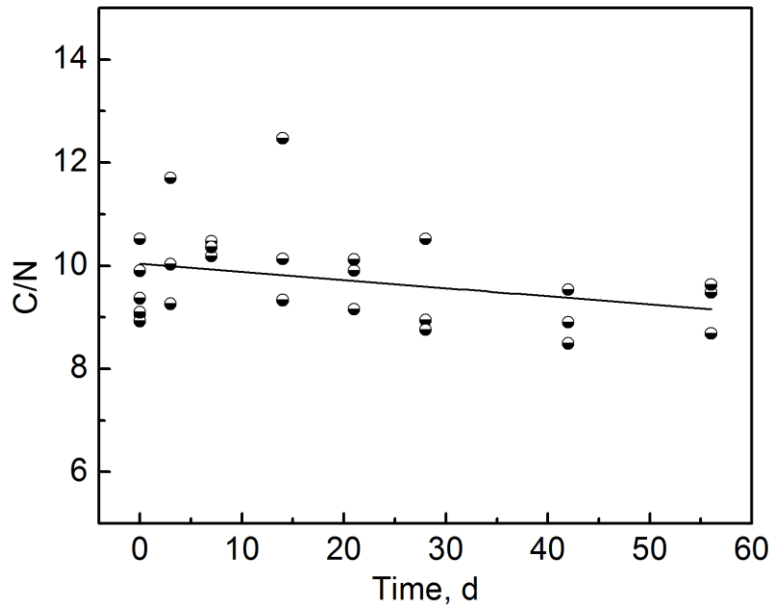


Figure 3.10 C/N of the compost as a function of time during the Nov14 test. The fitted line ($y=\beta x+\alpha$) is included for visual guidance only.

Besides the mineralization of carbon, one of the most important microbial processes is the mineralization of nitrogen [91]; microorganisms require nitrogen for their cell matter [54]. Under aerobic conditions, organic nitrogen is transformed into NH_3 or NH_4^+ during ammonification, subsequently into nitrites (NO_2^-) and finally into NO_3^- during nitrification [52,54,91,92]. In this context, nitrogen mineralization has been proposed to be used as a bio-indicator to evaluate the impact of biodegradable polymers in soil by measuring the concentrations of NH_4^+ , NO_2^- and NO_3^- during the biodegradation process [91,92]. Mature compost is expected to have appreciable amounts of NO_3^- [88]. The concentrations of NH_4^+ and NO_3^- as a function of time during the Nov14 test are shown in the Appendix 3I.

3.3.3.4 Compost activity

The ASTM D5338 and ISO 14855 standards recommend the compost to produce between 50 and 150 mg of CO_2 per gram of VS over the first 10 days as a measure of

the compost microbial activity [21,22]. **Figure 3.11** shows the production of CO₂ per gram of VS of the compost media used in the different biodegradation tests.

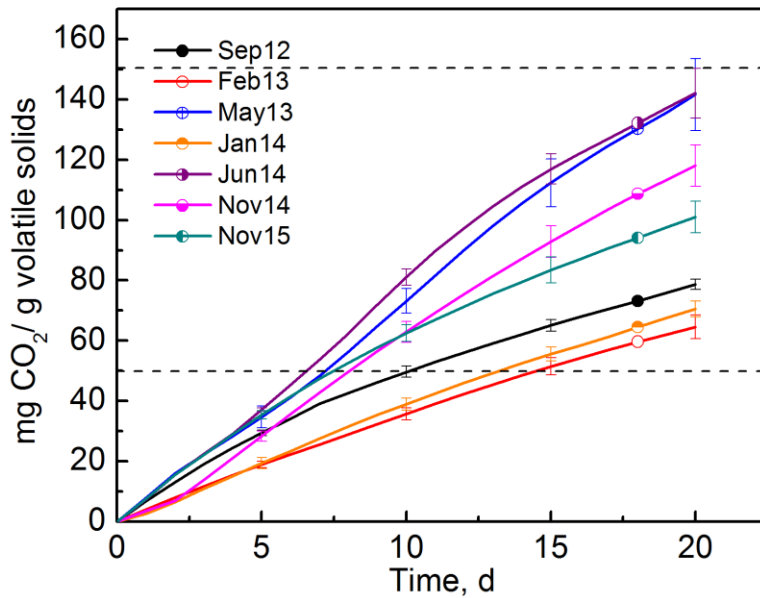


Figure 3.11 Microbial activity of the compost measured as the production of CO₂ per gram of VS. Variation between 30 and 80 mg of CO₂ per gram of VS is seeing at 10 d.

From **Figure 3.11**, the compost used in the Sep12 test was in the lower limit at 10 days, while the compost from the Feb13 and the Jan14 tests did not produce the 50 mg minimum until about 13 days. The compost from all other tests (May13, Jun14, Nov14, and Nov15 tests) produced an amount of CO₂ within the suggested range; and based on **Table 3.5**, these active composts had similar amounts of VS (39.1 – 44.6%), amounts of carbon (22.7 – 25.9%), C/N (10.3 – 10.9), and pH (7.4 – 8.5), except that the May13 test compost had a higher C/N and pH (22.9 and 9.1, respectively). However, even though the Feb13 and the May13 tests belong to the same compost pile A, they display a different activity. A similar situation occurs with the Jun14, the Nov14, and the Nov15 tests that belong to compost pile C.

While the compost activity (CO₂ production in the first 10 days) is only a recommendation in the ASTM D5338-15 standard, it is required in the ISO 14855-1:2005 for the validity of the results. This criteria seems to be based on the composting standards and guidelines for determination of compost stability, which is the rate or degree of OM decomposition [85]. Ge et al. (2006) state that for compost to be considered stable, it should have a CO₂ evolution rate less than or equal to 4 mg of carbon in the form of carbon dioxide per gram of VS per day (mg CO₂-C g⁻¹ VS d⁻¹) [85]; the California Compost Quality Council requires the compost to produce 2-8 mg CO₂-C g⁻¹ VS d⁻¹ [87]; the Woods End Research Laboratory Incorporated classifies compost stability based on the mg of CO₂ per gram of VS per day produced as follows: high (<1), medium-high (1-4), medium (4-8), medium-low (8-13), and low (>13) [88].

In this context, it is important to mention that starting a biodegradation test with a large number of samples requires considerable resources and preparation time. Considerable loss is incurred if the experiment is discarded because the compost does not produce the 50-150 mg of CO₂ per gram of VS over the first 10 days as required by the ISO 14855-1:2005 standard. In this scenario, it is more important to consider if the compost is stable enough so the blank bioreactors, which are the background, do not produce large amounts of CO₂ that can hinder measurement of the CO₂ evolved from the bioreactors containing the test materials. In fact, a low production of CO₂ from the background is desired to improve the sensitivity of the measurement.

3.3.3.5 Other nutrients

In general, it is assumed that with a reasonable C/N, all other nutrients required by the microorganisms are available in sufficient quantities [51]. **Table 3.6** shows the

physicochemical characteristics and the total nutrient analysis of the three different media used in the Nov15 test: compost, inoculated vermiculite, and uninoculated vermiculite.

The physicochemical parameters of compost and vermiculite media are quite different. Vermiculite is a clay mineral with excellent water holding capacity, while compost is a more heterogeneous and complex matrix which contains additional organic compounds that can be assimilated by the microorganisms other than the test material [93,94].

According to **Table 3.6**, the amount of VS in vermiculite is very low as expected. The pH in inoculated vermiculite is lower due to the mineral solution used, while the C/N is higher in uninoculated vermiculite since no extra source of nitrogen was provided. In any case, the C/N is expected to increase when the test material is added to the media. Other element concentrations are similar between inoculated and uninoculated vermiculite, except sodium and sulfur due to the mineral solution used for inoculation. The high concentration of aluminum was expected in the vermiculite media.

Table 3.6 Physicochemical parameters and total nutrient analysis of different media used in the Nov15 test

Parameter	Compost	Inoculated vermiculite	Uninoculated vermiculite
Dry solids, %	60.9	98	98.6
Volatile solids, %	39.1	2.0	1.4
pH	7.4	6.8	8.0
C/N ratio	10.9	7.2	27.1
Carbon, %	22.7	1.2	0.8
Nitrogen, %	2.08	0.16	0.03
Phosphorus, %	0.55	0.13	0.11
Potassium, %	2.48	4.32	4.26
Calcium, %	9.43	0.49	0.69
Magnesium, %	2.06	8.63	8.99
Sodium, %	0.40	0.15	0.03
Sulfur, %	0.42	0.05	0.01
Iron, ppm	15080	45330	47700
Zinc, ppm	163	80	86
Manganese, ppm	503	450	447
Copper, ppm	107	155	154
Boron, ppm	33	4	3
Aluminum, ppm	5955	42880	44200

Note: The total nutrient analysis was performed by inductively coupled plasma atomic emission spectroscopy (ICP-OES).

3.3.3.6 Priming effect

The priming effect is the over-degradation of the indigenous organic carbon present in the compost when testing materials like glucose and its polymers [46]. **Figure 3.12** shows an excellent example of the priming effect. In the Jan14 test, the GC curve displayed an unusual high production of CO₂ in comparison with CP and CS (also readily biodegradable materials), and a mineralization near 200%, which physically makes no sense; the additional carbon converted to CO₂ is coming from the compost and not from the sample material.

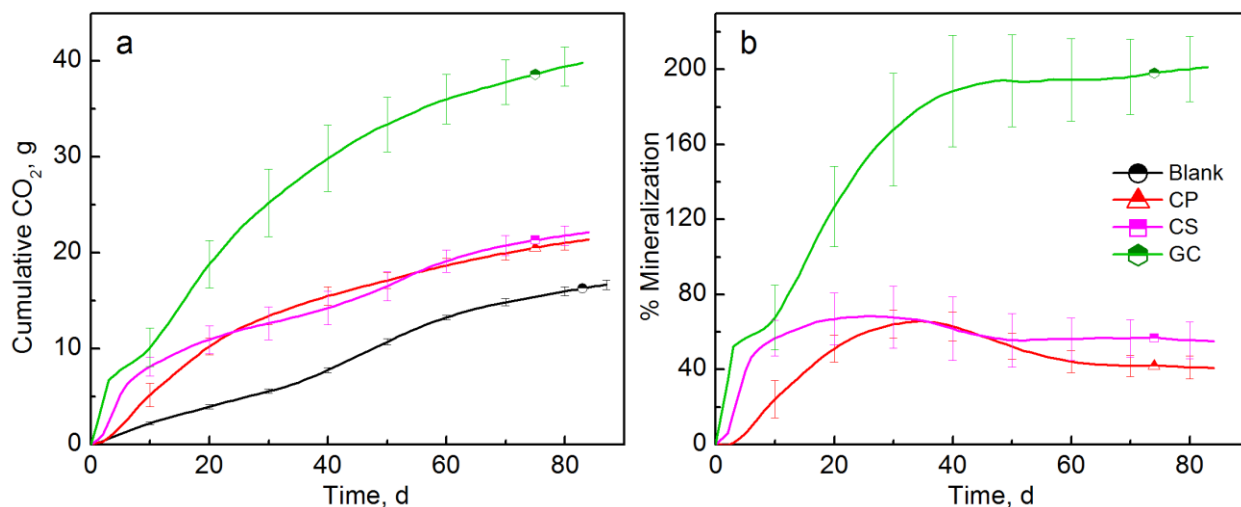


Figure 3.12 Cumulative CO₂ evolution (a) and mineralization (b) of CP, CS, and GC in the Jan14 test. Mineralization values larger than 100% are observed for GC.

It has been demonstrated that vermiculite is a good microbial carrier allowing the survival and full activity of the microorganisms, and it can be used as the solid media in biodegradation tests for avoiding the priming effect [46]. It has also been suggested that vermiculite increases reproducibility and aids in recovery of the by-products released during the degradation process, which is useful for determination of carbon balances [38,94].

3.3.4 Material-related factors affecting biodegradation

The physicochemical characteristics of the test materials such as chemical structure, hydrophilicity, crystallinity, molecular weight, shape, and surface area, among others, are also factors affecting the biodegradation rate and the biodegradability of the materials.

3.3.4.1 Chemical structure and properties

The intrinsic characteristics of the polymer such as mobility, tacticity, crystallinity, molecular weight, glass transition temperature (T_g), functional groups, plasticizers, and

additives highly influence its biodegradability [12]. The unique chemistry of the polymer also dictates that the microorganisms should have metabolic pathways capable of targeting the polymer for biodegradation [95].

Figure 3.13 shows the CO₂ evolution and mineralization of different materials from the Jun14 test, where there were two main groups of polymers tested. The first group, which included PE and LDPE polymers, did not show any meaningful mineralization ($3.7 \pm 1.6\%$ for PE) while the second group, consisting of CP, CS, and PLA, reached a maximum mineralization of 61.7 ± 9.3 , 48.0 ± 4.5 , and $47.4 \pm 9.8\%$, respectively.

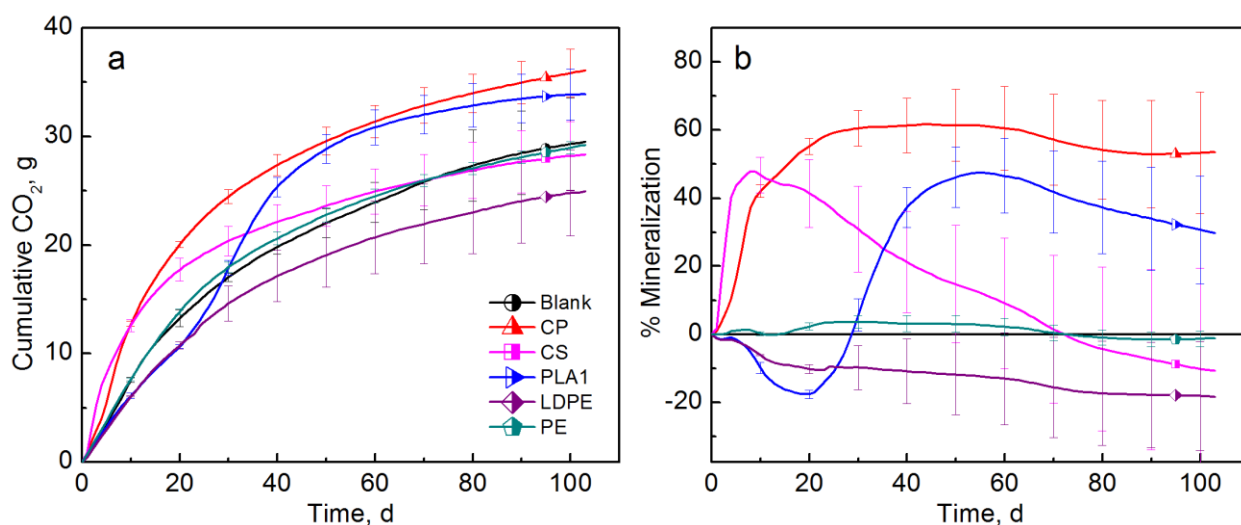


Figure 3.13 CO₂ evolution (a) and mineralization (b) of different materials in the Jun14 test. Large difference of % Mineralization is observed for the different materials.

The different behavior between these two groups is due to the difference in the intrinsic characteristics of the polymer. On one hand, polymers like LDPE are not easily degradable due to their hydrophobic characteristics and relatively high stability [95], provided by the presence of single bonds between carbon atoms in the polymer chain that are especially difficult to break [96]. On the other hand, polymers like cellulose and

starch tend to interact strongly with water due to their hydrophilic characteristics [96], and their biodegradation occurs relatively quickly. In the case of hydrolytically degradable polymers, the degradation rate is highly dependent on the nature of the functional groups comprising the polymer; some examples of functional groups contained in degradable polymers are: poly(α -hydroxy-esters), poly(β -hydroxy-esters), poly(ϵ -caprolactone), and poly(carbonates). A complete list of the different functional groups and their reactivity is provided elsewhere [47]. For example, polymers containing poly(α -hydroxy-esters), like PLA, tend to show lag periods due to the initial diffusion of water into the polymer matrix and the subsequent break down of the polymer into oligomers and monomers before actual biodegradation can take place. The biodegradation mechanism of PLA is discussed in more detail in Section 3.3.5.

In this context, Mezzanote *et al.* (2005) pointed out the question of whether it is correct or not to use cellulose as reference material since the microorganisms that are able to biodegrade materials like cellulose or starch are ubiquitous and perform cellulolytic activity, but it is not certain if they are equally able to perform esterase activity, which is required for the efficient and fast biodegradation of other materials like polyesters [49]. They have also suggested using biodegradable polyesters such as PCL as reference material besides cellulose. Similarly, other authors have proposed using PLA powder or PCL powder as reference materials for biodegradation tests [97,98].

Even if the test materials are the same, differences in composition and properties can highly influence their biodegradation rate. For example, **Figure 3.14** shows the biodegradation test results of two types of PLA evaluated in the Nov14 test. The PLA2 film is Ingeo™ 2003D while PLA4 film is Ingeo™ 4032D; the main difference between

these two types of PLA is their composition in terms of the L-Lactide and D-Lactide content, which in turn affects the crystallinity of the material. PLA2 has a crystallinity of $6.14 \pm 0.08\%$ as measured by differential scanning calorimetry (DSC) (data not shown), while PLA4 was found to be completely amorphous due to its higher amount of D-Lactide. PLA4 produced more CO₂ than PLA2, especially at the early stage of the test. Likewise, the mineralization of PLA4 was higher than 100% towards the end of the test, indicating a priming effect.

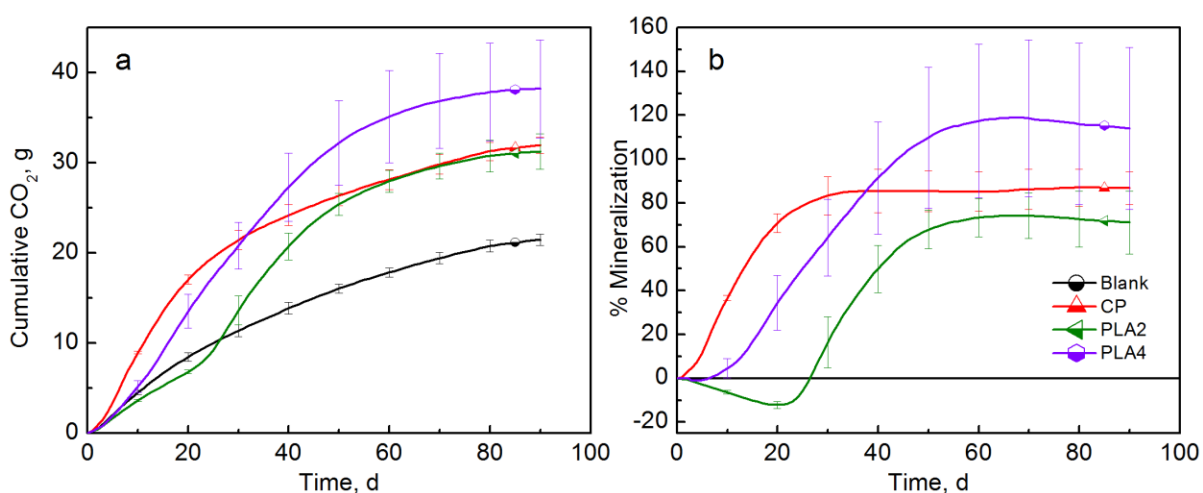


Figure 3.14 Cumulative CO₂ (a) and mineralization (b) of CP, PLA2, and PLA4 in the Nov14 test. PLA 4032D shows faster and larger mineralization than PLA 2003D.

These results are in agreement with the literature, in which other researchers have found that PLA with greater D-Lactide content presented higher and faster initial chemical hydrolytic degradation [99,100]. Besides, Tsuji and Miyauchi (2001) found that enzymatic hydrolysis, in which enzymes facilitate the cleavage of bonds, occurs mainly in the amorphous regions and on polymer chains with free ends [101]. However, these results may be also influenced by other factors such as molecular weight and thickness. PLA4 has lower M_n than PLA2 ($M_n = 82.9 \pm 6.7$ and 75.0 ± 1.4 kDa, for PLA2 and PLA4

respectively; on the other hand, PLA4 is much thicker than PLA2 (0.022 ± 0.003 and 0.255 ± 0.021 mm, for PLA2 and PLA4, respectively).

3.3.4.2 Concentration

ASTM D5338-15 and ISO 14855-1:2005 recommend the ratio of the dry mass of the compost to the dry mass of the test material be 6:1; for example, 600 g of dry solids of the inoculum mixed with 100 g of dry solids of the sample. However, in our case we found this ratio not to be the most convenient because most of our samples are tested as films (1 cm x 1 cm squares) and not as powder, and the volume and area occupied by thin films is too large for good exposure when mixed with the compost. For example, in our bioreactors we can only fit 400 g wet weight of compost; considering that the initial moisture content was adjusted to 50% and that 20% of that weight was vermiculite, then each bioreactor contained 160 g dry weight of compost. If we followed the compost-to-material ratio recommended by the standards the weight of the sample should be 26 g; the inconvenience with this amount is that 26 g of films with a thickness of 0.00254 cm is too large (*i.e.*, density of PLA=1.24 g/cm³, V=21 cm³, A_{film}=8,252 cm²) to be fit into the bioreactor and properly mixed with the compost. Moreover, if 26 g of cellulose were added to the bioreactor the production of CO₂ would be very high and fall outside the limits of the NDIR sensor. After many trial tests, we found that the optimal amount of material for our DMR system is 8 g or a 20:1 ratio (5% wt.). Again, similar to setting up the air flow rate mentioned earlier, the concentration of material should be adjusted in a way that the concentration of CO₂ is within the limits of the sensor and the production of CO₂ by the reference and the blank bioreactors are clearly differentiated.

Figure 3.15 shows the cumulative CO₂ and % mineralization of CP (5%) and PLA pellets with two different concentrations (5% and 15%) where 15% is closer to the 6:1 ratio suggested by the standards. As expected, the production of CO₂ in the 15% was higher than the one in the 5% since the amount of available carbon is higher, but the % mineralization was not affected. The PLA pellets in both concentrations reach the same mineralization by the end of the test.

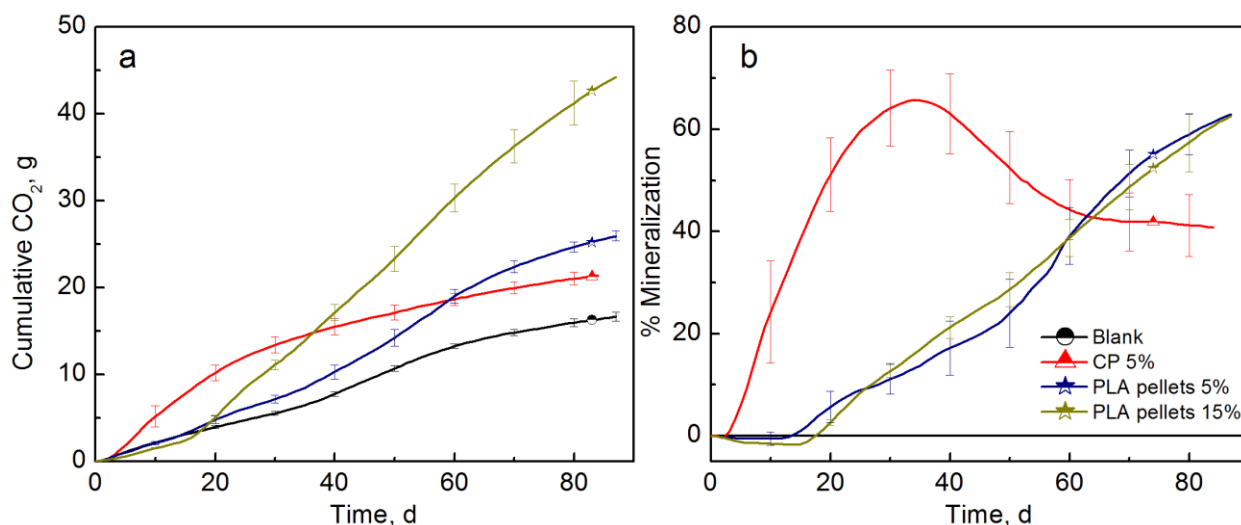


Figure 3.15 Cumulative CO₂ and % mineralization of CP and PLA pellets with two different concentrations: 5% and 15%, in the Jan14 test. % Mineralization was not affected regardless of the initial amount of PLA.

3.3.4.3 Shape

Biodegradation is usually, but not always, a surface erosion mechanism. Thus, materials in the form of powder usually degrade more easily since the area/volume ratio is maximized [8,76]. In this context, some researchers have suggested that the biodegradation test can be accelerated if the sample material is provided as a powder or small particles. For example, the plastic materials can be converted into very thin films and then fragmented via cryogenic milling [102].

Figure 3.16 shows the cumulative CO₂ evolution and % mineralization of CP and of PLA provided in different forms, *i.e.*, pellet and film, with surface area-to-volume ratio of ~12 and ~790, respectively. The production of CO₂, in this case, was not significantly different considering that the degradation of PLA via hydrolysis is a combination of both surface and bulk erosion [47].

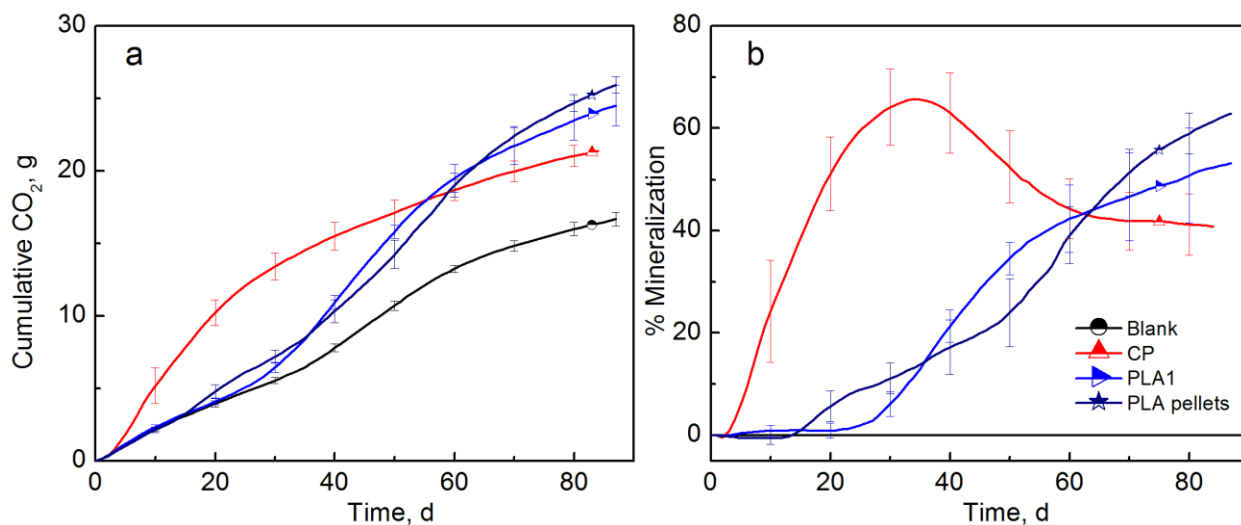


Figure 3.16 Cumulative CO₂ evolution (a) and mineralization (b) of CP and of PLA provided in different forms: pellet and film, in the Jan14 test. % Mineralization was not extensively different regardless of the shape of the material.

3.3.4.4 Comparison among different biodegradation tests

Even though it has been stated that comparing the results between different tests in a direct fashion would not be fair due to the many variables involved in the process, a possible way to perform such comparison would be to normalize against the mineralization of the positive reference, as suggested by ASTM D5338-15, in which the percentage of biodegradation relative to the positive reference (*e.g.*, cellulose) at the end of the test should be reported. In this context, if the t_i/t_T ratio, where t_i is the time at which the measurement was taken, and t_T the total time of the test, is plotted vs the ratio

of material mineralization and cellulose mineralization, a possible way to compare the results could be envisioned (**Figure 3.17**), assuming that the biodegradation behavior was similar in the tests being compared.

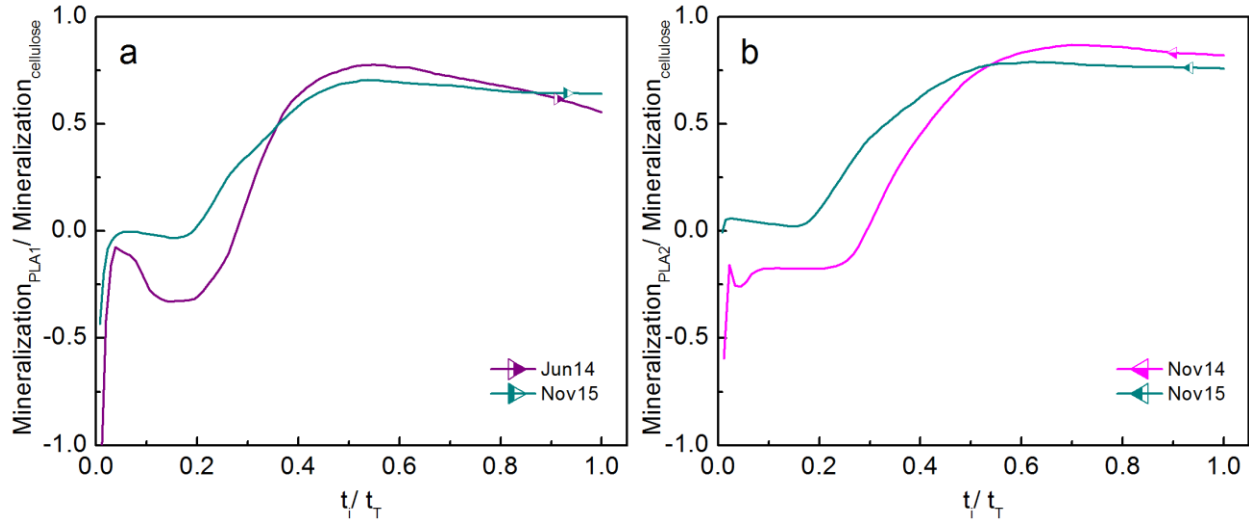


Figure 3.17 Comparison of the mineralization values obtained for PLA1 in the Jun14 and the Nov15 tests (a), and the mineralization values obtained for PLA2 in the Nov14 and the Nov15 tests (b). The mineralization ratio when adjusting the time span of the test seems to be similar when comparing the same test material.

Figure 3.17 shows that PLA1 reached a maximum mineralization ratio of 0.77 and 0.70 at a time ratio of 0.55 and 0.54 for the Jun14 test and the Nov15 test, respectively. Similarly, PLA2 reached a maximum mineralization ratio of 0.87 and 0.79 at a time ratio of 0.70 and 0.61 for the Nov14 test and the Nov15 test, respectively. This represents a difference of 9% between the mineralization ratio values in both cases. This approach to comparison should be further explored.

3.3.5 Study Case: Biodegradation of Poly(lactic acid)

In the case of natural polymers like cellulose and starch, the biodegradation process is relatively fast and starts with the depolymerization of the material by the action of microbial extracellular enzymes that reduce the polymer to a size that is water soluble and able to be transported through the cell wall for subsequent assimilation by the microbial metabolic pathways [26,103]. **Figure 3.18a** shows the biodegradation of cellulose.

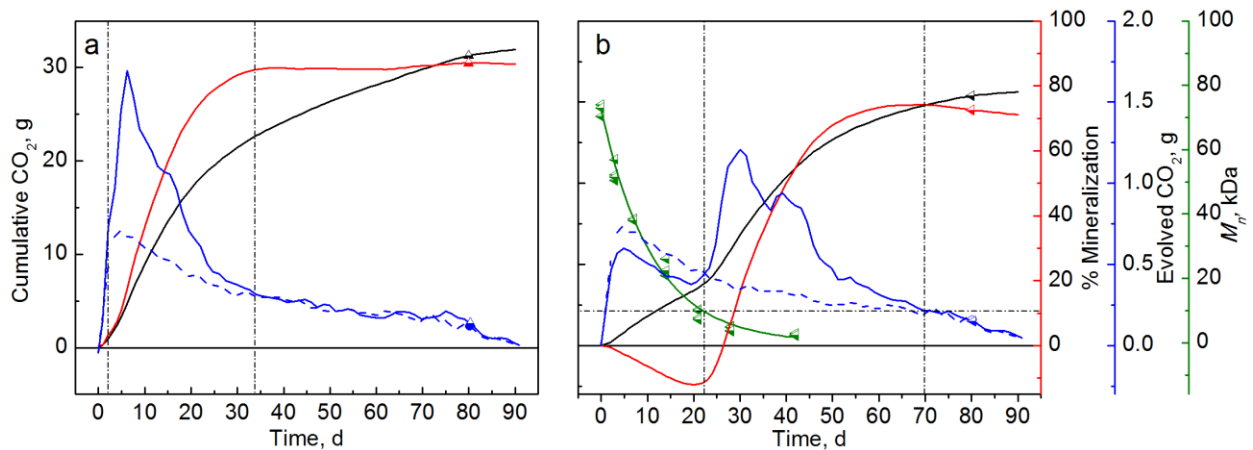


Figure 3.18 Biodegradation of CP (a) and PLA2 (b) during the Nov14 test. The black, red, blue, and green lines represent cumulative CO₂, mineralization, evolved CO₂ per measurement, and M_n reduction, respectively. The dashed blue line represents the evolved CO₂ per measurement of the blank bioreactors. The green line indicates a fitting of an equation of the form $M_n = M_{n0} \exp(-kt)$, where M_{n0} is the initial M_n , k is the rate constant and t is the time. The black dash-dot lines are used as reference to indicate the beginning and end of the biodegradation phase, and the M_n at which the biodegradation phase gets started. Different lag phases and biodegradation phases were observed for CP and PLA2.

Microorganisms drive the biodegradation but other abiotic processes (oxidative, thermal, chemical or photodegradation) may also take place before or in parallel, such as in the case of PLA, where biodegradation is well known to involve abiotic hydrolysis (**Figure 3.18b**) [104]. During the first step of PLA degradation, cleavage of ester linkages occurs due to their high susceptibility to water producing a significant reduction in the molecular weight of the polymer [103]. During the second step, the microorganisms are able to assimilate the low molecular weight lactic acid oligomers and monomers. We have found that the second step starts once the molecular weight is ≤ 10 kDa, as shown in **Figure 3.18b**.

Figure 3.18 shows that there are three phases in the biodegradation process: lag, biodegradation, and plateau phases. In the case of natural polymers like cellulose, the biodegradation phase starts almost immediately since fragmentation occurs quickly and the lag phase is assumed to occur due to the acclimatization of the microorganisms to the environment. In the case of polymers like PLA, there is an extended lag phase due to the relatively slow fragmentation of high molecular weight polymer chains. The biodegradation phase only occurs when enough low molecular weight oligomers and monomers become water soluble and are available for microbial assimilation [47].

The hydrolysis rate of the ester bonds in PLA can change depending on different factors such as water availability, pH, presence of ions, T_g , crystallinity, and molecular weight [47]. As previously mentioned, hydrolysis occurs mainly in the amorphous regions. As a result, during degradation, an increase in crystallinity can be observed. Furthermore, in the early stage of degradation, as T_g decreases from $64.0 \pm 0.8^\circ\text{C}$, as measured for PLA by DSC (data not shown), to temperatures below the test

temperature ($58 \pm 2^\circ\text{C}$), the oligomers and monomers have been reported to crystallize inside the PLA matrix since the polymer chains have sufficient mobility to rearrange into a more stable configuration [100,105].

Some researchers have suggested that during the early hydrolysis step no microorganisms are involved [103,106,107], while others consider that enzymatic hydrolysis plays an important role along with abiotic hydrolysis [108]. Therefore, to decouple abiotic and biotic degradation, PLA films with three different molecular weights (**Table 3.3**) were evaluated in inoculated vermiculite and uninoculated vermiculite during the Nov15 test and the results are shown in **Figure 3.19** and **Figure 3.20**. It is expected for polymers like PLA that both mechanisms compete against each other, with the fastest process the one that controls the initial degradation mechanism.

Figure 3.19 shows that there was no significant production of CO_2 from the samples tested in uninoculated vermiculite. On the other hand, the PLA1, PLA2, and PLA3 produced 5.2 ± 0.6 , 8.6 ± 0.9 , and 7.2 ± 0.3 g of CO_2 , respectively after 60 days of testing, and reached a mineralization of 34.6 ± 4.4 , 58.3 ± 5.8 , and $48.5 \pm 1.8\%$, respectively, in the same period of time.

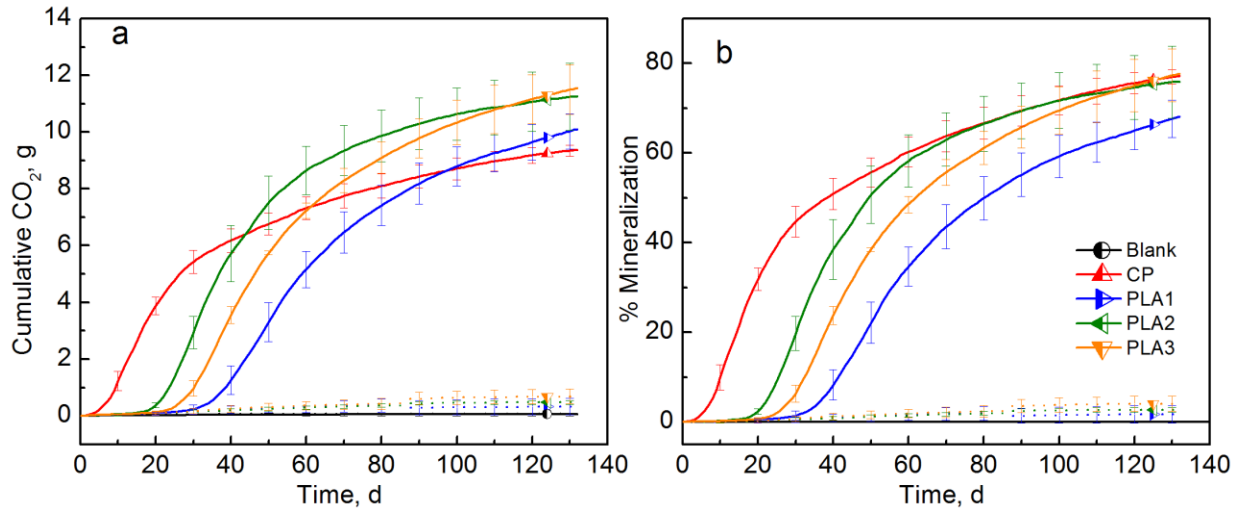


Figure 3.19 Cumulative CO₂ (a) and mineralization (b) of CP, PLA1, PLA2, and PLA3 in the Nov15 test. Solid lines and dotted lines represent inoculated vermiculite and uninoculated vermiculite, respectively.

Figure 3.20 shows the M_n as a function of time for the three PLA films tested in the three different media during the Nov15 test. The molecular weight decreased during the first three weeks and a first order reaction relationship was fitted to the experimental data. The M_n reduction of each sample material was not significantly different regardless of the testing media (*i.e.*, compost, inoculated vermiculite, and uninoculated vermiculite), indicating that the abiotic step or hydrolysis is the main contribution to the degradation process of PLA in the early stage of degradation, and therefore it is a limiting factor for the subsequent biodegradation of PLA [102,103,107]. **Figure 3.20** shows that the initial molecular weight also affects the hydrolysis rate and therefore the overall biodegradation. The PLA with higher M_n has longer polymer chains and more bonds to be cleaved, while the one with lower M_n has more polymer chains with free ends that can be cleaved producing more oligomers and monomers that are available for microbial assimilation.

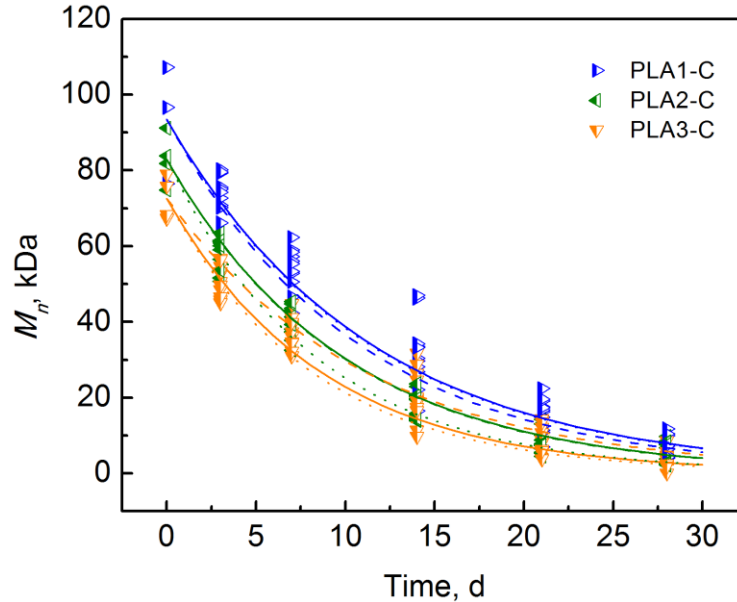


Figure 3.20 Molecular weight reduction as a function of time for PLA1, PLA2, and PLA3 in compost (solid line), inoculated vermiculite (dashed line), and uninoculated vermiculite (dotted line), in the Nov15 test. Lines indicate fitting of a first order reaction of the form $M_n = M_{n0} \exp(-kt)$, where M_{n0} is the initial M_n , k is the rate constant and t is the time.

In our experiment, the rate constants (k) were not significantly different. However, it could be possible that the hydrolytic degradation of PLA occurs faster in an abiotic environment due to the accumulation of by-products, such as oligomers and monomers of lactic acid, which in turn reduce the pH of the media. This lower pH can cause even more hydrolytic degradation due to an autocatalytic effect [47]. On the other hand, in a biotic environment the microorganisms ideally assimilate those by-products continuously and the pH does not change significantly, perhaps assisted by the natural buffering capacity of the compost [51].

3.4 Final Remarks

We have provided a comparative analysis of the results obtained from eight different biodegradation tests for cellulose, starch, glycerol, polyethylene, and poly(lactic acid). These tests were carried out in the same in-house built DMR system following the analysis of evolved CO₂ approach. The results along with the critical analysis of the information provided in the literature allowed us to identify low reproducibility as one of the main issues for this kind of evaluation, caused mainly by the difficult to control variables in measurements of the biodegradation process.

In order to further understand such sources of variability a critical review of the literature regarding the different factors affecting biodegradation was also provided. This analysis allowed us to identify some key parameters that can be more strictly monitored and controlled for an efficient biodegradation test, and therefore, to improve the current testing methodology.

Among the factors producing high variability is the quality and characteristics of the compost; therefore, a stricter control on moisture content, organic matter, and C/N should be required for the test, and all physicochemical parameters of the compost should be reported; otherwise, the interpretation of the results would not be complete. pH was found to be one of the easiest parameters to maintain due to the natural buffer capacity of the compost. If the test material is suspected to produce a priming effect, then biodegradation testing in vermiculite is recommended; also, in cases where recovering of the by-products or determination of carbon balances is relevant for the study. Amendment of vermiculite with a mineral solution is recommended since it provides many of the nutrients required by the microorganisms.

Regarding environmental factors, temperature was the easiest parameter to control while water content was the most difficult and crucial. Maintaining the moisture content of the compost constant throughout the composting period is vital for the survival and reproduction of the microorganisms and other processes like hydrolysis. The optimal flow rate and optimal material concentrations should be found for each specific system in a way that allows proper measurement of CO₂ by the sensor and a clear differentiation between the background and the sample material.

If the test material is not expected to be readily biodegradable or to follow a similar behavior to cellulose, then the use of an additional positive control should be recommended (*e.g.*, a standardized PCL or PLA powder). In hydrolytically degradable materials like PLA, the shape did not show any significant difference since degradation occurs simultaneously in the surface and the bulk. For other types of materials, the usual recommendation is to use powder or small particles to increase the area/volume ratio and the biodegradation rate. Other polymer characteristics such as chemical structure, glass transition temperature, crystallinity, molecular weight, and functional groups highly influence the biodegradability and biodegradation rate of the material.

The biodegradation of PLA requires prior hydrolytic degradation, which breaks down the polymer chain into lactic acid oligomers or monomers that are easily assimilated by microorganisms. Thus, abiotic hydrolysis is the main contribution to the degradation process of PLA in the early stage of degradation and becomes a limiting factor for the subsequent biodegradation of this material. However, the hydrolysis rate is also dependent on the specific PLA properties like crystallinity and initial molecular weight.

The CO₂ evolution test can always provide valuable information about the biodegradability of a test material. However, if the purpose of the study is not only to evaluate and/or certify a material as biodegradable or compostable, but also to understand its biodegradation mechanism and environmental impacts, then additional tests are required such as determination of carbon balances, ecotoxicity tests, and molecular ecological techniques, among others.

Further biodegradation tests in composting conditions using different standardized reference materials and more strictly controlled inoculum (compost and/or vermiculite) characteristics and testing parameters could be performed in different labs around the world (*e.g.*, round robin test) by the analysis of evolved CO₂ in a DMR system in an attempt to unify and to improve this testing methodology.

APPENDICES

APPENDIX 3A: Material processing

LDPE film production: The LDPE/LLDPE blend (30% LLDPE wt.) film was processed by using a Killion KLB 100 blown film extruder (Davis-Standard LLC, Pawcatuck, CT) with a screw diameter of 25.4 mm, screw L/D of 24, and annular die diameter of 5 cm. The temperature profile was 216, 216, 216, 213, 213, 210, 204 °C for barrel zones 1, 2, 3, clamp ring, adaptor, die 1, and die 2, respectively. The screw speed was 14 rpm and take up speed was 3 m per minute.

PLA film production: The Ingeo™ 2003D films were obtained by using a Microextruder model RCP-0625 (Randcastle Extrusion Systems, Inc., Cedar Grove, NJ) with a screw diameter of 15.9 mm, screw L/D of 24, and volume of 34 cm³. The PLA pellets were dried at 60°C for 24 h under vacuum (85 kPa) prior processing. The temperature profile and screw speed of the films is shown in **Table 3A.1**.

Table 3A.1 Temperature profile and screw speed used for the production of the PLA films

	PLA1	PLA2	PLA3
Zone 1, °C	193	193	193
Zone 2, °C	213	249	249
Zone 3, °C	216	249	249
Transfer tube, °C	216	249	249
Die, °C	210	216	216
Screw speed, rpm	49	33	28

APPENDIX 3B: Elemental analysis

The carbon, hydrogen, and nitrogen content of the different test materials were determined by using a PerkinElmer 2400 Series II CHNS/O Elemental Analyzer (Shelton, CT, USA), and values are presented in **Table 3B.1**.

Table 3B.1 Carbon, hydrogen, and nitrogen content of the tested materials

Material	ID	% Carbon^a	% Hydrogen^a	% Nitrogen^a
Cellulose powder	CP	42.50 ± 0.34	6.53 ± 0.05	0.04 ± 0.01
Cassava starch	CS	41.75 ± 0.35	6.69 ± 0.08	0.01 ± 0.00
Glycerol ^b	GC	39.12	8.77	0.00
Polyethylene powder	PE	85.76 ± 0.29	15.13 ± 0.09	0.01 ± 0.01
LDPE/LLDPE film	LDPE	86.83 ± 0.10	14.84 ± 0.04	0.00 ± 0.00
Ingeo™ 2003D pellet	PLA pellet	50.40 ± 0.28	5.65 ± 0.05	0.00 ± 0.01
	PLA1	50.05 ± 0.05	5.65 ± 0.02	0.01 ± 0.01
Ingeo™ 2003D film	PLA2	49.93 ± 0.11	5.56 ± 0.02	0.01 ± 0.01
	PLA3	49.99 ± 0.05	5.60 ± 0.01	0.01 ± 0.01
Ingeo™ 4032D sheet	PLA4	50.00 ± 0.08	5.61 ± 0.01	0.04 ± 0.02

^a Percentage by weight

^b Theoretical values based on chemical structure

APPENDIX 3C: Molecular weight determination

The M_n , M_w , and PI of PLA samples before and during composting were determined with a gel permeation chromatography (GPC) system from Waters Inc. (Milford, MA). The system is equipped with a Waters 1515 isocratic pump, a Waters 717 autosampler, a series of three columns (HR2, HR3, and HR4 Waters Styragel®), and a Waters 2414 refractive index detector interfaced with a Waters Breeze software. For each PLA sample, 20 mg were dissolved in 10 cm³ of tetrahydrofuran (THF) and filtered with a hydrophobic polytetrafluoroethylene (0.45 μm pore size) filter before injection. Then, 100 μL of each sample solution were injected into the system with a flow rate of 1 cm³/min, a run time of 45 min, and a temperature of 35°C. A third-order polynomial universal calibration curve was obtained from polystyrene standards ranging 1.37 – 2,480 kDa. The Mark-Houwink constants, $K= 0.000174$ dL/g and $\alpha= 0.736$, for PLA when dissolved in THF at 30°C [109], were used to obtain the absolute molecular weight values.

APPENDIX 3D: Compost source

The compost prepared at the MSU Composting Facility (East Lansing, MI) was produced by mixing dairy manure and straw in a proportion of 1:1. Manure, the fecal and urinary excretion of livestock, is rich in nitrogen content; hence, it was mixed with straw, a source of carbon, to achieve the desired carbon-nitrogen ratio (C/N) for the compost samples. The mixture was introduced into bays, turned 2-3 times a week. The material was allowed to naturally heat to about 55°C (132 °F) for 72 hours and turned at least three times. Then, the mixture was pulled out of the bay, and a pile was built up on an asphalt pad. After the active composting phase, a curing period of 6 to 12 months was required to finish the process and allow the compost to develop the desired characteristics. After curing, the compost was screened to remove large debris and inert materials [110].

APPENDIX 3E: Respirometric system

An enhanced direct measurement respirometric (DMR) system was built at the School of Packaging (SoP) in Michigan State University (MSU), East Lansing, MI, based on the system reported by [18]. This DMR system was designed to operate simultaneously with up to 95 bioreactors, and it is able to simulate different testing conditions by varying temperature and relative humidity (RH). A computer application was developed for controlling the system, as well as for measuring and recording the test variables. A non-dispersive infrared gas analyzer (NDIR), model LI-820 from LI-COR Inc., Lincoln, NE, was used to measure the concentration of CO₂ evolved from the bioreactors. **Figure 3E.1** shows a schematic diagram of the DMR; detailed information of the equipment can be found elsewhere [40].

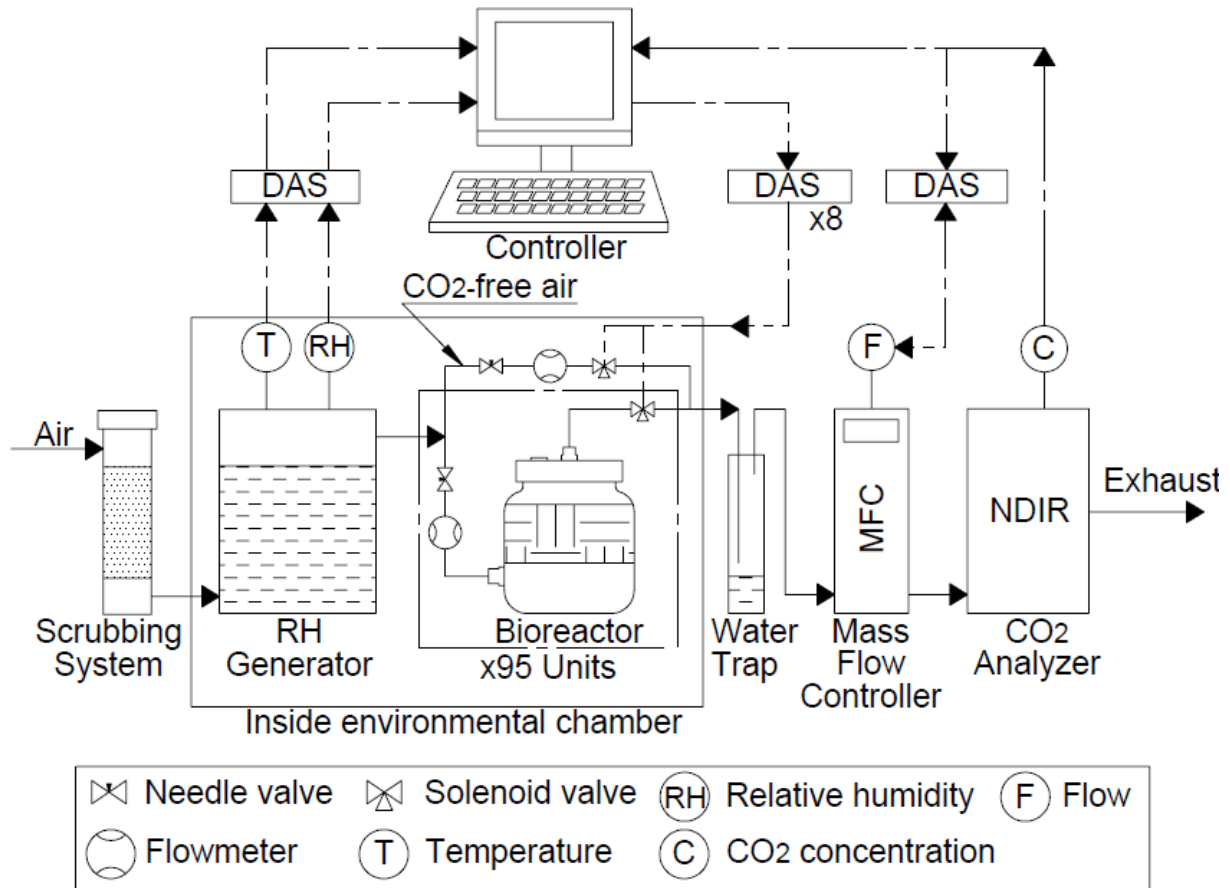


Figure 3E.1 Schematic diagram of a direct measurement respirometric system, reproduced from Castro-Aguirre, E. [40]. CO₂ from the incoming air is scrubbed by passing through a series of canisters containing soda lime. This CO₂-free air enters a water tank, located inside the environmental chamber at 58°C, to get humidified; then, CO₂-free water-saturated air is provided to the bioreactors with an upward flow direction. The respired air stream exits the bioreactors and the environmental chamber passing through a water trap, a mass flow controller (MFC) and a NDIR-CO₂ sensor for CO₂ concentration measurement. Temperature, relative humidity (RH), air flow rate, time and CO₂ concentration are measured and recorded by a data acquisition system (DAS).

APPENDIX 3F: Calculation method

In order to calculate the cumulative CO₂ evolved from the bioreactors and the mineralization of the sample materials, a number of parameters and variables are acquired by the DMR control software. It records the bioreactor number, the time stamp, the CO₂ concentration (ppm), the standard air flow rate (sccm), the temperature (°C), the relative humidity (%), the date (mm/dd/yyyy), and the time (hh:mm:ss), every 2 seconds during the last 30 seconds of each cycle time; *i.e.*, 15 measurements of each variable are recorded every cycle [40].

The cycle time is the period, set by the user, in which the solenoid valve of the selected bioreactor is opened by the control software allowing the respired air to flow through the NDIR sensor at a specified flow rate. This time is estimated according to the information presented in the Appendix 3G. All the information presented below regarding the calculation method can be found in more detail elsewhere [40].

The actual CO₂ concentration of each measurement is determined by multiplying the response CO₂ concentration by the calibration factor (Eq. 3F.1).

$$[C] = c * k \quad (\text{Eq. 3F.1})$$

where $[C]$ is the actual concentration of CO₂ of each sample (ppm), c the response concentration of CO₂ as measured by the NDIR analyzer (ppm), and k the calibration factor explained in the Appendix 3G.

The time (min) at which each measurement was done, relative to the starting time, is determined by Eq. 3F.2.

$$t_n = \frac{ts_n - ts_o}{60} \quad (\text{Eq. 3F.2})$$

where t_n is the time at which each measurement was done (min), ts_n is the time stamp at time t_n , and ts_o is the time stamp at time t_o corresponding to the time at which the experiment started.

The average time (min), average concentration (ppm), average flow rate (sccm), average temperature ($^{\circ}\text{C}$), and average RH (%) are calculated since 15 measurements of each variable are recorded every cycle and only a representative value per cycle is used for the CO_2 evolution calculation.

The concentration of CO_2 (ppm) is converted to mass of CO_2 (g) evolved from each bioreactor in the period of time between measurements (measurement interval) as described by the Eq. 3F.3.

$$E(\text{CO}_2) = \frac{F \times C \times T \times 44}{22414 \times 10^6} \quad (\text{Eq. 3F.3})$$

where $E(\text{CO}_2)$ is the mass of evolved CO_2 (g), F the flow rate (sccm), T the measurement interval, C the concentration of CO_2 evolved during the measurement interval, 22414 the volume of 1 mol of gas in cc at STP, 44 the molecular weight of CO_2 (g/mol), and 10^6 the ppm conversion factor [18].

If the time is plotted against the concentration, as shown in **Figure 3F.1**, then the area under the curve for a specific measurement interval represents the product $C \times T$ of the Eq. 3F.3 and it is determined by Eq. 3F.4.

$$A = \frac{([C]_n + [C]_{n-1}) \times (t_n - t_{n-1})}{2} \quad (\text{Eq. 3F.4})$$

where A is the area under the curve (ppm•min), t_n the time in which the measurement was done (min), t_{n-1} the time in which the previous measurement was done (min), $[C]_n$

the concentration of CO₂ (ppm) at time t_n , and $[C]_{n-1}$ is the concentration of CO₂ (ppm) at time t_{n-1} .

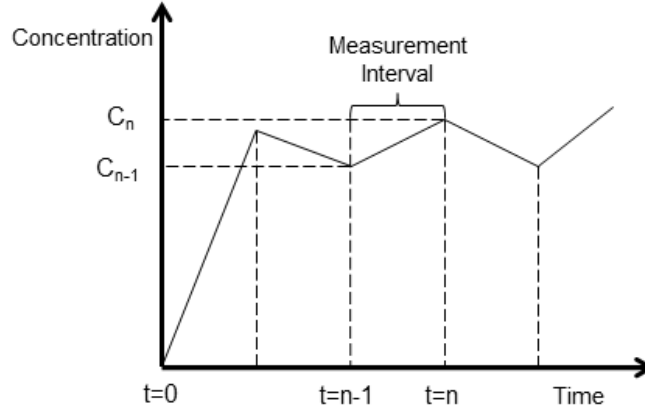


Figure 3F.1 Time vs. Concentration Plot, reproduced from Castro-Aguirre, E. [40]

The cumulative amount of evolved CO₂ in each bioreactor for each measurement interval is calculated using Eq. 3F.5.

$$C(CO_2) = E(CO_2)_n + C(CO_2)_{n-1} \quad (\text{Eq. 3F.5})$$

where $C(CO_2)$ is the cumulative mass of CO₂ (g), $E(CO_2)_n$ is the mass of CO₂ (g) evolved from the sample at time t_n , and $C(CO_2)_{n-1}$ is the cumulative mass of CO₂ (g) until the previous measurement (at time t_{n-1}).

Since the cumulative mass of CO₂ of the blank has to be subtracted from the cumulative mass of CO₂ of each sample at the same time interval for further calculating the percentage mineralization, the time is converted from minutes to days, and an interpolation of CO₂ values is performed with time intervals of one day using Eq. 3F.6.

$$I(CO_2) = C(CO_2)_L + (C(CO_2)_H - C(CO_2)_L) \frac{t_I - t_L}{t_H - t_L} \quad (\text{Eq. 3F.6})$$

where t_I (d) is the time interval, t_L (d) is the immediate lower value of the time interval, t_H (d) is the immediate higher value of the time interval, $I(CO_2)$ (g) is the interpolated

cumulative mass of CO₂ at time t_i , $C(CO_2)_L$ (g) is the cumulative mass of CO₂ at time t_L , and $C(CO_2)_H$ (g) is the cumulative mass of CO₂ at time t_H .

Once the cumulative mass of CO₂ of each bioreactor is obtained, the percentage mineralization of each bioreactor is calculated using Eq. 3F.7, expressing the relationship between the actual amount of CO₂ evolved from the test material and the theoretical amount of CO₂ that can be evolved from the same test material.

$$\% \text{ Mineralization} = \frac{(CO_2)_T - (CO_2)_B}{M_{TOT} \times C_{TOT} \times \frac{44}{12}} \times 100 \quad (\text{Eq. 3F.7})$$

where $\% \text{ Mineralization}$ is the percent carbon molecules converted to CO₂, $(CO_2)_T$ is cumulative mass of CO₂ (g) evolved from a sample bioreactor, $(CO_2)_B$ the average cumulative mass of CO₂ (g) evolved from the blank bioreactors, M_{TOT} the mass of test material (g), C_{TOT} is the proportion of total organic carbon in the total mass of test material (g/g), 44 the molecular weight of carbon dioxide, and 12 the atomic weight of carbon.

APPENDIX 3G: Determination of the calibration factor, optimal flow and cycle time

In this case, calibration refers to the process of establishing the relationship between the CO₂ analyzer signal (measured CO₂ concentration) and the known injected concentration of pure CO₂. Thus, when a measurement is made by the CO₂ analyzer, the signal measurement is multiplied by the calibration factor (*k*) to yield the actual concentration of CO₂ evolved from a sample (Eq. 3F.1) [40].

The calibration of the system was performed at 58 ± 2°C and 50 ± 5% RH. Known amounts of pure CO₂ gas (1, 5, 10, and 20 cc) were injected through a septum to empty bioreactors. Additionally, three air flow rates (20, 40, and 60 sccm) were used for determining the optimal flow. The actual concentration of CO₂ in the bioreactor was calculated using Eq. 3G.1, being 507, 2535, 5070, and 10140 ppm the corresponding actual concentration for 1, 5, 10, and 20 cc injected volume, respectively.

$$\text{Actual Concentration of } CO_2 = \frac{\text{Injected volume of } CO_2}{\text{Total volume of the bioreactor}} \quad (\text{Eq. 3G.1})$$

The response CO₂ concentration was measured by the NDIR and recorded along with the time every 2 seconds. Then, the calibration curve was determined by plotting the peak response concentrations against the actual concentrations as shown in **Figure 3G.1** [40].

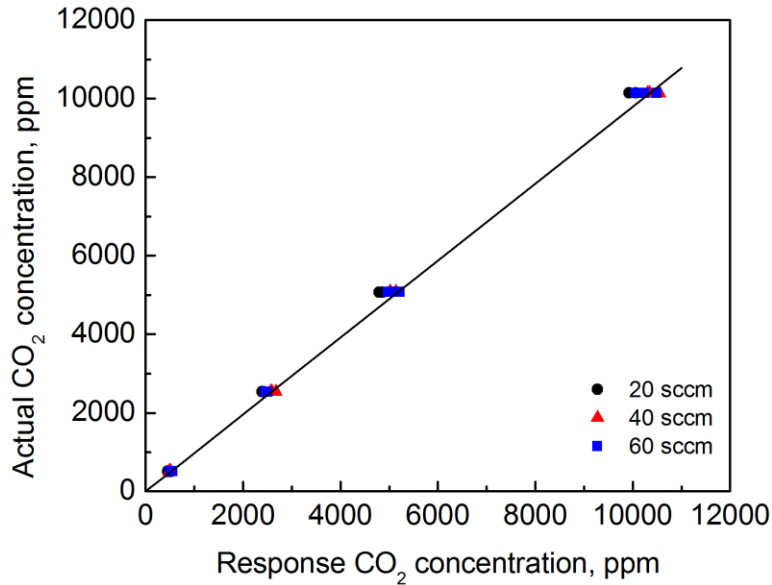


Figure 3G.1 Calibration curve at $58 \pm 2^\circ\text{C}$ and $55 \pm 5\%$ RH. A linear relationship of the form $[C] = c \cdot k$ was fitted to the data, where $[C]$ is the actual CO₂ concentration, c the response CO₂ concentration as measured by the NDIR analyzer, and k the calibration factor.

Figure 3G.2 shows that the response concentration is not affected when using different air flow rates, as long as the CO₂ concentration is allowed to reach its maximum value. **Figure 3G.3** shows that time to reach the maximum concentration was the lowest when using the highest air flow rate and vice versa. The small differences observed in the time among replicates of the same air flow rate are due to the different injected volumes of CO₂.

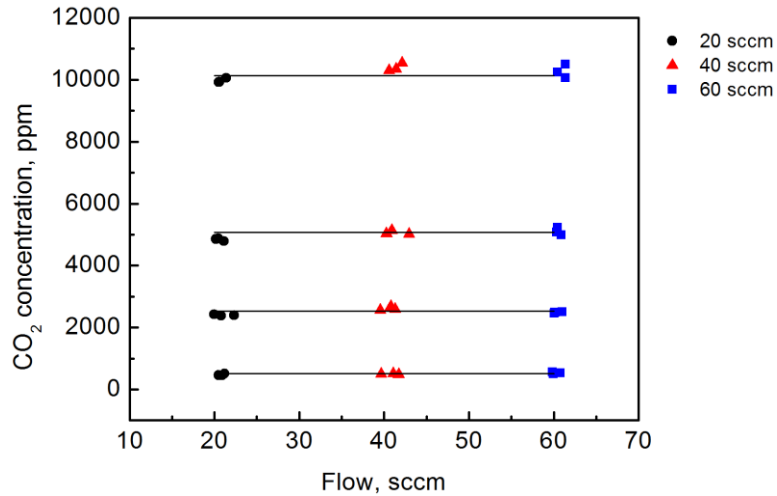


Figure 3G.2 Response CO₂ concentration obtained when using different injection volumes and air flow rates. The maximum concentration can be achieved in each case regardless the air flow rate used. Fitted lines of the form $y=\beta x+\alpha$ are included for visual guidance only, with $\beta= 0$, and $\alpha= 507, 2535, 5070$, and 10140 , corresponding to the different injection volumes used.

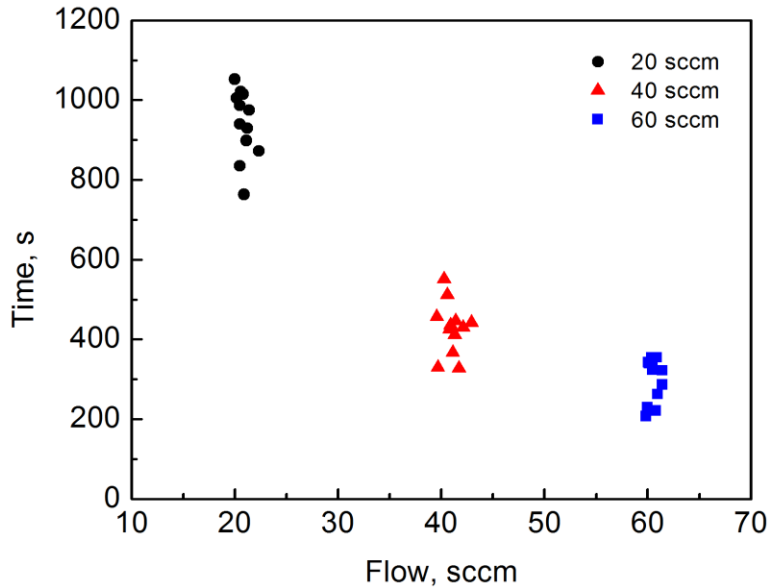


Figure 3G.3 Time to reach the maximum CO₂ concentration when using different air flow rates. The longest time to reach the maximum concentration was observed when using the lowest air flow rate.

The above findings are relevant when setting the parameters for performing the real biodegradation test in which the objective is to reach the CO₂ concentration at steady-state (instead of the maximum CO₂ concentration during calibration) before recording the measurement for a particular bioreactor. For example, if using a specific cycle time during the test, the bioreactors with the lower flow may show lower concentrations by the end of the cycle (measuring time), because there is not enough time to reach the steady-state. Therefore, it is important to select the appropriate air flow rate to be used during testing and based on that to determine the cycle time that would include the highest CO₂ concentration that could be expected from the testing materials. **Figure 3G.4** shows that the time to reach steady-state is depending on both CO₂ concentration and air flow rate.

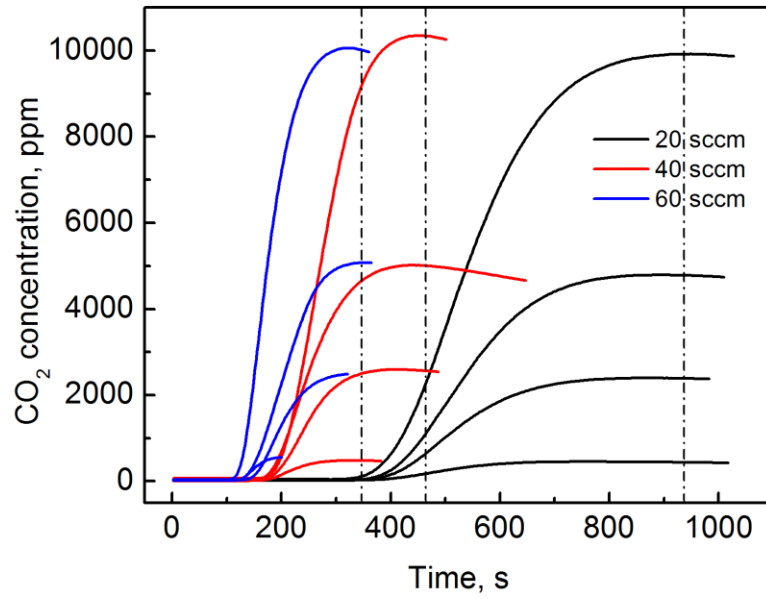


Figure 3G.4 Response concentration and time required for a selected bioreactor to reach the peak concentration for different injection volumes and air flow rates. The longest time was observed with the highest CO₂ concentration and the lowest air flow rate.

APPENDIX 3H: Compost physicochemical characteristics before and after the test

Table 3H.1 shows the compost physicochemical characteristics determined before and after the test for the Feb13 and the Nov14 tests. The carbon content decreased in both cases due to the mineralization of carbon, as expected. The C/N was also decreased being more pronounced in the compost with a higher initial C/N which is in agreement with the results obtained by Bernal et al. [89].

Table 3H.1 Physicochemical characteristics of the compost from the Feb13 and the Nov14 tests determined before and after the test

Parameter	Feb13		Nov14	
	Before	After	Before	After
Dry solids, %	54.9	50.8	41.5	82.6
Volatile solids, %	67.6	42.7	43.2	38.2
pH	8.9	7.8	8.5	8.1
Total Carbon, %	39.2	24.8	25.1	22.2
Total Nitrogen, %	2.3	2.6	2.43	2.17
C/N ratio	17.0	9.5	10.3	10.2

APPENDIX 3I: Compost nitrate and ammonium concentration

Figure 3I.1 shows the concentrations of NH_4^+ and NO_3^- as a function of time of the compost in the blank bioreactors and the compost in the CP bioreactors during the Nov14 test. Other researchers have found previously that during the composting process the NH_4^+ concentration decreases while the NO_3^- concentration increases due to the nitrification process [89,92].

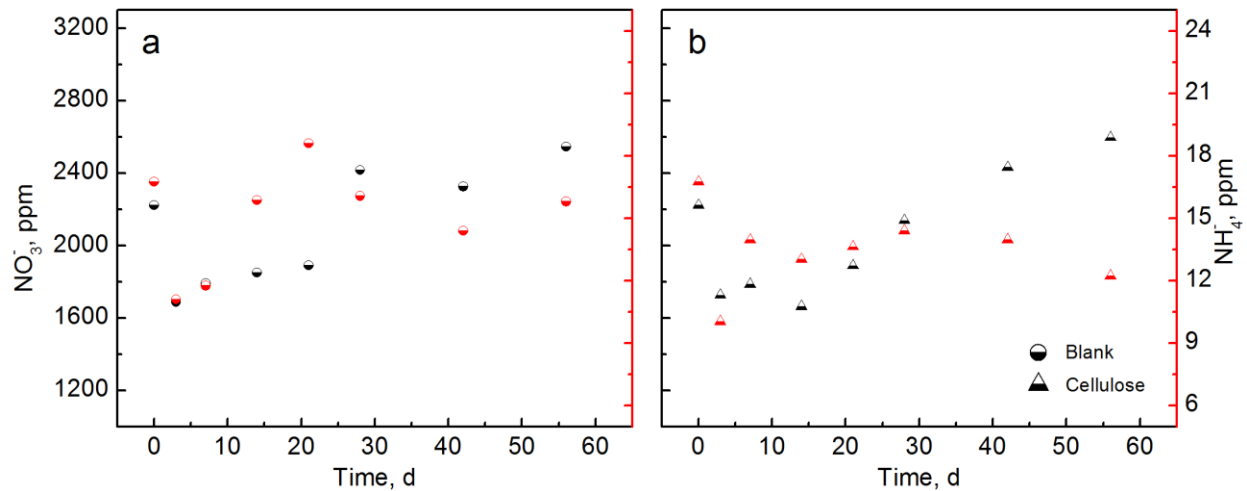


Figure 3I.1 Concentration of NO_3^- (left-black axis) and NH_4^+ (right-red axis) as a function of time of the compost in blank bioreactors (a) and CP bioreactors (b) during the Nov14 test.

APPENDIX 3J: Summary of the results obtained from the eight different biodegradation tests

A summary of the results obtained from the eight different biodegradation tests is provided in **Table 3J.1**.

Table 3J.1 Summary of the results obtained from the eight different biodegradation tests

Test	Sample	Media	g CO ₂ at 60 d	%Min. at 60 d	Max. %Min.	Days to achieve max. %Min.
Sep12	Blank	Compost	9.7 ± 0.2	N/A	N/A	N/A
	CP	Compost	17.8 ± 2.2	67.0 ± 18.4	77	139
	LDPE	Compost	8.9 ± 0.5	-3.3 ± 1.9	N/A	N/A
Feb13	Blank	Compost	18.3 ± 0.7	N/A	N/A	N/A
	CP	Compost	27.5 ± 4	67.7 ± 30.8	67.9	55
	LDPE	Compost	16.7 ± 1.5	-8.7 ± 6.2	N/A	N/A
May13	Blank	Compost	23.9 ± 4.1	N/A	N/A	N/A
	CP	Compost	33.6 ± 2.8	78.9 ± 23.1	79.5	52
	CS	Compost	26.5 ± 2.5	22.0 ± 21.0	28.1	43
	LDPE	Compost	25.1 ± 2.7	4.6 ± 4.8	6.8	20
Jul13	Blank	Compost	20.8 ± 2.3	N/A	N/A	N/A
	CP	Compost	33.7 ± 2.6	100.3 ± 20.5	100.8	65
	LDPE	Compost	22.2 ± 1.2	5.5 ± 4.8	6.1	68
Jan14	Blank	Compost	13.3 ± 0.2	N/A	N/A	N/A
	CP	Compost	18.7 ± 0.7	44.3 ± 5.9	65.7	34
	CS	Compost	19.1 ± 1.2	56.2 ± 11.2	68.3	26
	PE	Compost	10.7 ± 10.3	N/A	N/A	N/A
	GC	Compost	36 ± 2.6	194.5 ± 22.1	201.3	83
	PLA pellets (5%)	Compost	19 ± 0.8	39.2 ± 5.5	62.9	87
	PLA pellets (15%)	Compost	30.3 ± 1.6	38.8 ± 3.6	62.6	87
	PLA1	Compost	19.5 ± 1	42.4 ± 6.6	53.2	87

Table 3J.1 (cont'd)

Test	Sample	Media	g CO ₂ at 60 d	%Min. at 60 d	Max. %Min.	Days to achieve max. %Min.
Jan14	Blank	Inoculated vermiculite	0.5 ± 0.1	N/A	N/A	N/A
	CP	Inoculated vermiculite	4.9 ± 0.5	35.3 ± 3.9	41.7	79
	PLA pellets	Inoculated vermiculite	5.6 ± 0.4	34.5 ± 2.8	41.7	79
Jun14	Blank	Compost	23.9 ± 1.8	N/A	N/A	N/A
	CP	Compost	31.4 ± 1.5	60.6 ± 12.2	61.7	45
	CS	Compost	24.9 ± 2.1	9.1 ± 19.1	48	8
	PE	Compost	24.5 ± 0.6	2.2 ± 2.5	3.7	26
	LDPE	Compost	20.7 ± 3.4	-13.0 ± 13.5	N/A	N/A
	PLA1	Compost	30.8 ± 1.6	46.6 ± 11.0	47.4	55
Nov14	Blank	Compost	17.8 ± 0.5	N/A	N/A	N/A
	CP	Compost	28.1 ± 1.1	85.2 ± 9.0	87	82
	PLA2	Compost	28 ± 1.2	73.3 ± 8.7	74.2	69
	PLA4	Compost	35.1 ± 5.1	117.4 ± 35.0	118.9	68
Nov15	Blank	Compost	17.8 ± 1.1	N/A	N/A	N/A
	CP	Compost	29.3 ± 1.5	95.7 ± 12.1	98.2	94
	PLA1	Compost	27.1 ± 1.0	63.3 ± 6.7	68	72
	PLA2	Compost	27.7 ± 1.0	67.6 ± 7.1	76.9	86
	PLA3	Compost	31.2 ± 1.0	91.5 ± 7.0	109.1	120
	Blank	Inoculated vermiculite	0.0 ± 0.0	N/A	N/A	N/A
	CP	Inoculated vermiculite	7.3 ± 0.4	60.2 ± 3.3	75.6	120
	PLA1	Inoculated vermiculite	5.2 ± 0.6	34.6 ± 4.4	65	120
	PLA2	Inoculated vermiculite	8.6 ± 0.9	58.3 ± 5.8	74.7	120
	PLA3	Inoculated vermiculite	7.2 ± 0.3	48.5 ± 1.8	75.1	120

N/A: Not applicable
Min= Mineralization

REFERENCES

REFERENCES

- [1] T. Kijchavengkul, R. Auras, M. Rubino, S. Selke, M. Ngouajio, R.T. Fernandez, Formulation selection of aliphatic aromatic biodegradable polyester film exposed to UV/solar radiation, *Polym. Degrad. Stab.* 96 (2011) 1919–1926. doi:10.1016/j.polymdegradstab.2011.07.001.
- [2] P. Kunthadong, R. Molloy, P. Worajittiphon, T. Leejarkpai, N. Kaabbuathong, W. Punyodom, Biodegradable Plasticized Blends of Poly(L-lactide) and Cellulose Acetate Butyrate: From Blend Preparation to Biodegradability in Real Composting Conditions, *J. Polym. Environ.* 23 (2015) 107–113. doi:10.1007/s10924-014-0671-x.
- [3] Y.X. Weng, X.L. Wang, Y.Z. Wang, Biodegradation behavior of PHAs with different chemical structures under controlled composting conditions, *Polym. Test.* 30 (2011) 372–380. doi:10.1016/j.polymertesting.2011.02.001.
- [4] Y.L. Du, Y. Cao, F. Lu, F. Li, Y. Cao, X.L. Wang, Y.Z. Wang, Biodegradation behaviors of thermoplastic starch (TPS) and thermoplastic dialdehyde starch (TPDAS) under controlled composting conditions, *Polym. Test.* 27 (2008) 924–930. doi:10.1016/j.polymertesting.2008.08.002.
- [5] R. Iovino, R. Zullo, M.A. Rao, L. Cassar, L. Gianfreda, Biodegradation of poly(lactic acid)/starch/coir biocomposites under controlled composting conditions, *Polym. Degrad. Stab.* 93 (2008) 147–157. doi:10.1016/j.polymdegradstab.2007.10.011.
- [6] T. Kijchavengkul, R. Auras, M. Rubino, M. Ngouajio, R.T. Fernandez, Assessment of aliphatic-aromatic copolyester biodegradable mulch films. Part II: Laboratory simulated conditions, *Chemosphere.* 71 (2008) 1607–1616. doi:10.1016/j.chemosphere.2008.01.037.
- [7] M.R. Calil, F. Gaboardi, C.G.F. Guedes, D.S. Rosa, Comparison of the biodegradation of poly(ϵ -caprolactone), cellulose acetate and their blends by the Sturm test and selected cultured fungi, *Polym. Test.* 25 (2006) 597–604. doi:10.1016/j.polymertesting.2006.01.019.
- [8] T. Kijchavengkul, R. Auras, Compostability of polymers, *Polym. Int.* 57 (2008) 793–804. doi:10.1002/pi.2420.
- [9] E. Castro-Aguirre, F. Iñiguez-Franco, H. Samsudin, X. Fang, R. Auras, Poly(lactic acid)—Mass production, processing, industrial applications, and end of life, *Adv. Drug Deliv. Rev.* (2016). doi:10.1016/j.addr.2016.03.010.
- [10] G. Kale, T. Kijchavengkul, R. Auras, M. Rubino, S.E. Selke, S.P. Singh, Compostability of bioplastic packaging materials: An overview, *Macromol. Biosci.*

- 7 (2007) 255–277. doi:10.1002/mabi.200600168.
- [11] E.T.H. Vink, S. Davies, Life Cycle Inventory and Impact Assessment Data for 2014 Ingeo™ Polylactide Production, *Ind. Biotechnol.* 11 (2015) 167–180. doi:10.1089/ind.2015.0003.
- [12] A.A. Shah, F. Hasan, A. Hameed, S. Ahmed, Biological degradation of plastics: A comprehensive review, *Biotechnol. Adv.* 26 (2008) 246–265. doi:10.1016/j.biotechadv.2007.12.005.
- [13] J.C. Young, R.M. Cowan, *Respirometry for Environmental Science and Engineering*, SJ Enterprises, Springdale, Arkansas, 2004.
- [14] S. Selke, R. Auras, T.A. Nguyen, E. Castro Aguirre, R. Cheruvathur, Y. Liu, Evaluation of biodegradation-promoting additives for plastics, *Environ. Sci. Technol.* 49 (2015) 3769–3777. doi:10.1021/es504258u.
- [15] K. Dagnon, M. Pickens, V. Vaidyanathan, N. D'Souza, Validation of an Automated Multiunit Composting System, *J. Polym. Environ.* 22 (2014) 9–16. doi:10.1007/s10924-013-0596-9.
- [16] G. Lashermes, E. Barriuso, M. Le Villio-Poitrenaud, S. Houot, Composting in small laboratory pilots: Performance and reproducibility, *Waste Manag.* 32 (2012) 271–277. doi:10.1016/j.wasman.2011.09.011.
- [17] C. Way, D.Y. Wu, K. Dean, E. Palombo, Design considerations for high-temperature respirometric biodegradation of polymers in compost, *Polym. Test.* 29 (2010) 147–157. doi:10.1016/j.polymertesting.2009.10.004.
- [18] T. Kijchavengkul, R. Auras, M. Rubino, M. Ngouajio, R. Thomas Fernandez, Development of an automatic laboratory-scale respirometric system to measure polymer biodegradability, *Polym. Test.* 25 (2006) 1006–1016. doi:10.1016/j.polymertesting.2006.06.008.
- [19] R. Jayasekara, G.T. Lonergan, I. Harding, I. Bowater, P. Halley, G.B. Christie, An automated multi-unit composting facility for biodegradability evaluations, *J. Chem. Technol. Biotechnol.* 76 (2001) 411–417. doi:10.1002/jctb.388.
- [20] P. Dřimal, J. Hoffmann, M. Druřbık, Evaluating the aerobic biodegradability of plastics in soil environments through GC and IR analysis of gaseous phase, *Polym. Test.* 26 (2007) 729–741. doi:10.1016/j.polymertesting.2007.03.008.
- [21] ASTM Standard D5338-15, Standard Test Method for Determining Aerobic Biodegradation of Plastic Materials Under Controlled Composting Conditions, Incorporating Thermophilic Temperatures, ASTM B. Stand. (2015).
- [22] ISO 14855-1:2012, Determination of the ultimate aerobic biodegradability of plastic materials under controlled composting conditions — Method by analysis of

- evolved carbon dioxide — Part 1: General method, (2012) 20.
- [23] E. Rudnik, *Compostable polymer materials*, First Edit, Elsevier Ltd, Kidlington, Oxford, 2008.
- [24] M. Funabashi, F. Ninomiya, M. Kunioka, Biodegradability evaluation of polymers by ISO 14855-2, *Int. J. Mol. Sci.* 10 (2009) 3635–3654. doi:10.3390/ijms10083635.
- [25] M.P. Arrieta, J. Lopez, E. Rayon, A. Jimenez, Disintegrability under composting conditions of plasticized PLA-PHB blends, *Polym. Degrad. Stab.* 108 (2014) 307–318. doi:10.1016/j.polymdegradstab.2014.01.034.
- [26] E.F. Gómez, F.C. Michel Jr., Biodegradability of conventional and bio-based plastics and natural fiber composites during composting, anaerobic digestion and long-term soil incubation, *Polym. Degrad. Stab.* 98 (2013) 2583–2591. doi:10.1016/j.polymdegradstab.2013.09.018.
- [27] O. Cadar, M. Paul, C. Roman, M. Miclean, C. Majdik, Biodegradation behaviour of poly(lactic acid) and (lactic acid-ethylene glycol-malonic or succinic acid) copolymers under controlled composting conditions in a laboratory test system, *Polym. Degrad. Stab.* 97 (2012) 354–357. doi:10.1016/j.polymdegradstab.2011.12.006.
- [28] T. Kijchavengkul, R. Auras, M. Rubino, S. Selke, M. Ngouajio, R.T. Fernandez, Biodegradation and hydrolysis rate of aliphatic aromatic polyester, *Polym. Degrad. Stab.* 95 (2010) 2641–2647. doi:10.1016/j.polymdegradstab.2010.07.018.
- [29] E. Petinakis, X. Liu, L. Yu, C. Way, P. Sangwan, K. Dean, S. Bateman, G. Edward, Biodegradation and thermal decomposition of poly(lactic acid)-based materials reinforced by hydrophilic fillers, *Polym. Degrad. Stab.* 95 (2010) 1704–1707. doi:10.1016/j.polymdegradstab.2010.05.027.
- [30] R. Pradhan, M. Reddy, W. Diebel, L. Erickson, M. Misra, A. Mohanty, Comparative compostability and biodegradation studies of various components of green composites and their blends in simulated aerobic composting bioreactor, *Int. J. Plast. Technol.* 14 (2010). doi:10.1007/s12588-010-0009-z.
- [31] J.H. Song, R.J. Murphy, R. Narayan, G.B.H. Davies, Biodegradable and compostable alternatives to conventional plastics., *Philos. Trans. R. Soc. Lond. B. Biol. Sci.* 364 (2009) 2127–2139. doi:10.1098/rstb.2008.0289.
- [32] R. Mohee, G.D. Unmar, A. Mudhoo, P. Khadoo, Biodegradability of biodegradable/degradable plastic materials under aerobic and anaerobic conditions, *Waste Manag.* 28 (2008) 1624–1629. doi:10.1016/j.wasman.2007.07.003.

- [33] Y. Rudeekit, J. Numnoi, M. Tajan, P. Chaiwutthinan, T. Leejarkpai, Determining Biodegradability of Polylactic Acid under Different Environments, *J. Met. Mater. Miner.* 18 (2008) 83–87.
- [34] G. Kale, R. Auras, S.P. Singh, R. Narayan, Biodegradability of polylactide bottles in real and simulated composting conditions, *Polym. Test.* 26 (2007) 1049–1061. doi:10.1016/j.polymertesting.2007.07.006.
- [35] G. Kale, R. Auras, S.P. Singh, Comparison of the degradability of poly(lactide) packages in composting and ambient exposure conditions, *Packag. Technol. Sci.* 20 (2007) 49–70. doi:10.1002/pts.742.
- [36] Calrecycle, Performance Evaluation of Environmentally Degradable Plastic Packaging and Disposable Food Service Ware- Final Report, (2007) 75. <http://www.calrecycle.ca.gov/Publications/Documents/Plastics/43208001.pdf>.
- [37] G. Kale, R. Auras, S.P. Singh, Degradation of commercial biodegradable packages under real composting and ambient exposure conditions, *J. Polym. Environ.* 14 (2006) 317–334. doi:10.1007/s10924-006-0015-6.
- [38] R. Gattin, A. Copinet, C. Bertrand, Y. Couturier, Biodegradation study of a starch and poly(lactic acid) co-extruded material in liquid, composting and inert mineral media, *Int. Biodeterior. Biodegrad.* 50 (2002) 25–31. doi:10.1016/S0964-8305(02)00039-2.
- [39] U. Pagga, D.B. Beimborn, J. Boelens, B. De Wilde, Determination of the aerobic biodegradability of polymeric material in a laboratory controlled composting test, *Chemosphere.* 31 (1995) 4475–4487. doi:10.1016/0045-6535(95)00326-4.
- [40] E. Castro-Aguirre, Design and construction of a medium-scale automated direct measurement respirometric system to assess aerobic biodegradation of polymers, 2013.
- [41] D.W. Nelson, L.E. Sommers, Total carbon, organic carbon, and organic matter, in: D.L. Sparks (Ed.), *Methods Soil Anal., SSSA and ASA*, Madison, WI, 1996: pp. 961–1010.
- [42] J.M. Bremner, Nitrogen-Total, in: D.L. Sparks (Ed.), *Methods Soil Anal., SSSA and ASA*, Madison, WI, 1996: pp. 1085–1121.
- [43] D.W. Nelson, Determination of ammonium in KCl extracts of soils by the salicylate method, *Commun. Soil Sci. Plant Anal.* 14 (1983) 1051–1062.
- [44] S.A. Huffman, K.A. Barbarick, Soil nitrate analysis by cadmium reduction, *Commun. Soil Sci. Plant Anal.* 12 (1981) 79–89.
- [45] A. Esmaeili, A.A. Pourbabaee, H.A. Alikhani, F. Shabani, E. Esmaeili, Biodegradation of Low-Density Polyethylene (LDPE) by Mixed Culture of

- Lysinibacillus xylanilyticus and Aspergillus niger in Soil, PLoS One. 8 (2013) 1–10. doi:10.1371/journal.pone.0071720.
- [46] G. Bellia, M. Tosin, F. Degli-Innocenti, Test method of composting in vermiculite is unaffected by the priming effect, Polym. Degrad. Stab. 69 (2000) 113–120. doi:10.1016/S0141-3910(00)00048-3.
- [47] A. Gopferich, Mechanisms of Polymer Degradation and Elimination, in: Handb. Biodegrad. Polym., 1998: p. 451.
- [48] A. Hoshino, M. Tsuji, M. Momochi, A. Mizutani, H. Sawada, S. Kohnami, H. Nakagomi, M. Ito, H. Saida, M. Ohnishi, M. Hirata, M. Kunioka, M. Funabash, S. Uematsu, Study of the determination of the ultimate aerobic biodegradability of plastic materials under controlled composting conditions, J. Polym. Environ. 15 (2007) 275–280. doi:10.1007/s10924-007-0078-z.
- [49] V. Mezzanotte, R. Bertani, F.D. Innocenti, M. Tosin, Influence of inocula on the results of biodegradation tests, Polym. Degrad. Stab. 87 (2005) 51–56. doi:10.1016/j.polymdegradstab.2004.06.009.
- [50] C.L. Lauber, M. Hamady, R. Knight, N. Fierer, Pyrosequencing-based assessment of soil pH as a predictor of soil bacterial community structure at the continental scale, Appl. Environ. Microbiol. 75 (2009) 5111–5120. doi:10.1128/AEM.00335-09.
- [51] P.J. Stoffella, B.A. Kahn, Compost utilization in horticultural cropping systems, CRC Press LLC, Boca Raton, Florida, 2001.
- [52] M. Kumar, A. Kumar, J. Khan, P. Singh, J.W.C. Wong, A. Selvam, Evaluation of thermophilic fungal consortium for organic municipal solid waste composting, Bioresour. Technol. 168 (2014) 214–221. doi:10.1016/j.biortech.2014.01.048.
- [53] C. Song, M. Li, X. Jia, Z. Wei, Y. Zhao, B. Xi, C. Zhu, D. Liu, Comparison of bacterial community structure and dynamics during the thermophilic composting of different types of solid wastes: anaerobic digestion residue, pig manure and chicken manure, Microb. Biotechnol. 7 (2014) 424–433. doi:10.1111/1751-7915.12131.
- [54] D. Liu, M. Li, B. Xi, Z. Wei, C. Song, C. Zhu, Metaproteomics reveals major microbial players and their biodegradation functions in a large-scale aerobic composting plant, Microb. Biotechnol. 8 (2015) 950–960. doi:10.1111/1751-7915.12290.
- [55] M.N. Kim, W.G. Kim, H.Y. Weon, S.H. Lee, Poly (L-lactide)-Degrading Activity of a Newly Isolated Bacterium, J. Appl. Polym. Sci. 109 (2008) 234–239. doi:10.1002/app.26658.
- [56] M.N. Kim, S.T. Park, Degradation of Poly (L -lactide) by a Mesophilic Bacterium,

- J. Appl. Polym. Sci. 117 (2010) 67–74. doi:10.1002/app.31950.
- [57] M. Karamanlioglu, A. Houlden, G.D. Robson, Isolation and characterisation of fungal communities associated with degradation and growth on the surface of poly (lactic) acid (PLA) in soil and compost, *Int. Biodeterior. Biodegradation*. 95 (2014) 301–310. doi:10.1016/j.ibiod.2014.09.006.
- [58] T. Apinya, N. Sombatsompop, B. Prapagdee, Selection of a *Pseudonocardia* sp . RM423 that accelerates the biodegradation of poly (lactic) acid in submerged cultures and in soil microcosms, *Int. Biodeterior. Biodegradation*. 99 (2015) 23–30. doi:10.1016/j.ibiod.2015.01.001.
- [59] S. Sukkhum, S. Tokuyama, T. Tamura, V. Kitpreechavanich, A novel poly (L-lactide) degrading actinomycetes isolated from Thai forest soil , phylogenic relationship and the enzyme characterization, *J. Gen. Appl. Microbiol.* 55 (2009) 459–467. doi:10.2323/jgam.55.459.
- [60] N.R. Nair, V.C. Sekhar, K.M. Nampoothiri, Augmentation of a Microbial Consortium for Enhanced Polylactide (PLA) Degradation, *Indian J. Microbiol.* 56 (2016) 59–63. doi:10.1007/s12088-015-0559-z.
- [61] K. Tomita, H. Tsuji, T. Nakajima, Y. Kikuchi, Degradation of poly (D-lactic acid) by a thermophile, *Polym. Degrad. Stab.* 81 (2003) 167–171. doi:10.1016/S0141-3910(03)00086-7.
- [62] K. Tomita, T. Nakajima, Y. Kikuchi, N. Miwa, Degradation of poly (L -lactic acid) by a newly isolated thermophile, *Polym. Degrad. Stab.* 84 (2004) 433–438. doi:10.1016/j.polymdegradstab.2003.12.006.
- [63] E. Castro-Aguirre, R. Auras, M. Rubino, S.E. Selke, T. Marsh, Effect of Montmorillonite and Organo-modifier on the Aerobic Biodegradation of Poly(lactic acid) Bio-nanocomposites in composting conditions, in: 31st Polym. Degrad. Discuss. Gr. Conf., 2015.
- [64] S. Boonchan, M.L. Britz, G.A. Stanley, Degradation and Mineralization of High-Molecular-Weight Polycyclic Aromatic Hydrocarbons by Defined Fungal-Bacterial Cocultures, *Appl. Environ. Microbiol.* 66 (2000) 1007–1019. doi:10.1128/AEM.66.3.1007-1019.2000.
- [65] Z. Saadi, A. Rasmont, G. Cesar, Fungal Degradation of Poly (L-lactide) in Soil and in Compost, *J. Polym. Environ.* 20 (2012) 273–282. doi:10.1007/s10924-011-0399-9.
- [66] T. Teeraphatpornchai, M. Nakayama, Isolation and characterization of a bacterium that degrades various polyester-based biodegradable plastics, *Biotechnol. Lett.* 25 (2003) 23–28. doi:10.1023/A:1021713711160.
- [67] N. Hayase, H. Yano, E.M.I. Kudoh, C. Tsutsumi, K. Ushio, Y. Miyahara, S.

- Tanaka, Isolation and Characterization of Poly (Butylene Succinate-co-Butylene Adipate) -Degrading Microorganism, *J. Biosci. Bioeng.* 97 (2004) 131–133. doi:10.1016/S1389-1723(04)70180-2.
- [68] K. Tomita, N. Hayashi, N. Ikeda, Y. Kikuchi, Isolation of a thermophilic bacterium degrading some nylons, *Polym. Degrad. Stab.* 81 (2003) 511–514. doi:10.1016/S0141-3910(03)00151-4.
- [69] K. Tomita, K. Kojoh, A. Suzuki, Isolation of Thermophiles Assimilating Poly (Ethylene-co-Vinyl Alcohol), *J. Ferment. Bioeng.* 84 (1997) 400–402. doi:10.1016/S0922-338X(97)81998-8.
- [70] M.N. Kim, M.G. Yoon, Isolation of strains degrading poly (Vinyl alcohol) at high temperatures and their biodegradation ability, *Polym. Degrad. Stab.* 95 (2010) 89–93. doi:10.1016/j.polymdegradstab.2009.09.014.
- [71] F. Muroi, Y. Tachibana, Y. Kobayashi, T. Sakurai, K. Kasuya, Influences of poly(butylene adipate- co -terephthalate) on soil microbiota and plant growth, *Polym. Degrad. Stab.* 129 (2016) 338–346. doi:10.1016/j.polymdegradstab.2016.05.018.
- [72] P. Sangwan, D.Y. Wu, New Insights into Polylactide Biodegradation from Molecular Ecological Techniques, *Macromol. Biosci.* 8 (2008) 304–315. doi:10.1002/mabi.200700317.
- [73] W. Guo, J. Tao, C. Yang, Q. Zhao, C. Song, S. Wang, The rapid evaluation of material biodegradability using an improved ISO 14852 method with a microbial community, *Polym. Test.* 29 (2010) 832–839. doi:10.1016/j.polymertesting.2010.07.004.
- [74] T.L. Marsh, Terminal restriction fragment length polymorphism emerging method for characterizing diversity among homologous populations of amplification products, *Curr. Opin. Microbiol.* 2 (1999) 323–327. doi:10.1016/S1369-5274(99)80056-3.
- [75] T.L. Marsh, Culture-Independent Microbial Community Analysis with Terminal Restriction Fragment Length Polymorphism, *Methods Enzymol.* 397 (2005) 308–329. doi:10.1016/S0076-6879(05)97018-3.
- [76] S. Grima, V. Bellon-Maurel, P. Feuilloley, F. Silvestre, Aerobic biodegradation of polymers in solid-state conditions: A review of environmental and physicochemical parameter settings in laboratory simulations, *J. Polym. Environ.* 8 (2000) 183–196. doi:10.1023/A:1015297727244.
- [77] C. Sundberg, H. Jönsson, Higher pH and faster decomposition in biowaste composting by increased aeration, *Waste Manag.* 28 (2008) 518–526. doi:10.1016/j.wasman.2007.01.011.

- [78] H.F. Birch, Mineralization of plant nitrogen following alternate wet and dry conditions, *Plant Soil*. 20 (1964) 43–49. doi:10.1007/BF01378096.
- [79] P. Jarvis, A. Rey, C. Petsikos, L. Wingate, M. Rayment, J. Pereira, J. Banza, J. David, F. Miglietta, M. Borghetti, G. Manca, R. Valentini, Drying and wetting of Mediterranean soils stimulates decomposition and carbon dioxide emission: the “Birch effect,” *Tree Physiol*. 27 (2007) 929–940. doi:10.1093/treephys/27.7.929.
- [80] L. Berthe, C. Druilhe, C. Massiani, A. Tremier, A. de Guardia, Coupling a respirometer and a pycnometer, to study the biodegradability of solid organic wastes during composting, *Biosyst. Eng.* 97 (2007) 75–88. doi:10.1016/j.biosystemseng.2007.01.013.
- [81] J. Gu, S. Yang, R. Welton, D. Eberiel, S.P. Mccarthy, R.A. Gross, Effect of Environmental Parameters on the Degradability of Polymer Films in Laboratory-Scale Composting Reactors, *J. Environ. Polym. Degrad.* 2 (1994) 129–135. doi:10.1007/BF02074781.
- [82] M. Day, M. Krzymien, K. Shaw, L. Zaremba, W.R. Wilson, C. Botden, M. Krzymien, K. Shaw, L. Zaremba, W.R. Wilson, C. Botden, An Investigation of the Chemical and Physical Changes Occurring During Commercial Composting An Investigation of the Chemical and Physical Changes, *Compost Sci. Util.* 6 (1998) 44–66. doi:10.1080/1065657X.1998.10701920.
- [83] M. Tosin, F. Degli-Innocenti, C. Bastioli, Effect of the Composting Substrate on Biodegradation of Solid Materials Under Controlled Composting Conditions, *J. Environ. Polym. Degrad.* 4 (1996) 55–63. doi:10.1007/BF02083883.
- [84] W.F. Brinton, Compost quality standards and guidelines, 2000. <http://compost.css.cornell.edu/Brinton.pdf>.
- [85] B. Ge, D. McCartney, J. Zeb, Compost environmental protection standards in Canada, *J. Environ. Eng. Sci.* 5 (2006) 221–234. doi:10.1139/S05-036.
- [86] O.M. of the Environment, Ontario Compost Quality Standards, 2012. <https://www.ontario.ca/page/ontario-compost-quality-standards>.
- [87] C.C.Q. Council, Compost Maturity Index, 2001. <http://www.calrecycle.ca.gov/organics/products/quality/comp maturity.pdf>.
- [88] Woods End Research Laboratory Incorporated, Interpreting Waste and Compost Tests, 2005. <http://www.woods end.org/pdf-files/compost.pdf>.
- [89] M.P. Bernal, C. Paredes, M.A. Sanchez-Monedero, J. Cegarra, Maturity and stability parameters of compost prepared with a wide range of organic wastes, *Bioresour. Technol.* 63 (1998) 91–99. doi:10.1016/S0960-8524(97)00084-9.
- [90] G.F. Huang, J.W.C. Wong, Q.T. Wu, B.B. Nagar, Effect of C/N on composting of

- pig manure with sawdust, *Waste Manag.* 24 (2004) 805–813. doi:10.1016/j.wasman.2004.03.011.
- [91] International Standard ISO 14238:2012, Soil quality -- Biological methods -- Determination of nitrogen mineralization and nitrification in soils and the influence of chemicals on these processes, (2012) 12.
- [92] G.B. Ardisson, M. Tosin, M. Barbale, F. Degli-innocenti, Biodegradation of plastics in soil and effects on nitrification activity . A laboratory approach, *Front. Microbiol.* 5 (2014) 1–7. doi:10.3389/fmicb.2014.00710.
- [93] G. Bellia, M. Tosin, G. Floridi, F. Degli-Innocenti, Activated vermiculite, a solid bed for testing biodegradability under composting conditions, *Polym. Degrad. Stab.* 66 (1999) 65–79. doi:10.1016/S0141-3910(99)00053-1.
- [94] A. Longieras, J.-B. Tanchette, D. Erre, C. Braud, A. Copinet, Compostability of Poly(lactide): Degradation in an Inert Solid Medium, *J. Polym. Environ.* 15 (2007) 200–206. doi:10.1007/s10924-007-0061-8.
- [95] T. Leejarkpai, U. Suwanmanee, Y. Rudeekit, T. Mungcharoen, Biodegradable kinetics of plastics under controlled composting conditions, *Waste Manag.* 31 (2011) 1153–1161. doi:10.1016/j.wasman.2010.12.011.
- [96] E.S. Stevens, What makes green plastics green?, *Biocycle.* 44 (2003) 24–27.
- [97] M. Funabashi, F. Ninomiya, M. Kunioka, Biodegradation of polycaprolactone powders proposed as reference test materials for international standard of biodegradation evaluation method, *J. Polym. Environ.* 15 (2007) 7–17. doi:10.1007/s10924-006-0041-4.
- [98] M. Kunioka, F. Ninomiya, M. Funabashi, Biodegradation of poly(lactic acid) powders proposed as the reference test materials for the international standard of biodegradation evaluation methods, *Polym. Degrad. Stab.* 91 (2006) 1919–1928. doi:10.1016/j.polymdegradstab.2006.03.003.
- [99] G. Gorrasi, R. Pantani, Effect of PLA grades and morphologies on hydrolytic degradation at composting temperature: Assessment of structural modification and kinetic parameters, *Polym. Degrad. Stab.* 98 (2013) 1006–1014. doi:10.1016/j.polymdegradstab.2013.02.005.
- [100] R. Pantani, A. Sorrentino, Influence of crystallinity on the biodegradation rate of injection-moulded poly(lactic acid) samples in controlled composting conditions, *Polym. Degrad. Stab.* 98 (2013) 1089–1096. doi:10.1016/j.polymdegradstab.2013.01.005.
- [101] H. Tsuji, S. Miyauchi, Enzymatic Hydrolysis of Poly (lactide)s: Effects of Molecular Weight, L -Lactide Content, and Enantiomeric and Diastereoisomeric Polymer Blending, *Biomacromolecules.* 2 (2001) 597–604. doi:10.1021/bm010048k.

- [102] F. Degli-Innocenti, Biodegradation of plastics and ecotoxicity testing: When should it be done, *Front. Microbiol.* 5 (2014) 1–3. doi:10.3389/fmicb.2014.00475.
- [103] J. Lunt, Large-scale production, properties and commercial applications of polylactic acid polymers, *Polym. Degrad. Stab.* 59 (1998) 145–152. doi:10.1016/S0141-3910(97)00148-1.
- [104] P. Stloukal, S. Pekařová, A. Kalendova, H. Mattausch, S. Laske, C. Holzer, L. Chitu, S. Bodner, G. Maier, M. Slouf, M. Koutny, Kinetics and mechanism of the biodegradation of PLA/clay nanocomposites during thermophilic phase of composting process, *Waste Manag.* 42 (2015) 31–40. doi:10.1016/j.wasman.2015.04.006.
- [105] F. Iniguez-Franco, R. Auras, G. Burgess, D. Holmes, X. Fang, M. Rubino, H. Soto-Valdez, Concurrent solvent induced crystallization and hydrolytic degradation of PLA by water-ethanol solutions, *Polymer (Guildf)*. 99 (2016) 315–323. doi:10.1016/j.polymer.2016.07.018.
- [106] M. Agarwal, K.W. Koelling, J.J. Chalmers, Characterization of the degradation of polylactic acid polymer in a solid substrate environment, *Biotechnol. Prog.* 14 (1998) 517–526. doi:10.1021/bp980015p.
- [107] R.Y. Tabasi, A. Ajji, Selective degradation of biodegradable blends in simulated laboratory composting, *Polym. Degrad. Stab.* 120 (2015) 435–442. doi:10.1016/j.polymdegradstab.2015.07.020.
- [108] L. Husarova, S. Pekarova, P. Stloukal, P. Kucharzcyk, V. Verney, S. Commereuc, A. Ramone, M. Koutny, Identification of important abiotic and biotic factors in the biodegradation of poly(l-lactic acid), *Int. J. Biol. Macromol.* 71 (2014) 155–162. doi:10.1016/j.ijbiomac.2014.04.050.
- [109] J.R. Dorgan, J. Janzen, D.M. Knauss, S.B. Hait, B.R. Limoges, M.H. Hutchinson, Fundamental solution and single-chain properties of polylactides, *J. Polym. Sci. Part B Polym. Phys.* 43 (2005) 3100–3111. doi:10.1002/polb.20577.
- [110] T. Simon, MSU Composting Facility, (2015).

CHAPTER 4

IMPACT OF NANOCCLAYS ON THE BIODEGRADATION OF POLY(LACTIC ACID) NANOCOMPOSITES

A version of this chapter is published as:

Castro-Aguirre, E.; Auras, R.; Selke, S.; Rubino, M.; Marsh, T. Impact of Nanoclays on the Biodegradation of Poly(Lactic Acid) Nanocomposites. *Polymers*, 10.2 (2018) 202.

4.0 Abstract

Poly(lactic acid) (PLA), a well-known biodegradable and compostable polymer, was used in this study as a model system to determine if the addition of nanoclays affects its biodegradation in simulated composting conditions and whether the nanoclays impact the microbial population in a compost environment. Three different nanoclays were studied due to their different surface characteristics but similar chemistry: organo-modified montmorillonite (OMMT), Halloysite nanotubes (HNT), and Laponite[®] RD (LRD). Additionally, the organo-modifier of Cloisite[®] 30B, methyl, tallow, bis-2-hydroxyethyl, quaternary ammonium (QAC), was studied. PLA and PLA bio-nanocomposite (BNC) films were produced, characterized, and used for biodegradation evaluation with an in-house built direct measurement respirometer (DMR) following the analysis of evolved CO₂ approach. A biofilm formation assay and scanning electron microscopy were used to evaluate microbial attachment on the surface of PLA and BNCs. The results obtained from four different biodegradation tests with PLA and its BNCs showed a significantly higher mineralization of the films containing nanoclay in comparison to the pristine PLA during the first three to four weeks of testing, mainly attributed to the reduction in the PLA lag time. The effect of the nanoclays on the initial molecular weight during processing played a crucial role in the evolution of CO₂. PLA-LRD5 had the greatest microbial attachment on the surface as confirmed by the biofilm test and the SEM micrographs, while PLA-QAC0.4 had the lowest biofilm formation that may be attributed to the inhibitory effect also found during the biodegradation test when the QAC was tested by itself.

4.1 Introduction

Biodegradable polymers like poly(lactic acid) (PLA), poly(butylene adipate-co-terephthalate) (PBAT), and thermoplastic starch (TPS), have great potential to replace fossil-based polymers, avoid landfill disposal of most non-recyclable polymers, and help reduce environmental impacts. However, these materials have some properties and processing shortcomings that have limited their use in many applications, for example, brittleness, water sensitivity, low heat distortion temperature, medium to high gas permeability, and low melt viscosity [1,2]. Therefore, the creation of bio-nanocomposites (BNCs) in which the reinforcements have at least one dimension in the nanoscale dimension and the matrix is a biodegradable polymer, preferably a bio-based polymer, has garnered attention [1,3,4]. Ideally, BNCs could be recycled or treated together with other organic wastes in composting facilities and produce compost, a valuable soil conditioner and fertilizer [5].

One particularly useful class of nanofillers used to produce BNCs is inorganic layered silicate minerals, or nanoclays, due to their commercial availability, low cost, significant property enhancement and relatively simple processability [3]. Natural nanoclays, such as montmorillonite (MMT) with chemical structure $[\text{Na}_{0.38}\text{K}_{0.01}][\text{Si}_{3.92}\text{Al}_{0.07}\text{O}_8][\text{Al}_{1.45}\text{Mg}_{0.55}\text{O}_2(\text{OH})_2] \cdot 7\text{H}_2\text{O}$, and synthetic nanoclays, such as Laponite[®] RD (LRD) with chemical structure $\text{Na}_{0.7}[(\text{Si}_8\text{Mg}_{5.5}\text{Li}_{0.3}) \text{O}_{20}(\text{OH})_4]_{0.7}$, and halloysite nanotubes (HNT) with chemical structure $\text{Al}_2(\text{OH})_4\text{Si}_2\text{O}_5(2\text{H}_2\text{O})$, offer a unique route for enhancing the mechanical, physical and barrier properties of biodegradable polymers at low levels of loading (<5% wt.), especially when the nanoclay particles are well dispersed in the polymer matrix [2,6]. However, the dispersion of hydrophilic

nanofillers in a polymer matrix is challenging. Organophilization, or organic modification, is a technique that improves clay compatibility with organic polymers by reducing the surface energy between the clay layers. Increasing the clay inter-gallery spacing facilitates the intercalation and exfoliation of the clay in the polymer matrix [2,3]. The exfoliation into individual layers depends on the clay's ability for surface modification in which the interlayer inorganic ions are exchanged with organic cations [4,7].

The most broadly studied organo-modifiers are ammonium alkyls. When the clay inorganic ions are exchanged with these organic cations, the inter-gallery spacing increases due to the bulkiness of the alkyl-ammonium ions [7]. For example, organo-modified montmorillonite (OMMT), in which its inorganic ions (*e.g.*, Na⁺, K⁺, Ca²⁺ and Mg²⁺) have been replaced by organic alkyl-ammonium ions improving the wetting with the polymer chains [1,3]. Several researchers have reported improvement in the properties and performance of PLA with addition of OMMT. For example, Ray et al., through a series of papers, demonstrated that the addition of montmorillonite has a significant effect in the improvement of PLA properties (in both solid and melt states), crystalline behavior, and biodegradability in comparison with pristine PLA. Among the different mechanical properties that have been improved are storage modulus, flexural modulus, flexural strength, tensile modulus and elongation at break [8–10]. Additional benefits in performance have been reported such as increased glass transition and thermal degradation temperatures [3,11]. Another reported advantage, other than enhancement of the mechanical and thermal properties, is improvement in the barrier properties due to the enhanced tortuous path provided by the silicate layers to gases like oxygen [9,12,13]. The decreased transparency is a minor disadvantage of these

BNCs [3]. Other researchers have found significant improvement in thermo-mechanical and barrier properties of BNCs based on PLA and OMMT [14,15].

Halloysite is another type of nanoclay that has received great attention as filler for polymer/clay nanocomposites due to its biocompatibility, natural abundance, and relatively low cost. HNT has almost no surface charge and does not require organic modification for adequate dispersion [16,17]. However, functionalized HNT has shown improved dispersion during processing and enhanced mechanical and thermal properties [18,19]. HNT has been used as filler for several polymers like poly(propylene) (PP), vinyl ester, polyamide (PA), poly(vinyl chloride) (PVC), epoxy, and natural rubber for enhancing properties such as mechanical, thermal, crystallinity, and fire resistance [18,19]. Researchers have found that PLA-HNT nanocomposites exhibited improvement in properties like tensile strength, Young modulus, impact properties, flexural properties, and storage modulus, but no significant modification in the thermal properties in comparison with pure PLA [16,20–22]. The addition of HNT promotes crystallization and formation of different crystalline phases [21,22]. HNT was also found to slightly increase water absorption [23]. However, other researchers found increased thermal and flame retardant properties besides improvement in mechanical properties [19]. Esmā et al. also found enhanced thermal properties but in their case mechanical properties were not significantly improved [24]. Similarly, Kim et al. found decreased tensile strength with clay loading higher than 5% wt. but enhanced rheological properties [17].

Laponite® (LRD), another clay that might lead to novel properties, has not been widely investigated for the development of PLA-based nanocomposites. LRD is an entirely synthetic hectorite clay that belongs to the group of smectite phyllosilicate

minerals, and it has great capacity for swelling and exfoliation [25,26]. The advantage of using synthetic clays like LRD is the high structural regularity, single layer dispersions of nanoparticles, and low level of impurities (*e.g.*, silica, iron oxides, and carbonates). Due to its gelation properties, LRD has been used for different pharmaceutical and cosmetic applications; for example, toothpastes, creams, and glazes [27–30]. Zhou et al. studied PLA-LRD composite films and found improvement in the thermal stability, tensile strength and hydrophilicity of PLA, especially when the LRD content is below 0.2% wt. [31,32]. Similarly, Tang et al. studied nanocomposites based on starch, poly vinyl alcohol (PVOH), and LRD and found that an increase in LRD content (0–20%) enhanced tensile strength and decreased water vapor permeability [26].

Besides performance limitations, one of the drawbacks of some biodegradable polymers, like PLA, is that they do not biodegrade as fast as other organic wastes during composting, which in turn affects their general acceptance in industrial composting facilities [33]. Therefore, increasing their biodegradation rate in the composting environment should facilitate and encourage their disposal through these facilities by degrading in a time frame comparable with other organic materials.

Several researchers studied the effect of OMMT on the biodegradation of biodegradable polymers like polycaprolactone (PCL) [34], poly(3-hydroxybutyrate-co-3-hydroxyvalerate) (PHBV) [35], TPS [36], and PLA [10,33,37–45]. Their results indicated that, in general, these BNCs biodegraded faster than their respective pristine polymer. Therefore, the incorporation of nanoclays into a biodegradable polymer matrix represents a promising approach not only for enhancing the polymer performance but also for increasing its biodegradation rate in composting conditions. However, the effect

of different nanoclays and organo-modifiers on the abiotic and biotic degradation of PLA is still unclear and needs further investigation. Even though it is well known that the biodegradation mechanism of PLA involves chemical hydrolysis, the role of microorganisms and how they are affected by the presence of nanoparticles is still not well understood [44].

Thus, this study aimed to understand the biodegradation mechanisms of BNCs made of PLA and compounded with OMMT, HNT, and LRD, and to identify the main factors contributing to their biodegradation rate such as those related to the polymer structure and also those related to the soil/compost environments or to the microbial populations that could be impacted by the presence of nanoparticles.

4.2 Materials and Methods

4.2.1 Materials

Poly(lactic acid) resin (Ingeo™ 2003D) was obtained from NatureWorks LLC. (Minnetonka, MN) with 3.8-4.2% D-LA, number average molecular weight (M_n) of 121.1 ± 7.5 kDa, polydispersity index (PDI) of 1.9 ± 0.1 , and melt flow index (MFI) of 6 g/10 min (210°C, 2.16 kg). Cellulose powder (particle size ~ 20 μm) and Halloysite nanotubes (HNT) were purchased from Sigma-Aldrich (St. Louis, MO). Organo-modified montmorillonite (OMMT) (Cloisite® 30B) and Laponite® RD (LRD) were acquired from BYK Additives Inc. (Gonzales, TX). Additionally, Tomamine™ Q-T-2 (QAC) with 60 - 70% purity of a methyl, tallow, bis-2-hydroxyethyl, quaternary ammonium, the organo-modifier of Cloisite® 30B, was obtained from Air Products and Chemicals Inc. (Butler, IN). Tetrahydrofuran (THF) was obtained from Pharmco-AAPER (North East, CA). The composition per liter of the R2 broth (R2B) used was 0.5 g yeast extract, 0.5 g proteose

peptone #3, 0.5 g casamino acids, 0.5 g dextrose, 0.5 g soluble starch, 0.3 g sodium pyruvate, 0.3 g dipotassium phosphate, and 0.05 g magnesium sulfate. The composition per liter of the M9 minimal medium was 12.8 g $\text{Na}_2\text{HPO}_4 \cdot 7\text{H}_2\text{O}$, 3 g KH_2PO_4 , 0.5 g NaCl, 1 g NH_4Cl , and 1 g of 1 mM MgSO_4 , 1 mM CaCl_2 , 3×10^{-9} M $(\text{NH}_4)_6\text{Mo}_7\text{O}_{24} \cdot 4\text{H}_2\text{O}$, 4×10^{-7} M H_3BO_3 , 3×10^{-8} M $\text{CoCl}_2 \cdot 6\text{H}_2\text{O}$, 1×10^{-8} M $\text{CuSO}_4 \cdot 5\text{H}_2\text{O}$, 8×10^{-8} M $\text{MnCl}_2 \cdot 4\text{H}_2\text{O}$, 1×10^{-8} M $\text{ZnSO}_4 \cdot 7\text{H}_2\text{O}$, 1×10^{-6} M $\text{FeSO}_4 \cdot 7\text{H}_2\text{O}$. All the chemicals and reagents were commercial products of the highest available grade.

4.2.2 Processing of the PLA bio-nanocomposites

PLA-BNCs (PLA-OMMT, PLA-LRD, and PLA-HNT) were produced in a two-step process. First, masterbatches were prepared in a ZSK 30 twin-screw extruder (Werner Pfleiderer, NJ) and pelletized. Second, PLA-BNC films (1 and 5% wt. nanoclay) were produced in a cast film microextruder model RCP-0625 (Randcastle Extrusion Systems, Inc., Cedar Grove, NJ). Two PLA-QAC films (0.4 and 1.5% wt. organo-modifier) were produced in a similar fashion. Three PLA films (PLA1, PLA2, and PLA3) with different molecular weight were obtained by varying the processing conditions, and used as control films. In all cases, the materials were dried at 60°C for 8 h under vacuum (85 kPa) prior to processing. The thickness of the films was measured using a digital micrometer (Testing Machines Inc., New Castle, DE). More details regarding the film processing are provided in **Table 4A.1** of the Appendix 4A.

4.2.3 Characterization of the PLA bio-nanocomposites

To evaluate the presence and dispersion of the nanoclays in the PLA matrix, X-ray diffraction (XRD) and transmission electron microscopy (TEM) were performed. PLA and BNC films were embedded in paraffin blocks and microtomed in 100 nm sections

for bright field imaging using an Ultramicrotome MYX (RMC Boeckeler Instruments, Tucson, AZ). TEM micrographs were obtained using a JEOL 2200FS transmission electron microscope (JEOL USA, Inc., Peabody, MA) operating at an acceleration voltage of 200 kV. XRD analysis was conducted in a Rigaku Rotaflex Ru-200BH X-ray diffractometer equipped with a Ni-filtered Cu K α radiation source setting at 45 kV and 100 mA. The interlayer spacing was calculated according to Bragg's Law [46]. The carbon, hydrogen and nitrogen content, as well as the amount of nanoclay present in each BNC film was determined by elemental analysis (CHN) and are reported in **Table 4B.1** of the Appendix 4B. Additional methodologies, such as differential scanning calorimetry (DSC), thermal gravimetric analysis (TGA), moisture isotherm, electrical conductivity, and contact angle, used for characterization of the BNCs are provided in the Appendix 4B.

4.2.4 Biodegradation evaluation

The aerobic biodegradation of PLA and BNCs was evaluated through a series of experiments (**Table 4.1**) by analysis of evolved CO₂ under controlled composting conditions (at 58°C), using an in-house built direct measurement respirometer (DMR) with a CO₂ non-dispersive infrared gas analyzer (NDIR). Manure compost from the MSU Composting Facility (East Lansing, MI) was used. The compost was sieved on a 10 mm screen and preconditioned at 58°C for 3 days prior to use. Deionized water was incorporated to adjust the moisture content to about 50%. Saturated vermiculite premium grade (Sun Gro Horticulture Distribution Inc., Bellevue, WA) was mixed with the compost (1:4 parts, dry wt. compost) for better aeration. Compost samples were sent to the Soil and Plant Nutrient Laboratory at Michigan State University (East

Lansing, MI, USA) for determination of the physicochemical parameters (dry solids, volatile solids, C/N ratio, and pH) and are reported in **Table 4C.1** of the Appendix 4C. Detailed information about the methods used for compost characterization can be found elsewhere [47].

Table 4.1 Key for biodegradation test and labels of the samples

Test ID	Samples tested
I	Blank, Cellulose, OMMT, HNT, LRD, PLA1, PLA-OMMT5
II	Blank, Cellulose, OMMT, OMMT5, QAC, QAC5, PLA1, PLA-OMMT1, PLA-OMMT5, PLA-OMMT7.5
III	Blank, Cellulose, PLA2, PLA-OMMT1, PLA-OMMT5, PLA-HNT1, PLA-HNT5, PLA-LRD1, PLA-LRD5, PLA-QAC1.5, PLA-QAC0.4
IV	Blank, Cellulose, PLA1, PLA2, PLA3, PLA-OMMT5, PLA-QAC0.4

The bioreactors were loaded with 400 g of compost (or vermiculite) and mixed thoroughly with 8 g of polymer sample (unless otherwise specified). Film samples were cut to 1 cm² pieces and triplicates of each test material were analyzed. Additionally, triplicates of blank bioreactors (with compost or vermiculite only) were evaluated. To simulate composting conditions, the bioreactors were placed in an environmental chamber set at a constant temperature of 58 ± 2°C. Water-saturated CO₂-free air was provided to each bioreactor with a flow rate of 40 ± 2 sccm (cm³/min at standard temperature and pressure). The bioreactors were incubated in the dark for at least 45 d or until the evolved CO₂ reached a plateau. For all the biodegradation studies, the results are presented as average (*n*=3) and standard deviation.

4.2.5 Size Exclusion Chromatography (SEC)

The number average molecular weight (M_n), weight average molecular weight (M_w), and polydispersity index (PDI) of PLA and BNCs before and during composting were determined by SEC with a system from Waters Inc. (Milford, MA) as previously described [47]. Shortly, 20 mg of films were dissolved in 10 cm³ of THF and filtered with a hydrophobic polytetrafluoroethylene (0.45 μ m pore size) filter. Then, 100 μ L of each sample solution were injected. A third-order polynomial calibration curve was obtained from polystyrene (PS) standards ranging 0.5 – 2,480 kDa, and the Mark-Houwink constants, $K= 0.000164$ dL/g and $\alpha= 0.704$, for PS were used.

4.2.6 Microbial attachment

Biofilm Assay: The biofilm forming ability of microorganisms on the surface of PLA and BNCs was assessed with a biofilm assay in 24-well polystyrene plates as described elsewhere [48,49]. For this test, sterilized PLA films and BNC films were added to the wells of a microtiter plate (24 wells). The films were sterilized by rinsing with 70% ethanol, followed by irradiation with ultraviolet light for 5 min prior to testing. Four replicates of each sample were tested. Each well contained 600 μ L of R2B and 200 μ L of compost extract (CE), which was prepared by vigorously mixing dry compost with deionized water (1:2 wt./vol.) on vortex for 2 min. The mix was allowed to settle for 20 minutes and then the supernatant was passed through a sieve with 1 mm mesh. A sterile compost extract (SCE) was prepared for a control by passing the CE twice through a 0.22 μ m filter. The inoculated plates were incubated for 48 hours at 58°C gently shaking at 100 rpm. *Pseudomonas aeruginosa* (PA) strain PAO1, a biofilm producing bacterium, was used as a positive control at 23°C, and uninoculated wells

were considered as a negative control. To determine the level of biofilm formed on the surface of PLA and BNCs after incubation, the films were transferred to clean Eppendorf tubes and treated in parallel with the microtiter plates. The broth was removed from the plates and the wells and films were gently washed with water three times. The biofilm was stained with 800 μ L of 0.5% crystal violet for 15 min followed by washing three times with water. After the plates and films had air-dried, 800 μ L of 30% acetic acid was added, followed by incubation for 15 min. Measurements were done using an Epoch™ Microplate Spectrophotometer (BioTek Instruments, Inc., Winooski, VT) at 600 nm directly on the wells and following decantation of the films. Decanted acetic acid from films was transferred into clean microtiter plates for absorbance measurement at 600 nm. The biofilm formation was quantified by subtracting the average absorbance of the cognate controls from the average absorbance of the inoculated samples.

Scanning Electron Microscopy (SEM): Similar to the biofilm test, sterilized PLA films and PLA-LRD5 films were added to an Erlenmeyer flask containing R2B (2x) and an overnight culture of the compost extract (CE) on R2B at 58°C (3:1 vol.). The samples were incubated for 48 hours at 58°C. The films were removed from the flasks, gently washed with water three times, and air-dried. The samples were mounted on aluminum stubs using high vacuum carbon tabs (SPI Supplies, West Chester, PA), and coated with osmium. SEM micrographs were obtained at various magnifications using a JEOL 6610LV (tungsten hairpin emitter) scanning electron microscope (JEOL Ltd., Tokyo, Japan) operating at a voltage of 10 kV to observe the biofilm formation.

4.2.7 Statistical Analysis

All statistical analyses were performed using Minitab18 software (Minitab Inc., State College, PA) by analysis of variance (one-way ANOVA), and Tukey test with a p-value threshold of 0.05 as for level of significance. Data are reported as mean and standard deviations.

4.3 Results and Discussion

4.3.1 Characterization of the PLA bio-nanocomposites

Figure 4.1 and **Figure 4.2** show the XRD spectra and TEM micrographs of the BNCs, respectively. These methods were used to evaluate the presence and dispersion of the nanoclays in the PLA matrix. Depending on the degree of dispersion, a layered silicate nanocomposite can be either intercalated or exfoliated. Intercalation occurs when the polymer chains penetrate into the interlayer regions of the clay, while exfoliation is observed when the clay layers are delaminated and randomly dispersed in the polymer matrix [3]. As observed in **Figure 4.1a**, in the case of PLA-OMMT5 film, OMMT is not fully exfoliated but intercalated in the PLA matrix, which is represented by the shift of the peak to the left, *i.e.*, the increase in the interlayer distance from 1.85 nm, for the pristine OMMT, to 3.42 nm, for the OMMT present in the film. The organic modification of the MMT through exchange of cationic ions allows for better dispersion and exfoliation of the silicate layers into the PLA matrix [1,3,7]. However, in the case of PLA-OMMT5 it was not enough to obtain a fully exfoliated BNC. This was confirmed by the TEM micrograph (**Figure 4.2a**), which shows some small agglomerations. However, it seems that the OMMT is evenly distributed in the PLA matrix. PLA-OMMT1 showed a better dispersion of the OMMT in the polymer matrix, but in general, full exfoliation is difficult to

achieve, and most nanocomposites are a mixture of both structures, which is usually referred to as disordered morphology or orderly exfoliated morphology [4].

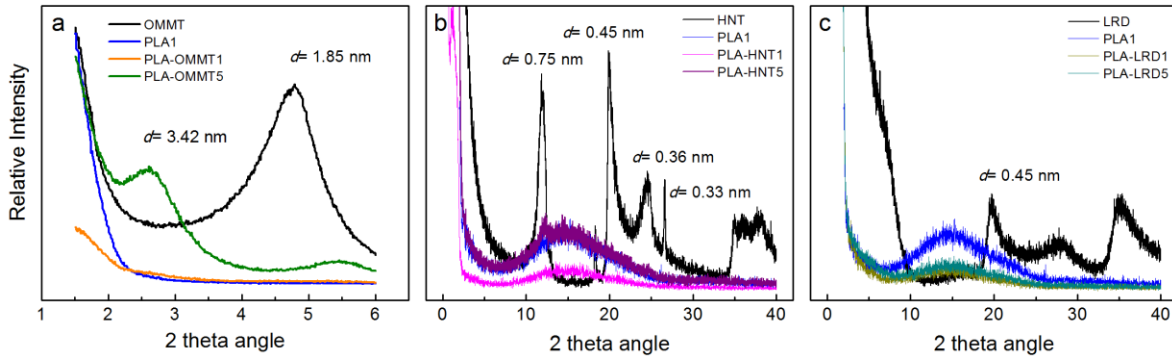


Figure 4.1 XRD spectra of the different nanoclays, PLA1, and (a) OMMT, (b) HNT, and (c) LRD bio-nanocomposite films.

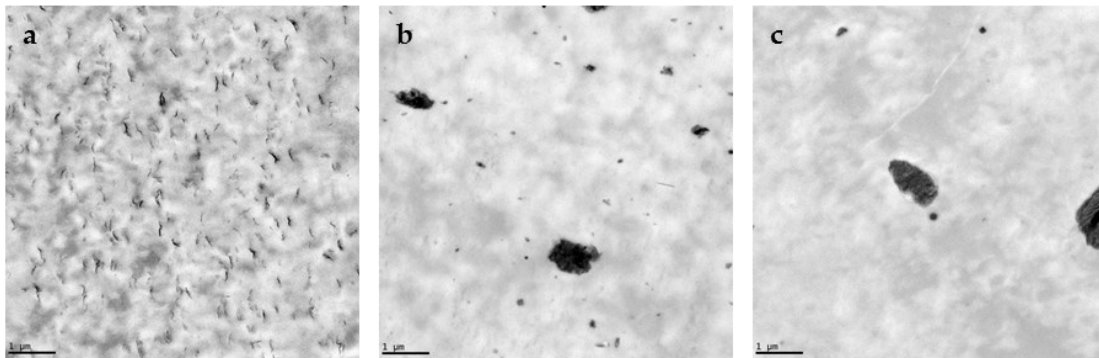


Figure 4.2 TEM micrographs of (a) PLA-OMMT5, (b) PLA-HNT5, and (c) PLA-LRD5 bio-nanocomposites at 10kx. The bar in the left bottom represents 1 μm .

Similarly, **Figure 4.1b** and **Figure 4.1c** show the XRD spectra of HNT and LRD nanocomposites, respectively. In both cases, the profiles showed broad peaks around a 2θ angle of 16 which are representative of amorphous PLA samples [50,51]. HNT is an alumina-silicate clay with an elongated hollow tubular structure consisting of an external surface composed of siloxane (Si-O-Si) groups and an inner side and edges consisting of (Al-OH) groups [16,24,52]. In the XRD spectrum of the HNT nanoclay (**Figure 4.1b**),

the presence of three main peaks at 2θ angles of 12.02, 19.99, and 24.54 can be observed, corresponding to the basal d-spacing of 0.75, 0.45, and 0.36 nm, respectively. Similar diffraction patterns are reported elsewhere [24,53–57]. In the case of PLA-HNT5, the presence of a peak at 2θ angle of 12.25 was observed. The small shift to the right, from the 12.02 of the pristine HNT, indicates a reduction in the d-spacing. This behavior has been observed by other researchers, and was attributed to the formation of a micro-filled composite [24,54]. The disappearance of the other peaks, such in the case of PLA-HNT5 and PLA-HNT1, has been explained as due to the interaction of the polymer chains with the nanotubes, and also due to the preferential orientation of nanotubes during processing of the film [19,24]. It was also observed that the intensity of the characteristic peaks depends on the level of loading of nanoclay [53,54].

LRD particles have a disk-like shape with two external tetrahedral silica sheets that present continuous corner-shared tetrahedral SiO_4 units arranged in hexagonal rings, and a central octahedral magnesia sheet which is composed of bivalent or trivalent cations sharing the edges coordinated to hydroxyl groups. The excess negative charge is compensated by the presence of Na ions between the silicate layers [25,27–29]. In the XRD spectrum of the LRD nanoclay (**Figure 4.1c**), the presence of the characteristic LRD peak at 2θ angle of 19.8 can be observed, corresponding to the basal d-spacing of 0.45 nm. Similar diffraction patterns are reported for LRD elsewhere [25,26]. In the XRD spectra of the PLA-LRD, no diffraction peaks were observed. This behavior has been attributed, in the literature, to separated LRD platelets dispersed

individually in the polymer matrix [25]. The nanoclay dispersion was also confirmed by TEM.

Figure 4.2b and **Figure 4.2c** show the TEM micrographs of HNT and LRD nanocomposites, respectively. In the case of PLA-HNT5, **Figure 4.2b** shows the presence of big agglomerations indicating that HNT was not evenly distributed in the PLA matrix. Similar observations have been reported in the literature for PLA-HNT nanocomposites [20,53]. A similar distribution was also found for the PLA-LRD5 film (**Figure 4.2c**).

Other factors influencing the nanoclay dispersion in the PLA matrix are the level of loading and the size of the nanoparticles [26]. For example, HNT and LRD are bigger particles than MMT. While MMT has layers with 1 nm thickness and tangential dimensions from 300 °A to a few microns [1,3,7], HNT has inner and outer diameters of the tube ranging from 10 to 40 nm and 40 to 70 nm, respectively, while the length ranges from 0.2 to 3 µm [16,24,52]. LRD usually has dimensions around 25-30 nm in diameter and 1 nm in thickness [26,27,29].

4.3.2 Biodegradation evaluation

The DMR system was used to perform four different biodegradation tests in which the CO₂ evolved from each bioreactor was measured with controlled temperature, RH, and air flow rate. For the data analysis, the average cumulative CO₂ and % mineralization of each test material was calculated and plotted as a function of time. Detailed information about the concepts and calculations is provided elsewhere [47,58–60]. The blank bioreactors contain the solid media only (*i.e.*, compost or vermiculite). In all cases, cellulose powder was used as a positive reference material since it is a well-known

easily biodegradable material. The cumulative CO₂ and % mineralization curves obtained from the different biodegradation tests for the evaluation of PLA and PLA-BNCs, as well as the different nanoclays and surfactant, are presented in **Figure 4.3** to **Figure 4.11**.

To evaluate the effect of the nanoclays on the compost microbial population, the three different nanoclays were tested in the powder form as received. **Figure 4.3** shows the CO₂ evolved from the bioreactors containing the three different nanoclays. A significant difference between the CO₂ evolved from cellulose and the one from the nanoclays was observed. During the first 40 days of the test, OMMT and LRD bioreactors produced a significantly higher amount of CO₂ than the blank indicating that there was no inhibition. On the contrary, the HNT bioreactors produced equal or less CO₂ than the blank, especially after 35 days, indicating some kind of inhibition in which HNT may limit the availability and/or the distribution of carbon and other nutrients for basic microorganism functions.

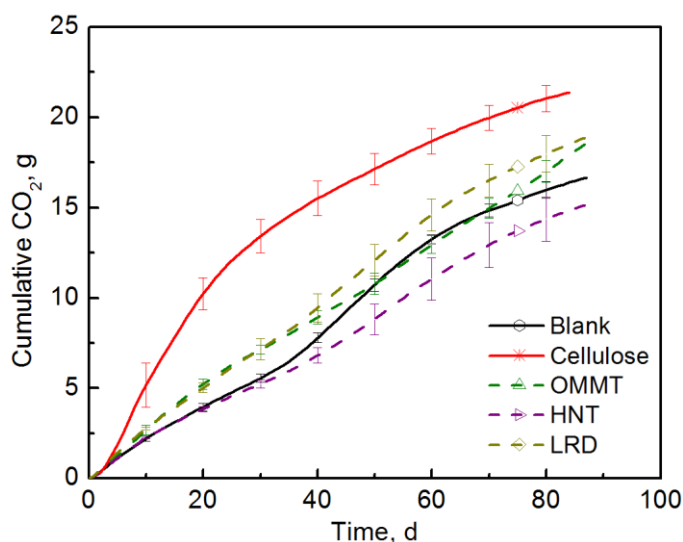


Figure 4.3 CO₂ evolution of the three different nanoclays (Test I in compost).

Figure 4.4 shows the CO₂ and % mineralization of the pristine PLA film and PLA-OMMT5. The typical PLA biodegradation behavior with the presence of a lag time of around 25 days was observed [47,61]. The lag time observed in the biodegradation of PLA has been explained by the low diffusion rate of the byproducts formed during the hydrolytic degradation and present inside the sample [62]. Cellulose reached a maximum mineralization of 65.7% after 34 days while PLA and PLA-OMMT5 reached 53.2 and 59.6% after 87 days, respectively. The decrease in the mineralization curve of cellulose indicates that these bioreactors were no longer producing more CO₂ than the blank bioreactors. This behavior may be explained by a rapid and large increase of the microbial population at the beginning of the test when there are plenty of resources easily available for microbial assimilation. Then, a decrease in the mineralization curve is observed when these resources are depleted and/or limited [47]. Even though by the end of the test, the mineralization of PLA and PLA-OMMT5 was not significantly different, it was clearly observed that the lag phase of the pristine PLA was longer than the PLA-OMMT5. The mineralization of PLA-OMMT5 was significantly higher before day 60. Among the different explanations for this accelerated biodegradation due to OMMT found in the literature is the relatively high hydrophilicity of the nanoclay, which improves the diffusion of water into the PLA polymeric matrix and in turn promotes hydrolytic degradation [33,37,38,44,62]. Another reason is that the presence of terminal hydroxyl groups in the silicate layers and in some organo-modifiers promotes the hydrolytic degradation of PLA [10,44,63]. However, the molecular weight of the PLA-OMMT5 films and the thickness can play a crucial role and influence the observed results [47].

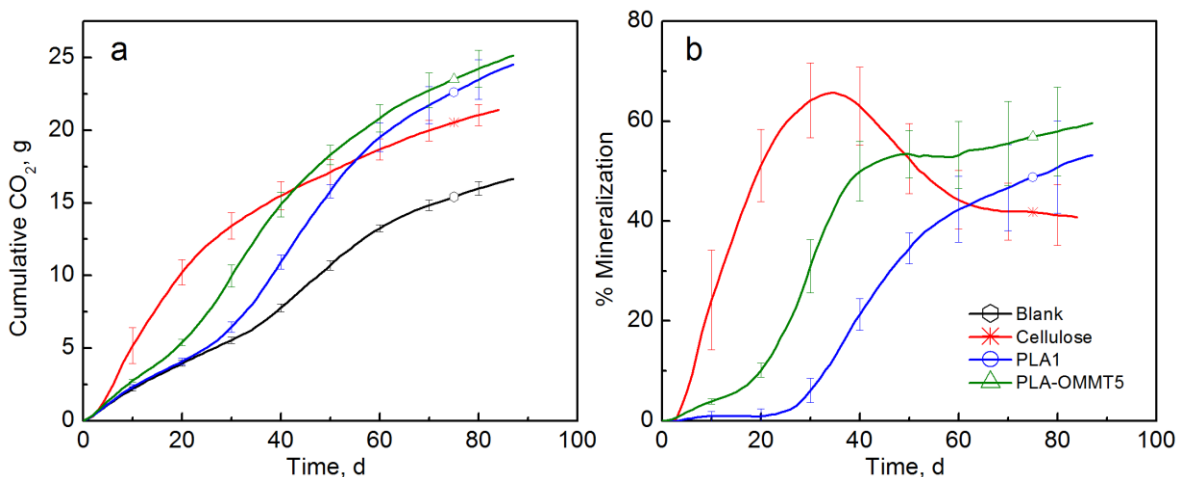


Figure 4.4 (a) CO₂ evolution and (b) % Mineralization of PLA and PLA-OMMT5 films (Test I in compost).

To evaluate the effect of clay loading on the biodegradation of PLA, three films with different loadings of OMMT (1, 5, and 7.5% wt.) were tested. **Figure 4.5** shows the CO₂ evolution and % mineralization of PLA and PLA-OMMT films. Cellulose reached a maximum mineralization of 61.7% after 45 days of testing. The biodegradation behavior of the pristine PLA and PLA-OMMT1 was similar, again with a typical lag time at the beginning of the biodegradation test. The negative mineralization values observed in **Figure 4.5b** are generated as an artifact when the blank bioreactors produce more CO₂ than the sample material bioreactors. This effect might be caused because of the physical barrier offered by the polymer film at this early stage of the test, contrary to the PLA-OMMT5 and PLA-OMMT7.5 in which their biodegradation phase started much earlier. The observed shorter lag time of PLA-OMMT5 is in agreement with the previous test results, but in this case the average mineralization was significantly higher than the PLA control. It seems that PLA-OMMT7.5 has the highest average mineralization and the fastest biodegradation rate in which the lag time was only around 5 days. However,

mineralization values above 100% indicate the presence of a priming effect, in which the additional carbon converted to CO₂, is not coming from the sample material but from the over-degradation of the indigenous organic carbon present in the compost [47,64]. Again, the initial molecular weight of the films should influence the observed results. It is important to mention that during the processing of the films, with different nanoclay loading, the resulting molecular weight was affected even though, in this case, the same processing conditions were maintained, with the higher clay loading corresponding to the lower molecular weight. Furthermore, Roy et al. analyzed the water-soluble degradation products by electrospray ionization-mass spectrometry (ESIMS), and their results indicated a catalytic effect of MMT in hydrolysis of PLA since shorter lactic acid oligomers were formed in the case of PLA/MMT composites [41]. Some researchers have attributed a plasticizing effect to the degradation byproducts (*i.e.*, lactic acid oligomers and monomers), represented by a decrease in the T_g of PLA and BNCs. In this context, faster biodegradation of the PLA and BNC could also be induced by the increased segmental mobility of backbone chains and the expanded amorphous regions of the polymeric matrix [44,62,65]. Another factor influencing the biodegradation rate of the BNCs is the crystallinity of the material. The presence of nanoclays could affect the degree of crystallization of PLA (**Table 4B.2**), with the amorphous parts preferentially biodegrading [47].

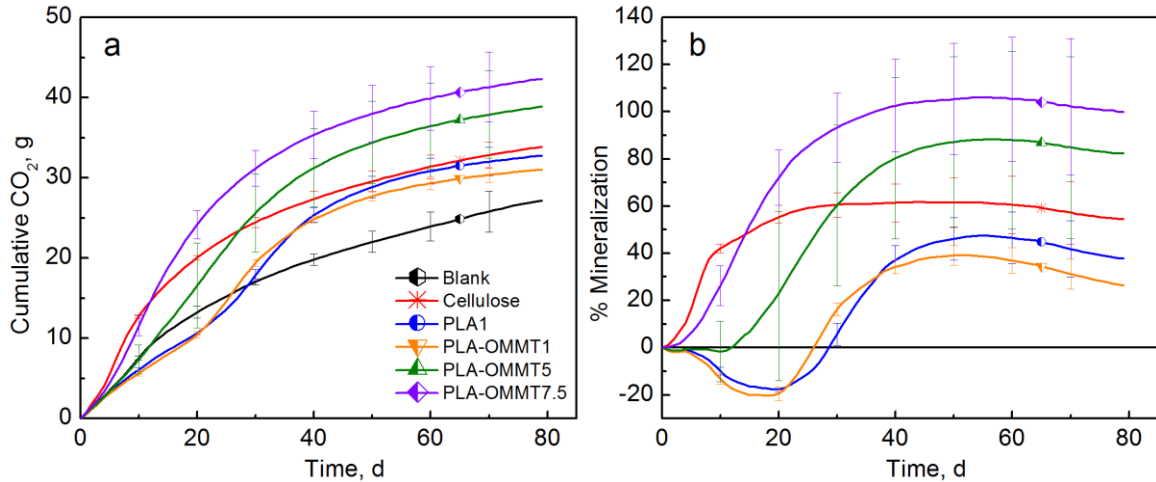


Figure 4.5 (a) CO₂ evolution and (b) % Mineralization of PLA and PLA-OMMT films with three different levels of loading (1, 5, and 7.5%) (Test II in compost).

The effect of the amount/concentration of clay and surfactant on the compost microbial populations was evaluated and the results are shown in **Figure 4.6**. In this case, OMMT refers to 8 g of the tested sample material while OMMT5 refers to the theoretical amount of nanoclay contained in 8 g of PLA-OMMT5 film. Similarly, QAC refers to 8 g of the tested sample material and QAC5 to the theoretical amount of surfactant contained in 8 g of PLA-OMMT5 film. Regardless of the concentration of either OMMT or QAC, the CO₂ evolution was always significantly lower than the blank, indicating that there was clear inhibition of the microbial activity when these materials were present by themselves.

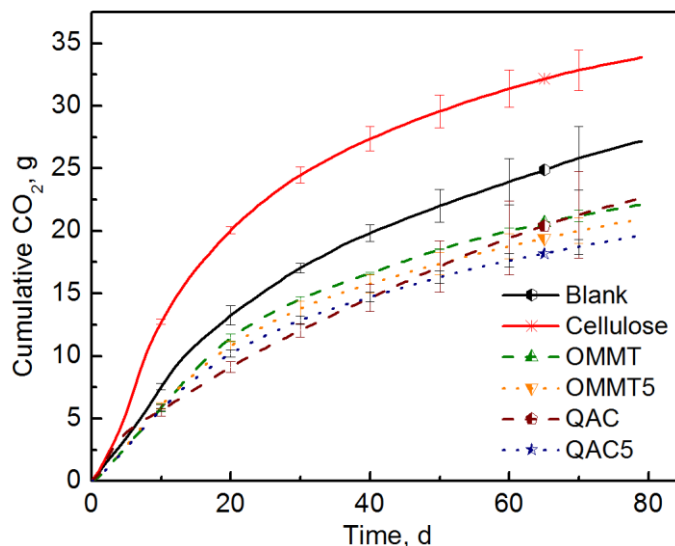


Figure 4.6 CO₂ evolution of OMMT nanoclay and QAC surfactant (Test II in compost).

Figure 4.7 shows the results of a different biodegradation test in which the PLA-OMMT and the PLA-QAC films were evaluated. Cellulose reached a mineralization of 85.5% after 38 days of testing, while the PLA control reached 74.2% after 69 days. As in the previous test, there was no significant difference between the pristine PLA and the PLA-OMMT1 films (**Figure 4.7b**). However, PLA-OMMT5 had significantly higher mineralization and a shorter lag time than the PLA control. A priming effect was observed with mineralization values over 100%. The PLA films containing the surfactant (QAC) also showed reduced lag time and a significantly higher amount of evolved CO₂ than the PLA control, and in both cases a priming effect was observed (**Figure 4.7d**). This may be due to the lower initial molecular weight of these films. In Chapter 3, it was demonstrated that the PLA film with the lowest M_n presented a priming effect when tested in compost, but it was not observed in inoculated vermiculite, having mineralization values closer to the other two tested PLA films with higher M_n [47]. PLA-OMMT5 and PLA-QAC0.4 were also tested in inoculated and uninoculated vermiculite,

and the results are later shown in **Figure 4.11**. Similarly, the priming effect was not observed in this case.

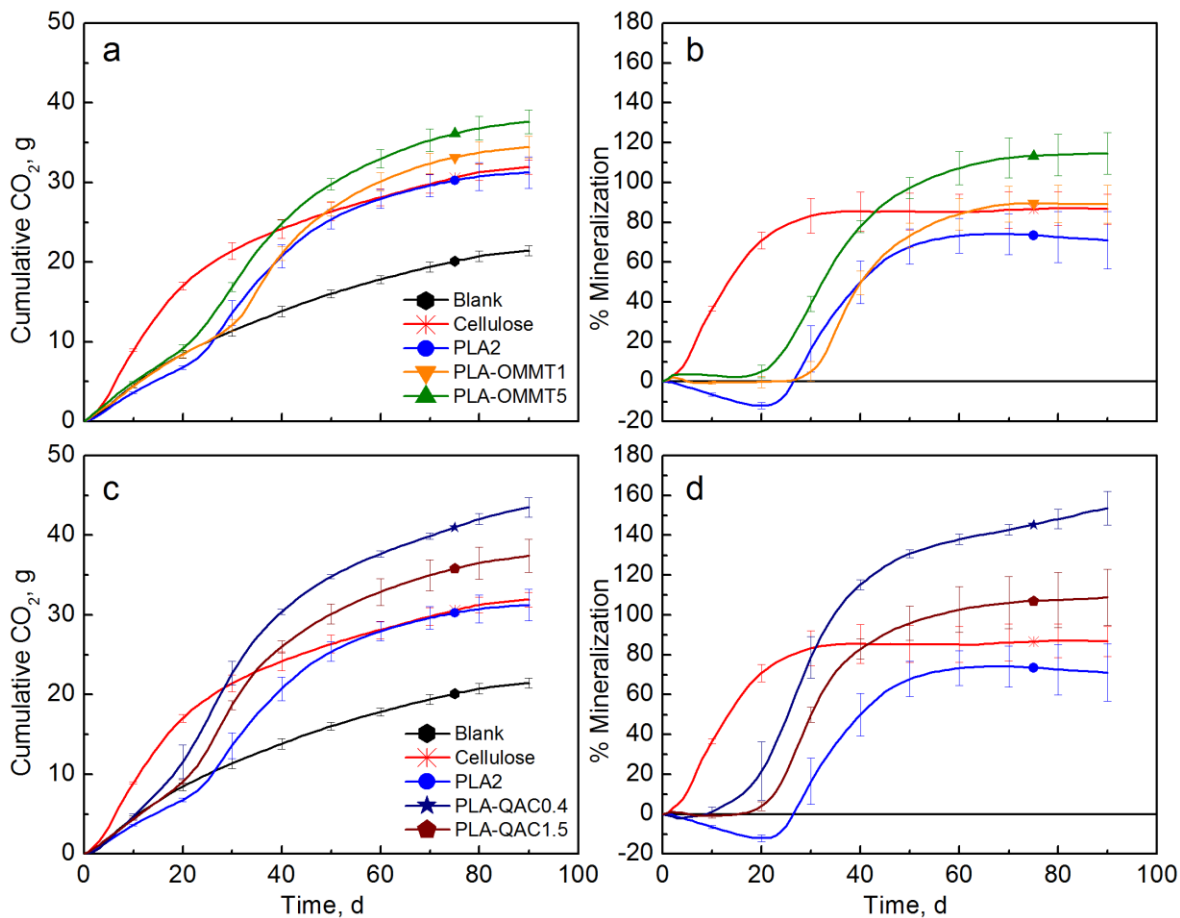


Figure 4.7 CO₂ evolution and % Mineralization of PLA-OMMT films (a & b) and PLA-QAC films (c & d) (Test III in compost).

Figure 8 shows that the mineralization of PLA-HNT films was not significantly different from the PLA control by the end of the test (90 days). However, it can be clearly observed that with both levels of loading the lag time was reduced and the mineralization was significantly different before day 45. A higher variability and also a priming effect were observed in the biodegradation of PLA-HNT1 film. PLA-HNT films

reached their maximum mineralization after 50 days of testing with an average of 86.9 and 74.6% for PLA-HNT1 and PLA-HNT5, respectively.

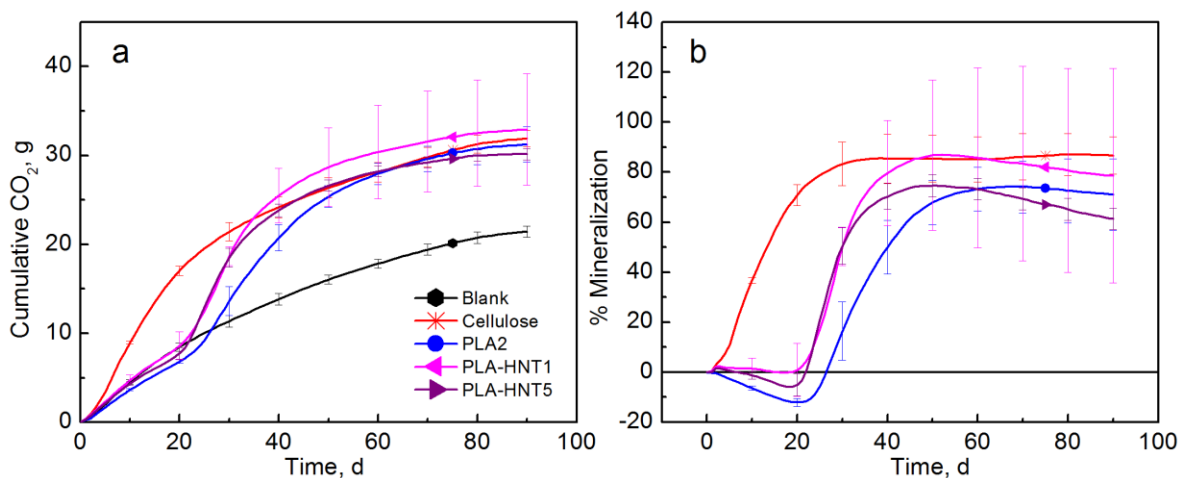


Figure 4.8 (a) CO₂ evolution and (b) % Mineralization of PLA-HNT films (Test III in compost).

As observed in **Figure 4.9**, PLA-LRD5 showed significantly higher mineralization than the pristine PLA and the PLA-LRD1 films. In this case, the lag time was not reduced but the PLA-LRD5 showed a priming effect. PLA-LRD films reached their maximum mineralization by the end of the test with an average of 82.5 and 112.5% for PLA-LRD1 and PLA-LRD5, respectively.

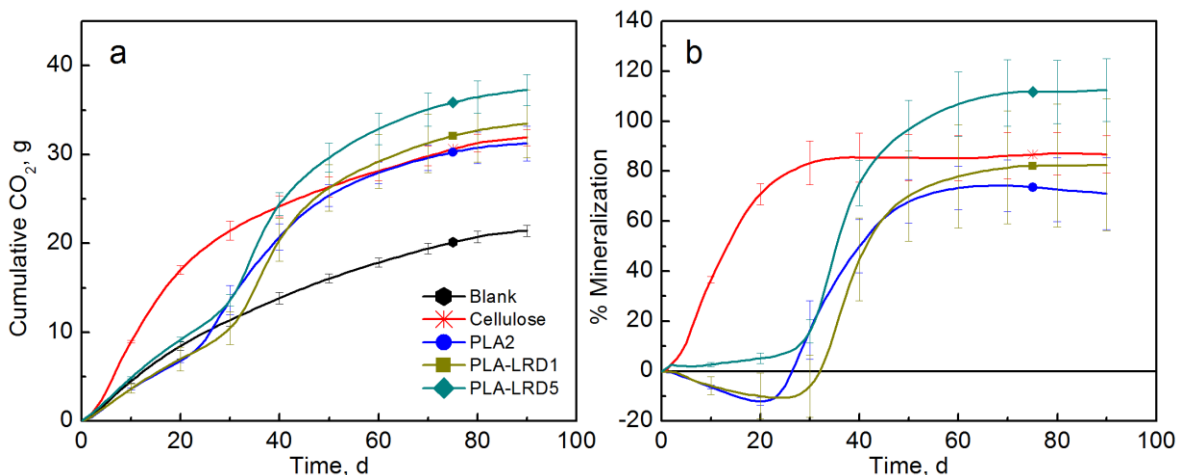


Figure 4.9 (a) CO₂ evolution and (b) % Mineralization of PLA-LRD films (Test III in compost).

To avoid the priming effect observed in the previous tests, a specific new biodegradation test was performed in three different solid environments (compost, inoculated vermiculite, vermiculite) as described elsewhere [47]. When tested in compost (**Figure 4.10**), there was no significant difference in the mineralization of these materials by the end of the test (132 days). However, it seems that the mineralization of PLA-OMMT5 was significantly higher than the PLA during the first 45 days of testing. Similarly to the previous tests, PLA-OMMT5 showed a reduced lag time and a priming effect could be occurring due to the low molecular weight of both films. The maximum average mineralization for PLA and PLA-OMMT5 was 110.4 and 100.2%, respectively.

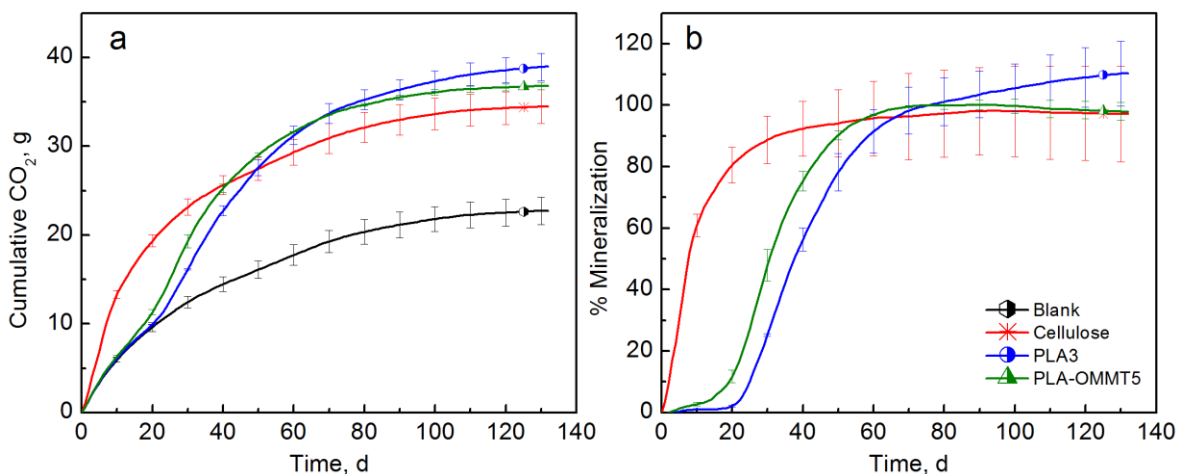


Figure 4.10 (a) CO₂ evolution and (b) % Mineralization of PLA and PLA-OMMT5 films (Test IV in compost).

The biodegradation test with inoculated vermiculite should avoid the priming effect as previously demonstrated [47,64,66]. **Figure 4.11** shows that there was no significant difference in the mineralization of the tested materials at the end of the test (132 days). However, both PLA-OMMT5 and PLA-QAC0.4 showed significantly higher mineralization than the PLA control before 70 days of testing, and a much shorter lag time. The PLA control reached 77.7% mineralization after 132 days while PLA-OMMT5 reached the same mineralization after 83 days of testing and a maximum average mineralization of 83.3%. PLA-QAC reached a mineralization of 77.3%. It is important to mention that longer testing times were expected in this case since the biodegradation in inoculated vermiculite occurs at a slower rate than in compost. Even though the initial molecular weight of the films has a strong effect on their mineralization and priming effect, it seems that the addition of OMMT also accelerated the initial degradation of the samples. As previously mentioned, this behavior may be explained by the improved diffusion of water into PLA due to the high hydrophilicity of the nanoclay, which in turn promotes hydrolytic degradation [33,37,38,44,62].

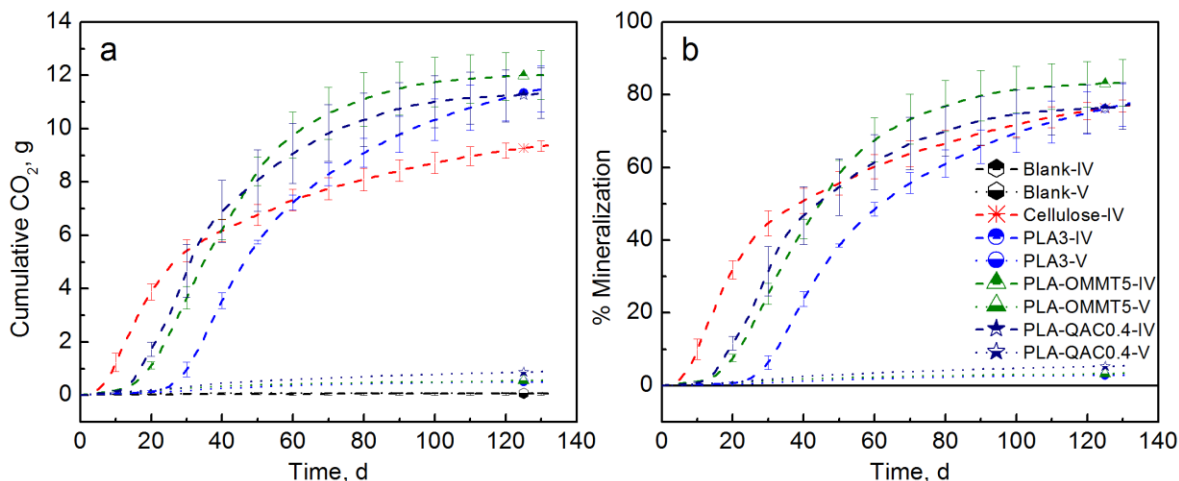


Figure 4.11 (a) CO₂ evolution and (b) % Mineralization of PLA, PLA-OMMT5, and PLA-QAC0.4 (Test IV in inoculated vermiculite (dashed lines) and uninoculated vermiculite (dotted lines)).

Figure 4.11 also shows the results when testing with uninoculated vermiculite. As expected, there was no significant evolution of CO₂ in the abiotic degradation test, and there was no significant difference in the mineralization values. For the biodegradation test III, film samples were taken at different periods of time in order to track the changes in the molecular weight and the results are explained in section 4.3.3.

4.3.3 Molecular Weight

Figure 4.12 shows the initial molecular weight distribution (MWD) of the PLA film and BNCs. As previously mentioned, the addition of nanoclay resulted on a reduction of the M_n during processing. This reduction in M_n was more pronounced in the case of PLA-OMMT5, PLA-QAC1.5, and PLA-QAC0.4. More detailed information about the initial M_n , M_w , and PDI, of PLA and BNCs films is provided in **Table 4D.1** of the Appendix 4D.

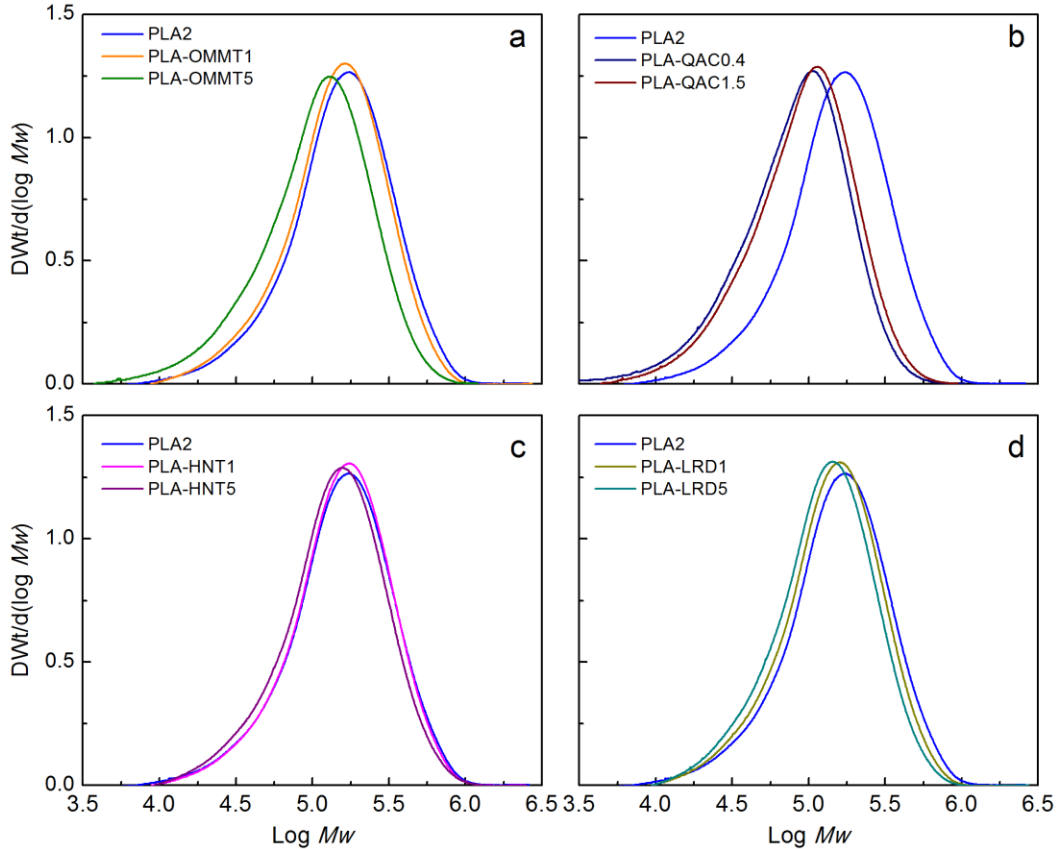


Figure 4.12 Initial molecular weight of PLA and BNCs.

Figure 4.13 shows the decrease of molecular weight of the PLA control film as function of time during the biodegradation test III, represented by the shift of the peak to the left. This behavior was previously reported in the literature during the hydrolytic degradation of PLA, and was attributed to the chain scission preferentially occurring in the bulk of the polymer matrix rather than the surface [67]. The broadening of the peaks over time indicates an increase in the PDI due to the fragmentation of the PLA chains. The change in the MWD from monomodal to multimodal after day 14 has also been previously observed during hydrolytic degradation of PLA and was attributed to the formation of crystalline residues due to the rearrangement of the new shorter polymer chains into a more stable configuration (*i.e.*, crystalline structures) [51,67]. The

formation of more defined and higher peaks, as observed at days 42 and 56, has been attributed to the predominant degradation of the amorphous regions [68]. During the biodegradation tests a whitening effect in PLA and BNC was observed. It has been reported that this effect indicates increased crystallinity and opacity due to the beginning of the hydrolytic degradation phase of the biodegradation process [44,45,62]. The whitening effect occurs because a change in the refraction index of the polymer is induced by the absorbed water and/or the byproducts, *e.g.*, carboxylic end-groups that are able to catalyze ester hydrolysis [45,62].

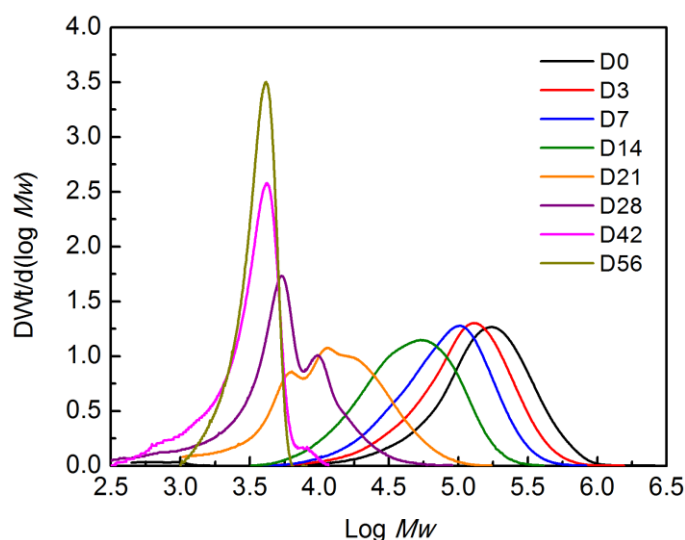


Figure 4.13 Change in molecular weight of PLA2 film (Test III in compost).

Figure 4.14 shows the changes in the MWD of the BNCs as function of time until day 28 since it was not possible to collect samples for SEC analysis after that period of time (except for PLA control as shown in **Figure 4.13**). Similarly to the PLA control, the BNCs showed multimodal peaks after day 14, although more evidently after day 21. In general, this behavior was less pronounced for PLA-OMMT1, PLA-LRD1, and PLA-LRD5, and it may be attributed to a slower formation of crystalline residuals. From **Figure 4.14**, it can be observed that the reduction of molecular weight was slower for

PLA-OMMT1 and PLA-LRD1, in comparison with the pristine PLA. Similarly, the MWD of PLA-OMMT5 and PLA-QAC15 have a similar trend with an evident multimodal peak at day 21, while the reduction of molecular weight of PLA-HNT5 and PLA-LRD5 films seems to be slower than PLA control.

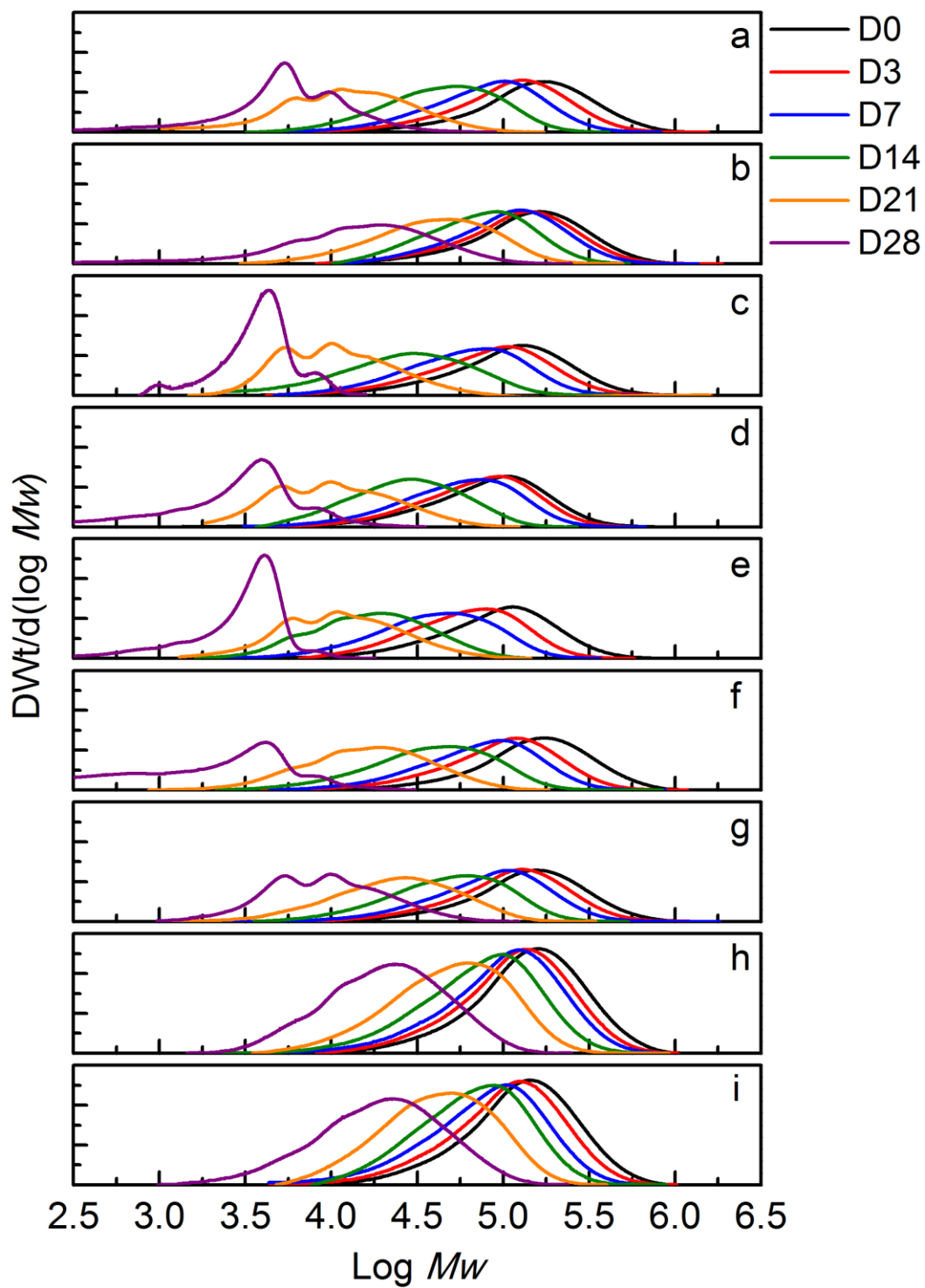


Figure 4.14 Change in molecular weight of (a) PLA2, (b) PLA-OMMT1, (c) PLA-OMMT5, (d) PLA-QAC0.4, (e) PLA-QAC1.5, (f) PLA-HNT1, (g) PLA-HNT5, (h) PLA-LRD1, and (i) PLA-LRD5 films (Test III in compost).

Deconvolution of the peaks was performed due to the multimodal MWD observed in the previous results, followed by kinetics analysis (Appendix 4D). The M_n reduction rate (k) constant was calculated for PLA and the BNCs, fitting of a first order reaction of the form $M_n / M_{n0} = \exp(-kt)$, where M_{n0} is the initial M_n , and t is the time. The results (**Figure 4D.3** and **Table 4D.2**) show that the BNCs, especially PLA-LRD films, have a lower M_n reduction rate than the PLA control ($k = 0.1008 \pm 0.0037$) until day 28. Ray and Okamoto analyzed the molecular weight of PLA and PLA nanocomposites and found that the reduction was almost the same for all the samples [10]. In contrast, Paul et al. found that the M_n of PLA decreased ~40% with respect to its initial value while for the PLA nanocomposites M_n decreased 70-80% [38]. In this case, even though the M_n reduction rate of the BNC was the same or lower than the PLA control, a higher evolution of CO₂ from the bioreactors supplemented with the BNC was generally observed during the biodegradation tests. Therefore, it is also relevant to understand the role of the microorganisms and how they are affected by the presence of these nanoclays. For example, Annamalai et al. suggested that the clay nanoparticles improve the absorption of UV light and promote polymer photo-oxidation due to the catalytic effect of metal ion impurities. That increased oxidation at the surface of the nanocomposites could favor the adhesion, accumulation and growth of the microorganisms [69].

4.3.4 Microbial attachment

Biofilm assays were performed to evaluate the ability of the microorganisms present in the compost to attach to the surface of PLA film and BNCs (*i.e.*, PLA-OMMT5, PLA-QAC0.4, PLA-HNT5, and PLA-LRD5). Even though biofilm formation does not

necessarily mean that the material is biodegraded by the attached populations [70], it is an important aspect of microbial performance and survival [71]. When biofilm-forming microorganisms release exopolymeric substances (EPS) (e.g., carbohydrates, nucleic acids, and proteins) such resources become available for other microorganisms, including secreted enzymes that degrade PLA and derivatives. Secreting extracellular digestive enzymes after forming a biofilm would localize the effect of extracellular digestion and increase the benefit to biofilm-forming strains. Biofilm production is a common trait among microorganisms living in soil which are usually exposed to low moisture conditions. Biofilms can contribute to water retention in the soil matrix, prevent microorganisms from being washed out, and confer tolerance to other environmental stressors [71].

An initial test of the biofilm assay is shown in the Appendix 4E. **Figure 4.15**, **Table 4E.3** and **Table 4E.4** show the results of the biofilm test. A positive control was performed using *Pseudomonas aeruginosa* (PA) strain PAO1, a high biofilm forming strain, at 23°C [72,73]. Looking at the control with PA at 23°C (Figure 15.a), it is observed that the control wells (R2B only) have an absorbance (A600 nm) of 1.226-1.332, with uninoculated control wells ranging from 0.060 to 0.065, which is in agreement with the values reported by Satti et al. [49]. The wells containing PLA, PLA-QAC0.4, PLA-HNT5, and PLA-LRD5 were approximately the same as the control lacking any film (R2B only). However, the wells containing PLA-OMMT5 showed significantly more biofilm formation (average 2.042), suggesting that the OMMT had an indirect stimulation on biofilm formation by PA. For the biofilm formed on the surface of the films by PA at 23°C, PLA ranged from 0.501 to 0.752, which is also in agreement

with the values previously observed [49]. In this case, the values of PLA-OMMT5 and PLA-HNT5 were significantly different from PLA-QAC0.4. PLA-HNT5 had one of the highest average values with 1.254. Looking at the total biofilm formation, PLA-OMMT5 and PLA-QAC0.4 were significantly different from pristine PLA and the rest of the BNCs with the highest (2.917) and lowest (1.107) values, respectively. The total average biofilm values (wells + film) for PA at 23°C in descending order are as follows PLA-OMMT5 > PLA-HNT5 > PLA > PLA-LRD5 > PLA-QAC0.4.

Regarding the biofilm estimates with CE at 58°C (**Figure 4.15b**), the sterile controls (SCE) have values that are between 0.101 and 0.124, which are slightly greater than what was seen with low nutrient media at 23°C. This is probably due to significant amounts of humic material in the CE. The control wells (CE only) have values of 0.381-0.588. These values are less than the ones for PA at 23°C which is expected since PA is a well-known biofilm former and because microbial growth and survival is generally more challenging at 58°C and CE contains a diverse collection of microbial populations, many of which do not form biofilm under these conditions. The wells supplemented with PLA and BNCs ranged from 0.122-0.603 with no statistically significant difference among them. Biofilm formation was observed on the surface of PLA and BNCs with CE at 58°C. PLA-LRD5 has significantly higher value (0.519) than the rest of the BNCs. The lowest average values were observed for PLA-QAC0.4 and PLA with 0.113 and 0.090, respectively. In this case, the total biofilm was also not significantly different among the sample materials.

In general, the PLA-LRD5 biofilm was the largest among the different samples, indicating that population in CE have a preference for PLA-LRD5 at 58°C. In contrast, a

pure culture, *Pseudomonas aeruginosa*, clearly preferred PLA-OMMT5 at 23°C. Overall the biofilms at 58°C are smaller than the biofilm at 23°C. At both temperatures, PLA-QAC0.4 was the film producing the lowest average amount of biofilm which may be attributed to inhibition due to the surfactant. This is supported by the biodegradation test where the surfactant was tested alone. Further investigation is recommended to understand which are the specific microbial strains present in the compost that bind to and preferentially degrade PLA and the BNCs.

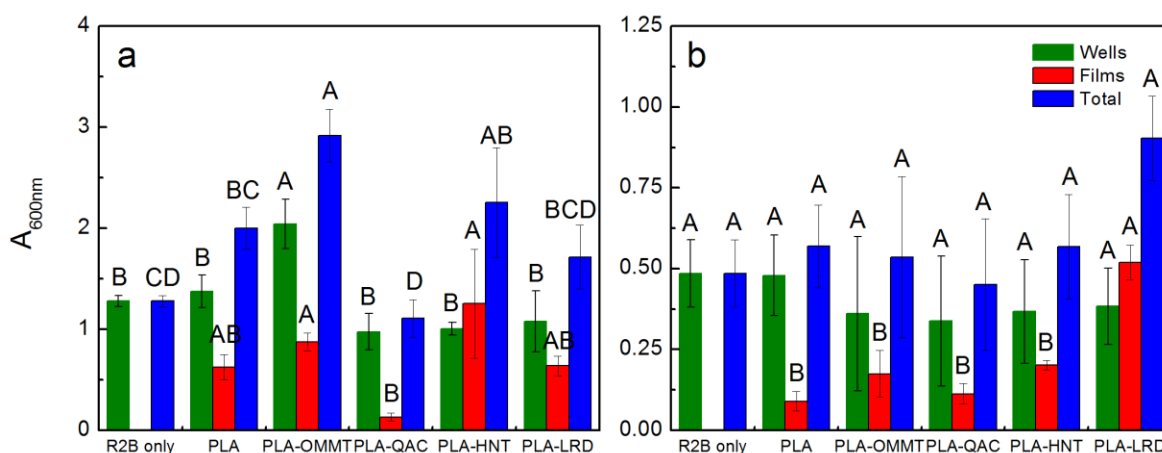


Figure 4.15 Absorbance (600 nm) of (a) PA at 23°C, and (b) CE at 58°C for second biofilm test. Columns with the same letter within a group (*i.e.*, wells, films, or total) are not significantly different at $p \leq 0.05$ (Tukey test).

Due to the significant differences between pristine PLA and PLA-LRD5 found in the biofilm formed on the surface of the films during the test at 58°C with CE, several SEM micrographs were taken from samples coated with osmium. **Figure 4.16** shows the difference in microbial attachment between pristine PLA and PLA-LRD5 at a magnification of 1000x. It can be clearly observed that the surface of PLA-LRD5 is much more heavily populated by microorganisms, in agreement with the biofilm test results (**Figure 4.15b**).

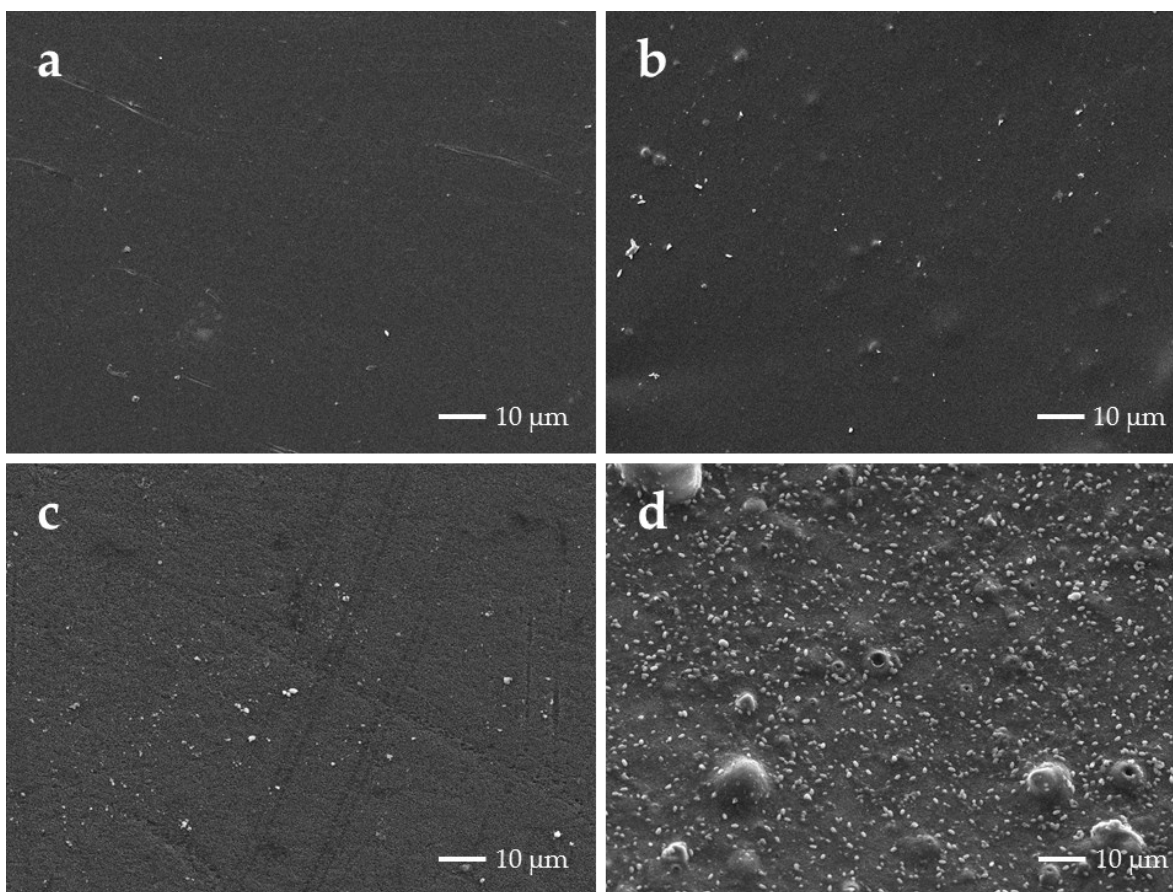


Figure 4.16 SEM micrographs of (a) PLA and (b) PLA-LRD at 1000x before incubation, (c) PLA and (d) PLA-LRD5 after incubation for 48 h at 58°C with compost extract in R2B.

4.4 Final Remarks

The effect of three different nanoclays, OMMT, HNT, and LRD, as well as the OMMT organo-modifier (QAC) on the biodegradation of PLA was evaluated with an in-house built DMR system following the analysis of evolved CO₂ approach. The results obtained from four different biodegradation tests along with the study of microbial attachment on the surface of PLA and its BNCs show that the biodegradation phase of the films containing nanoclay started earlier than that for pristine PLA. This behavior was confirmed by the results obtained from different tests for PLA-OMMT5, even when

tested in inoculated vermiculite. The tests performed in vermiculite allowed untangling the observed priming effect even though longer testing times were required. The effect of the nanoclays on the initial molecular weight during processing played a crucial role in the biodegradation studies, also since a lower M_{n0} (≤ 60 kDa) seems to be correlated to the priming effect in compost. Further investigation is recommended using PLA and BNCs with the same initial molecular weight and thickness, a task not easy to achieve in lab settings. When the different nanoclays and surfactant were tested alone, it was observed that HNT, OMMT, and QAC showed some inhibition regardless of the amount introduced in the bioreactors. PLA-LRD5 showed a priming effect with mineralization values exceeding 100%. This behavior may be explained by the lower initial molecular weight and by the results observed during the microbial attachment tests, in which PLA-LRD5 showed the greatest biofilm formation on the surface as confirmed by the SEM micrographs. PLA-QAC0.4 had the lowest biofilm formation, which may be attributed to the inhibitory effect also found during the CO₂ evolution test when QAC was tested alone. Under the experimental conditions used to investigate biofilm formation, it was noted that significant biofilm was established in only 48 hours; however, the timing may be different in composting conditions. Further investigation is required on the specific microbial strains that are capable of biodegrading PLA and its BNCs and how they can affect the biodegradation rate. Disposable products like packaging would greatly benefit from the biodegradable features of PLA since it would allow its disposal along with other organic wastes in composting facilities.

APPENDICES

APPENDIX 4A: Material processing

Masterbatch (MB) production: The PLA-BNCs (PLA-OMMT, PLA-HNT, and PLA-LRD) masterbatches (15 – 20% nanoclay wt.) were prepared in a ZSK 30 twin-screw extruder (Werner Pfleiderer, NJ) and pelletized. A PLA-QAC masterbatch (10% QAC wt.) was prepared in a similar fashion. Pristine PLA was processed in the twin-screw extruder and used for the processing of PLA1 control film. **Table 4A.1** shows the general MB processing conditions.

Film production: All films were produced by using a Microextruder model RCP-0625 (Randcastle Extrusion Systems, Inc., Cedar Grove, NJ) with a screw diameter of 15.9 mm, screw L/D of 24, and volume of 34 cm³. **Table 4A.1** shows the processing conditions of the films and their thickness as measured with a digital thickness micrometer. However, it was observed that the measurement of the BNC's thickness with the digital micrometer may not be the best approach due to the presence of the nanoclay. The thickness of PLA-OMMT1 and PLA-OMMT5 was measured from the SEM cross-section of the films and it was found to be 0.020 ± 0.004 , and 0.010 ± 0.002 mm, respectively.

Table 4A.1 Processing conditions of the sample materials

Material	Conc., wt%	Type	Temp. range, °C	rpm	Thickness, mm
PLA	0%	MB	146-186	130	N/A
PLA-OMMT	20%	MB	146-186	130	N/A
PLA-QAC	10%	MB	148-189	130	N/A
PLA-HNT	15%	MB	159-181	40	N/A
PLA-LRD	15%	MB	159-181	40	N/A
PLA1	0%	Film	194-216	49	0.031 ± 0.006
PLA2	0%	Film	193-249	33	0.022 ± 0.003
PLA3	0%	Film	193-249	28	0.034 ± 0.009
PLA-OMMT	1%	Film	193-243	18	0.044 ± 0.007
PLA-OMMT	5%	Film	193-248	18	0.073 ± 0.014
PLA-OMMT	7.5%	Film	193-243	18	0.089 ± 0.013
PLA-QAC	0.4%	Film	143-173	31	0.039 ± 0.008
PLA-QAC	1.5%	Film	143-173	31	0.036 ± 0.011
PLA-HNT	1%	Film	193-216	23	0.037 ± 0.007
PLA-HNT	5%	Film	193-216	23	0.050 ± 0.006
PLA-LRD	1%	Film	193-216	23	0.064 ± 0.013
PLA-LRD	5%	Film	193-216	23	0.127 ± 0.011

N/A: Not applicable

APPENDIX 4B: Material characterization

Elemental Analysis (CHN): The carbon, hydrogen, and nitrogen content of the different test materials was determined by using a PerkinElmer 2400 Series II CHNS/O Elemental Analyzer (Shelton, CT, USA), and values are presented in **Table 4B.1**. The amount of filler present in each of the films was confirmed by CHN, considering the theoretical chemical structure of PLA and each of the components.

Table 4B.1 Carbon, hydrogen, and nitrogen content of the tested materials

Material	ID	% Carbon ^a	% Hydrogen ^a	% Nitrogen ^a
Cellulose powder	Cellulose	42.50 ± 0.34	6.53 ± 0.05	0.04 ± 0.01
	PLA1	50.05 ± 0.05	5.65 ± 0.02	0.01 ± 0.01
Ingeo™ 2003D film	PLA2	49.93 ± 0.11	5.56 ± 0.02	0.01 ± 0.01
	PLA3	49.99 ± 0.05	5.60 ± 0.01	0.01 ± 0.01
Cloisite® 30B	OMMT	19.22 ± 0.06	3.84 ± 0.02	0.99 ± 0.00
Laponite® RD	LRD	0.18 ± 0.01	1.19 ± 0.04	0.02 ± 0.01
Halloysite	HNT	0.09 ± 0.02	1.83 ± 0.05	0.01 ± 0.00
Tomamine™	QAC	59.28 ± 0.60	12.28 ± 0.05	2.55 ± 0.02
PLA-OMMT 1% ^a	PLA-OMMT1	49.49 ± 0.07	5.54 ± 0.04	0.03 ± 0.02
PLA-OMMT 5% ^a	PLA-OMMT5	48.76 ± 0.07	5.49 ± 0.02	0.07 ± 0.01
PLA-OMMT 7.5% ^a	PLA-OMMT7.5	47.75 ± 0.11	5.43 ± 0.01	0.09 ± 0.00
PLA-HNT 1% ^a	PLA-HNT1	49.67 ± 0.12	5.60 ± 0.06	0.70 ± 0.34
PLA-HNT 5% ^a	PLA-HNT5	48.22 ± 0.10	5.44 ± 0.01	1.68 ± 0.43
PLA-LRD 1% ^a	PLA-LRD1	49.58 ± 0.17	5.54 ± 0.05	2.43 ± 0.42
PLA-LRD 5% ^a	PLA-LRD1	47.70 ± 0.11	5.39 ± 0.06	6.43 ± 1.82
PLA-QAC 0.5%	PLA-QAC0.5	49.98 ± 0.08	5.55 ± 0.02	0.01 ± 0.00
PLA-QAC 1.5%	PLA-QAC1.5	50.55 ± 0.04	5.78 ± 0.02	0.05 ± 0.01

^a Percentage by weight

Differential Scanning Calorimetry (DSC): The glass transition (T_g) and melting (T_m) temperatures of PLA and BNCs films were determined using a DSC model Q-100 (TA Instruments, New Castle, DE) and the TA Instruments Universal Analysis 2000 software (Version 4.5A). The testing temperature was from 5°C to 210°C with a ramping rate of 10°C/min. The results are shown in **Figure 4B.1** and **Table 4B.2**.

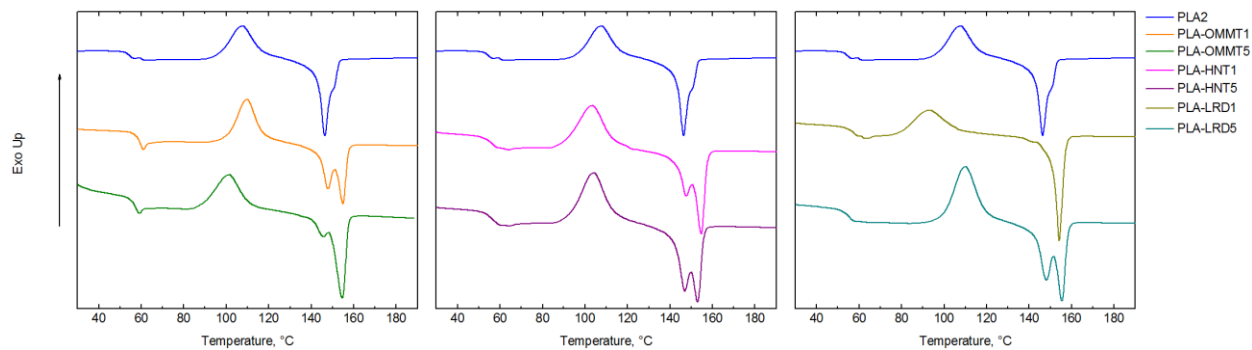


Figure 4B.1 DSC of the PLA and BNCs films (1st cycle).

Thermogravimetric Analysis (TGA): The degradation temperature (T_d) of the PLA and PLA-OMMT films was measured with a TGA model Q50 from Thermal Analysis Inc. (New Castle, DE). The testing temperature was from 23°C to 600°C with a ramping rate of 10°C/min. The results are shown in **Figure 4B.2** and **Table 4B.2**.

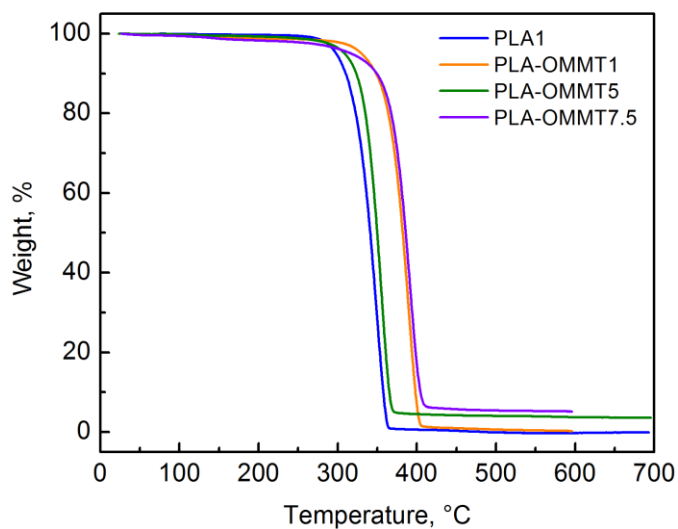


Figure 4B.2 TGA of the PLA and PLA-OMMT films.

Table 4B.2 Thermal properties of the PLA and BNCs

Sample	T _g , °C	T _c , °C	T _m , °C	T _d , °C	% X _c
PLA1	63.3	N/A	152.0	349.0	25.0
PLA2	54.4	107.1	146.4	N/A	4.6
PLA-MMT1	59.8	109.8	154.9	389.2	1.6
PLA-MMT5	57.8	101.5	154.6	355.0	4.3
PLA-MMT7.5	57.9	90.3	152.8	391.5	12.3
PLA-HNT1	56.8	103.1	154.7	N/A	4.0
PLA-HNT5	56.7	103.7	153.0	N/A	4.5
PLA-LRD1	57.9	92.0	154.2	N/A	11.6
PLA-LRD5	55.6	109.7	155.5	N/A	2.7

N/A: Not available

Moisture sorption isotherm: The moisture sorption isotherms of the nanoclays, PLA, and BNCs films were examined by gravimetric analysis using an SGA-100 from VTI Corp. (Hialeah, FL). The samples (5-10 mg) were exposed to relative humidity (RH) between 0 and 95 ± 2% with RH steps of 10, at 23 ± 0.1°C. The results are shown in

Figure 4B.3.

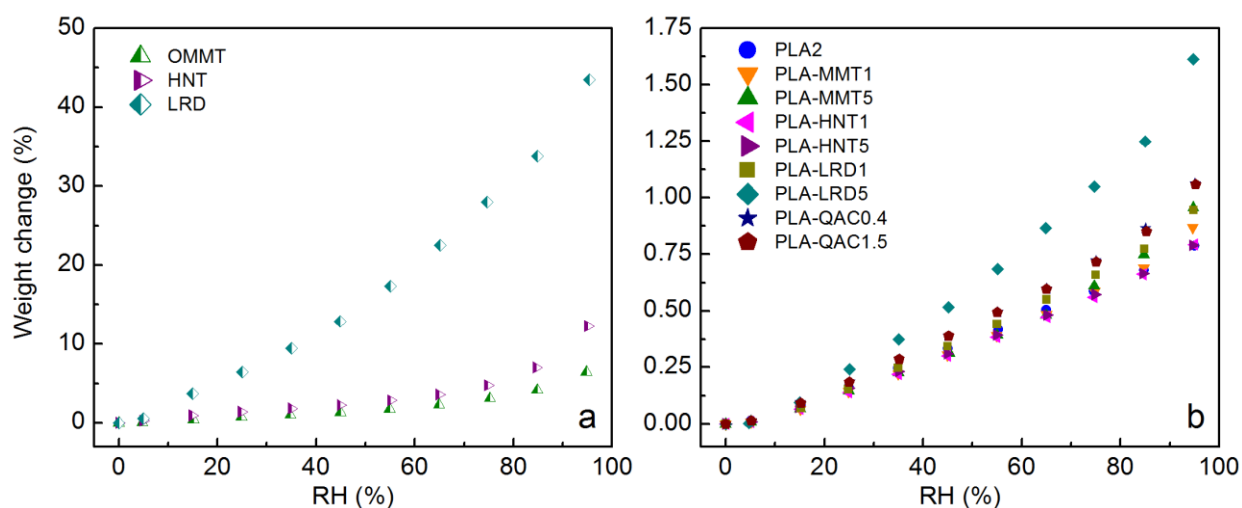


Figure 4B.3 Moisture sorption isotherms of the nanoclays, PLA and BNCs films.

Electrical conductivity: The measurements were carried out using an electrochemical impedance spectroscopy (EIS) system (Gamry Instruments,

Warminster, PA) for 2.54 cm² film samples. Copper foil tape with conductive adhesive was located on the surface of the film from both sides, and the electrodes were attached to each extreme of the tape. The Gamry Framework software was used for the analysis using the Potentiostatic EIS mode. The conductivity was measured over a frequency range of 1 x 10⁵ to 0.1 Hz with an applied potential of 20 mV at room temperature (23°C). The resistivity values presented in **Table 4B.3** were calculated using the impedance (Z) value at a frequency of 0.1 Hz.

Table 4B.3 Resistivity of the PLA and BNCs

Sample	Resistivity		
PLA2	3.96E+13	±	1.47E+11 AB
PLA-OMMT5	3.31E+13	±	5.05E+12 B
PLA-QAC0.4	3.77E+13	±	1.00E+12 AB
PLA-HNT5	3.61E+13	±	4.21E+12 AB
PLA-LRD5	4.15E+13	±	6.20E+11 A

Note: Values with the same letter are not significantly different at $p \leq 0.05$ with Tukey-Kramer Test.

Contact angle: Surface wettability of the PLA and BNCs films was evaluated by contact angle measurements using a goniometer (Drop Shape Analysis System, DSA10 Mk2, Krüss GmbH, Hamburg, Germany), equipped with a diffuse light source and a CCD camera, at room temperature (23°C). A drop of HPLC grade water (3 µL) was deposited on the film surface and a magnified image of the drop profile was conveyed to a computer. The contact angle was measured with the Drop Shape Analysis Software using the tangent method. Ten measurements per film were performed and the values reported in **Table 4B.4** are the average of contact angles measured on both sides of the drop.

Table 4B.4 Contact angle of the PLA and BNCs measured with water at room temperature

Sample	Contact angle
PLA2	71.6 ± 2.1 ^D
PLA-OMMT5	96.4 ± 4.2 ^A
PLA-QAC0.4	83.3 ± 4.5 ^C
PLA-HNT5	93.2 ± 2.5 ^B
PLA-LRD5	85.6 ± 3.9 ^C

Note: Values with the same letter are not significantly different at $p \leq 0.05$ with Tukey-Kramer Test.

APPENDIX 4C: Physicochemical characteristics of the compost

Samples of the compost used in the different biodegradation tests were sent to the Soil and Plant Nutrient Laboratory at Michigan State University (East Lansing, MI, USA) for determination of the physicochemical parameters (dry solids, volatile solids, C/N ratio, pH, and microbial activity) as shown in **Table 4C.1**. Detailed information about the methods used for compost characterization can be found elsewhere [47].

Table 4C.1 Physicochemical characteristics of the compost used in the different biodegradation tests

Parameters	ISO^b	I	II	III	IV
Dry solids, %	50-55	53.3	52.7	41.5	60.9
Volatile solids, %	<30	26.4	44.3	43.2	39.1
pH	7-9	7.8	7.9	8.5	7.4
Total Carbon, %	N/A ^a	15.3	25.7	25.1	22.7
Total Nitrogen, %	N/A ^a	0.9	2.4	2.4	2.1
C/N ratio	10-40	17.4	10.8	10.3	10.9
Compost activity ^c	50-150	39.0	81.1	63.0	62.5

^a Not applicable or not available

^b Values based on ISO 14855-1:2005 standard

^c Average values measured in mg of CO₂ per g of VS in the first 10 days

APPENDIX 4D: Molecular weight determination

Initial molecular weight: The number average molecular weight (M_n), weight average molecular weight (M_w), and polydispersity index (PDI) of the samples before and during composting were determined by size exclusion chromatography (SEC) with a system from Waters Inc. (Milford, MA), equipped with a Waters 1515 isocratic pump, a Waters 717 autosampler, a series of three columns (HR2, HR3, and HR4 Waters Styragel®), and a Waters 2414 refractive index detector interfaced with Waters Breeze software [47]. **Table 4D.1** shows the initial M_n , M_w , and PDI of the samples as measured before each of the different biodegradation tests.

Table 4D.1 Initial M_n , M_w , and PDI of the PLA samples

Biodegradation test	Sample	M_n , kDa	M_w , kDa	PDI
I	PLA1	113.1 ± 0.1 ^A	208.0 ± 0.8 ^A	1.8 ± 0.0 ^B
	PLA-OMMT5	59.8 ± 1.1 ^B	118.9 ± 0.9 ^B	2.0 ± 0.0 ^A
II	PLA1	113.1 ± 0.1 ^A	208.0 ± 0.8 ^A	1.8 ± 0.0 ^A
	PLA-OMMT1	82.9 ± 2.2 ^B	157.3 ± 1.7 ^B	1.9 ± 0.0 ^A
	PLA-OMMT5	59.8 ± 1.1 ^C	118.9 ± 0.9 ^C	2.0 ± 0.0 ^A
	PLA-OMMT7.5	37.5 ± 2.3 ^D	76.7 ± 1.3 ^D	2.1 ± 0.2 ^A
III	PLA2	88.8 ± 0.9 ^A	172.0 ± 1.3 ^A	1.9 ± 0.0 ^C
	PLA-OMMT1	82.9 ± 2.2 ^{ABC}	157.3 ± 1.7 ^B	1.9 ± 0.0 ^C
	PLA-OMMT5	52.8 ± 0.7 ^D	116.1 ± 0.3 ^D	2.2 ± 0.0 ^A
	PLA-HNT1	91.4 ± 3.3 ^A	171.1 ± 1.2 ^A	1.9 ± 0.1 ^C
	PLA-HNT5	79.7 ± 3.8 ^{BC}	153.0 ± 2.5 ^B	1.9 ± 0.1 ^{BC}
	PLA-LRD1	84.2 ± 1.7 ^{AB}	155.5 ± 1.4 ^B	1.8 ± 0.0 ^C
	PLA-LRD5	75.3 ± 0.9 ^C	139.0 ± 0.7 ^C	1.8 ± 0.0 ^C
	PLA-QAC0.4	43.5 ± 3.8 ^E	88.7 ± 1.6 ^F	2.0 ± 0.1 ^{ABC}
PLA-QAC1.5	45.0 ± 2.4 ^E	96.7 ± 1.3 ^E	2.2 ± 0.1 ^{AB}	
IV	PLA1	119.0 ± 11.3 ^A	234.4 ± 16.9 ^A	2.0 ± 0.1 ^B
	PLA2	101.1 ± 11.8 ^{AB}	206.2 ± 23.1 ^A	2.0 ± 0.1 ^{AB}
	PLA3	84.8 ± 6.9 ^B	167.4 ± 3.2 ^B	2.0 ± 0.2 ^B
	PLA-OMMT5	45.5 ± 5.8 ^C	108.6 ± 11.6 ^C	2.4 ± 0.2 ^A
	PLA-QAC0.4	54.5 ± 9.5 ^C	118.2 ± 5.8 ^C	2.2 ± 0.3 ^{AB}

Note: Values with the same letter within the same group (*i.e.*, biodegradation test) and in the same column are not significantly different at $p \leq 0.05$ with Tukey-Kramer Test.

Molecular Weight Reduction during Biodegradation: Due to the observed multimodal MWD in the results presented in Section 4.3.3, deconvolution of the MWD peaks was necessary for conducting kinetics analysis, in which the M_n reduction rate (k) constant was calculated for PLA and the BNCs. Therefore, a curve fitting and data analysis program, Fityk version 1.3.0, developed by Marcin Wojdyr [74], was used for deconvolution using a log normal function as was used by Perejon et al., which is more appropriate to fit asymmetrical functions [75] such as the ones observed for the MWD (**Figure 4.13** and **Figure 4.14**). **Figure 4D.1** shows an example of the deconvolution of the PLA control peaks at day 7, 14, 21, and 28. To confirm whether deconvolution of a

peak was necessary or not, and which are the main peaks of the MWD, the area fraction was used. **Figure 4D.2** shows the PLA control as an example of the methodology used. **Figure 4D.2a** shows the M_n calculated from the different deconvoluted peaks as function of time while **Figure 4D.2b** shows the area fraction of those different peaks, in which the first peak has the main contribution until day 21. For PLA control on days 28 and 42, it seems that the first and second peaks may have similar contribution in some cases and the contribution of the other peaks is minimal. In the case of PLA control for day 56 a single peak was observed. This analysis was performed for all the BNCs in a similar fashion and the main peaks were selected case by case for the determination of k . In most cases, no deconvolution was required for days 0, 3, and 7.

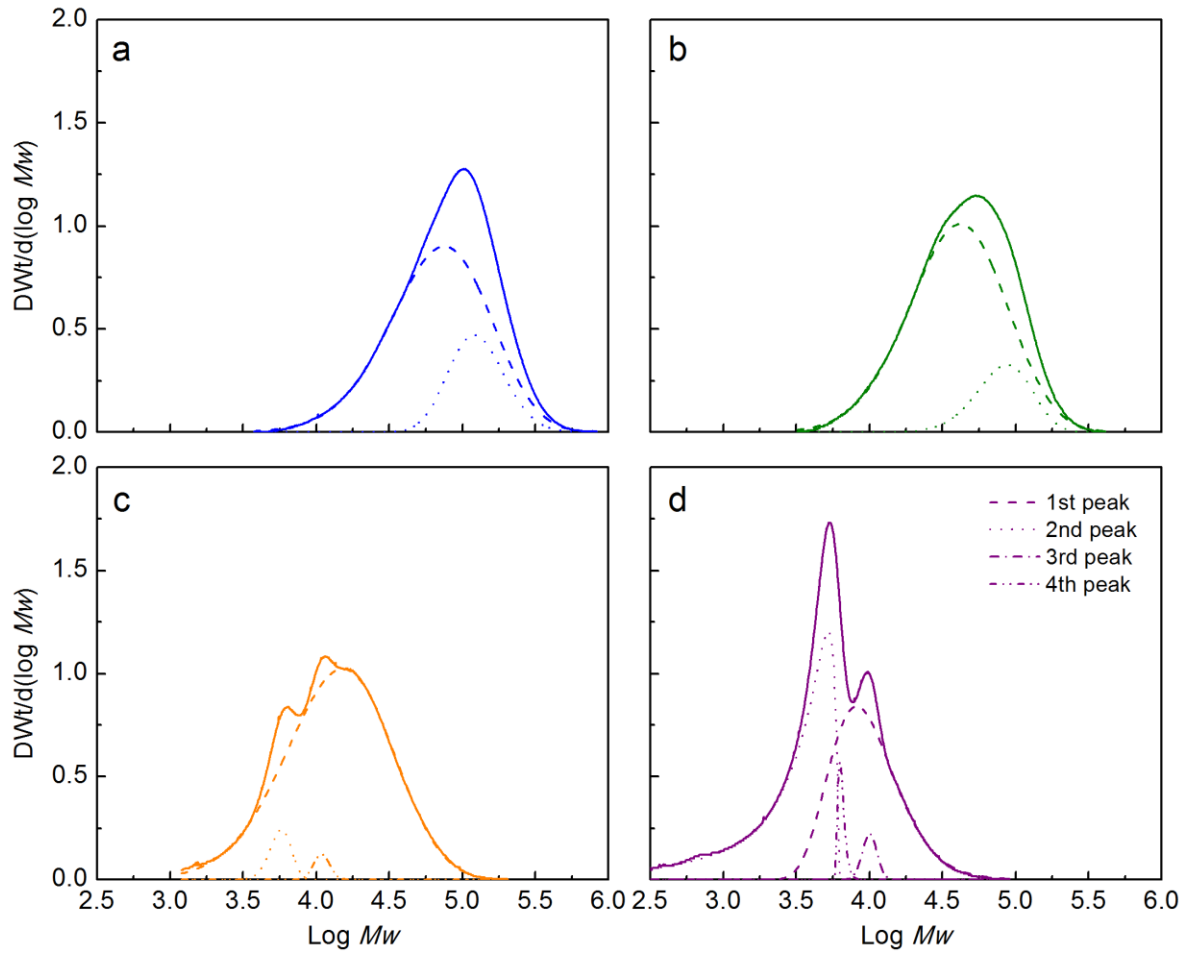


Figure 4D.1 Deconvolution of the PLA2 peaks at days (a) 7, (b) 14, (c) 21, and (d) 28 (Test III in compost).

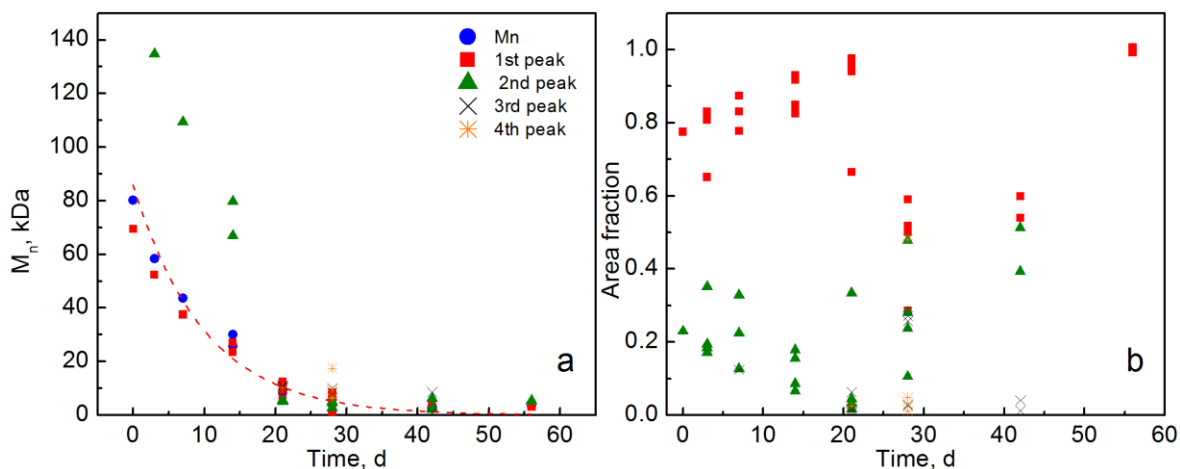


Figure 4D.2 (a) M_n and (b) area fraction as function of time for PLA2 film (Test III in compost).

Figure 4D.3 and **Table 4D.2** show the M_n reduction as a function of time for PLA and PLA-BNCs. The dashed lines indicate fitting of a first order reaction of the form $M_n/M_{n0} = \exp(-kt)$, where M_{n0} is the initial M_n , k is the rate constant and t is the time. It can be observed that the initial molecular weight has a real effect on the biodegradation rate, especially until day 21, in which the abiotic degradation (*i.e.*, hydrolysis) takes place, and therefore the overall biodegradation. A material with low M_n has more polymer chains with free ends that can be cleaved, thus producing more oligomers and monomers that are available for the microorganisms in comparison with one of higher M_n [47]. **Figure 4D.3** also shows that for each of the BNCs the film with 1% and 5% filler loading follow a similar pattern. PLA-HNT films (**Figure 4D.3c**) are the ones with the closest initial molecular weight to the PLA control and they follow a very similar pattern, especially after the third day. PLA-HNT and PLA-LRD films seem to have a lower rate than the PLA control, which is in agreement with previous results.

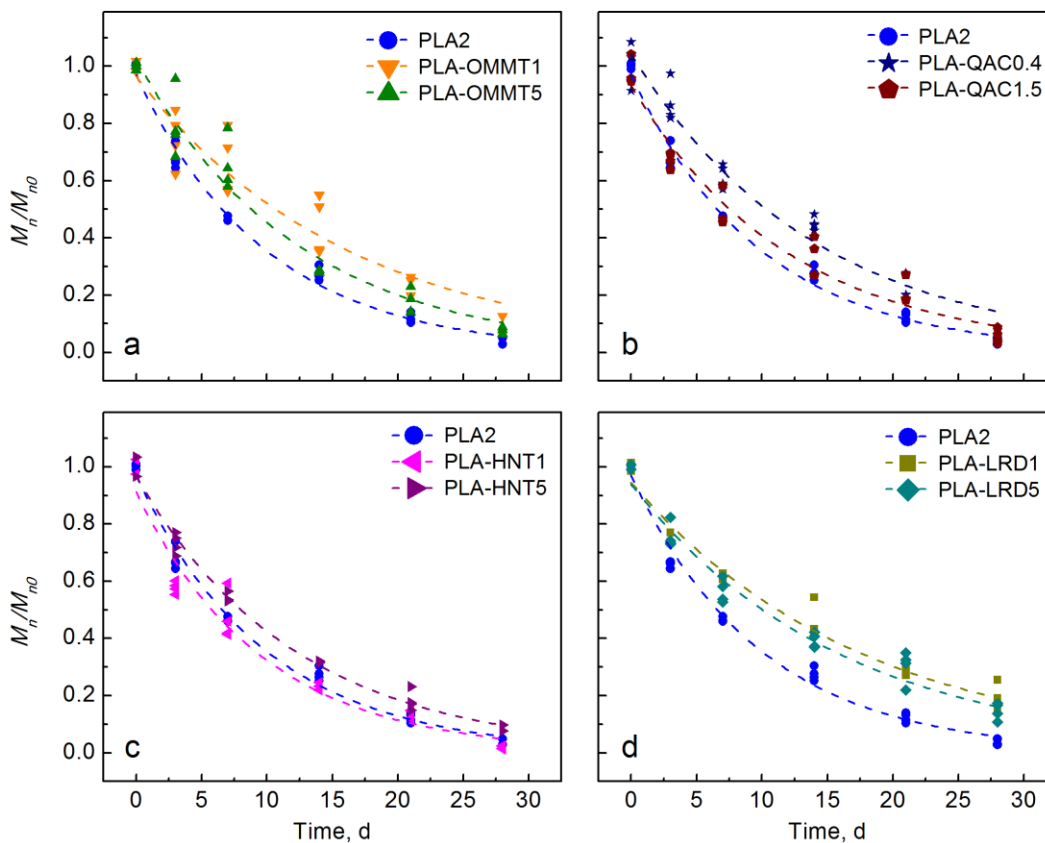


Figure 4D.3 Molecular weight reduction as function of time for PLA2 and (a) PLA-OMMT, (b) PLA-QAC, (c) PLA-HNT, and (d) PLA-LRD films (Test III in compost).

Dashed lines indicate fitting of a first order reaction of the form $M_n/M_{n0} = \exp(-kt)$, where

M_{n0} is the initial M_n , k is the rate constant and t is the time.

Table 4D.2 Initial molecular weight and reduction rate of PLA and BNCs as estimated by the first order reaction of the form $M_n = M_{n0} \exp(-kt)$

Sample	M_{n0} , kDa	K , d ⁻¹
PLA2	86.0 ± 1.5 ^A	0.1008 ± 0.0037 ^A
PLA-OMMT1	80.0 ± 3.5 ^{ABC}	0.0616 ± 0.0058 ^C
PLA-OMMT5	54.1 ± 1.8 ^E	0.0815 ± 0.0057 ^B
PLA-HNT1	83.4 ± 3.3 ^{AB}	0.1037 ± 0.0078 ^A
PLA-HNT5	77.2 ± 1.3 ^C	0.0824 ± 0.0029 ^B
PLA-LRD1	79.6 ± 1.8 ^{BC}	0.057 ± 0.0027 ^C
PLA-LRD5	70.7 ± 1.9 ^D	0.0628 ± 0.0034 ^C
PLA-QAC04	44.9 ± 1.3 ^F	0.0711 ± 0.0045 ^{BC}
PLA-QAC15	42.8 ± 1.4 ^F	0.0828 ± 0.0056 ^B

Note: Values with the same letter within the same column are not significantly different at $p \leq 0.05$ with Tukey-Kramer Test.

APPENDIX 4E: Biofilm formation

Figure 4E.1, Table 4E.1 and Table 4E.2 show the results of the first iteration of the biofilm test. Looking at the control with PA at 23°C (Figure 4E.1a), the control wells (R2B – No polymer) have an absorbance (600 nm) of 1.628-2.029 (uninoculated control wells ranged from 0.065 to 0.067). There was no significant difference in the wells supplemented with PLA and BNCs (Table 4E.1). The wells supplemented with PLA-LRD5 had the highest average value of 2.028. At 23°C, *P. aeruginosa* did form biofilm on the surface of the films. The quantitation of biofilm on PLA ranged from 0.409 to 0.966, which is in accordance with the values observed by Satti et al. [49]. There was no significant difference between PLA and BNCs. However, PLA-HNT5 and PLA-LRD5 showed the highest average values of 1.105 and 1.137, respectively. Then, viewing the total biofilm formed by PA (i.e., wells plus films), PLA-LRD5 had the highest average total of 3.165 while the total average for the pristine PLA was 2.390.

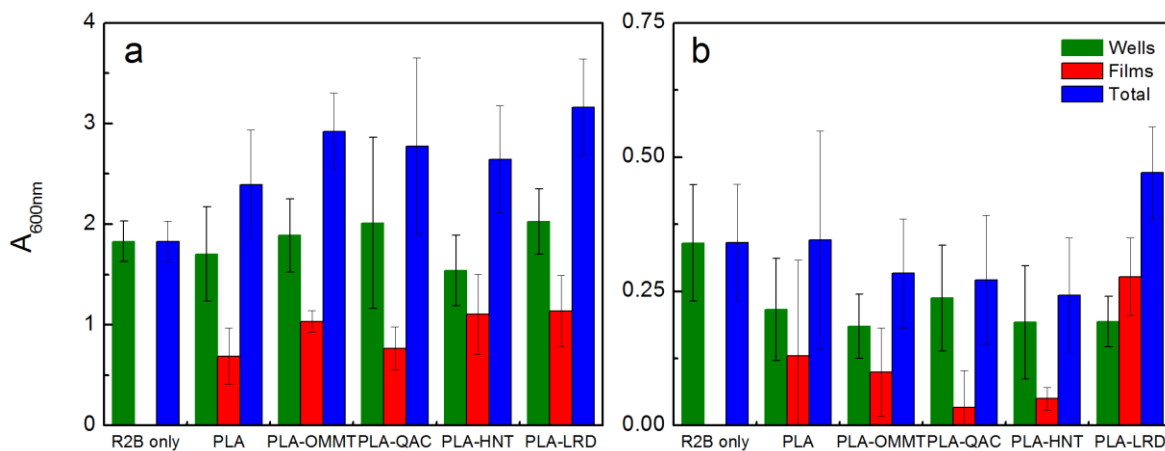


Figure 4E.1 Absorbance (600 nm) of (a) PA at 23°C, and (b) CE at 58°C first iteration.

Table 4E.1 Absorbance (600 nm) of a) PA at 23°C first iteration

Sample	Wells	Films	Total
w/o PLA	1.829 ± 0.201 ^A	N/A	1.829 ± 0.201 ^A
PLA	1.703 ± 0.467 ^A	0.688 ± 0.279 ^A	2.390 ± 0.544 ^A
PLA-OMMT	1.889 ± 0.363 ^A	1.035 ± 0.108 ^A	2.924 ± 0.379 ^A
PLA-QAC	2.012 ± 0.850 ^A	0.764 ± 0.214 ^A	2.776 ± 0.876 ^A
PLA-HNT	1.541 ± 0.351 ^A	1.105 ± 0.397 ^A	2.646 ± 0.530 ^A
PLA-LRD	2.028 ± 0.325 ^A	1.137 ± 0.353 ^A	3.165 ± 0.480 ^A

Note: Values with the same letter within the same column are not significantly different at $p \leq 0.05$ with Tukey-Kramer Test.

Regarding the test with CE at 58°C (**Figure 4E.1b**), the sterile controls (SCE) have values that are between 0.54 and 0.57, which are low values considering that the CE still contains humics and other compounds that can bind to polystyrene. The control wells (CE – No polymer) have values of 0.231-0.449. These values were less than the ones for PA at 23°C which is expected since PA is a pure culture of good biofilm former. The wells supplemented with PLA and BNCs look consistent overall in biofilm with values ranging from 0.087-0.312 and no statistically significant difference among them (**Table 4E.2**). In this case, the control well showed the highest average value of 0.340. PLA-LRD5 has an average value of 0.194. Biofilm formation was detected on PLA and BNCs with CE at 58°C. In this case, PLA-LRD5 has significantly higher value (0.277) than the rest of the BNCs. PLA showed an average value of 0.130 while the lowest average value (0.034) was observed with PLA-QAC0.4. The total biofilm (*i.e.*, wells plus films) was not significantly different among the sample materials.

Table 4E.2 Absorbance (600 nm) of a) CE at 58°C first iteration

Sample	Wells	Films	Total
w/o PLA	0.340 ± 0.109 ^A	N/A	0.341 ± 0.109 ^A
PLA	0.216 ± 0.095 ^A	0.130 ± 0.179 ^A	0.346 ± 0.203 ^A
PLA-OMMT	0.185 ± 0.060 ^A	0.099 ± 0.082 ^A	0.284 ± 0.102 ^A
PLA-QAC	0.237 ± 0.098 ^A	0.034 ± 0.069 ^A	0.271 ± 0.120 ^A
PLA-HNT	0.192 ± 0.105 ^A	0.050 ± 0.021 ^A	0.242 ± 0.107 ^A
PLA-LRD	0.194 ± 0.047 ^A	0.277 ± 0.072 ^A	0.471 ± 0.086 ^A

Note: Values with the same letter within the same column are not significantly different at $p \leq 0.05$ with Tukey-Kramer Test.

Similarly, **Table 4E.3** and **Table 4E.4** show the results of the biofilm test discussed in section 4.3.4 and **Figure 4.15**, with PA at 23°C and CE at 58°C.

Table 4E.3 Absorbance (600 nm) of PA at 23°C during the biofilm test

Sample	Wells	Films	Total
R2B only	1.279 ± 0.053 ^B	N/A	1.279 ± 0.053 ^{CD}
PLA2	1.376 ± 0.160 ^B	0.626 ± 0.125 ^{AB}	2.002 ± 0.204 ^{BC}
PLA-OMMT5	2.042 ± 0.243 ^A	0.875 ± 0.089 ^A	2.917 ± 0.259 ^A
PLA-QAC0.4	0.977 ± 0.180 ^B	0.131 ± 0.040 ^B	1.107 ± 0.185 ^D
PLA-HNT5	1.044 ± 0.061 ^B	1.254 ± 0.539 ^A	2.258 ± 0.542 ^{AB}
PLA-LRD5	1.078 ± 0.301 ^B	0.639 ± 0.097 ^{AB}	1.717 ± 0.316 ^{BCD}

Note: Values with the same letter within the same column are not significantly different at $p \leq 0.05$ with Tukey-Kramer Test.

Table 4E.4 Absorbance (600 nm) of CE at 58°C during the biofilm test

Sample	Wells	Films	Total
R2B only	0.485 ± 0.103 ^A	N/A	0.485 ± 0.103 ^A
PLA2	0.479 ± 0.124 ^A	0.090 ± 0.030 ^B	0.569 ± 0.128 ^A
PLA-OMMT5	0.360 ± 0.238 ^A	0.175 ± 0.073 ^B	0.536 ± 0.249 ^A
PLA-QAC0.4	0.338 ± 0.201 ^A	0.113 ± 0.032 ^B	0.451 ± 0.204 ^A
PLA-HNT5	0.367 ± 0.161 ^A	0.201 ± 0.014 ^B	0.568 ± 0.161 ^A
PLA-LRD5	0.384 ± 0.118 ^A	0.519 ± 0.054 ^A	0.903 ± 0.130 ^A

Note: Values with the same letter within the same column are not significantly different at $p \leq 0.05$ with Tukey-Kramer Test.

REFERENCES

REFERENCES

- [1] A.P. Kumar, D. Depan, N.S. Tomer, R.P. Singh, Nanoscale particles for polymer degradation and stabilization — Trends and future perspectives, *Prog. Polym. Sci.* 34 (2009) 479–515. doi:10.1016/j.progpolymsci.2009.01.002.
- [2] J.M. Lagaron, Nanotechnology for bioplastics: opportunities , challenges and strategies, *Trends Food Sci. Technol.* 22 (2011) 611–617. doi:10.1016/j.tifs.2011.01.007.
- [3] H.M.C. De Azeredo, Nanocomposites for food packaging applications, *Food Res. Int.* 42 (2009) 1240–1253. doi:10.1016/j.foodres.2009.03.019.
- [4] J.-M. Raquez, Y. Habibi, M. Murariu, P. Dubois, Polylactide (PLA)-based nanocomposites, *Prog. Polym. Sci.* 38 (2013) 1504–1542. doi:10.1016/j.progpolymsci.2013.05.014.
- [5] T. Kijchavengkul, R. Auras, Compostability of polymers, *Polym. Int.* 57 (2008) 793–804. doi:10.1002/pi.2420.
- [6] D.A.P. De Abreu, P.P. Losada, I. Angulo, J.M. Cruz, Development of new polyolefin films with nanoclays for application in food packaging, *Eur. Polym. J.* 43 (2007) 2229–2243. doi:10.1016/j.eurpolymj.2007.01.021.
- [7] M.M. Reddy, S. Vivekanandhan, M. Misra, S.K. Bhatia, A.K. Mohanty, Biobased plastics and bionanocomposites: Current status and future opportunities, *Prog. Polym. Sci.* 38 (2013) 1653–1689. doi:10.1016/j.progpolymsci.2013.05.006.
- [8] S.S. Ray, P. Maiti, M. Okamoto, K. Yamada, K. Ueda, New Polylactide/ Layered Silicate Nanocomposites. 1. Preparation, Characterization, and Properties, *Macromolecules.* 35 (2002) 3104–3110.
- [9] S.S. Ray, K. Yamada, M. Okamoto, K. Ueda, New polylactide-layered silicate nanocomposites. 2. Concurrent improvements of material properties, biodegradability and melt rheology, *Polymer (Guildf).* 44 (2003) 857–866.
- [10] S.S. Ray, K. Yamada, M. Okamoto, A. Ogami, K. Ueda, New polylactide/ layered silicate nanocomposites, 4. Structure, properties and biodegradability, *Compos. Interfaces.* 10 (2003) 435–450. doi:10.1163/156855403771953687.
- [11] S. Bourbigot, G. Fontaine, S. Duquesne, R. Delobel, PLA nanocomposites: quantification of clay nanodispersion and reaction to fire, *Int. J. Nanotechnol.* 5 (2008) 683–692.
- [12] S.S. Ray, K. Yamada, M. Okamoto, Y. Fujimoto, A. Ogami, K. Ueda, New polylactide/ layered silicate nanocomposites. 5. Designing of materials with

- desired properties, *Polymer* (Guildf). 44 (2003) 6633–6646. doi:10.1016/j.polymer.2003.08.021.
- [13] E. Picard, E. Espuche, R. Fulchiron, Effect of an organo-modified montmorillonite on PLA crystallization and gas barrier properties, *Appl. Clay Sci.* 53 (2011) 58–65. doi:10.1016/j.clay.2011.04.023.
- [14] G. Lo Re, S. Benali, Y. Habibi, J. Raquez, P. Dubois, Stereocomplexed PLA nanocomposites: From in situ polymerization to materials properties, *Eur. Polym. J.* 54 (2014) 138–150. doi:10.1016/j.eurpolymj.2014.03.004.
- [15] S. Ligot, S. Benali, R. Ramy-Ratiarison, M. Murariu, R. Snyders, P. Dubois, Mechanical, Optical and Barrier Properties of PLA-layered silicate nanocomposites coated with Organic Plasma Polymer Thin Films, *Mater. Sci. Eng. with Adv. Res.* 1 (2015) 1–11. doi:10.24218/msear.2015.04.
- [16] Y. Chen, L.M. Geever, J.A. Killion, J.G. Lyons, C.L. Higginbotham, D.M. Devine, Halloysite Nanotube Reinforced Polylactic Acid Composite, (2015) 1–8. doi:10.1002/pc.
- [17] Y.H. Kim, S.H. Kwon, H.J. Choi, K. Choi, N. Kao, N. Bhattacharya, R.K. Gupta, Thermal, Mechanical, and Rheological Characterization of Polylactic Acid / Halloysite Nanotube Nanocomposites, 2348 (2016). doi:10.1080/00222348.2016.1187054.
- [18] A. Kausar, Review on Polymer/Halloysite Nanotube Nanocomposite, *Polym. Plast. Technol. Eng.* 0 (2017) 1–17. doi:10.1080/03602559.2017.1329436.
- [19] M. Liu, Z. Jia, D. Jia, C. Zhou, Recent advance in research on halloysite nanotubes-polymer nanocomposite, *Prog. Polym. Sci.* 39 (2014) 1498–1525. doi:10.1016/j.progpolymsci.2014.04.004.
- [20] M. Murariu, A.-L. Dechief, Y. Paint, S. Peeterbroeck, L. Bonnaud, P. Dubois, Poly(lactide) (PLA)— Halloysite Nanocomposites: Production, Morphology and Key-Properties, *J. Polym. Environ.* 20 (2012) 932–943. doi:10.1007/s10924-012-0488-4.
- [21] K. Prashantha, B. Lecouvet, M. Sclavons, M.F. Lacrampe, P. Krawczak, Poly(lactic acid)/ Halloysite Nanotubes Nanocomposites: Structure, Thermal, and Mechanical Properties as a Function of Halloysite Treatment, *J. Appl. Polym. Sci.* (2013) 1895–1903. doi:10.1002/app.38358.
- [22] W. Wu, X. Cao, Y. Zhang, G. He, Poly(lactide)/ Halloysite Nanotube Nanocomposites: Thermal, Mechanical Properties, and Foam Processing, *J. Appl. Polym. Sci.* (2013) 443–452. doi:10.1002/app.39179.
- [23] P. Russo, S. Cammarano, E. Bilotti, T. Peijs, P. Cerruti, D. Acierno, Physical Properties of Poly Lactic Acid / Clay Nanocomposite Films: Effect of Filler Content

- and Annealing Treatment, *Journ.* 5 (2014) 1–8. doi:10.1002/app.39798.
- [24] C. Esmā, Y. Erpek, G. Ozkoc, U. Yilmazer, Effects of Halloysite Nanotubes on the Performance of Plasticized Poly (lactic acid)-Based Composites, *Polym. Compos.* (2015). doi:10.1002/pc.
- [25] F.A. Aouada, L.H.C. Mattoso, E. Longo, A simple procedure for the preparation of lapo- nite and thermoplastic starch nanocomposites: Structural, mechanical, and thermal characterizations, *J. Thermoplast. Compos. Mater.* 0 (2011) 1–14. doi:10.1177/0892705711419697.
- [26] X. Tang, S. Alavi, Structure and Physical Properties of Starch/Poly Vinyl Alcohol/ Laponite RD Nanocomposite Films, *J. Agric. Food Chem.* 60 (2012) 1954–1962.
- [27] W. Loyens, P. Jannasch, F.H.J. Maurer, Poly (ethylene oxide)/ Laponite nanocomposites via melt-compounding: effect of clay modification and matrix molar mass, *Polymer (Guildf)*. 46 (2005) 915–928. doi:10.1016/j.polymer.2004.11.076.
- [28] L.A. Utracki, M. Sepehr, E. Boccaleri, Synthetic, layered nanoparticles for polymeric nanocomposites (PNCs), *Polym. Adv. Technol.* 18 (2007) 1–37. doi:10.1002/pat.852.
- [29] G.F. Perotti, J. Tronto, M.A. Bizeto, C.M.S. Izumi, M.L.A. Temperini, A.B. Lugao, D.F. Parra, V.R.L. Constantino, Biopolymer-Clay Nanocomposites: Cassava Starch and Synthetic Clay Cast Films, *J. Brazilian Chem.* 25 (2014) 320–330.
- [30] C.-J. Wu, A.K. Gaharwar, P.J. Schexnailder, G. Schmidt, Development of Biomedical Polymer-Silicate Nanocomposites: A Materials Science Perspective, *Materials (Basel)*. 3 (2010) 2986–3005. doi:10.3390/ma3052986.
- [31] G.X. Zhou, M.W. Yuan, L. Jiang, M.L. Yuan, H.L. Li, The Preparation and Property Research on Laponite-Poly (L-Lactide) Composite Film, *Adv. Mater. Res.* 750 (2013) 1919–1923.
- [32] H.L. Li, G.X. Zhou, Y.K. Shan, M.L. Yuan, The Mechanical Properties and Hydrophilicity of Poly (L-Lactide)/Laponite Composite Film, *Adv. Mater. Res.* 706 (2013) 340–343.
- [33] P. Stloukal, S. Pekařová, A. Kalendova, H. Mattausch, S. Laske, C. Holzer, L. Chitu, S. Bodner, G. Maier, M. Slouf, M. Koutny, Kinetics and mechanism of the biodegradation of PLA/clay nanocomposites during thermophilic phase of composting process, *Waste Manag.* 42 (2015) 31–40. doi:10.1016/j.wasman.2015.04.006.
- [34] T. Wu, T. Xie, G. Yang, Preparation and characterization of poly (ϵ -caprolactone)/ Na + -MMT nanocomposites, *Appl. Clay Sci.* 45 (2009) 105–110. doi:10.1016/j.clay.2009.02.009.

- [35] M.C.S. Correa, M.C. Branciforti, E. Pollet, J.A.M. Agnelli, P.A.P. Nascente, L. Averous, Elaboration and Characterization of Nano-Biocomposites Based on Plasticized Poly (Hydroxybutyrate-Co-Hydroxyvalerate) with Organo-Modified Montmorillonite, *J. Polym. Environ.* 20 (2012) 283–290. doi:10.1007/s10924-011-0379-0.
- [36] N.F. Magalhães, C.T. Andrade, Thermoplastic corn starch/ clay hybrids: Effect of clay type and content on physical properties, *Carbohydr. Polym.* 75 (2009) 712–718. doi:10.1016/j.carbpol.2008.09.020.
- [37] S.-R. Lee, H. Park, H. Lim, T. Kang, X. Li, W.-J. Cho, C.-S. Ha, Microstructure, tensile properties, and biodegradability of aliphatic polyester/ clay nanocomposites, *Polymer (Guildf)*. 43 (2002) 2495–2500.
- [38] M.A. Paul, C. Delcourt, M. Alexandre, P. Degee, F. Monteverde, P. Dubois, Polylactide/ montmorillonite nanocomposites: study of the hydrolytic degradation, *Polym. Degrad. Stab.* 87 (2005) 535–542. doi:10.1016/j.polymdegradstab.2004.10.011.
- [39] Y.H. Lee, J.H. Lee, I. An, C. Kim, D.S. Lee, Y.K. Lee, J. Nam, Electrospun dual-porosity structure and biodegradation morphology of Montmorillonite reinforced PLLA nanocomposite scaffolds, *Biomaterials.* 26 (2005) 3165–3172. doi:10.1016/j.biomaterials.2004.08.018.
- [40] K. Fukushima, C. Abbate, D. Tabuani, M. Gennari, G. Camino, Biodegradation of poly (lactic acid) and its nanocomposites, *Polym. Degrad. Stab.* 94 (2009) 1646–1655. doi:10.1016/j.polymdegradstab.2009.07.001.
- [41] P.K. Roy, M. Hakkarainen, A. Albertsson, Nanoclay effects on the degradation process and product patterns of polylactide, *Polym. Degrad. Stab.* 97 (2012) 1254–1260. doi:10.1016/j.polymdegradstab.2012.05.032.
- [42] S. Molinaro, M.C. Romero, M. Boaro, A. Sensidoni, C. Lagazio, M. Morris, J. Kerry, Effect of nanoclay-type and PLA optical purity on the characteristics of PLA-based nanocomposite films, *J. Food Eng.* 117 (2013) 113–123. doi:10.1016/j.jfoodeng.2013.01.021.
- [43] P.M.S. Souza, A.R. Morales, M.A. Marin-Morales, L.H.I. Mei, PLA and Montmorillonite Nanocomposites: Properties , Biodegradation and Potential Toxicity, *J. Polym. Environ.* 21 (2013) 738–759. doi:10.1007/s10924-013-0577-z.
- [44] A. V. Machado, A. Araújo, M. Oliveira, Assessment of polymer-based nanocomposites biodegradability, (2014).
- [45] M.P. Balaguer, C. Aliaga, C. Fito, M. Hortal, Compostability assessment of nano-reinforced poly(lactic acid) films, *Waste Manag.* 48 (2016) 143–155. doi:10.1016/j.wasman.2015.10.030.

- [46] J.M. Cowley, *Diffraction Physics*, 3rd ed., Elsevier B.V., Amsterdam, 1995.
- [47] E. Castro-Aguirre, R. Auras, S. Selke, M. Rubino, T. Marsh, Insights on the aerobic biodegradation of polymers by analysis of evolved carbon dioxide in simulated composting conditions, *Polym. Degrad. Stab.* 137 (2017) 251–271. doi:10.1016/j.polymdegradstab.2017.01.017.
- [48] J.H. Merritt, D.E. Kadouri, G.A. O’Toole, Growing and analyzing static biofilms, *Curr. Protoc. Microbiol.* (2011) 1–18. doi:10.1002/9780471729259.mc01b01s22.
- [49] S.M. Satti, A.A. Shah, R. Auras, T.L. Marsh, Isolation and characterization of bacteria capable of degrading poly(lactic acid) at ambient temperature, *Polym. Degrad. Stab.* 144 (2017) 392–400. doi:10.1016/j.polymdegradstab.2017.08.023.
- [50] G. Gorrasi, R. Pantani, Effect of PLA grades and morphologies on hydrolytic degradation at composting temperature: Assessment of structural modification and kinetic parameters, *Polym. Degrad. Stab.* 98 (2013) 1006–1014. doi:10.1016/j.polymdegradstab.2013.02.005.
- [51] F. Iñiguez-Franco, R. Auras, G. Burgess, D. Holmes, X. Fang, M. Rubino, H. Soto-Valdez, Concurrent solvent induced crystallization and hydrolytic degradation of PLA by water-ethanol solutions, *Polym.* (United Kingdom). 99 (2016) 315–323. doi:10.1016/j.polymer.2016.07.018.
- [52] W.L. Tham, T. Poh, Z. Arifin, M. Ishak, W.S. Chow, Characterisation of Water Absorption of Biodegradable Poly (lactic Acid)/ Halloysite Nanotube Nanocomposites at Different Temperatures, 12 (2016) 13–25.
- [53] R.T. De Silva, M. Soheilmoghaddam, K.L. Goh, M.U. Wahit, S. Bee, A. Hamid, S. Chai, P. Pasbakhsh, Influence of the Processing Methods on the Properties of Poly (lactic acid)/ Halloysite Nanocomposites, (2014) 1–9. doi:10.1002/pc.
- [54] A.H. Touny, A.D. Jones, Effect of electrospinning parameters on the characterization of PLA / HNT nanocomposite fibers, (2010) 857–865. doi:10.1557/JMR.2010.0122.
- [55] N. Cai, Q. Dai, Z. Wang, Toughening of electrospun poly (L -lactic acid) nanofiber scaffolds with unidirectionally aligned halloysite nanotubes, (2015) 1435–1445. doi:10.1007/s10853-014-8703-4.
- [56] Y. Dong, J. Marshall, H.J. Haroosh, S. Mohammadzadehmoghadam, D. Liu, X. Qi, K. Lau, Composites : Part A Polylactic acid (PLA)/ halloysite nanotube (HNT) composite mats : Influence of HNT content and modification, *Compos. PART A.* 76 (2015) 28–36. doi:10.1016/j.compositesa.2015.05.011.
- [57] G. Gorrasi, R. Pantani, M. Murariu, P. Dubois, PLA / Halloysite Nanocomposite Films : Water Vapor Barrier Properties and Specific Key Characteristics, (2012) 20–22. doi:10.1002/mame.201200424.

- [58] ASTM Standard D5338-15, Standard Test Method for Determining Aerobic Biodegradation of Plastic Materials Under Controlled Composting Conditions, Incorporating Thermophilic Temperatures, ASTM B. Stand. (2015).
- [59] ISO 14855-1:2012, Determination of the ultimate aerobic biodegradability of plastic materials under controlled composting conditions — Method by analysis of evolved carbon dioxide — Part 1: General method, (2012) 20.
- [60] T. Kijchavengkul, R. Auras, M. Rubino, M. Ngouajio, R. Thomas Fernandez, Development of an automatic laboratory-scale respirometric system to measure polymer biodegradability, *Polym. Test.* 25 (2006) 1006–1016. doi:10.1016/j.polymertesting.2006.06.008.
- [61] E. Castro-Aguirre, F. Iñiguez-Franco, H. Samsudin, X. Fang, R. Auras, Poly(lactic acid)—Mass production, processing, industrial applications, and end of life, *Adv. Drug Deliv. Rev.* 107 (2016) 333–366. doi:10.1016/j.addr.2016.03.010.
- [62] K. Fukushima, E. Giménez, L. Cabedo, J.M. Lagarón, J.L. Feijoo, Biotic degradation of poly (DL -lactide) based nanocomposites, *Polym. Degrad. Stab.* 97 (2012) 1278–1284. doi:10.1016/j.polymdegradstab.2012.05.029.
- [63] K. Fukushima, D. Tabuani, M. Dottori, I. Armentano, J.M. Kenny, G. Camino, Effect of temperature and nanoparticle type on hydrolytic degradation of poly (lactic acid) nanocomposites, *Polym. Degrad. Stab.* 96 (2011) 2120–2129. doi:10.1016/j.polymdegradstab.2011.09.018.
- [64] G. Bellia, M. Tosin, F. Degli-Innocenti, Test method of composting in vermiculite is unaffected by the priming effect, *Polym. Degrad. Stab.* 69 (2000) 113–120. doi:10.1016/S0141-3910(00)00048-3.
- [65] D.N. Bikiaris, Nanocomposites of aliphatic polyesters: An overview of the effect of different nanofillers on enzymatic hydrolysis and biodegradation of polyesters, *Polym. Degrad. Stab.* 98 (2013) 1908–1928. doi:10.1016/j.polymdegradstab.2013.05.016.
- [66] G. Bellia, M. Tosin, G. Floridi, F. Degli-Innocenti, Activated vermiculite, a solid bed for testing biodegradability under composting conditions, *Polym. Degrad. Stab.* 66 (1999) 65–79. doi:10.1016/S0141-3910(99)00053-1.
- [67] H. Tsuji, Y. Ikada, Blends of crystalline and amorphous poly(lactide) .3. Hydrolysis of solution-cast blend films, *J. Appl. Polym. Sci.* 63 (1997) 855–863. doi:papers://590F92D9-0B76-4B88-8729-9AF064BE5AC8/Paper/p4495.
- [68] H. Tsuji, T. Saeki, T. Tsukegi, H. Daimon, K. Fujie, Comparative study on hydrolytic degradation and monomer recovery of poly(l-lactic acid) in the solid and in the melt, *Polym. Degrad. Stab.* 93 (2008) 1956–1963. doi:10.1016/j.polymdegradstab.2008.06.009.

- [69] P.K. Annamalai, D.J. Martin, P.K. Annamalai, D.J. Martin, Can clay nanoparticles accelerate environmental biodegradation of polyolefins?, *Mater. Sci. Technol.* 30 (2014) 593–602. doi:10.1179/1743284713Y.0000000498.
- [70] J.P. Eubeler, M. Bernhard, T.P. Knepper, Environmental biodegradation of synthetic polymers II. Biodegradation of different polymer groups, *TrAC - Trends Anal. Chem.* 29 (2010) 84–100. doi:10.1016/j.trac.2009.09.005.
- [71] J.T. Lennon, B.K. Lehmkuhl, A trait-based approach to bacterial biofilms in soil, *Environ. Microbiol.* 18 (2016) 2732–2742. doi:10.1111/1462-2920.13331.
- [72] S.G. Ali, M.A. Ansari, H.M. Khan, M. Jalal, A.A. Mahdi, S.S. Cameotra, Crataeva nurvala nanoparticles inhibit virulence factors and biofilm formation in clinical isolates of *Pseudomonas aeruginosa*, *J. Basic Microbiol.* 57 (2017) 193–203. doi:10.1002/jobm.201600175.
- [73] J. Overhage, S. Lewenza, A.K. Marr, R.E.W. Hancock, Identification of genes involved in swarming motility using a *Pseudomonas aeruginosa* PAO1 mini-Tn5-lux mutant library, *J. Bacteriol.* 189 (2007) 2164–2169. doi:10.1128/JB.01623-06.
- [74] M. Wojdyr, Fityk: A general-purpose peak fitting program, *J. Appl. Crystallogr.* 43 (2010) 1126–1128. doi:10.1107/S0021889810030499.
- [75] A. Perejón, P.E. Sánchez-Jiménez, J.M. Criado, L.A. Pérez-Maqueda, Kinetic Analysis of Complex Solid-State Reactions. A New Deconvolution Procedure, *J. Phys. Chem. B.* 115 (2011) 1780–1791. doi:10.1021/jp110895z.

CHAPTER 5

ENHANCING THE BIODEGRADATION RATE OF POLY(LACTIC ACID) FILMS AND PLA BIO-NANOCOMPOSITES IN SIMULATED COMPOSTING THROUGH BIOAUGMENTATION

A version of this chapter is published as:

Castro-Aguirre, E., Auras, R., Selke, S., Rubino, M., Marsh, T. Enhancing the biodegradation rate of poly(lactic acid) films and PLA bio-nanocomposites in simulated composting through bioaugmentation, *Polymer Degradation and Stability*, 154 (2018) 46

– 54.

5.0 Abstract

Biodegradable polymers provide an opportunity to divert plastic waste from landfills, with composting as an alternative disposal route. However, some biodegradable polymers, such as poly(lactic acid) (PLA), do not biodegrade as fast as other organic wastes during composting, affecting their general acceptance in industrial composting facilities. Bioaugmentation, the addition of specific microbial strains, is a promising technique to accelerate the biodegradation of compostable plastics, so that they biodegrade in comparable time frames with other organic materials. In this study, we evaluated the effect of bioaugmentation on the biodegradation of PLA and PLA biocomposites (BNCs) in simulated composting conditions. PLA, PLA with 5% organo-modified montmorillonite (PLA-OMMT5), and PLA with 0.4% surfactant (PLA-QAC0.4) films were produced and fully characterized. PLA-degrading bacteria were isolated through an enrichment technique with PLA as the sole carbon source at 58°C. Isolates were identified as *Geobacillus* using 16S rRNA gene sequencing and the NCBI database, and further used to study the effect of bioaugmentation on the biodegradation rate of PLA and BNCs in solid environments. The biotic and abiotic degradation was assessed in compost, inoculated vermiculite, and uninoculated vermiculite at 58°C by analysis of evolved CO₂ using an in-house built direct measurement respirometer. Size exclusion chromatography was also used to measure and to monitor the change in molecular weight of the film samples retrieved every week during the biodegradation test. The microbial attachment on the surface of PLA of the isolated microbial strain and other microorganisms present in the compost was evaluated by a biofilm forming assay in wells incubated at 58°C. Bioaugmentation with *Geobacillus* increased the evolution of

CO₂ and accelerated the biodegradation phase of PLA and BNCs when tested in compost and inoculated vermiculite with compost mixed culture. Bioaugmentation could commercially be used to accelerate the biodegradation of PLA in compost environments.

5.1 Introduction

Plastics represent 12.9% of the 258 million tons of municipal solid waste (MSW) generated in 2014 in the USA, from which only 9.5% was recovered (*i.e.*, recycling and composting), the recycled plastics were mostly polyethylene and polyethylene terephthalate. Hence, most plastic waste (25.1 million tons) ended up accumulating in landfills, which is a major environmental concern [1]. Compostable polymers, like poly(lactic acid) (PLA), represent a promising way to divert plastic waste from landfills, replacing conventional polymers for some applications, especially for non-durable goods and single-use products like packaging, disposable plates and cutlery, and contaminated plastic waste (*e.g.*, food packaging and agricultural mulch films) [2]. However, such benefit is only accomplished if PLA-based products reach the desired disposal system at their end of life. The ideal scenario is one in which these products/ packaging would be collected and sent along with the organic wastes to commercial composting facilities. However, one of the main current challenges for PLA-based materials to be widely accepted in composting facilities at their end of life is that their biodegradation in composting is usually slower than that for other organic wastes [3]. In Chapter 4, we studied the impact of different nanoclays (*e.g.*, organo-modified montmorillonite, OMMT, and its organo-modifier, methyl, tallow, bis-2-hydroxyethyl, quaternary ammonium, QAC) on the biodegradation rate of PLA bio-nanocomposites

(BNCs) in different solid environments (*i.e.*, compost and vermiculite), and on microbial attachment using a “*mixed culture*” extracted from the compost. It was found that the presence of OMMT seems to accelerate the initial phase of biodegradation, but not the final mineralization phase, and to promote microbial attachment in comparison to the pristine PLA under certain conditions [3]. Therefore, there is interest in knowing which specific microbial strains present in the compost can bind to PLA and preferentially biodegrade PLA and its BNCs, and whether they can be purposely used to accelerate the biodegradation mechanism.

Some researchers have identified the microbial consortia present in the compost environment [4–7], and others have reported the isolation and identification of several species capable of biodegrading PLA [8–15], and other polymers [16–24] by 16S rRNA sequence analysis. In this context, bioaugmentation (*i.e.*, the addition of specific microbial strains) is a promising technique that can be studied and used to accelerate the biodegradation of compostable plastics, so that they biodegrade in comparable time frames with other organic wastes. Increasing the biodegradation rate of PLA should facilitate its disposal through composting since PLA-based products and organic materials could biodegrade in a similar period of time.

This study aimed first to isolate and to identify the microbial strains present in the compost capable of biodegrading PLA, and second, to evaluate the effect of introducing such microbial strains on the biodegradation rate of PLA and its BNCs in simulated composting conditions (*i.e.*, in a solid environment at 58°C), since most of the studies found in the literature have been performed in liquid media, which do not necessarily represent real composting conditions.

5.2 Materials and Methods

5.2.1 Materials

Ingeo™ 2003D resin, poly(lactic acid), was acquired from NatureWorks LLC. (Minnetonka, MN, USA). Cellulose powder with particle size ~20 µm was purchased from Sigma-Aldrich (St. Louis, MO, USA). Cloisite® 30B, organo-modified montmorillonite (OMMT), was obtained from BYK Additives Inc. (Gonzales, TX, USA). Tomamine™ Q-T-2 (QAC) with 60 - 70% purity of a methyl, tallow, bis-2-hydroxyethyl, quaternary ammonium, the organo-modifier of Cloisite® 30B, was obtained from Air Products and Chemicals Inc. (Butler, IN, USA). The composition per liter of the R2 broth (R2B) used was 0.5 g yeast extract, 0.5 g proteose peptone #3, 0.5 g casamino acids, 0.5 g dextrose, 0.5 g soluble starch, 0.3 g sodium pyruvate, 0.3 g dipotassium phosphate, and 0.05 g magnesium sulfate. Additionally, GELRITE® gellan gum (CP Kelco, Inc., San Diego, CA, USA) was used to produce R2A plates. The composition per liter of the M9 minimal medium was 12.8 g Na₂HPO₄·7H₂O, 3 g KH₂PO₄, 0.5 g NaCl, 1 g NH₄Cl, and 1 g of 1 mM MgSO₄, 1 mM CaCl₂, 3×10⁻⁹ M (NH₄)₆Mo₇O₂₄·4H₂O, 4×10⁻⁷ M H₃BO₃, 3×10⁻⁸ M CoCl₂·6H₂O, 1×10⁻⁸ M CuSO₄·5H₂O, 8×10⁻⁸ M MnCl₂·4H₂O, 1×10⁻⁸ M ZnSO₄·7H₂O, 1×10⁻⁶ M FeSO₄·7H₂O. All the materials were used as received unless indicated.

5.2.1.1 Material processing and characterization

PLA pellets were dried prior to processing for 8 h under vacuum (85 kPa) at 60°C. PLA-OMMT5 (5% wt. OMMT) and PLA-QAC0.4 (0.4% surfactant) films were processed in two steps: 1) masterbatches were processed in a ZSK 30 twin-screw extruder (Werner Pfleiderer Co., Ramsey, NJ, USA) with temperature range of 146-186°C and screw

speed of 130 rpm; 2) the films were extruded in a RCP-0625 microextruder model (Randcastle Extrusion Systems, Inc., Cedar Grove, NJ, USA), screw diameter of 1.59 cm, L/D ratio of 24, and volume of 34 cc. The processing temperature range for the PLA-OMMT film was 193 – 248°C with a screw speed of 18 rpm, and for the PLA-QAC film was 143 – 173°C with a speed of 31 rpm. A pristine PLA film was produced in the same film extruder with processing temperature range of 193 – 249°C and screw speed of 28 rpm. The thicknesses were 0.073 ± 0.014 , 0.039 ± 0.008 , and 0.034 ± 0.009 mm for PLA-OMMT5, PLA-QAC0.4 and PLA films, respectively.

The extruded films were fully characterized, as described in Chapter 4 [3]. The carbon, hydrogen, and nitrogen contents of the different films were obtained with a CHNS/O Elemental Analyzer, PerkinElmer 2400 Series II (Shelton, CT, USA), and values are presented in **Table 5.1**.

Table 5.1 Carbon, hydrogen, and nitrogen content of the tested materials

Material	% Carbon^a	% Hydrogen^a	% Nitrogen^a
Cellulose	42.50 ± 0.34	6.53 ± 0.05	0.04 ± 0.01
PLA	49.99 ± 0.05	5.60 ± 0.01	0.01 ± 0.01
PLA-OMMT5	48.76 ± 0.07	5.49 ± 0.02	0.07 ± 0.01
PLA-QAC0.4	49.98 ± 0.08	5.55 ± 0.02	0.01 ± 0.00

^a Percentage by weight

5.2.2 Isolation of PLA-degrading microbial strain

The isolation of PLA-degrading microbial strains was performed through a serial enrichment technique. Compost (1 g) was inoculated in 25 mL of fresh M9 minimal media in a 100-mL Erlenmeyer flask containing twenty PLA pellets as sole carbon source and incubated in a shaker at 58°C and 70 rpm. After a week, five PLA pellets were aseptically transferred to fresh M9 medium containing twenty new PLA pellets along with 100 µL of the previous culture and incubated for 7 days under the same

conditions. This procedure was repeated for six more consecutive transfers to capture potential PLA-degrading microbial strains. The final enrichment (100 mL) was spread across R2A plates using serial dilution techniques and incubated at 58°C. Six isolated colonies were selected and purified using the streak-plating method after three consecutive transfers that were performed every three days. Purified strains were stored in 20% glycerol at –80°C for further analyses.

5.2.3 Identification of PLA-degrading microbial strain

Microbial isolates were identified using 16S rRNA gene sequencing. Overnight broth cultures of isolates were used for genomic DNA extraction by mixing 20 µL of culture with 200 µL of Alkaline-PEG lysis reagent [25] and incubating for 5 min at 55°C and then store at -20°C. DNA extractions (2 µL) were used as templates for polymerase chain reaction (PCR) amplification of 16S rRNA using bacterial primers 27F (50-AGAGTTTGATCCTGGCTCAG-30) and 1389R (50-ACGGGCGGTGTGTACAAG-30). Each PCR reaction mix contained 25 µL of master mix (GoTaq® Master Mix, Promega, Madison, WI, USA), 2 µL of template, 1.2 µL of each primer and the rest was Milli Q® water to adjust the volume to 50 µL. The PCR amplifications were performed using an Applied Biosystems™ 2720 Thermal Cycler (Thermo Fisher Scientific Inc., Wilmington, DE, USA) with the following reaction conditions: initial denaturation of DNA at 94°C for 5 min followed by the amplification cycle with denaturation at 94°C for 45 s, annealing at 55.5°C for 45 s, and extension at 72°C for 1 min. The cycling concluded with an extension at 72°C for 7 min, and then it was kept at 4°C. The PCR products were purified using QIAquick® PCR Purification Kit (50) (Qiagen Sciences Inc., Germantown, MD, USA) following the instructions from the manufacturer. The concentration of DNA in

the purified samples was obtained with a NanoDrop® ND-1000 spectrophotometer and ND-1000 V3.1.8 software (Thermo Fisher Scientific Inc., Wilmington, DE, USA). The purified PCR products were mixed with the 27F or 1389R primer (~60ng of PCR product with 30 pmoles of primer) and sent for Sanger sequencing at the Research Technology Support Facility (RTSF) at Michigan State University (MSU). Identification of the microbial strains was performed using the Sequence Match function of the Ribosomal Database Project (RDP) from the Center for Microbial Ecology at MSU (rdp.cme.msu.edu), based on the National Center for Biotechnology Information (NCBI) taxonomy [26].

5.2.4 Biodegradation evaluation

5.2.4.1 Preparation of the compost and vermiculite

The aerobic biodegradation of the PLA, PLA-OMMT5, and PLA-QAC0.4 films was evaluated by CO₂ analysis in simulated composting at 58°C, using the direct measurement respirometer (DMR) and methodology described elsewhere [27]. In brief, compost was obtained from the Composting Facility at MSU (East Lansing, MI, USA) and then mixed with saturated vermiculite (Premium grade, Sun Gro Horticulture Distribution Inc., Bellevue, WA, USA) using a 1:4 ratio of dry weight compost. The moisture content of the mix was increased to ~50% by adding deionized water. Biodegradation tests were also carried out with uninoculated and inoculated vermiculite to study abiotic degradation and bioaugmentation. In the case of inoculation with a *mixed culture* (i.e., microbial consortia extracted from compost), vermiculite was mixed in a proportion of 1:4 (wt.) with the inoculum solution prepared by combining compost extract with a mineral solution at a 1:1 ratio. Detailed information about the preparation

of the mineral solution and the compost extract can be found elsewhere [27,28]. In the case of bioaugmentation studies in vermiculite, the inoculum solution was prepared by combining the mineral solution with a pure culture of the PLA-degrading microbial strain. The initial physicochemical parameters of the compost and vermiculite were determined in the Soil and Plant Nutrient Laboratory at MSU (East Lansing, MI, USA) and shown in **Table 5.2**. A complete list of the compost and vermiculite total nutrient analysis is provided in the Appendix 5A (**Table 5A.1**).

Table 5.2 Initial physicochemical parameters of the compost and vermiculite used for biodegradation tests

Parameters	ISO ^b	Biodegradation Test		
Type of media ^c	C	C	IV	V
Dry solids, %	50-55	51.8	21.4	18.9
Volatile solids, %	<30	41.3	2.8	3.1
pH	7-9	7.9	6.8	8.2
Total Carbon, %	N/A ^a	24.0	1.6	1.8
Total Nitrogen, %	N/A ^a	2.4	0.2	0.03
C/N ratio	10-40	9.9	10.2	59.9

^a Not applicable or not available

^b Values based on ISO 14855-1:2005 standard for compost

^c C= compost; IV= inoculated vermiculite; V= uninoculated vermiculite

5.2.4.2 Bioreactor setup

The bioreactors were filled with a mixture of 400 g (wet wt.) of media (either compost, inoculated or uninoculated vermiculite) and 8 g of film samples (1 cm x 1 cm pieces). Triplicates of each sample material, positive controls (cellulose powder), and blanks (media only) were analyzed. The bioreactors were provided with water-saturated CO₂-free air at a flow rate of 40 ± 2 sccm (standard cubic centimeters per minute) and incubated in the dark at 58 ± 2°C. Detailed information on the testing conditions using the DMR system can be found elsewhere [27].

5.2.4.3 Bioaugmentation

For the bioaugmentation studies, all media were inoculated with a pure culture of the PLA-degrading strain. First, the purified strain was inoculated in 25 mL of R2B in a 100-mL Erlenmeyer flask and incubated overnight at 58°C in an Innova™ 4300 shaker (New Brunswick Scientific Co., Edison, NJ, USA). Then, this culture was used as inoculum for a 500 mL culture, also in R2B, and incubated for 48 hours in the shaker at 58°C. Direct cell counting was performed to determine the number of microorganisms in the culture using disposable counting slides (Nexcelom Bioscience LLC., Lawrence, MA, USA) following the instructions of the manufacturer. Cells were counted on a Nikon Eclipse E600 microscope (Nikon Instruments Inc., Melville, NY, USA) using phase-contrast at 1000x final magnification. This pure culture was used to inoculate the bioreactors by adding cells equivalent to 1% of the total community in a bioreactor, assuming that there was approximately 1×10^8 bacteria/g in compost. The 48-hour culture was diluted with either water (for compost) or the inoculum solution (for vermiculite) to reach the 1% target.

5.2.5 Biofilm formation

The microbial attachment of the PLA-degrading strain on PLA, PLA-OMMT5, and PLA-QAC0.4 was evaluated through a biofilm formation test using a standard microtiter plate assay (24-well Corning®, Corning Inc., Corning, NY, USA) as previously described [3]. In brief, sterilized film samples were mixed with 600 µL of R2B and 200 µL of an overnight grown culture of the purified strain and incubated in a shaker (100 rpm) at 58°C for 48 hours (4 replicates tested). As explained in the previous study, *Pseudomonas aeruginosa* (PA), strain PAO1, was used as a positive control at 23°C,

and uninoculated wells as a negative control [3]. After incubation, wells and films were gently rinsed with water, stained with 800 μ L of 0.5% crystal violet for 15 min, and resolubilized for measurement in 800 μ L of 30% acetic acid for 15 min. The absorbance at 600 nm was determined with an Epoch™ Microplate Spectrophotometer (BioTek Instruments, Inc., Winooski, VT, USA).

5.2.6 Size Exclusion Chromatography (SEC)

The molecular weight distribution (*MWD*) and number average molecular weight (*Mn*) of the PLA, PLA-OMMT5 and PLA-QAC0.4 film samples collected at different periods of time during the bioaugmentation test were obtained by SEC as previously described [3,27]. In brief, 10 mg of sample were dissolved in 5 mL of tetrahydrofuran (THF) and filtered prior to injection (1 cm³/min flow rate for 50 min at 35°C) in a gel permeation chromatography system (Waters Inc., Milford, MA, USA). Polystyrene standards (0.5 – 2,480 kDa) were used for the calibration of the system.

5.2.7 Statistical Analysis

Minitab18 software (Minitab Inc., State College, PA, USA) was used to conduct analysis of variance (one-way ANOVA) and Tukey-Kramer tests with $p \leq 0.05$. All the results show mean and standard deviation.

5.3 Results and Discussion

5.3.1 Isolation and identification of PLA-degrading bacteria

A serial enrichment technique was used with M9 minimal media and PLA as the sole carbon source, and compost as the only source of microorganisms (initial stage) to determine the microbial strains able to biodegrade PLA. The incubation temperature was set at 58°C to simulate an active composting phase. This procedure was followed

by isolation through the streak-plating method, and identification using 16S rRNA Sanger sequencing. The results from the MSU-RDP Sequence Match based on the NCBI database (**Table 5.3**) showed that the isolates were *Geobacillus*, closest to *G. thermoleovorans*. The sequence matching function was configured so it only retrieved the strains from the NCBI database closest to the isolated strains (KNN = 1). *Geobacillus thermoleovorans*, referred to from now on, as *Geobacillus* only, were further used to study the effect of bioaugmentation on the biodegradation rate of PLA in solid environments, and biofilm formation on the surface of the PLA film and BNCs. *Geobacillus* spp. can be found in terrestrial and marine environments and are capable of surviving in extreme environments like high temperature and limited resources [29,30]. They can grow under low nitrogen and low oxygen conditions [31]. They are Gram-positive, thermophilic, motile, rod-shaped, spore-forming bacteria [29–32]. *Geobacillus* spp. have optimal growth temperatures ranging from 55 to 65°C and pH ranging from 6.0 to 8.5 [30–32]. These attributes are consistent with conditions found in composting environments. Moreover, it has been reported that *Geobacillus* are able to utilize a variety of sugars, carboxylic acids and hydrocarbons [30], and they can grow on R2A broth, lactose, lactate, and C13-C20 *n*-alkanes [31]. A complete list of current valid species for the genus *Geobacillus* can be found elsewhere [33].

Table 5.3 Identification of the microbial isolates using the MSU-RDP Sequence Match and the NCBI database

Isolate ID	No. bases of sequence	Sab Score	Closest strain	GenBank Accession number
EC-1	1406	0.978	<i>Geobacillus themoleovorans</i>	MH183210
EC-2	1406	0.989	<i>Geobacillus themoleovorans</i>	MH183211
EC-3	1406	0.977	<i>Geobacillus thermoleovorans</i>	MH183212
EC-4	1406	0.985	<i>Geobacillus themoleovorans</i>	MH183213
EC-5	1406	0.962	<i>Geobacillus themoleovorans</i>	MH183214
EC-6	1406	0.994	<i>Geobacillus themoleovorans</i>	MH183215

5.3.2 Biodegradation Test

The biodegradation of PLA, PLA-OMMT5, and PLA-QAC0.4 was evaluated by analysis of evolved CO₂ with the DMR system at 58°C. The experiments were conducted using different types of solid media: compost, inoculated vermiculite, and uninoculated vermiculite. In the following biodegradation results, cellulose is the reference material, and blank refers to those bioreactors without polymer films. **Figure 5.1a**, shows that regardless of testing in compost or vermiculite inoculated with the *mixed culture*, all samples produced significantly higher amounts of CO₂ than their respective blanks, so no inhibition was observed due to the presence of the films. **Figure 5.1b**, shows that PLA-OMMT5 and PLA-QAC0.4 have shorter lag times than the pristine PLA, initiating the biodegradation phase earlier in both types of media. Biodegradation in inoculated vermiculite is slower than in compost, so longer testing times were expected. The high mineralization values reached in PLA-QAC0.4 are an indication of the priming effect occurring in the compost media, which was clearly avoided when testing in inoculated

vermiculite as shown in **Figure 5.1b**. As expected, neither significant CO₂ production nor mineralization was observed from the bioreactors with uninoculated vermiculite since there are no microorganisms present. The degradation in this case is mostly attributed to an abiotic hydrolytic process. The results of this initial test using a *mixed culture* from the compost showed that vermiculite is an excellent media for testing bioaugmentation using a single purified strain like *Geobacillus*.

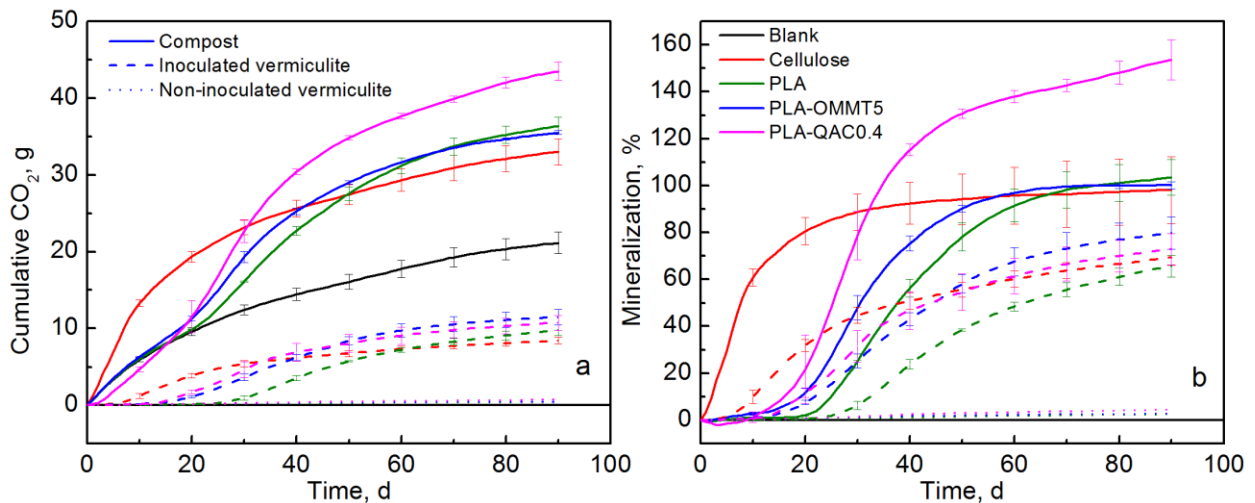


Figure 5.1 (a) CO₂ evolution and (b) % Mineralization of cellulose, PLA, and PLA-OMMT5, and PLA-QAC0.4 in compost (solid lines), inoculated vermiculite with mixed culture (dashed lines), and uninoculated vermiculite (dotted lines); adapted from Castro-Aguirre et al. [3].

Figure 5.2 shows the cumulative CO₂ and % mineralization of PLA and PLA-OMMT5 in compost with and without the inoculation of *Geobacillus*. **Figure 5.2a** shows that the compost alone (solid line) and the compost with *Geobacillus* (dashed line) did not produce significantly different amounts of CO₂. However, when an additional source of carbon was introduced (*i.e.*, cellulose or PLA), there was significantly higher production of CO₂ in the presence of *Geobacillus* at the early stage of the test (<25 d).

This behavior has been attributed to the synergistic effect of *Geobacillus* with the other microbial strains present in the compost and confirmed by the bioaugmentation test in vermiculite. Furthermore, **Figure 5.2b** shows that in all cases the lag time was reduced with the presence of the *Geobacillus* (dashed lines), indicated by the shift of the curve to the left, meaning that the biodegradation phase started earlier in comparison to the samples without *Geobacillus* (solid lines). When comparing by material (**Figure 5.2b**), the lag time is shorter in the PLA-OMMT5 film than in the PLA film. This in agreement with previous reported results in which faster biodegradation was attributed mostly to the initial lower molecular weight of the PLA-OMMT5 films, but also to the higher initial hydrolytic degradation promoted by the presence of OMMT [3].

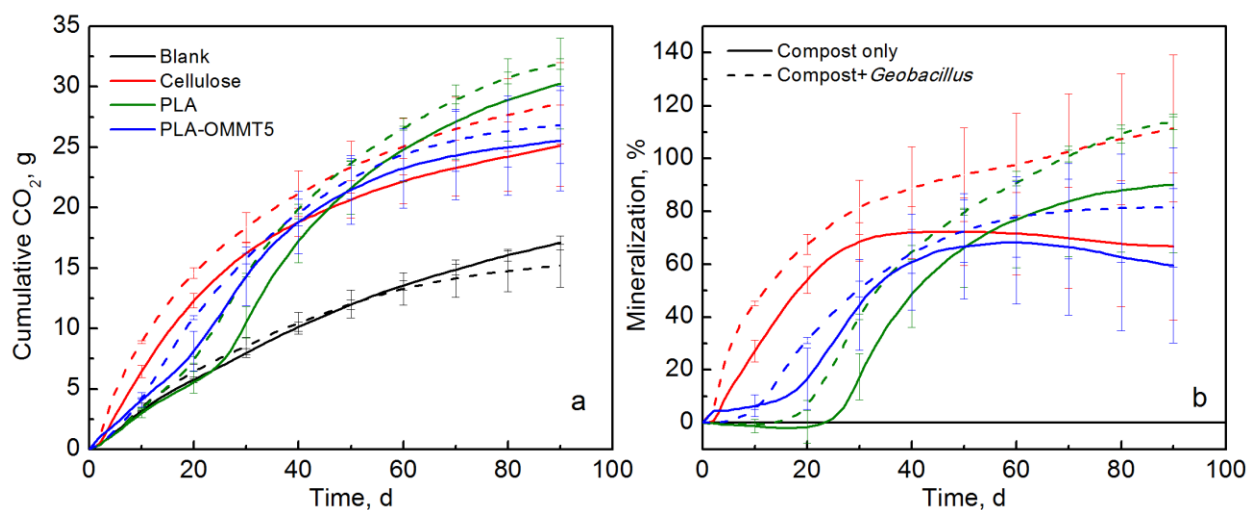


Figure 5.2 (a) CO₂ evolution and (b) % Mineralization of cellulose, PLA, and PLA-OMMT5 in compost without *Geobacillus* (solid lines) and with *Geobacillus* (dashed lines).

Figure 5.3 and **Figure 5.4** show the results of biodegradation tests with bioaugmentation in vermiculite with 4 different levels of inoculation: 1) uninoculated vermiculite, 2) vermiculite inoculated with *Geobacillus* only, 3) vermiculite inoculated

with the *mixed culture* from the compost extract, and 4) vermiculite inoculated with *mixed culture and Geobacillus*. Similar to the results observed in compost, the samples in vermiculite inoculated with *mixed culture and Geobacillus*, produced a statistically significant higher amount of CO₂ than the samples in vermiculite inoculated with the *mixed culture only*, especially PLA-OMMT5 (**Figure 5.3c**), in which the lag time was reduced almost by half (from ~20 d to ~10 d). In all cases, the same mineralization levels were reached towards the end of the test. As previously mentioned, no significant production of CO₂ was expected in the uninoculated bioreactors. Surprisingly, *Geobacillus* by itself did not produce as much CO₂ as when it was together with the *mixed culture*. There was no significant CO₂ production or mineralization when *Geobacillus* was inoculated alone. The observed behavior can be attributed to the *Geobacillus* metabolic activity and to the synergistic effect with other microorganisms. Some researchers have reported that *Geobacillus* spp. have high extracellular esterase and lipase activity [31,32], and are able to utilize a wide range of sugars, carboxylic acids, lactose, lactate, and even hydrocarbons (e.g., C₁₃-C₂₀ *n*-alkanes) [30,31]. Esterases, which break down organic molecules with ester bonds, are extracellular enzymes present on the surface and/or within the biofilm [34]. Thus, the extracellular enzymes produced by *Geobacillus* become resources that may be available for other microorganisms contributing to their growth and activity. Tomita *et al.*, suggested that esterases secreted by *Geobacillus thermocatenuatus* are involved in PLA degradation [15]. Similarly, Sakai *et al.*, showed that degradation of PLA was related to the esterases secreted by *Bacillus smithii* [35]. Moreover, it has been observed that some *Geobacillus* spp. are involved in symbiotic relationships with other microorganisms

providing metabolites from cell lysis [32]. PLA-degrading bacteria may not be limited to the genus *Geobacillus*; other researchers have found members of the family *Bacillaceae* being dominant degraders during composting [7,36]. Further investigation is needed to understand the metabolism and synergistic behavior of *Geobacillus* with other microbial consortia present in the compost for the optimal biodegradation of PLA.

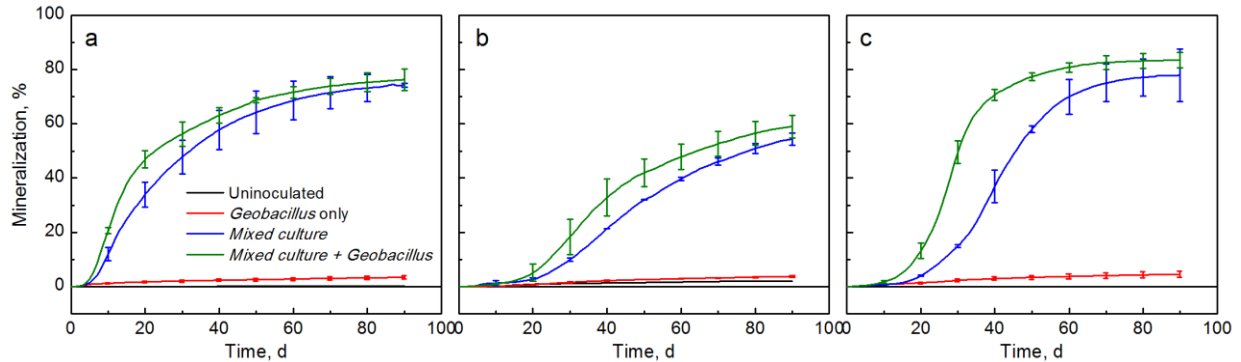


Figure 5.3 % Mineralization of (a) Cellulose, (b) PLA, and (c) PLA-OMMT5 in vermiculite with different levels of inoculation.

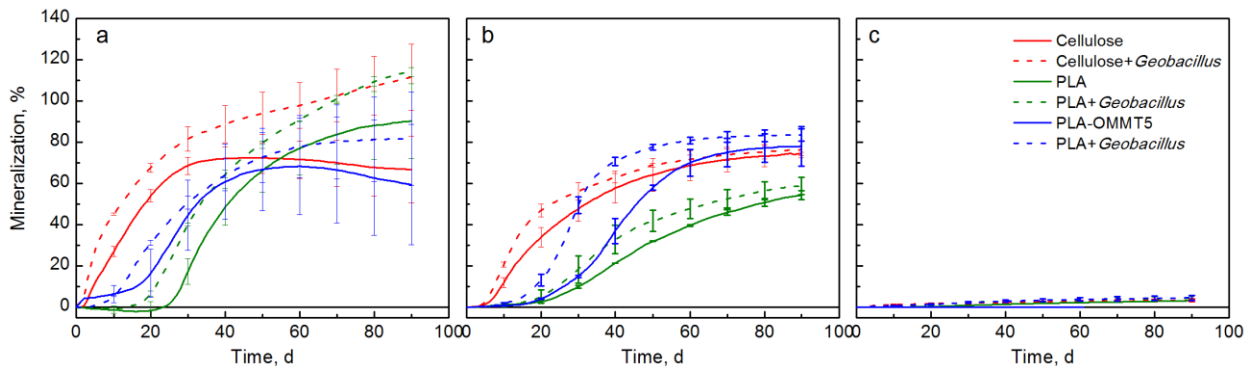


Figure 5.4 % Mineralization of cellulose, PLA, and PLA-OMMT5 in (a) compost (same as **Figure 5.2b**), (b) vermiculite inoculated with mixed culture, and (c) uninoculated vermiculite. Solid lines represent samples without *Geobacillus* while dashed lines represent samples inoculated with *Geobacillus*.

5.3.3 Molecular Weight

Samples of the different materials were retrieved at different time intervals during the biodegradation test to evaluate the change in molecular weight. **Figure 5.5** shows the reduction of M_n of the film samples as function of time. The observed M_n reduction is typical of a bulk degradation mechanism, which can be best represented by a first order reaction fitting with the equation: $M_n = M_{n0} \exp(-kt)$, where M_{n0} is the initial M_n , t is the time, and k is the M_n reduction rate constant [37,38]. **Table 5B.1** of the Appendix 5B shows that the rate constants were not significantly different for the samples tested in *Geobacillus* only, *mixed culture*, and *mixed culture with Geobacillus*. In Chapter 4, we showed that looking at M_n may not be the best approach to studying the molecular weight reduction, and that looking at the changes in the *MWD* may provide more insights about the biodegradation behavior [3].

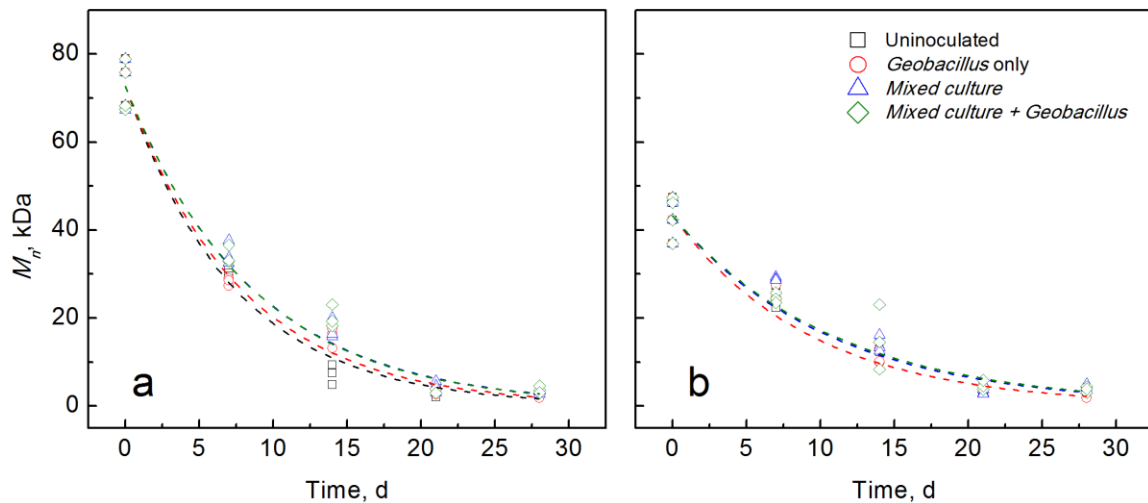


Figure 5.5 Molecular weight reduction as function of time for (a) PLA and (b) PLA-OMMT5 in vermiculite with different levels of inoculation. Lines represent the fitting of the equation $M_n = M_{n0} \exp(-kt)$, where M_{n0} is the initial M_n , k is the rate constant and t is the time.

Figure 5.6 shows the *MWD* of the PLA film as function of time during the biodegradation in vermiculite with the different levels of inoculation. In all cases, a shift of the *MWD* peak to the left represents a decrease of the molecular weight due to bulk hydrolysis of the film while the broadening of the peak represents a higher polydispersity index (*PI*) caused by chain fragmentation [39]. The observed change in the *MWD* from single peak to multiple peaks, especially after days 14 and 21, has been attributed to the rearrangement of the newly formed short polymer chains into crystalline structures [39,40]. The presence of higher and sharper peaks at day 28 indicates that the amorphous regions are being preferably degraded [41]. Therefore, increased crystallinity can be expected during and after the initial degradation [42–44]. In this case (**Figure 5.6**), all the samples have the same initial *MWD* (black line). Regardless of the level of inoculation, all the samples seem to have similar behavior until day 7, where the peak shifted to the left. At day 14, the peak of uninoculated vermiculite became broader and showed the presence of more than one peak. The peaks of *mixed culture* and *mixed culture with Geobacillus* show similar behavior. For the days 21 and 28, the broadening of the peaks and the presence of a multimodal peak is more evident. In all the cases, the biggest reduction of the molecular weight happened between days 14 and 21, with an increase in the lower molecular weight tail. Similar observations were previously reported for pristine PLA and PLA bio-nanocomposite films in simulated composting conditions [3,27]. Moreover, it can be noticed between days 21 and 28 that there was not a significant shift of the peak to the left, instead, the peaks became higher and sharper indicating degradation in the amorphous zone and the consumption of the low molecular weight chains like monomers and oligomers of lactic acid by the

microorganisms. This finding is supported by the significant increase on the production of CO₂ and on the mineralization observed during these days. **Figure 5.6d** shows that the *MWD* of the *mixed culture with Geobacillus* remains around the same position between days 21 and 28, but the low molecular weight tail disappears. A similar observation was found for PLA-OMMT5 films during biodegradation in vermiculite with different levels of inoculation (**Figure 5B.1** of the Appendix 5B). However, this behavior between days 21 and 28 was not observed in the PLA and PLA-OMMT5 samples tested in compost *only* during our previous work [3]. This may indicate that bioaugmentation with *Geobacillus* promotes the rapid microbial assimilation of low molecular weight PLA chains and agrees with the results from the biodegradation test in which the degree of mineralization of PLA and PLA-OMMT5 significantly increased with the presence of *Geobacillus* in both compost and inoculated vermiculite (*i.e.*, with mixed culture).

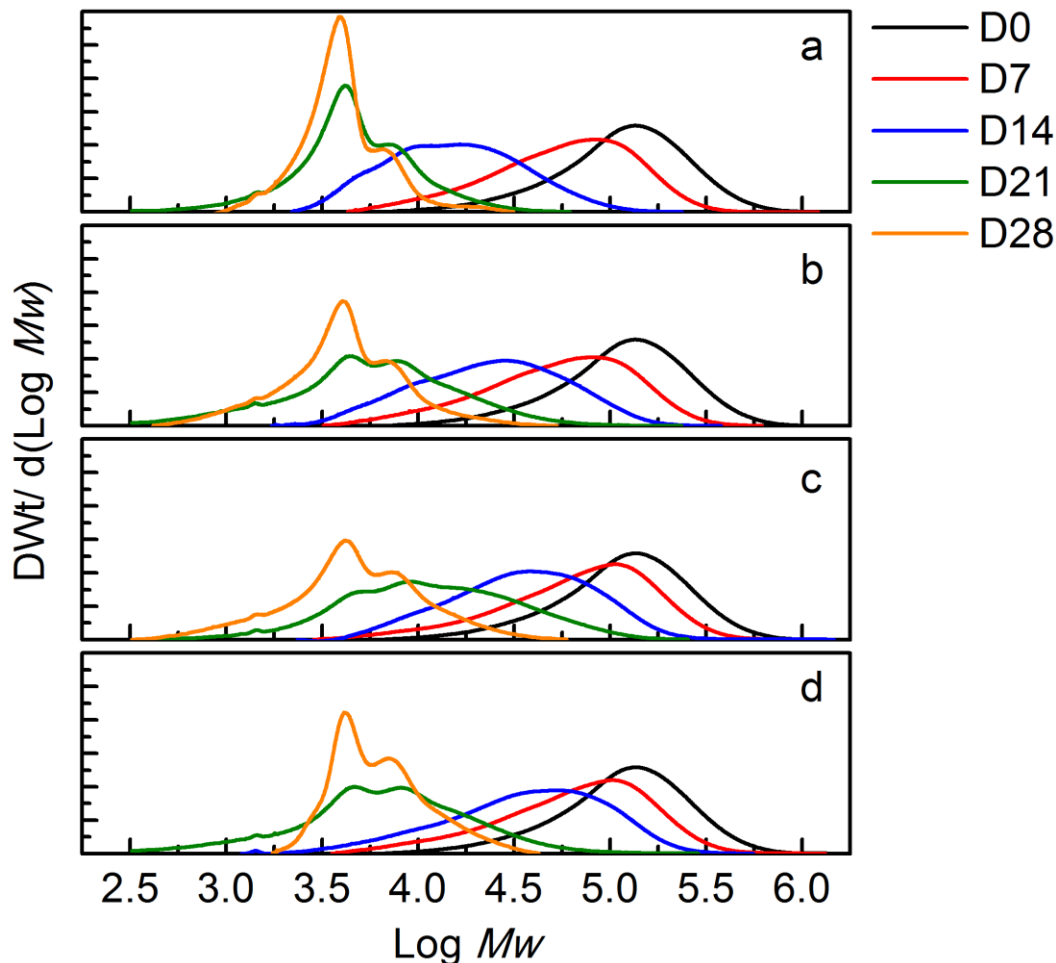


Figure 5.6 MWD of PLA samples in vermiculite with different levels of inoculation (a) uninoculated, (b) *Geobacillus* only, (c) mixed culture, (d) mixed culture and *Geobacillus*.

5.3.4 Biofilm test

Table 5.4 and **Table 5.5**, and **Figure 5C.1** and **Figure 5C.2** of the Appendix 5C, show the *Geobacillus* biofilm formation test results. In **Table 5.4**, the positive control (R2B wells) with PA at 23°C showed an absorbance (A_{600}) of 1.016-1.100, while the negative control (uninoculated wells) had an A_{600} of 0.059-0.067. These values are similar to previously reported values [3,45]. The wells containing PLA and BNCs show no statistically significant difference from the control lacking any film (R2B only). In the case of the test with PA at 23°C, the biofilm formation individual values ranged from

0.013 to 0.155 for PLA, from 0.177 to 0.554 for PLA-OMMT5, and from 0.005 to 0.084 for PLA-QAC0.4 samples. A statistically significant difference was found between the PLA-OMMT5 and PLA-QAC0.4 absorbance values. For the total biofilm formation (wells + film), the same behavior was observed in which the average biofilm values were as follows PLA-OMMT5 \geq PLA \geq PLA-QAC0.4 (**Figure 5C.1a**). These observations are in agreement with the results previously reported, and in which it was suggested that the OMMT may have an indirect stimulation on biofilm formation by PA, while QAC may have an inhibitory effect (**Figure 5C.2a**) [3]. Some researchers have reported that QACs are toxic to microorganisms with significant inhibition of growth of soil microbes at higher concentrations by affecting microbial processes, such as dehydrogenase activity and nitrification [46]. Furthermore, the use of QACs has been studied as a way to inhibit and reduce the attachment of microorganisms in tissues [47]. A list of the minimum inhibitory concentration (MIC) and non-inhibitory concentration (NIC) values of different QACs and different microorganisms can be found elsewhere [48]. Further research is needed to better understand the effect of QACs on the compost microbial consortia.

Table 5.4 Absorbance (600 nm) of biofilm formation samples with *Pseudomonas aeruginosa* (PA) at 23°C

Sample	Wells	Films	Total
R2B only	1.058 \pm 0.042 ^A	N/A	1.058 \pm 0.042 ^B
PLA	1.237 \pm 0.252 ^A	0.084 \pm 0.071 ^{AB}	1.321 \pm 0.262 ^{AB}
PLA-OMMT5	1.488 \pm 0.388 ^A	0.366 \pm 0.189 ^A	1.853 \pm 0.431 ^A
PLA-QAC0.4	1.021 \pm 0.127 ^A	0.040 \pm 0.044 ^B	1.060 \pm 0.134 ^B

Note: Values with the same letter within the same column are not statistically significantly different at $p \leq 0.05$ with Tukey-Kramer test.

Table 5.5 Absorbance (600 nm) of biofilm formation samples with *Geobacillus* at 58°C

Sample	Wells	Films	Total
R2B only	0.231 ± 0.008 ^A	N/A	0.231 ± 0.008 ^A
PLA	0.151 ± 0.067 ^A	0.061 ± 0.036 ^A	0.212 ± 0.076 ^A
PLA-OMMT5	0.199 ± 0.060 ^A	0.090 ± 0.046 ^A	0.289 ± 0.076 ^A
PLA-QAC0.4	0.169 ± 0.042 ^A	0.048 ± 0.032 ^A	0.216 ± 0.053 ^A

Note: Values with the same letter within the same column are not statistically significantly different at $p \leq 0.05$ with Tukey-Kramer test.

Table 5.5 shows the biofilm values with *Geobacillus* at 58°C. The control wells (R2B only) have individual values ranging from 0.223 to 0.240. This absorbance is significantly lower than the absorbance for PA, a known biofilm forming strain, at 23°C. We have observed similar behavior in our previous work with compost extract that was attributed to more challenging conditions for microbial growth and survival at 58°C [3]. However, biofilm abundance also depends on the bacterial strains present [24,49]. The wells supplemented with PLA, PLA-OMMT5 and PLA-QAC0.4 had an average absorbance of 0.151, 0.199, and 0.169, respectively. No statistically significant difference was found between the samples. Biofilm formation by *Geobacillus* at 58°C was observed on the surface of all the films (**Figure 5C.1b**). However, no statistically significant difference was found among the sample materials. The same behavior was observed for the total biofilm formation (wells + film). Although *Geobacillus* was able to attach to the surface of the different films at 58°C, it did not show any preference towards a specific material. In contrast, the pure culture of PA clearly preferred PLA-OMMT5 at 23°C. The fact that the biofilm formation by *Geobacillus* was lower than that by the compost extract at 58°C (**Figure 5C.2b**) agrees with the results from the biodegradation test, in which the mineralization was significantly lower when *Geobacillus* was tested alone. However, there may be other environmental conditions

that are more stimulatory to *Geobacillus* biofilm. For example, the formation of biofilms by *Geobacillus* spp. has been studied in the dairy industry since they are heat-resistant spore-forming bacteria. Some researchers found that *Geobacillus* preferentially form biofilms on surfaces at air-liquid interfaces rather than on submerged surfaces [50]. Moreover, the presence of cations may influence the structural integrity and cohesion of biofilms formed by *Geobacillus* spp., affecting not only the surface-biofilm interaction, but also the metabolism and physiology of these microorganisms [51]. Even though biofilm formation is not a direct indication of biodegradation, it plays an important role in the microbial performance and survival [11,52]. Synergistic effects are commonly observed in which some microbial strains release resources that become available for other microorganisms (e.g., extracellular digestive enzymes able to degrade PLA and derivatives) [11,52]. Furthermore, biofilms are beneficial for other microorganisms since they retain water in the compost, provide tolerance to environmental stressors, and prevent microorganisms from being washed out [52]. Further investigation is still needed to fully understand the synergistic behavior of *Geobacillus* with other populations present in the compost for the biodegradation of PLA-based films.

5.4 Final Remarks

This study aimed to isolate and to identify PLA-degrading microbial strains present in compost, and to evaluate the effect of introducing such microbial strains on the biodegradation rate of PLA and PLA bio-nanocomposites in simulated composting conditions. *Geobacillus thermoleovorans* was identified as the microbial strain present in the compost capable of degrading PLA at 58°C. *Geobacillus* was further used to study bioaugmentation in compost and vermiculite with different levels of inoculation.

Bioaugmentation with *Geobacillus* increased the evolution of CO₂ and shortened the lag phase when tested in compost and vermiculite with mixed culture. *Geobacillus* inoculated alone in vermiculite did not produce significant mineralization of either PLA or PLA-OMMT5 films. Further investigation is recommended to understand this behavior. The lag time was shorter in the PLA-OMMT5 than in the PLA, results that agree with previous results. In all cases the lag time was reduced by the presence of the *Geobacillus*, so more CO₂ was produced at the early stage of biodegradation. *Geobacillus* was able to form biofilm and attach to the surface of PLA, but in amounts less than the compost-derived *mixed culture* at 58°C and PA at 25°C. Moreover, PLA-OMMT5 provided a surface more readily colonized by *P. aeruginosa* and *Geobacillus*, suggesting that polymer modification may provide a way to enhance colonization and therefore degradation of polymers. If the biodegradation rate of PLA and PLA-based products can be accelerated and/or tailored, it could greatly benefit their general use and acceptance in industrial composting facilities. So, using bioaugmentation to enhance the biodegradation rate of these compostable polymers can create a novel method to fast track their biodegradation, so that they can be easily accepted and biodegraded with other compostable organic materials. In turn, if more solid wastes can be disposed through composting, the amount of waste disposed in landfills could be reduced along with the social and environmental impacts associated with landfilling.

APPENDICES

APPENDIX 5A: Compost and vermiculite nutrient analysis

Table 5A.1 shows the physicochemical characteristics and the total nutrient analysis of the different media used: compost, inoculated vermiculite, and uninoculated vermiculite.

Table 5A.1 Physicochemical parameters and total nutrient analysis of different media used in the biodegradation test

Parameter	Compost	Inoculated vermiculite	Uninoculated vermiculite
Dry solids, %	51.8	21.4	18.9
Volatile solids, %	41.3	2.8	3.1
pH	7.9	6.8	8.2
C/N ratio	9.9	10.2	59.9
Carbon, %	24.0	1.6	1.8
Nitrogen, %	2.42	0.16	0.03
Phosphorus, %	0.72	0.21	0.13
Potassium, %	2.56	4.20	3.40
Calcium, %	7.69	0.62	0.57
Magnesium, %	2.08	8.74	8.33
Sodium, %	0.49	0.14	0.04
Sulfur, %	0.50	0.05	0.01
Iron, ppm	5542	51300	48010
Zinc, ppm	206	72	66
Manganese, ppm	404	418	374
Copper, ppm	102	222	207
Boron, ppm	40	3	1
Aluminum, ppm	2640	40280	37930

Note: The total nutrient analysis was performed by inductively coupled plasma atomic emission spectroscopy (ICP-OES).

APPENDIX 5B: Molecular weight

Table 5B.1 Molecular weight reduction rate of PLA and PLA-OMMT5 in vermiculite with different levels of inoculation as estimated by the first order reaction of the form M_n/M_{n0}

$$= \exp(-kt)$$

Level of inoculation	k_{PLA}, d^{-1}	$k_{PLA-OMMT5}, d^{-1}$
<i>Uninoculated</i>	0.136 ± 0.008^A	0.095 ± 0.005^A
<i>Geobacillus only</i>	0.128 ± 0.004^{AB}	0.107 ± 0.008^A
<i>Mixed culture</i>	0.117 ± 0.003^B	0.095 ± 0.005^A
<i>Mixed culture+Geobacillus</i>	0.117 ± 0.006^B	0.092 ± 0.008^A

Note: Values with the same letter within the same column are not significantly different at $p \leq 0.05$ with Tukey-Kramer Test.

Figure 5B.1 shows the molecular weight distribution (*MWD*) of the PLA-OMMT5 film as function of time during the biodegradation in vermiculite with the different levels of inoculation. PLA-OMMT5 follows a similar behavior as pristine PLA with higher and sharper peaks on days 21 and 28 attributed to the assimilation of the low molecular weight chains by the microorganisms and the remaining of the newly formed crystalline structures.

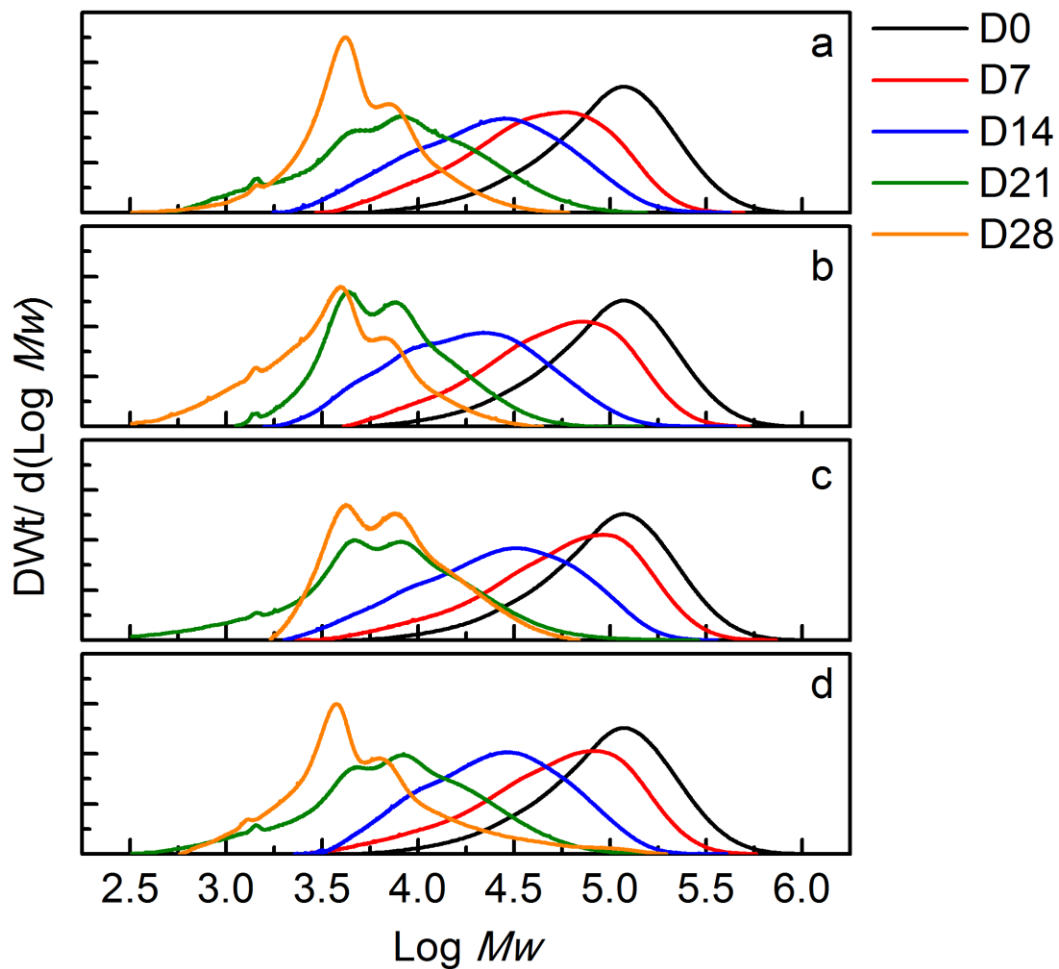


Figure 5B.1 MWD of PLA-OMMT5 samples in vermiculite with different levels of inoculation (a) uninoculated, (b) *Geobacillus* only, (c) mixed culture, (d) mixed culture and *Geobacillus*.

APPENDIX 5C: Biofilm Test

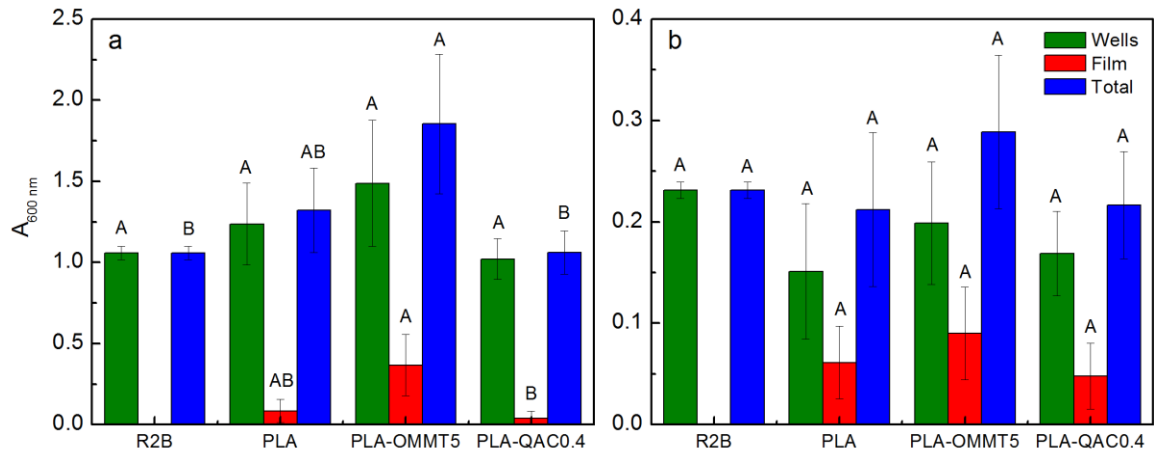


Figure 5C.1 Absorbance (600 nm) of (a) PA at 23°C, and (b) *Geobacillus* at 58°C of biofilm formation samples. Bars with the same letter within a group (*i.e.*, wells, films, or total) are not statistically significantly different at $p \leq 0.05$ with Tukey-Kramer test.

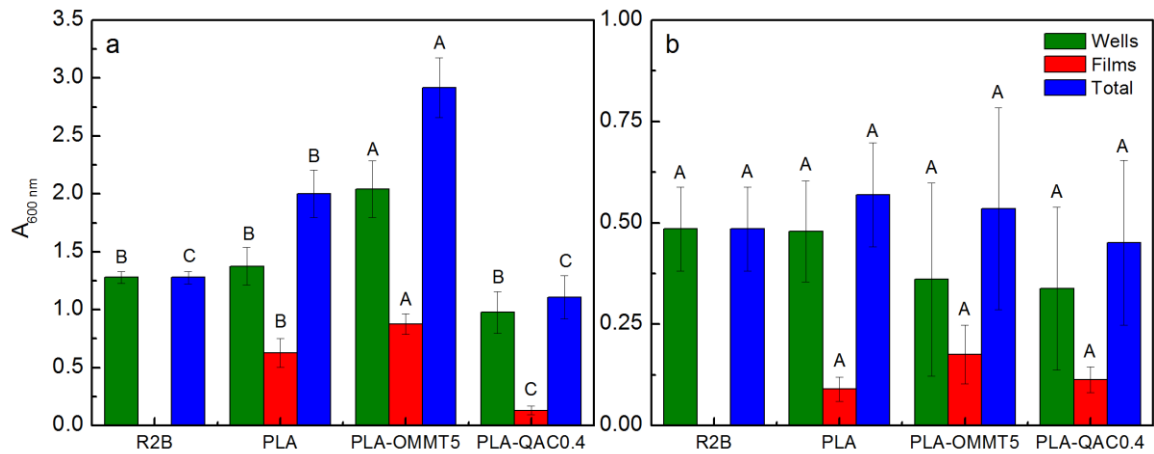


Figure 5C.2 Absorbance (600 nm) of (a) PA at 23°C, and (b) *mixed culture* at 58°C for biofilm test. Bars with the same letter within a group (*i.e.*, wells, films, or total) are not significantly different at $p \leq 0.05$ (Tukey-Kramer test). Adapted from Castro-Aguirre et al. [1].

REFERENCES

REFERENCES

- [1] EPA, Advancing Sustainable Materials Management: 2014 Tables and Figures, (2016) 1–65.
- [2] E. Castro-Aguirre, F. Iñiguez-Franco, H. Samsudin, X. Fang, R. Auras, Poly(lactic acid)—Mass production, processing, industrial applications, and end of life, *Adv. Drug Deliv. Rev.* 107 (2016) 333–366. doi:10.1016/j.addr.2016.03.010.
- [3] E. Castro-Aguirre, R. Auras, S. Selke, M. Rubino, T. Marsh, Impact of Nanoclays on the Biodegradation of Poly (Lactic acid) Nanocomposites, *Polymers (Basel)*. 10 (2018) 1–24. doi:10.3390/polym10020202.
- [4] M. Kumar, A. Kumar, J. Khan, P. Singh, J.W.C. Wong, A. Selvam, Evaluation of thermophilic fungal consortium for organic municipal solid waste composting, *Bioresour. Technol.* 168 (2014) 214–221. doi:10.1016/j.biortech.2014.01.048.
- [5] C. Song, M. Li, X. Jia, Z. Wei, Y. Zhao, B. Xi, C. Zhu, D. Liu, Comparison of bacterial community structure and dynamics during the thermophilic composting of different types of solid wastes: anaerobic digestion residue, pig manure and chicken manure, *Microb. Biotechnol.* 7 (2014) 424–433. doi:10.1111/1751-7915.12131.
- [6] D. Liu, M. Li, B. Xi, Z. Wei, C. Song, C. Zhu, Metaproteomics reveals major microbial players and their biodegradation functions in a large-scale aerobic composting plant, *Microb. Biotechnol.* 8 (2015) 950–960. doi:10.1111/1751-7915.12290.
- [7] A. Hassen, K. Belguith, N. Jedidi, A. Cherif, M. Cherif, A. Boudabous, Microbial characterization during composting of municipal solid waste, *Bioresour. Technol.* 80 (2001) 217–225. doi:10.1016/S0960-8524(01)00065-7.
- [8] M.N. Kim, W.G. Kim, H.Y. Weon, S.H. Lee, Poly (L-lactide)-Degrading Activity of a Newly Isolated Bacterium, *J. Appl. Polym. Sci.* 109 (2008) 234–239. doi:10.1002/app.26658.
- [9] M.N. Kim, S.T. Park, Degradation of Poly (L -lactide) by a Mesophilic Bacterium, *J. Appl. Polym. Sci.* 117 (2010) 67–74. doi:10.1002/app.31950.
- [10] M. Karamanlioglu, A. Houlden, G.D. Robson, Isolation and characterisation of fungal communities associated with degradation and growth on the surface of poly (lactic) acid (PLA) in soil and compost, *Int. Biodeterior. Biodegradation.* 95 (2014) 301–310. doi:10.1016/j.ibiod.2014.09.006.
- [11] T. Apinya, N. Sombatsompop, B. Prapagdee, Selection of a *Pseudonocardia* sp . RM423 that accelerates the biodegradation of poly (lactic) acid in submerged

- cultures and in soil microcosms, *Int. Biodeterior. Biodegradation*. 99 (2015) 23–30. doi:10.1016/j.ibiod.2015.01.001.
- [12] S. Sukkhum, S. Tokuyama, T. Tamura, V. Kitpreechavanich, A novel poly (L-lactide) degrading actinomycetes isolated from Thai forest soil , phylogenetic relationship and the enzyme characterization, *J. Gen. Appl. Microbiol.* 55 (2009) 459–467. doi:10.2323/jgam.55.459.
- [13] N.R. Nair, V.C. Sekhar, K.M. Nampoothiri, Augmentation of a Microbial Consortium for Enhanced Polylactide (PLA) Degradation, *Indian J. Microbiol.* 56 (2016) 59–63. doi:10.1007/s12088-015-0559-z.
- [14] K. Tomita, H. Tsuji, T. Nakajima, Y. Kikuchi, Degradation of poly (D-lactic acid) by a thermophile, *Polym. Degrad. Stab.* 81 (2003) 167–171. doi:10.1016/S0141-3910(03)00086-7.
- [15] K. Tomita, T. Nakajima, Y. Kikuchi, N. Miwa, Degradation of poly (L -lactic acid) by a newly isolated thermophile, *Polym. Degrad. Stab.* 84 (2004) 433–438. doi:10.1016/j.polymdegradstab.2003.12.006.
- [16] S. Boonchan, M.L. Britz, G.A. Stanley, Degradation and Mineralization of High-Molecular-Weight Polycyclic Aromatic Hydrocarbons by Defined Fungal-Bacterial Cocultures, *Appl. Environ. Microbiol.* 66 (2000) 1007–1019. doi:10.1128/AEM.66.3.1007-1019.2000.
- [17] Z. Saadi, A. Rasmont, G. Cesar, Fungal Degradation of Poly (L-lactide) in Soil and in Compost, *J. Polym. Environ.* 20 (2012) 273–282. doi:10.1007/s10924-011-0399-9.
- [18] T. Teeraphatpornchai, M. Nakayama, Isolation and characterization of a bacterium that degrades various polyester-based biodegradable plastics, *Biotechnol. Lett.* 25 (2003) 23–28. doi:10.1023/A:1021713711160.
- [19] N. Hayase, H. Yano, E.M.I. Kudoh, C. Tsutsumi, K. Ushio, Y. Miyahara, S. Tanaka, Isolation and Characterization of Poly (Butylene Succinate-co-Butylene Adipate) -Degrading Microorganism, *J. Biosci. Bioeng.* 97 (2004) 131–133. doi:10.1016/S1389-1723(04)70180-2.
- [20] K. Tomita, N. Hayashi, N. Ikeda, Y. Kikuchi, Isolation of a thermophilic bacterium degrading some nylons, *Polym. Degrad. Stab.* 81 (2003) 511–514. doi:10.1016/S0141-3910(03)00151-4.
- [21] K. Tomita, K. Kojoh, A. Suzuki, Isolation of Thermophiles Assimilating Poly (Ethylene-co-Vinyl Alcohol), *J. Ferment. Bioeng.* 84 (1997) 400–402. doi:10.1016/S0922-338X(97)81998-8.
- [22] M.N. Kim, M.G. Yoon, Isolation of strains degrading poly (Vinyl alcohol) at high temperatures and their biodegradation ability, *Polym. Degrad. Stab.* 95 (2010)

89–93. doi:10.1016/j.polymdegradstab.2009.09.014.

- [23] A. Esmaeili, A.A. Pourbabaee, H.A. Alikhani, F. Shabani, E. Esmaeili, Biodegradation of Low-Density Polyethylene (LDPE) by Mixed Culture of *Lysinibacillus xylanilyticus* and *Aspergillus niger* in Soil, *PLoS One*. 8 (2013) 1–10. doi:10.1371/journal.pone.0071720.
- [24] F. Muroi, Y. Tachibana, Y. Kobayashi, T. Sakurai, K. Kasuya, Influences of poly(butylene adipate-co-terephthalate) on soil microbiota and plant growth, *Polym. Degrad. Stab.* 129 (2016) 338–346. doi:10.1016/j.polymdegradstab.2016.05.018.
- [25] P. Chomczynski, M. Rymaszewski, Alkaline polyethylene glycol-based method for direct PCR from bacteria, eukaryotic tissue samples, and whole blood, *Biotechniques*. 40 (2006) 454–458. doi:10.2144/000112149.
- [26] J.R. Cole, Q. Wang, J.A. Fish, B. Chai, D.M. McGarrell, Y. Sun, C.T. Brown, A. Porras-Alfaro, C.R. Kuske, J.M. Tiedje, Ribosomal Database Project: Data and tools for high throughput rRNA analysis, *Nucleic Acids Res.* 42 (2014) 633–642. doi:10.1093/nar/gkt1244.
- [27] E. Castro-Aguirre, R. Auras, S. Selke, M. Rubino, T. Marsh, Insights on the aerobic biodegradation of polymers by analysis of evolved carbon dioxide in simulated composting conditions, *Polym. Degrad. Stab.* 137 (2017) 251–271. doi:10.1016/j.polymdegradstab.2017.01.017.
- [28] ISO 14855-1:2012, Determination of the ultimate aerobic biodegradability of plastic materials under controlled composting conditions — Method by analysis of evolved carbon dioxide — Part 1: General method, (2012) 20.
- [29] M.K.L.M. Sakaff, A.Y.A. Rahman, J.A. Saito, S. Hou, M. Alam, Complete genome sequence of the thermophilic bacterium *Geobacillus thermoleovorans* CCB_US3_UF5, *J. Bacteriol.* 194 (2012) 1239–1239. doi:10.1128/JB.06580-11.
- [30] T.N. Nazina, E. V. Lebedeva, A.B. Poltarau, T.P. Tourova, A.A. Grigoryan, D.S. Sokolova, A.M. Lysenko, G.A. Osipov, *Geobacillus gargensis* sp. nov., a novel thermophile from a hot spring, and the reclassification of *Bacillus vulcani* as *Geobacillus vulcani* comb. nov, *Int. J. Syst. Evol. Microbiol.* 54 (2004) 2019–2024. doi:10.1099/ijs.0.02932-0.
- [31] M.F. DeFlaun, J.K. Fredrickson, H. Dong, S.M. Pfiffner, T.C. Onstott, D.L. Balkwill, S.H. Streger, E. Stackebrandt, S. Knoessen, E. van Heerden, Isolation and characterization of a *Geobacillus thermoleovorans* strain from an ultra-deep South African gold mine, *Syst. Appl. Microbiol.* 30 (2007) 152–164. doi:10.1016/j.syapm.2006.04.003.
- [32] I.M. Banat, R. Marchant, *Geobacillus* Activities in Soil and Oil Contamination Remediation, in: N.A. Logan, P. De Vos (Eds.), *Endospore-Forming Soil Bact.*,

- Springer, Berlin, Heidelberg, Berlin, 2011: pp. 259–270. doi:10.1007/978-3-642-19577-8.
- [33] A.C. Parte, LPSN - List of prokaryotic names with standing in nomenclature, *Nucleic Acids Res.* 42 (2014) 613–616. doi:10.1093/nar/gkt1111.
- [34] T.J. Battin, Assessment of fluorescein diacetate hydrolysis as a measure of total esterase activity in natural stream sediment biofilms, *Sci. Total Environ.* 198 (1997) 51–60. doi:10.1016/S0048-9697(97)05441-7.
- [35] K. Sakai, H. Kawano, A. Iwami, M. Nakamura, M. Moriguchi, Isolation of a thermophilic poly-L-lactide degrading bacterium from compost and its enzymatic characterization, *J. Biosci. Bioeng.* 92 (2001) 298–300. doi:10.1016/S1389-1723(01)80266-8.
- [36] W. Guo, J. Tao, C. Yang, Q. Zhao, C. Song, S. Wang, The rapid evaluation of material biodegradability using an improved ISO 14852 method with a microbial community, *Polym. Test.* 29 (2010) 832–839. doi:10.1016/j.polymertesting.2010.07.004.
- [37] F. Iñiguez-Franco, R. Auras, K. Dolan, S. Selke, D. Holmes, M. Rubino, H. Soto-Valdez, Chemical recycling of poly(lactic acid) by water-ethanol solutions, *Polym. Degrad. Stab.* 149 (2018) 28–38. doi:10.1016/j.polymdegradstab.2018.01.016.
- [38] F. Iñiguez-Franco, R. Auras, J. Ahmed, S. Selke, M. Rubino, K. Dolan, H. Soto-Valdez, Control of hydrolytic degradation of Poly(lactic acid) by incorporation of chain extender: From bulk to surface erosion, *Polym. Test.* 67 (2018) 190–196. doi:10.1016/j.polymertesting.2018.02.028.
- [39] H. Tsuji, Y. Ikada, Blends of crystalline and amorphous poly(lactide) .3. Hydrolysis of solution-cast blend films, *J. Appl. Polym. Sci.* 63 (1997) 855–863. doi:papers://590F92D9-0B76-4B88-8729-9AF064BE5AC8/Paper/p4495.
- [40] F. Iñiguez-Franco, R. Auras, G. Burgess, D. Holmes, X. Fang, M. Rubino, H. Soto-Valdez, Concurrent solvent induced crystallization and hydrolytic degradation of PLA by water-ethanol solutions, *Polym. (United Kingdom)*. 99 (2016) 315–323. doi:10.1016/j.polymer.2016.07.018.
- [41] H. Tsuji, T. Saeki, T. Tsukegi, H. Daimon, K. Fujie, Comparative study on hydrolytic degradation and monomer recovery of poly(l-lactic acid) in the solid and in the melt, *Polym. Degrad. Stab.* 93 (2008) 1956–1963. doi:10.1016/j.polymdegradstab.2008.06.009.
- [42] K. Fukushima, E. Giménez, L. Cabedo, J.M. Lagarón, J.L. Feijoo, Biotic degradation of poly (DL -lactide) based nanocomposites, *Polym. Degrad. Stab.* 97 (2012) 1278–1284. doi:10.1016/j.polymdegradstab.2012.05.029.
- [43] A. V. Machado, A. Araújo, M. Oliveira, Assessment of polymer-based

nanocomposites biodegradability, (2014).

- [44] M.P. Balaguer, C. Aliaga, C. Fito, M. Hortal, Compostability assessment of nano-reinforced poly(lactic acid) films, *Waste Manag.* 48 (2016) 143–155. doi:10.1016/j.wasman.2015.10.030.
- [45] S.M. Satti, A.A. Shah, R. Auras, T.L. Marsh, Isolation and characterization of bacteria capable of degrading poly(lactic acid) at ambient temperature, *Polym. Degrad. Stab.* 144 (2017) 392–400. doi:10.1016/j.polymdegradstab.2017.08.023.
- [46] B. Sarkar, M. Megharaj, Y. Xi, G.S.R. Krishnamurti, R. Naidu, Sorption of quaternary ammonium compounds in soils: Implications to the soil microbial activities, *J. Hazard. Mater.* 184 (2010) 448–456. doi:10.1016/j.jhazmat.2010.08.055.
- [47] P.J. Breen, C.M. Compadre, E.K. Fifer, H. Salary, D.C. Serbus, D.L. Lattin, Quaternary Ammonium Compounds Inhibit and Reduce the Attachment of Viable *Salmonella typhimurium* to Poultry Tissues, *J. Food Sci.* 60 (1995) 1191–1196. doi:10.1111/j.1365-2621.1995.tb04553.x.
- [48] R.J.W. Lambert, J. Pearson, Susceptibility testing: accurate and reproducible minimum inhibitory concentration (MIC) and non-inhibitory concentration (NIC) values, *J. Appl. Microbiol.* 88 (2000) 784–790. doi:10.1046/j.1365-2672.2000.01017.x.
- [49] M. Walczak, M. Swiontek, A. Sionkowska, M. Michalska, U. Jankiewicz, E. Dejasikora, Biofilm formation on the surface of polylactide during its biodegradation in different environments, *Colloids Surfaces B Biointerfaces.* 136 (2015) 340–345.
- [50] Y. Zhao, M.P.M. Caspers, K.I. Metselaar, P. De Boer, G. Roeselers, R. Moezelaar, M.N. Groot, R.C. Montijn, T. Abee, R. Korta, Abiotic and Microbiotic Factors Controlling Biofilm Formation by Thermophilic Sporeformers, *Appl. Environ. Microbiol.* 79 (2013) 5652–5660. doi:10.1128/AEM.00949-13.
- [51] B. Somerton, S. Flint, J. Palmer, J. Brooks, D. Lindsay, Preconditioning with cations increases the attachment of *Anoxybacillus flavithermus* and *Geobacillus* species to stainless steel, *Appl. Environ. Microbiol.* 79 (2013) 4186–4190. doi:10.1128/AEM.00462-13.
- [52] J.T. Lennon, B.K. Lehmkuhl, A trait-based approach to bacterial biofilms in soil, *Environ. Microbiol.* 18 (2016) 2732–2742. doi:10.1111/1462-2920.13331.

CHAPTER 6

CONCLUSIONS AND RECOMMENDATIONS

6.0 Conclusions

Poly(lactic acid) (PLA) is likely the most popular polymer derived from renewable resources. It is recyclable and biodegradable under composting conditions, thus providing an alternative disposal route. PLA is already used in different applications for the medical, textile, plasticulture, and packaging industries with products manufactured *via* established polymer-processing techniques (*i.e.*, extrusion, injection molding, blow molding, thermoforming, foaming, and spinning) as critically reviewed in Chapter 2. The range of applications of PLA keeps increasing with the development of novel materials in which PLA is blended with other polymers and/or compounded with different fillers to achieve the desired performance properties. Therefore, with the development of these new PLA-based materials, there is also a need for methodologies to evaluate their biodegradability and understand their biodegradation mechanisms if composting is their intended end of life.

In this context, chapter 3 presented a summary of the literature with the different methods that have been used to test the biodegradation of several materials. This information along with a comparative analysis of the results obtained from our own biodegradation tests (performed by analysis of evolved CO₂), allowed us to identify some key factors that should be more strictly controlled for an efficient biodegradation test, especially those related to the characteristics of the compost (*e.g.*, organic matter, carbon-nitrogen ratio, and pH). Regarding environmental factors, temperature was the easiest parameter to control throughout the testing period while water content was the

most crucial and difficult to adjust. Chapter 3 also discussed the biodegradation of PLA as a study case based on our experiments. The results advocated that abiotic hydrolysis is the main contribution to the degradation process of PLA in the early stage of degradation and becomes a limiting factor for the subsequent biodegradation of this material, with the degradation rate depending also on the specific properties of the material (*e.g.* crystallinity and initial molecular weight).

Throughout this work, we emphasized that one of the current limitations for composting as PLA end-of-life scenario is that this material does not biodegrade as fast as other organic wastes which affects its general acceptance in industrial composting facilities. Two approaches were proposed and studied to accelerate the biodegradation rate of PLA: the addition of nanoclays to the polymer matrix and bioaugmentation (*i.e.*, the addition of selective PLA-degrading microbial strains).

In chapter 4, we evaluated the effect of three different nanoclays and a surfactant (OMMT, HNT, LRD, and QAC) on the biodegradation rate of PLA. The results suggested that the biodegradation phase of the films containing nanoclay started earlier than that for pristine PLA. However, the initial molecular weight and thickness of the samples played a crucial role in these biodegradation studies. When the different nanoclays and surfactant were tested alone, it was observed that HNT, OMMT, and QAC presented some inhibition regardless of the amount introduced in the bioreactors.

The effect of nanoclays on the microbial attachment was also evaluated with a biofilm formation assay. The results showed that PLA-LRD had the greatest biofilm formation (as confirmed by the SEM micrographs). On the other hand, PLA-QAC had

the lowest biofilm formation, which was attributed to an inhibitory effect also observed during the biodegradation test when QAC was tested alone.

Further investigation on the specific microbial strains capable of degrading PLA and on how they can affect the biodegradation rate of PLA was presented in Chapter 5. *Geobacillus thermoleovorans* was identified as the PLA-degrading microbial strain present in the compost at 58°C, and it was used to study bioaugmentation in simulated composting conditions. The results showed that bioaugmentation with *Geobacillus* increased the evolution of CO₂ and shortened the lag phase of PLA and PLA-OMMT when tested in compost and vermiculite inoculated with a compost-derived mixed culture. *Geobacillus* inoculated alone in vermiculite did not produce significant mineralization of either PLA or PLA-OMMT films.

Microbial attachment was also investigated in Chapter 5. *Geobacillus* was able to form biofilm and attach to the surface of PLA, but in lower amounts than the compost-derived mixed culture at 58°C and *Pseudomonas aeruginosa* (PA) at 23°C. The results also suggested that PLA-OMMT provided a surface more readily colonized by PA and *Geobacillus*, indicating enhanced colonization.

In general, if the biodegradation rate of PLA and PLA-based materials (e.g. BNCs) can be accelerated and/or tailored, it will greatly benefit their general use and acceptance in industrial composting facilities. Therefore, incorporating nanoclays on the PLA matrix and/or using bioaugmentation with specific microbial strains have been proved to be effective methods for enhancing the biodegradation rate of PLA, so PLA products can be easily biodegraded along with other compostable organic materials.

6.1 Recommendations

The results presented in this work from our different biodegradation tests along with the information provided in the literature allowed us to identify that one of the main issues of biodegradation testing is the low reproducibility due to the number of variables involved in the biodegradation process, making it difficult to provide fair comparisons of samples that are not within the same test. We have recommended performing a biodegradation test in different labs around the world (e.g., round robin test) by the analysis of evolved CO₂ in a DMR system using different standardized reference materials (e.g., cellulose, PLA, and PCL), and more strictly controlled compost physicochemical characteristics and testing parameters, in an attempt to unify and to improve this testing methodology.

Regarding the studies made with PLA bio-nanocomposites, we have identified that the incorporation of nanoclays affected the initial molecular weight and thickness of the PLA films even when maintaining the same processing conditions as the control films. The results suggested that these two factors (*i.e.*, initial molecular weight and thickness) played a crucial role in the evolution of CO₂. Therefore, it is recommended for future biodegradation testing to produce samples with no significant difference in molecular weight and thickness, even though it can be challenging.

During the bioaugmentation studies, we observed that the presence of *Geobacillus* significantly increased the evolution of CO₂ when tested in compost and vermiculite inoculated with a compost-derived mixed culture. However, when *Geobacillus* was inoculated alone in vermiculite, no significant mineralization of the samples was observed. Therefore, further studies are recommended to understand this behavior, as well as the different interactions of *Geobacillus* with other microbial strains

present in the compost that may have a synergistic effect on the biodegradation of materials.

Future work should also concentrate on studying other microbial strains that have been reported in the literature and that are able to assimilate PLA and its degradation by-products. In this context, most of the studies found in the literature were performed in liquid media, so it is essential to understand the biodegradation behavior in solid environments such as compost and vermiculite. It would also be relevant to study the changes in the phylogenetic composition and the different microbial interactions during composting using molecular ecological techniques (*e.g.* next generation sequencing and metaproteomics).

For future biodegradation testing, and especially for bioaugmentation studies, we recommend the use of vermiculite. This media has been proven to be an excellent solid environment to simulate composting conditions in a more controlled manner, *e.g.*, avoiding priming effect produced by some testing materials, the incorporation of specific microbial strains, and the possible recovery of degradation by-products that can be potentially used for a complete carbon balance analysis.

Future work should continue focus on finding approaches to tailor the biodegradation rate of PLA. If such rate is accelerated, PLA and PLA-based products can be accepted in industrial composting facilities and treated together with other organic wastes, which is the ideal end-of-life scenario for this type of products. In turn, if more solid wastes can be disposed through composting, the amount of waste disposed in landfills could be reduced along with the social and environmental impacts associated with landfilling.

Finally, in a wider perspective, future work need to be done so PLA-based products can reach their intended end-of-life scenarios (*i.e.*, recycling and composting). Currently, there are still limitations due to the lack of suitable infrastructure for collecting post-consumer PLA products, sorting, recycling, and/or composting. So, efforts should be centered on active collaboration with industries, commodity groups, industry associations, and government groups to improve the recovery rate of PLA.